Sensory adaptations in shrimp from deep hydrothermal vents : Comparison of chemo- and thermo-sensory abilities in the vent species Mirocaris fortunata and the coastal species Palaemon elegans

Julia Machon

Sorbonne Université – Muséum National d'Histoire Naturelle

Ecole doctorale « Sciences de la Nature et de l'Homme » (ED227)

UMR 7208 Biologie des ORganismes et Ecosystèmes Aquatiques (BOREA)

Equipe Adaptations aux Milieux Extrêmes (AMEX)

Adaptations sensorielles chez les crevettes hydrothermales profondes : Comparaison des facultés chimio- et thermo-sensorielles de la crevette hydrothermale *Mirocaris fortunata* et de la crevette côtière *Palaemon elegans*

Sensory adaptations in shrimp from deep hydrothermal vents: Comparison of chemo- and thermosensory abilities in the vent species *Mirocaris fortunata* and the coastal species *Palaemon elegans*

Par **Julia Machon**

Thèse de doctorat de Biologie Marine

Dirigée par **Juliette Ravaux** et **Magali Zbinden**

Présentée et soutenue publiquement le 2 octobre 2018

Devant un jury composé de :

Thierry PEREZ / Rapporteur
Directeur de Recherche. Institut Méditerranéen de Biodiversité et d'Ecologie Marine et Continentale

Chris HAUTON / Rapporteur
Maître de Conférences. Ocean and Earth Science, University of Southampton

Florence PRADILLON / Examinateur
Chargé de Recherche. Ifremer, Centre de Brest

Martine MAÏBECHE / Examinateur
Professeur des Universités. Institut d'Ecologie et des Sciences de l'Environnement de Paris

Philippe LUCAS / Examinateur
Directeur de Recherche. Institut d'Ecologie et des Sciences de l'Environnement de Paris

Magali ZBINDEN / Directrice de Thèse
Maître de Conférences. Sorbonne Université

Remerciements

Acknowledgements

Cette thèse conclut trois années de travail qui furent heureuses et passionantes grâce à l'aide et le soutien de nombreuses personnes.

Tout d'abord, je suis infiniment reconnaissante envers mes directrices de thèse, Juliette & Magali, pour leur confiance, leur temps et leurs nombreux conseils qui m'ont permis de m'améliorer tout du long. Merci pour votre soutien scientifique et moral, votre bienveillance et d'avoir rendu tout cela possible.

Je remercie sincèrement Philippe, qui a amplement contribué au bon déroulement de cette thèse, du début à la fin. Merci pour ton aide, ta bonne humeur et m'avoir accueillie dans ton laboratoire où j'ai beaucoup appris.

Je remercie bien sûr Bruce, Louis, Nelly, Bérénice, Sébastien, Kamil, Alison et Céline qui ont fait partie de mon aventure au sein de l'équipe AMEX et l'ont rendue si positive.

Je remercie spécialement Bruce, Magali, Juliette et Marie-Anne de m'avoir donné l'opportunité incroyable de participer à la mission océanographique BICOSE2 et la chance de plonger avec le Nautile. Magali, Louis, Bruce, merci d'avoir rendu cette expérience inoubliable. Je remercie par la même occasion l'équipage du navire Pourquoi Pas ?, l'équipe Nautile, les nombreux scientifiques avec qui j'ai vécu cette mission et particulièrement Aurélie, qui a égaillé mes journées.

Je remercie chaleureusement Thomas et Nicolas pour leur contribution, leurs conseils et leur humour. Un grand merci à Nicolas pour m'avoir permis de participer aux enseignements de biologie animale.

I am profusely thankful to Steffen for welcoming me in its laboratory in Greifswald, to Jakob for its precious help, and to Rebecca, Andy, Veronica, Marie and Matthes as part of this very nice team.

Je remercie toutes les personnes que j'ai côtoyées à l'INRA de St-Cyr, où les déjeuners furent captivants, notamment Michel, Nina, Jean-Pierre, Didier, Elodie et Christelle.

Je remercie Dominique, Jean-Marie et tous les membres de l'aquarium Océanopolis qui m'ont accueillie plusieurs fois et aidé à réaliser de nombreuses expériences.

Je remercie beaucoup Nelly pour son soutien quotidien et nos nombreux échanges. Merci également à Latifa et Paula pour leur joie contagieuse.

Je remercie Nicolas pour nous avoir ramené tant de fois des crevettes côtières, mais aussi pour m'avoir passionné pour la biologie animale dès la première année de licence.

Je remercie Anne, Sylvie et tous les membres de l'UMR BOREA avec qui j'ai pu échanger.

Je remercie Matthieu pour ses conseils précieux avec les statistiques et le logiciel R.

Je remercie Géraldine et Chakib pour leur aide en microscopie électronique.

Enfin, je remercie mes proches qui ont partagé mon enthousiasme tout au long de cette thèse. Je remercie tendrement ma mère pour son réconfort et ses blagues, ma sœur pour son intérêt et son soutien, Boris pour ses conseils avisés et pour m'avoir motivée chaque jour, et plus que tout mon père, pour m'avoir encouragée très tôt à être curieuse, rationnelle et zen, et pour avoir insisté sur l'importance de développer un esprit critique.

Table of Contents

List of Figures

List of Tables

Introduction

Along mid-oceanic ridges, deep hydrothermal vents are dynamic environments where geothermally heated seawater, called hydrothermal fluid, discharges from chimneys and cracks in the seafloor. The pure hydrothermal fluid is warm (up to 350°C), anoxic, acid and enriched in potentially toxic minerals and dissolved gases (Charlou et al. 2000, 2002, 2010). The dilution of this fluid with the surrounding cold (2°C) and oxygenated seawater creates steep variations of temperature and chemical concentrations around active vents (Johnson et al. 1986). In spite of these hostile conditions, added to high hydrostatic pressure and darkness, vents are colonized by dense macrofaunal communities (Tunnicliffe et al. 1991, 1998, van Dover et al. 1995, Desbruyères et al. 2000, Wolff 2005). These vent ecosystems rely on chemoautotrophic bacteria as primary producers, which convert reduced chemicals through oxidation, providing the energy to fix carbon and to produce organic matter that serves as a nutritional basis for primary consumers (Jannasch and Mottl 1985, Childress and Fisher 1992, van Dover 2000, Fisher et al. 2007, Ponsard et al. 2013). In light of their habitat, lifestyle and the fairly extreme abiotic conditions they must cope with, vent animals are fascinating models to investigate biological adaptations.

Alvinocaridid shrimp are an emblematic faunal taxon of vents from the Mid-Atlantic Ridge (Segonzac et al. 1993, Desbruyères et al. 2000, 2001), with four endemic species (*Rimicaris exoculata*, *Rimicaris chacei*, *Mirocaris fortunata* and *Alvinocaris markensis*) that are widely distributed along the ridge and commonly reported, depending on the species, from 850 to 4000 m depth (Lunina and Vereshchaka 2014). Several studies show that these shrimp possess a range of morphological, anatomical and physiological adaptations to the hydrothermal environment, related to ectosymbiosis with bacteria (Casanova et al. 1993, Zbinden et al. 2004, Ponsard et al. 2013), respiration in hypoxic conditions (Lallier and Truchot 1997, Hourdez and Lallier 2007), or thermal stress (Ravaux 2003, Cottin et al. 2010) for instance. However, sensory adaptations have only been partially investigated (Jinks et al. 1998) despite their importance in understanding the maintenance of these species, their life cycle and their long-term evolution. The mechanisms used by vent shrimp for orientation in the absence of sunlight are still enigmatic. Vent shrimp colonize the close surrounding of active chimneys, suggesting that they might detect attractants to choose their microhabitat, such as abiotic factors of the hydrothermal fluid emissions (Segonzac et al. 1993, Sarrazin et al. 1999). This refers to short-distance detection (i.e. few meters). The detection and selection of distant active vents is also questioning. The

abundance of shrimp and other vent organisms along the Mid-Atlantic Ridge indicates that they are successful colonizers, but it is unclear how vent species locate and settle in new vents, that can be a few to hundreds of kilometers apart (Teixeira et al. 2012, 2013). The main hypothesis is that larval stages ensure dispersion in the water currents, and can detect cues of the scattering hydrothermal fluid, called plume, emanating from an active vent (Rittschoff et al. 1998, Herring and Dixon 1998, Tyler and Young 2003). Long-distance detection of hydrothermal cues also concerns vent shrimp adults, which sometimes disperse in the surrounding abyssal water at tens of meters from the active chimneys, and must orient theirselves towards the vent to return to their habitat (Segonzac et al. 1993). Hence, emissions of hydrothermal fluids are likely to play a major role for the orientation within both local and remote habitats of vent shrimp, which may present specific sensory abilities to detect the hydrothermal fluid.

The understanding of the mechanisms used by vent shrimp to detect their habitat is crucial considering the current societal and economic context where the seafloor is the target of mining industries. There is a rising demand for precious and rare metals, and consequently over the past decade the interest has shifted from the overexploited terrestrial resources towards hydrothermal vents as source of metals (van Dover 2011). Venting creates massive sulfide deposits which contain valuable metals such as copper, gold, silver, and zinc (Krasnov et al. 1995). After prospection, exploration and resource assessment phases, the first large-scale excavation of seafloor massive sulfides is planned to start at 1600 m depth in the waters of Papua New Guinea (Filer and Gabriel 2017) using specific designed remotely operated underwater vehicles (Teague et al. 2018). Aside from the direct perturbations (e.g. turbidity, noise) on a mining zone, the sediment plumes created by the extraction process could have various impacts on vent fauna. The release of mineral particles and potentially toxic compounds will modify the water column properties, which could impact the physiology of animals (Gwyther 2009, Hauton et al. 2017). The plume dispersal could also act as a lure for vent organisms during dispersion processes (Boschen et al. 2013). Hence, studying vent shrimp sensory abilities is part of the scientific background necessary to evaluate how these animals might cope with deep-sea mining disturbances.

Sensory perception rules species interactions with their environment and congeners, and is therefore central to most animal behaviors. In light of their vast diversity, crustaceans are excellent models to use in comparative studies to reveal evolutionary sensory adaptations to diverse habitats and lifestyles (Derby and Weissburg 2014). Caridean shrimp are particularly relevant for such

approaches, with a broad distribution from shallow-waters to the deep ocean, but studies on their sensory systems are scarce. In the vent habitat, Alvinocaridid shrimp (belonging to the Caridea) are further interesting since the species that live on the Mid-Atlantic Ridge exhibit different lifestyles, primarily linked to their trophic behavior. For example, *R. exoculata* relies on the primary production of episymbiotic bacteria, and consequently needs to stay close to the hydrothermal fluid to supplement its symbionts in reduced compounds (Zbinden et al. 2008, Durand et al. 2009, Petersen et al. 2010, Ponsard et al. 2013), whereas *M. fortunata* is a secondary consumer that lives in the periphery of the main chimneys (Gebruk et al. 1997, Desbruyères et al. 2001). Hence, these species might not be sensitive to the same attractants. These differences within Alvinocaridid species make vent shrimp excellent models to investigate sensory adaptations to habitats and lifestyles and to complement the current knowledge on crustacean sensory biology.

The dim light emitted at vents, temperature and chemicals (especially sulfide) have been proposed as potential attractants for the detection of hydrothermal fluid emissions (Pelli and Chamberlain 1989, Segonzac et al. 1993, Renninger et al. 1995, Jinks et al. 1998). Due to their unusual highly modified eyes, vision has been relatively well studied in vent shrimp (van Dover et al. 1989, Gaten et al. 1998, Chamberlain 2000). They possess a highly sensitive retina which cannot form images but might detect the thermal radiation of the hot fluid at the chimney exits (van Dover et al. 1989, Pelli and Chamberlain, 1989). Such very dim light is detectable only at short-distance, likely less than two meters (Segonzac et al. 1993). Next, temperature may be a key factor for shrimp positioning in their habitat (Segonzac et al. 1993), and attraction to warm temperatures has been reported for *R. exoculata* (Ravaux et al. 2009). Temperature is relevant for both the short- and long-distance detection of an active vent field, since spreading hydrothermal plumes are characterized by fine temperature anomalies (Tao et al. 2017). But it is not known if vent shrimp present specific adaptations of their thermosensory systems, for which mechanisms are not yet understood in crustaceans (Lagerspetz and Vainio 2006). Finally, the chemicals extensively released at vents might be used as orientation cues (Renninger et al. 1995, Desbruyères et al. 2000). Chemical gradients occur from the fluid emission point, and can be either steep or gradual depending on the chemical (Klevenz et al. 2011). For example, sulfide rapidly disappears around the chimneys after reacting with seawater and hydrothermal fluid constituents (Mottl and McConachy 1990, Zhang and Millero 1993), whereas methane, manganese or iron are more conservative (de Angelis et al. 1993, Aumond 2013, Waeles et al. 2017). Thus, depending on their stability, chemicals can be relevant either for short- or long-distance detection of the hydrothermal fluid and plume. Only Renninger and collaborators (1995) have to date investigated the

chemosensory abilities of a vent shrimp, *R. exoculata*, for which the antennae were responsive to sulfide, and the authors proposed chemotaxis as an orientation mechanism for vent shrimp.

To further investigate the potential sensory adaptations of vent shrimp that would allow the detection of the thermal and chemical signature of the hydrothermal fluid, a multi-approaches study of chemo- and thermosensory abilities in the vent shrimp *M. fortunata* is presented in this thesis. The approaches were conducted in parallel on the coastal related species *Palaemon elegans* for comparison, in order to highlight potential adaptations to the vent habitat. The main objectives of this work are:

- to determine if vent shrimp present specificities of their chemosensory system compared to a related shallow-water species, with potential dissimilarities at structural, functional and molecular levels that could reflect adaptive traits,

- to evaluate the relevance of chemical and thermal guidance for vent shrimp orientation in their habitat, through electrophysiological and behavioral experiments.

This thesis presents both published and unpublished results, with several approaches of investigation (structural, neurophysiological, behavioral and molecular) detailed in distinct chapters. Accordingly, the manuscript does not follow a publication plan. Thesis publications are presented at the end of the manuscript, and published results are indicated at the beginning of the corresponding sections.

Chapter I is the background of the study, with presentation of the hydrothermal environment, the shrimp species living at the Mid-Atlantic Ridge, and the equipments developed for *in vivo* studies on vent fauna. The chapter also reviews the current state of knowledge on chemo- and thermosensory mechanisms in marine crustaceans.

Chapter II contains the materials and methods, including sampling and maintenance of specimens, and protocols for imaging approaches, electrophysiology, behavior experiments and molecular studies.

Chapter III presents a structural analysis of the chemosensory organs and integrative centers in *M. fortunata* and *P. elegans*, with the morphology of the antennal appendages, the ultrastructure of the olfactory aesthetasc sensilla and a description of the chemosensory centers in the brain.

Numerical aspects used to infer on chemodetection efficiency are compared between the two species to discuss on potential adaptations of the vent species.

Chapter IV investigates the detection of hydrothermal fluid chemicals by the antennal appendages. An electroantennography method on marine shrimp was developed for this purpose and is presented. Detection of sulfide, iron, manganese and food-related odors were tested on both *M. fortunata* and *P. elegans* to investigate potential dissimilar response profiles.

Chapter V deals with the use of the food-related odors and hydrothermal fluid chemical and thermal signature as orientation cues in vent shrimp. Several behavioral experiments were conducted at atmospheric pressure on *M. fortunata* and *P. elegans*, and at *in situ* pressure on *M. fortunata* and *R. exoculata*, to test attraction to food-related odors, sulfide and warm temperature.

Chapter VI presents first insights into the molecular basis of chemo- and thermodetection in vent shrimp. Identification and expression pattern within the chemosensory organs of a well conserved co-ionotropic receptor, IR25a, is conducted on four vent shrimp species and on *P. elegans*. Preliminary results of a transcriptome analysis of the chemosensory organs in the four vent shrimp species are also presented as they reveal several classes of chemo- and thermoreceptor candidates.

These chapters are followed by a conclusion integrating the main results from each chapter, and the perspectives for future researches. Thesis publications, communications list, the glossary[1] and the abbreviations are presented at the end of the manuscript.

[1] Scientific terms defined in the glossary are indicated at first use.

Chapter I

Sensing at depths: background

I. The deep hydrothermal environment

1. Formation of hydrothermal vents and fluid characteristics
2. Vent ecosystems and trophic networks

II. Vent shrimp lifestyle on Mid-Atlantic Ridge

1. Classification
2. Distributions and trophic behaviors
3. Physicochemical characteristics of the habitat and related adaptations
    - 3.1. Chemical environment
    - 3.2. Temperature
    - 3.3. Hydrostatic pressure
4. Dispersal and colonization processes
5. Sensory abilities
    - 5.1. Vision
    - 5.2. Chemodetection
    - 5.3. Other sensory modalities

III. Isobaric recovery and maintenance for *in vivo* studies of vent fauna

1. Isobaric recovery and transfer with PERISCOP and BALIST
2. Maintenance at *in situ* pressure in the IPOCAMP and VISIOCAMP aquaria
3. The AbyssBox project

IV. Chemo- and thermosensory mechanisms in marine crustaceans

1. Chemodetection
    - 1.1. Context
    - 1.2. Two chemosensory pathways
    - 1.3. Detection of chemicals
        - 1.3.1. Chemoreceptors
        - 1.3.2. Chemosensory sensilla and neurons
        - 1.3.3. Flicking of the antennules
    - 1.4. Central integration of the chemical stimulus
        - 1.4.1. Overview of the central nervous system
        - 1.4.2. First-order chemosensory centers
        - 1.4.3. Higher-order integrative centers
    - 1.5. Assumptions on olfactory abilities from comparative studies
2. Thermodetection

V. Models used in the present study

1. The vent species *Mirocaris forutnata*
    - 1.1. Selection criteria
    - 1.2. Distribution
    - 1.3. Gross morphology
    - 1.4. Trophic behavior
    - 1.5. Habitat and chemical and thermal environment
2. The shallow-water species *Palaemon elegans*
    - 2.1. Selection criteria
    - 2.2. Distribution, feeding habits and gross morphology

I. The deep hydrothermal environment

Hydrothermal vents and related fauna were first discovered off the coast of the Galapagos Islands in 1977 (Lonsdale 1977, Corliss et al. 1979). Further explorations have determined that hydrothermal vents occur in all oceans from shallow-waters to depths exceeding 5000 m (Beaulieu et al. 2013). They are mostly located in tectonic areas where active rifting occurs, such as the Mid-Atlantic Ridge (MAR), and on zones of subduction processes and local spreading (Figure 1). Over the 60 000 km of oceanic ridges, only hundreds of kilometers have been explored, so a large number of potential hydrothermal vents remains to be discovered (Beaulieu et al. 2015, Baker et al. 2016).

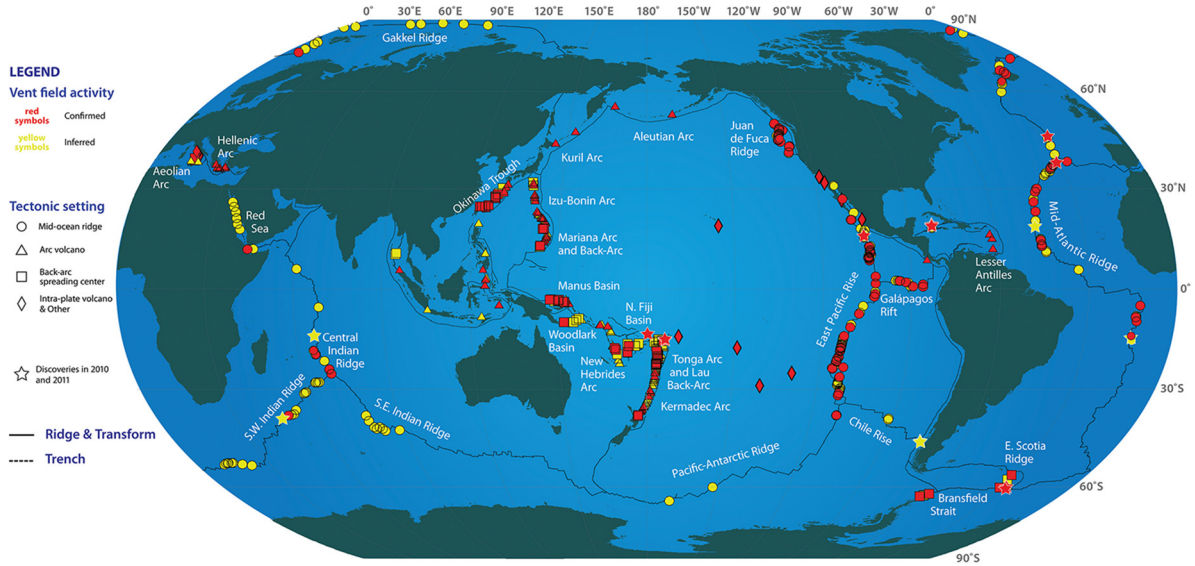

Figure 1 Global distribution of hydrothermal vents
From InterRidge Vents Database v.2.1.

(Credits: S. Beaulieu, K. Joyce, J. Cook and S.A. Soule / WHOI, InterRidge)

1. Formation of hydrothermal vents and fluid characteristics

Along oceanic ridges, hydrothermal vents are a consequence of the tectonic pressure that is exerted on the oceanic crust in rifting areas, where the upper mantle of the Earth is molted and ascend to form new crusts (Pomerol et al. 2005). Seawater infiltrates into the resulting cracks in the seafloor to 2 to 3 km depth and is warmed up to several hundreds of degrees near magmatic chambers (Edmond et al. 1982) (Figure 2). High temperature and hydrostatic pressure conditions trigger the ascent of the warmed seawater, which interacts with the surrounding crust and gets enriched in

various minerals and dissolved gases (Kelley et al. 2005, Charlou et al. 2002, 2010). This highly modified seawater is called hydrothermal fluid. Hydrothermal fluids vary in composition depending on the rock stratums encountered during the ascent, but they are commonly warm (up to 350°C), anoxic, acidic (pH from 2-4) and rich in gases (e.g. hydrogen sulfide, methane, hydrogen…) and metals (e.g. iron, zinc, copper…) (Jannasch and Mottl 1985, Johnson et al. 1986, Humphris et al. 1995, von Damm 1995, Charlou et al. 2010).

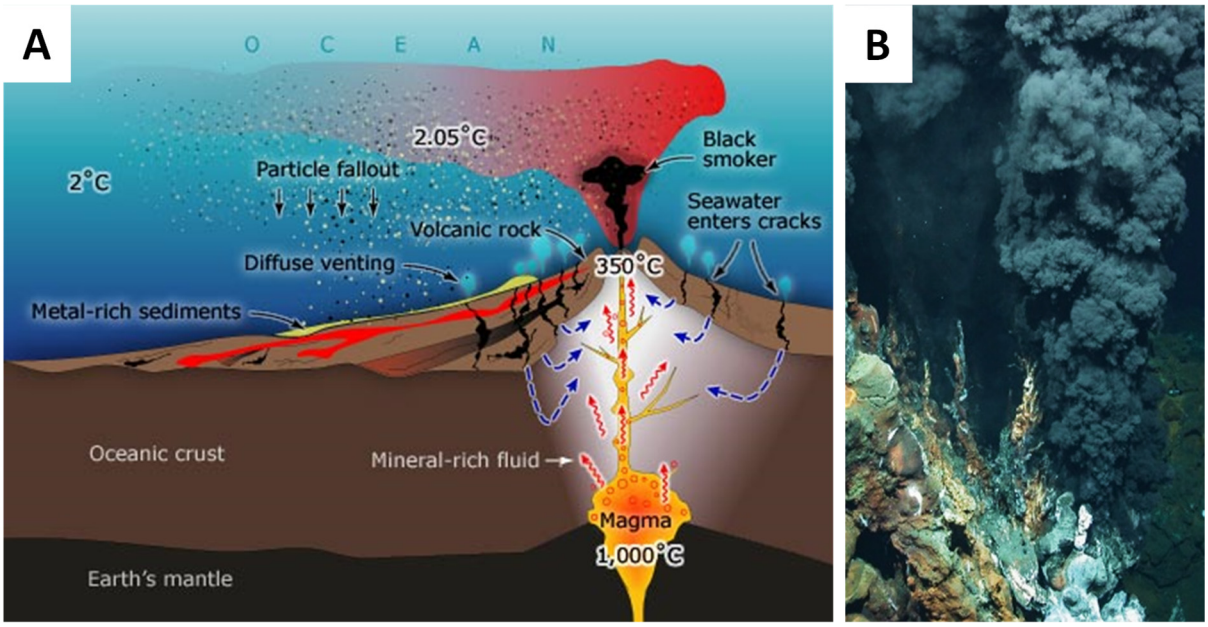

Figure 2 Formation of hydrothermal vents

A. Schematic description of hydrothermal vent functioning (Credits: GNS Science).
B. Black smoker from the Turtle Pits vent site on the Mid-Atlantic Ridge (Credits: University of Bremen, Center for Marine Environmental Research).

When expelled through fissures in the seafloor, the hydrothermal fluid is diluted with the cold and oxygenated surrounding seawater, which triggers mineral precipitation. These precipitations lead to the formation of chimneys and deposits of mineral particles around the vent fields (Figure 2A,B). The release of fluid also generates hydrothermal plumes(GLOSSARY) that raise in the water column, because of their high temperature which reduces the fluid density. While ascending and further mixing with seawater, the plume temperature decreases until reaching a neutral buoyancy stage that will spread horizontally. Around active chimneys, subsea-floor dilution of the hydrothermal fluid also occurs over areas up to several meters, and leads to diffuse vents where warm (5-60°C) fluids diffuse through seafloor and mineral deposits (Figure 2A) (Tunnicliffe et al. 1998). The duration of venting at one site depends on the speed of accretion of the ridge, from tens of years for fast ridges (e.g. East Pacific Rise) to thousands of years for slow ridges (e.g. MAR) (Rona et al. 1993, Lalou et al. 1995).

Table 1 presents the physicochemical characteristics of hydrothermal fluids from different vent sites at the MAR, for which the environmental conditions differ in relation with depths and subjacent rocks. The vent sites Trans Atlantic Geotraverse (TAG), Snake Pit, Lucky Strike and Menez Gwen occur on basaltic(GLOSSARY) substrata, from which emanate fluids rich in hydrogen sulfide but impoverished in methane and minerals such as copper and iron (Charlou et al. 2000, Douville et al. 2002). In contrast, the vent sites Rainbow and Logatchev are situated over ultramafic(GLOSSARY) rocks from which emanate fluids rich in methane and hydrogen, but impoverished in hydrogen sulfide (Charlou et al. 2002, 2010, Douville et al. 2002).

Table 1 Physicochemical characteristics of hydrothermal fluids from several vent sites at the Mid-Atlantic Ridge, compared to abyssal seawater

From Charlou et al. 2002, Schmidt et al. 2007 and references therein.

	Seawater	Menez Gwen	Lucky Strike	Snake Pit	TAG	Rainbow	Logatchev
Type		basaltic	basaltic	basaltic	basaltic	ultramafic	ultramafic
Depth (m)		850	1700		3670	2300	3000
Temp. (°C)	2	275-284	170-364	3050	290-321	365	347-352
pH (25°C)	7.8	4.2-4.3	3.5-3.7	3.7	3.1	2.8	3.3
$Si(OH)_4$ (mM)	<0.2	7.7-11.6	11.5-16.3		22	6.9	8.2
Cl (mM)	546	357-381	422-533	550	659	750	515
Br (µM)	838	666-710	735-924	-	880-1045	1178	818
SO_4 (mM)	28.2	0	0	-	0	0	0
Na (mM)	464	312-319	347-446	515	584	553	430
Li (µM)	26	238-274	278-357	835	411	340	245
K (mM)	9.8	22.1-23.8	21.1-26.7	23	18	20.4	21.9
Rb (µM)	1.3	20.3-29.4	22.7-39.1	-	10	36.9	27.7
Cs (nM)	2.3	330	200-280	170	110	333	385
Mg (mM)	53	0	0	0	0	0	0
Ca (mM)	10.2	29.7-33.1	31.3-38.2	11	26	66.6	27.3
Sr (µM)	87	100-111	67-19	54	99	200	138
Ba (µM)	0.14	>12	19268	-	<19	>67	>4.5
Fe (µM)	<0.001	<2-18	30-863	2400	1640	24050	2500
Mn (µM)	<0.001	59-71	84-446	400	1000	2250	330
Cu (µM)	0.007	0.6-3	46113	35	150	121-162	15-50
Zn (µM)	0.01	2.4-4.3	20941	53	46	115-185	25-30
Gases							
H_2S (mM)	0	<1.5	2.5-3	6	6.7	1.2	0.5-0.8
CO_2 (mM)	2.3	17-20	13-28	-	2.9-3.4	16	10.1
CH_4 (mM)	0.0003	1.35-2.63	0.5-0.97	-	0.124-0.147	2.5	2.1
Ar (µM)	16	11-38	11-30	-	20-40	-	12
N_2 (mM)	0.59	0.6-1.9	0.61-0.97	-	0.9-0.89	1.8	3
H_2 (mM)	0.0004	0.024-0.048	0.02-0.73	-	0.15-0.37	16	12

2. Vent ecosystems and trophic networks

Deep-sea hydrothermal vent ecosystems share characteristic forms of energy sources, assemblage structures, trophic relationships and environmental biotic and abiotic interactions (van Dover 2000). Vents are colonized by an extremely high biomass of macrofauna (500 to 1000 times superior to the biomass in abyssal plains [Fustec et al. 1988]), with approximately 70 % of species endemic to vents (Wolff 2005, Galkin and Sagalevich 2017). These communities are concentrated in the mixing zone of the hydrothermal fluid with the surrounding seawater. They are sustained by a microbial chemosynthetic primary production (Fisher et al. 2007). Chemoautotrophic bacteria use the energy produced by the oxidation of reduced compounds of the hydrothermal fluid (such as sulfide and methane) to fix inorganic carbon and produce organic matter (Jannash and Mottl 1985, Fisher 1990). These bacteria can be directly ingested by primary consumers, can grow on their body surface or be involved in endo- or ectosymbiosis relationships (Tunnicliffe et al. 1991, Segonzac et al. 1993).

Several vent species rely directly on hydrothermal fluid supplies because they depend on products from symbiotic chemoautotrophic bacteria as a source of energy, for instance: *Riftia pachyptila* (Vestimentifera) (Figure 3A), *Alvinella pompejana* (Annelid), *Alviniconcha* species and *Ifremeria nautilei* (Gasteropods) (Figure 3B), *Bathymodiolus* species (Bivalvia) (Figure 3C) and *Rimicaris* species (Crustacea) (Figure 3D) (Levin and Michener 2002, Bergquist et al. 2007, Le Bris and Duperron 2010, Govenar 2012, Govenar et al. 2015). Next, the primary consumers provide organic matter for predator and scavenger species (crab, fish, shrimp…) that do not rely directly on the chemosynthetic primary production (Tunnicliffe et al. 1991).

Vent communities differ widely among biogeographic regions (Figure 3) (Ramirez-LLodra et al. 2007). For instance, at vents in the Pacific Ocean, sessile Vestimentifera and Annelid are the dominant taxa, whereas the MAR communities are dominated by Bivalvia and vagile Alvinocarididae (Gebruk et al. 1997, Desbruyères et al. 2006). Different vents within a region support different assemblages of species, and within one vent the species composition and abundance vary between the top and the base of the chimneys (van Dover et al. 2018). These different patterns of distribution are likely determined by the physicochemical *preferendum* of each species (Tunnicliffe 1991, Sarrazin et al. 1997, Desbruyères et al. 2000).

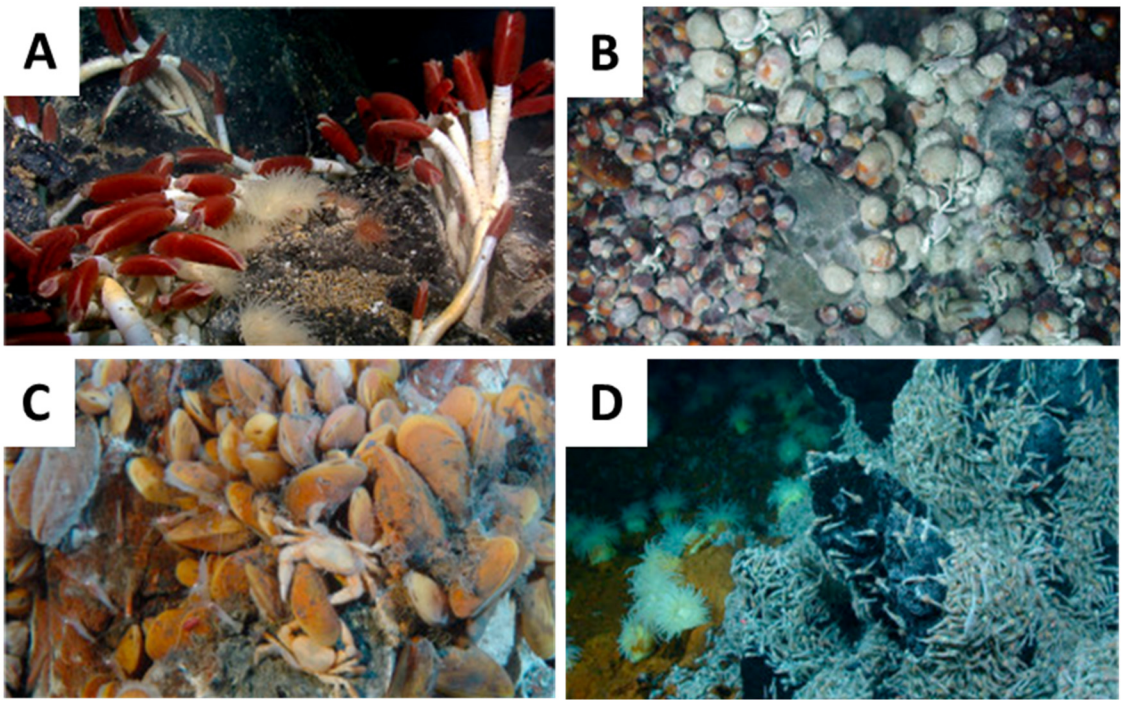

Figure 3 Examples of vent fauna communities from different locations
Modified from van Dover et al. 2018.

A. Giant tubeworms (*Riftia pachyptila*) with limpets and anemones at Galapagos spreading center, Eastern Pacific Ocean (Credits: Wikimedia).
B. Hairy (*Alviniconcha* spp.) and black (*Ifremeria nautilei*) snails with bythograeid crabs at Tu'I Malila vent field, Lau Basin, Western Pacific Ocean (Credits:WHOI).
C. Mussels (*Bathymodiolus azoricus*) with bythograeid crabs at the Lucky Strike vent field, Atlantic Ocean (Credits: Ifremer).
D. Swarming shrimps (*Rimicaris hybisae*) and anemones at Beebe vent, Mid-Cayman Rise, Caribbean Sea (Credits: WHOI).

II. Vent shrimp lifestyle on the Mid-Atlantic Ridge

1. Classification

Four shrimp species are widely distributed at vents from the Mid-Atlantic Ridge (MAR): *Rimicaris exoculata* (Williams and Rona 1986), *Rimicaris chacei* (Williams and Rona 1986) (*R. chacei* was later transferred to the genus *Chorocaris* [Martin and Hessler 1990], and recently reassigned to its original genus *Rimicaris* [Vereshchaka et al. 2015]), *Mirocaris fortunata* (Martin and Christiansen 1995) and *Alvinocaris markensis* (Williams 1988). They are all part of the Alvinocarididae family (Christoffersen 1986, Komai and Segonzac 2003) inside the Caridea infraorder (Li et al. 2011, Aznar-Cormano et al. 2015) (Figure 4A) among the Decapoda (Crustacea phylogeny is presented in Figure 11 and Figure 12). The phylogenetic relationships inside Alvinocarididae are still discussed but the genus are well defined (Vereshchaka et al. 2015) (Figure 4B).

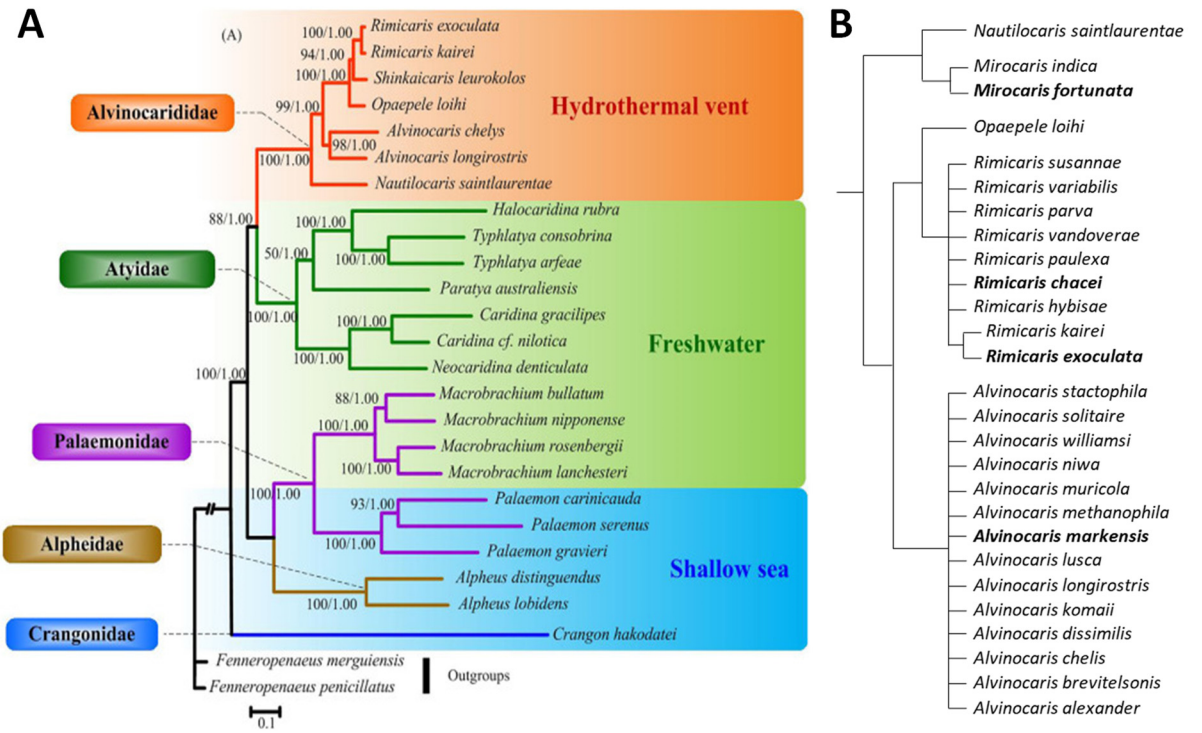

Figure 4 Position among Caridea and phylogeny of Alvinocarididae

A. Phylogenetic tree of the Caridea infraorder derived from Maximum Likehood and Bayesian analyses based on partitioned nucleotide sequences of 13 mitochondrial protein-coding genes; sequences from Dendrobranchiata species were used as an outgroup (from Sun et al. 2018).
B. Hypothetic phylogenetic tree of Alvinocarididae (modified from Vereshchaka et al. 2015). Species from the Mid-Atlantic Ridge used in the present study are indicated in bold.

2. Distributions and trophic behaviors

Vent shrimp species from the MAR exhibit different morphologies, behaviors and distribution patterns around active chimneys (Gebruk et al. 2000). They are presented separately hereafter.

R. exoculata (**Figure 5**A) is by far the most abundant shrimp species on the MAR sites (van Dover et al. 1988, Segonzac et al. 1993, Gebruk et al. 1997a, Desbruyères et al. 2001), except the shallowest ones (Lucky Strike, 1700 m depth and Menez Gwen, 850 m depth) (Gebruk et al. 2000, Pond et al. 2000). It forms very dense and motile swarms (1500 to 3000 individuals per square meter) on the walls of active chimneys (**Figure 5**A') (van Dover et al. 1988, Segonzac et al. 1993, Gebruk et al. 1997a, 2000). *R. exoculata* is a primary consumer that relies on the chemosynthetic primary production of symbiotic bacteria harvested in the cephalothorax. Indeed, this species presents a dense epibiotic community of chemoautotrophic bacteria in its gill chambers (Zbinden et al. 2004). These bacteria could oxide sulphide, iron, methane and hydrogen (Zbinden et al. 2008, Hügler et al. 2011), and there is a direct nutritional transfer of the organic matter from the epibionts to the host, by transtegumental absorption across the gill chamber integument (Ponsard et al. 2013). Hence, the strong attraction behavior to the hydrothermal fluid close suroundings observed in *R. exoculata* (Segonzac et al. 1993, Renninger et al. 1995) might be explained by its need to sustain its symbiotic bacterial community on which it relies for its nutritional supply.

R. chacei (Figure 5B) is much less abundant than *R. exoculata* (e.g. 200-300 ind./m² at the TAG site, Segonzac et al. 1993; less than 10 ind./m² at the Rainbow site, Desbruyères et al. 2001). It lives from the periphery of *R. exoculata* swarms to the surrounding areas of the chimneys, close to diffuse vents. This species also hosts bacteria in its gill chambers (Casanova et al. 1993, Apremont 2017), but in a less extent than *R. exoculata* (Apremont 2017). Hence, *R. chacei* relies both on chemoautotrophic production via its symbiotic bacteria and on classical food sources, being a predatory secondary consumer and scavenging on *R. exoculata* and other invertebrates (Segonzac et al. 1993, Gebruk et al. 2000).

➔

A. *Rimicaris exoculata* (Credits: P. Briand / Ifremer). **A'.** Swarm of *R. exoculata* around a black smoker (Credits: Ifremer, Victor 6000). **B.** *Rimicaris chacei* (Credits: L. Corbari / MNHN). **C.** *Mirocaris fortunata* (Credits: Océanopolis). **D.** *Alvinocaris markensis* (Credits: L. Corbari / MNHN). **D'.** *A. markensis* on *Bathymodiolus* mussels (Credits: NOAA Vent Program).
Scale bars = 1 cm.
Nb: all species feeding on bacterial mats are technically primary consumers, but in the present study we restrain primary consumers to those supplied in energy by symbiotic bacteria.

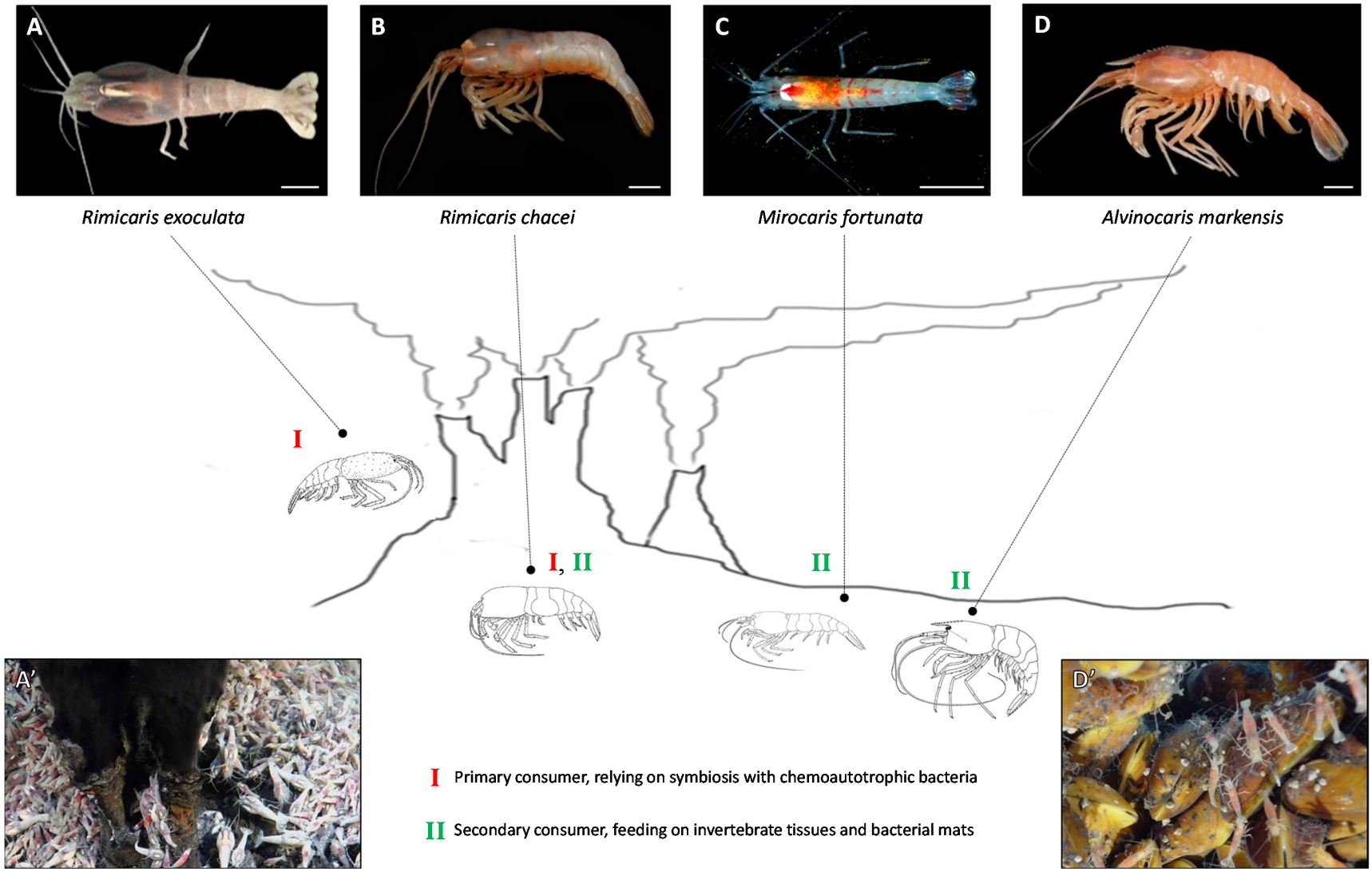

Figure 5 General distribution patterns and lifestyles of alvinocaridid shrimp species from Mid-Atlantic Ridge

Legend previous page.

A. markensis and *M. fortunata* (**Figure 5**C,D) are usually present in low abundances on the surrounding areas of the chimneys and on mussel assemblages (**Figure 5**D'). They are opportunist secondary consumers (Gebruk et al. 2000), necrophageous (Segonzac et al. 1993) and apparently do not rely on a symbiotic relationship with chemoautotrophic bacteria.

A transitional series has been proposed from the "*Alvinocaris-type*", closest in appearance to non-vent caridean shrimp, to the "*Rimicaris-type*", with *Mirocaris* falling between these two pairs, and *R. exoculata* being the most specialized species (Segonzac et al. 1993, Vereshchaka 1996a, Gebruk et al. 1997a). The authors proposed that this sequence reflects a pattern of increasing morphological adaptation and trophic specialization to the hydrothermal environment. This concept is also supported by the evolution of eyes in alvinocaridid shrimp (Gaten et al. 1998 and see section II.5.1.).

3. Physicochemical characteristics of the habitat and related adaptations

Table 2 *In situ* measurements of temperature, pH and chemical concentrations in habitats of Alvinocaridid shrimp from the Mid-Atlantic Ridge

Species	Site	Temp. (°C)	pH	S (µM)	CH_4 (µM)	Fe (µM)	Cu (µM)	References
R. exoculata	Rainbow	4.7-25	6.3-7.8	0.4-22	21.9	58-1470	0.14-320	Geret et al. 2002, Desbruyères et al. 2001, Schmidt et al. 2008
	TAG	2.8-17.4	6.8-8.1	0.5-77	0.1-5.7	2.8-140	-	Schmidt et al. 2008, Cathalot et al. 2018
	Snake Pit	5-37	7-7.4	1.3-8.5	-	3-34	-	Segonzac et al. 1993, Cathalot et al. 2018
R. chacei	Lucky Strike	6.5-7.49	6	18.7-38.31	-	1.22-3.53	0.25-1.62	Sarrazin et al 2015
M. fortunata	Rainbow	11.2	7.1	7.2	6.5	-	-	Desbruyères et al. 2001
	Lucky Strike	5.39-13.7	6.3-7.3	5.11-38.31	0.8	0.54-3.53	0.25-1.7	Sarrazin et al 2015, Desbruyères et al. 2001
A. markensis	Lucky Strike	6.5-8.79	6	18.7-40.07	-	1.22-5.25	0.25-0.46	Sarrazin et al 2015

As described earlier (see section I.1.), the chemical composition of the hydrothermal fluids from different sites along the MAR varies according to the nature of the underlying rock stratum. The vent shrimp are present on all sites along the MAR, hence their chemical environment is different at each site. At the scale of one site, fluid composition can also vary from one chimney to another (e.g. at the Lucky Strike site, Desbruyères et al. 2001). Next, the different positioning of the shrimp species around the active chimneys (**Figure 5**) implies that each species faces different thermal and chemical

conditions, in relation to the level of dilution of the hydrothermal fluid in their microhabitat. In addition, the hydrothermal habitat is characterized by an important temporal and spatial variability of abiotic conditions, since the continuous emission of hydrothermal fluid and its mixing with seawater creates steep gradients of temperature and chemical concentrations (Bates et al. 2010, Cuvelier et al. 2011, Sarrazin et al. 2015). However, *in situ* measurements of temperature, pH and chemicals concentrations can give an idea of the range values for these factors in the shrimp environments (Table 2).

3.1. Chemical environment

In the vent habitat, sulfides (H_2S, HS^- and S^{2-}) and dissolved metals (Fe, Cu, Zn, Pb…) can reach concentrations potentially toxic for animals. H_2S inhibits the cytochrome c oxidase and consequently blocks the production of ATP in the respiratory electron transport chain of mitochondria (Powell and Somero 1986). Sulfide concentrations of few micromolar are considered toxic for most animals (Smith and Gosselin 1979), but in basaltic vent sites sulfide concentrations can exceed 30 $\mu mol.L^{-1}$ in the vent shrimp microhabitats (Sarrazin et al. 2015, Cathalot et al. 2018). High concentrations of iron, copper and zinc have been measured in the gills and the digestive glands of *R.exoculata* and *M. fortunata*, superior to those of shallow-water species from polluted coastal environments (Geret et al. 2002, Kadar et al. 2007). Among the various protection mechanisms in vent animals (Grieshaber and Volkel 1998), the symbiotic bacteria were proposed to be involved in the detoxification of sulfide and metals (Alayse-Danet et al. 1987, Zbinden et al. 2004, 2008).

Because the pure hydrothermal fluid is anoxic, the mixing zone is furthermore characterized by low oxygen concentrations that add to the toxicity potential of the environment (Childress and Fisher 1992). To cope with the low availability of oxygen, vent crustacean hemocyanin presents a high affinity for O_2, superior to the one displayed by shallow-water species (Sanders et al. 1988, Lallier and Truchot 1997, Chausson et al. 2001, 2004).

3.2. Temperature

The dilution of the hot hydrothermal fluid (up to 350°C) in the cold surrounding seawater (2°C) creates abrupt temperature gradients around active chimneys. Such spatial and temporal variability makes the characterization of vent thermal environments difficult (Bates et al. 2010), but *in situ* measurements of temperature are informative on the level of dilution of the hydrothermal fluid in the seawater (Johnson et al. 1988a, Childress and Fisher 1992, Sarradin et al. 1998).

Temperature is considered as a major determinant of spatial distribution of vent species (Sarrazin et al. 1997, Lee 2003). *R. exoculata* lives close to chimney exits and consequently is frequently exposed to warm temperatures (>20°C), whereas the microhabitat of other shrimp species rarely exceeds 10°C. *In vivo* experiments at *in situ* pressure revealed that the critical thermal temperature is 38±2 °C for *R. exoculata* (Ravaux et al. 2003, Shillito et al. 2006) and 36±1 °C for *M. fortunata* (Shillito et al. 2006). These species are hence not functionally adapted to high temperatures but might present other adaptations to cope with steep thermal variations, such as behavioral responses (e.g. low avoidance threshold) or molecular adaptations (Ravaux et al. 2003).

3.3. Hydrostatic pressure

Vent shrimp can handle hydrostatic pressure up to 400 bars at the deepest MAR sites (Ashadze, 4000 m depth). Restoring the natural pressure is essential for the long-term maintenance of most vent animals in a good physiological state (Childress and Fisher 1992, Shillito et al. 2004, 2006, 2008). Pressure impacts biological systems in several ways, for example by modifying cellular volumes, molecular interactions, chemical reaction kinetics and gene expression patterns (Somero 1992b, Pradillon and Gaill 2007, Mestre et al. 2009, Pradillon 2012). Evidence of a large range of tolerance to pressure in the vent crab *Bythograea thermydron* (Mickel and Childress 1982, Airries and Childress 1994) suggests that vent species might present homeoviscous adaptations(GLOSSARY) of their cellular membranes.

4. Dispersal and colonization processes

Due to the ephemeral nature of hydrothermal vents, vent communities face risks of local extinction and must have developed propagation strategies in the course of evolution. Because adults and juveniles vent shrimp need to stay close to active vents to find food or to supplement their symbiotic bacteria in reduced compounds, their migratory capacity is limited (Ponsard et al. 2013, Teixeira et al. 2013). It is hypothesized that dispersion and colonization processes are performed at larval stages and/or post-larval stages (Herring and Dixon 1998). In Alvinocarididae, the first larval stage (Zoe I) (Figure 6A) is lecithotrophic(GLOSSARY), with an important storage of lipids (Pond et al. 1997) and poorly developed mouthparts (Hernandez-Avila et al. 2015). This stage is likely followed by a stage feeding on particles of photosynthetic origin that sink in the aphotic zone (Cowen et al. 2001), which could extend the stage duration and accordingly confer a high dispersal potential (Hernandez-Avila et al. 2015).

Over the MAR, strong convection currents near active vents might transport the larvae at the level of the buoyant plume, at 200-300 m over the seafloor, and horizontal transport might be driven by currents constrained in the axis of the ridge (Kim et al. 1994). The mechanisms that could be used by the larvae to detect an active site to settle are unknown. However, the high abundance of shrimp along the MAR and the evidence of a large-scale connectivity between sites (Teixeira et al. 2012, 2013) indicate that vent shrimp are successful colonizers. Larval settlement may be driven by numerous factors, such as co-specific odors, vibration, or chemical cues (Rittschof et al. 1998). For the latter, Renninger and collaborators (1995) and Rittschof and collaborators (1998) proposed sulphide as a settlement cue, and Cuomo and collaborators (1985) reported attraction to gels containing sulfide on larvae of vent polychaete worms during *in situ* experiments. Chemosensory abilities of vent shrimp larvae are unknown, but they possess olfactory aesthetasc[(GLOSSARY)] sensilla on their antennules (Figure 6B) and numerous sensilla[(GLOSSARY)] on the antennae (Figure 6C) (Hernandez-Avilla et al. 2015) for which sensory functions could be hypothesized with an ultrastructural analysis.

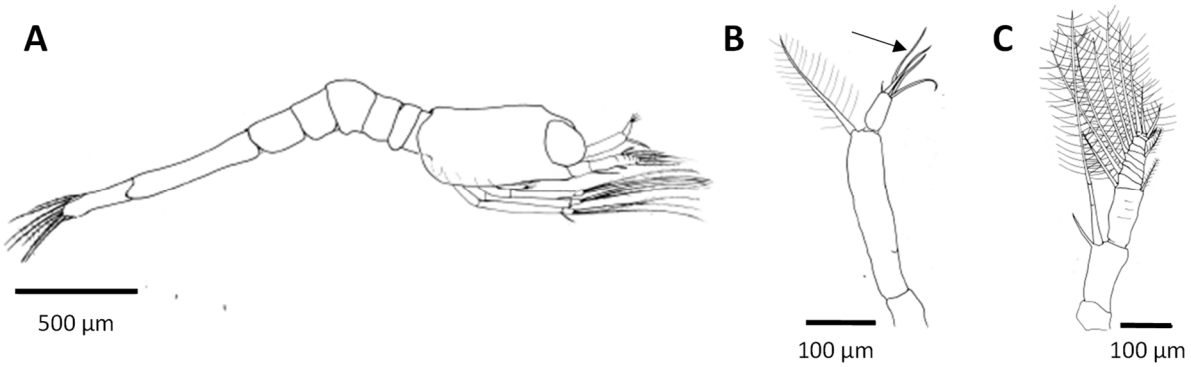

Figure 6 First larval stage of *Mirocaris fortunata*
Modified from Hernandez-Avila et al. 2015.

A. Right view. **B.** Antennule. Arrow, aesthetasc. **C.** Antenna.

5. Sensory abilities

As pointed out by Segonzac et al. (1993), the long-term occurrence of vent shrimp in the fairly hostile hydrothermal environment must have been run in parallel to an evolution of the sensory abilities to efficiently detect their habitat, from short- and long-distance, and to locate food sources. Among the sensory modalities that could be involved in the detection of active vents, vision has received the most attention since the eyes of vent shrimp are highly modified. Other senses have been considered although not thoroughly investigated.

5.1. Vision

The anatomy of the visual system of Alvinocarididae species from the MAR has been extensively described (van Dover et al. 1989, O'Neill et al. 1995, Nuckley et al. 1996, Lakin et al. 1997, Gaten et al. 1998a,b, Chamberlain et al. 2000). It was proposed that they possess highly sensitive "eyes" adapted to perceive the radiation emitted by the very hot fluid (thermal radiation), which may be a signal for vent shrimp to locate and/or avoid heat sources (Pelli and Chamberlain 1989, van Dover et al. 1989, O'Neill et al. 1995, Nuckley et al. 1996).

In *R. exoculata*, van Dover et al. (1989) noticed that the pink organs beneath the dorsal carapace (Figure 7B) were connected to the brain in a position similar to the optic nerves in shallow-water species. Transverse sections of these organs revealed that they are actually highly modified retina, for which the general anatomy is similar between *R. exoculata*, *R. chacei* and *M. fortunata* (Figure 7A). These species lack crystalline cones, which focus the light to the photoreceptor units and consequently allow the formation of images. The rhabdoms, which are organelles that receive the light and transfer it to the retinal cells, are hypertrophied in *R. exoculata*, *R. chacei* and *M. fortunata*, but poorly developed *in A. markensis* which may be totally blind (Lakin et al. 1997). A white tapetum underlies the rhabdoms and might have a reflective function to maximize the absorption of light. The number of pigments (identified as rhodopsin [van Dover et al. 1989], a common photosensitive pigment in Arthropods) is higher in vent shrimps compared to shallow-water species (Nuckley et al. 1996). Altogether these transformations reduce the spatial resolution but greatly enhance the sensitivity of the retina. The effective use of vision in vent shrimp is further supported by the presence of optic neuropils(GLOSSARY) in the brain (Charmantier-Daures and Segonzac 1998).

Gaten et al. (1998a) highlighted a gradual transformation of the eyes in vent shrimp (Figure 7C), supporting the evolution sequence theory from the most epibenthic-like shrimp *Alvinocaris* to the specialized *Rimicaris*. In an ancestral deep-sea shrimp, similar to a shallow-water shrimp, the eyes are stalked and the brain optic neuropils are located in the eyestalks. In *A. markensis*, the eyestalks are reduced and the optic neuropils have migrated on the posterior side of the brain. In *M. fortunata* (Figure 7D) and *R. chacei*, the retina expends on the dorsal side. In *R. exoculata* the anterior eye disappears while the dorsal eye is enlarged. In addition, this latter species exhibits the highest volume density of rhabdoms (Gaten et al. 1998b).

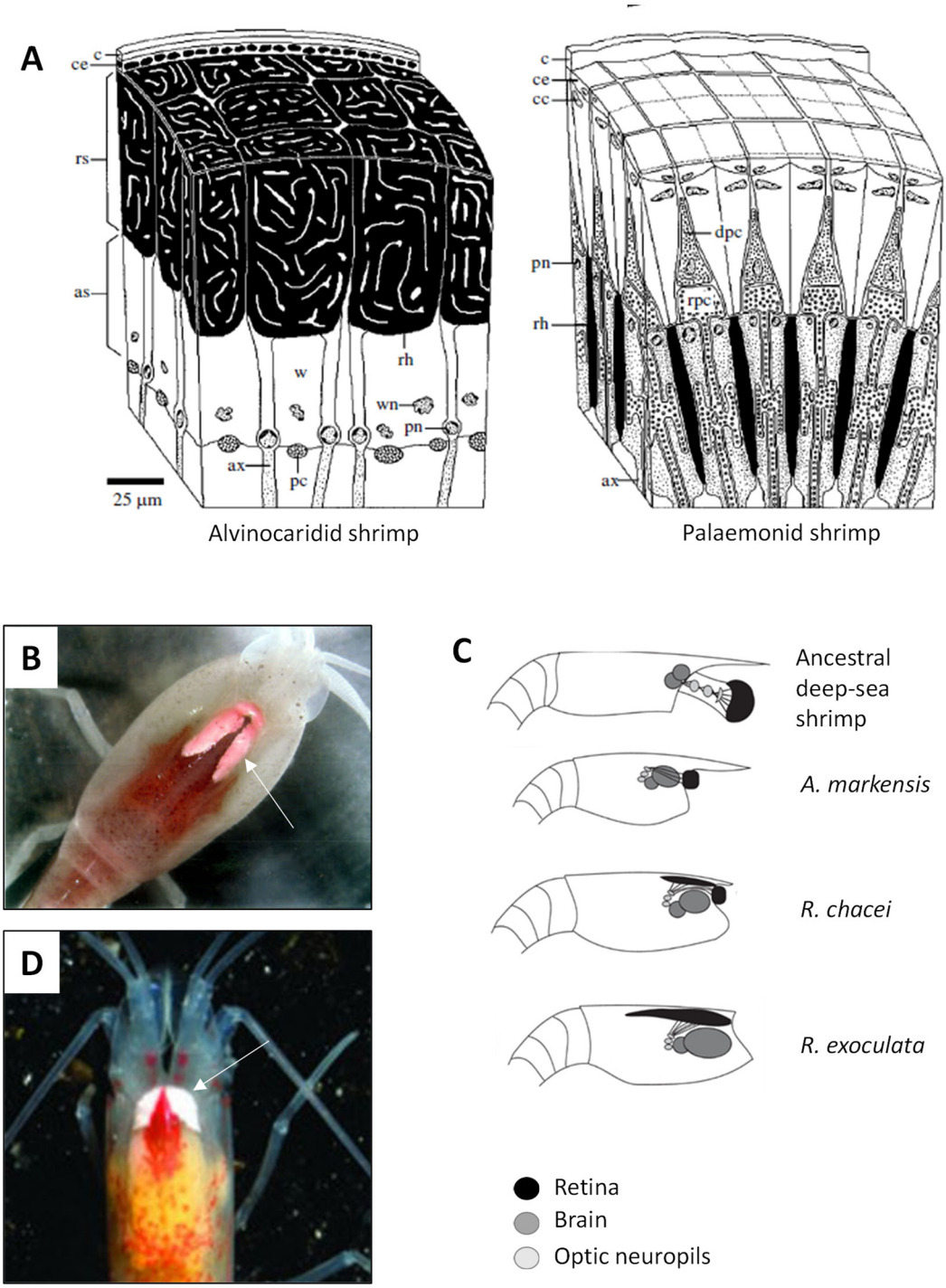

Figure 7 The "eyes" of Alvinocaridid shrimp

A. Diagram of the typical cellular organization of the retina of an Alvinocaridid shrimp (adapted for photodetection in very dim light) compared with that of a shallow-water Palaemonid shrimp (adapted for pattern vision in daylight) (from Chamberlain 2000). as, arhabdomeral segment; ax, photoreceptor axon; c, cornea; cc, cone cell; ce, corneal epidermis; dpc, distal pigment cell; pc, screening pigment cell; pn, photoreceptor nucleus; rh, rhabdom; rpc, reflecting pigment cell; rs, rhabdomeral segment; w, white diffusing cell; wn, nucleus of white diffusing cell.

B. Dorsal view of *R. exoculata*. The arrow indicates the retina (Credits: Wikimedia).

C. Schematic diagram showing the evolution of the dorsal eye of *Rimicaris* from the stalked compound eye of an ancestral deep-sea shrimp (modified from Gaten et al. 1998a).

D. Dorsal view of *M. fortunata*. The arrow indicates the retina (Credits: Océanopolis).

The hypothesis of thermal radiation detection by vent shrimp was first supported by the observation of a very dim light at chimney exits with a wavelength of 450 to 550 nm, which fits to the absorbance spectrum of the rhodopsin, the pigment identified in the retina of *R. exoculata* (van Dover et al. 1989). However, Segonzac et al. (1993) reminded that temperature rapidly decreases when the fluid dilutes in the seawater (from 300°C in the chimney to 35°C 20 cm over the chimney exit) and so does the radiation intensity, and that the distance of effective visual detection is reduced by the light attenuation in seawater. The visual sense of vent shrimp as proposed by van Dover et al. (1989) is thus likely to fit only for a very short distance detection (likely less than one meter) of the hot fluid at the chimney exits.

Recently, Phillips et al. (2016) suggested from *in situ* video footages that vent shrimp may produce bioluminescent light, and that their visual system may hence allow the detection of this bioluminescence. Although the existence of this bioluminescence signal is speculative for now, the persistence of the visual system in vent shrimp and the hypertrophy of the rhabdoms definitely allow the detection of any low-intensity light signals in the vent habitat.

5.2. Chemodetection

Localization of vents by chemotaxis has been considered for both short- (few meters) and long-distance (tens of meters) detection. Sulfide, as an obvious signature for hydrothermal habitats, has been proposed as a settlement cue (Rittschof et al. 1998). Renninger and collaborators (1995) demonstrated that *R. exoculata* can detect sulfide via its antennae and reported observations suggesting attraction to sulfide. The authors used for comparison a shallow-water species (*Penaeus aztecus*) for which they recorded antennal responses to the basic pH of the sulfide solutions rather than sulfide itself. They concluded that the sulfide response they found in *R. exoculata* might be an adaptation of a widespread sulfide sensitivity in vent shrimp to the vent environment.

Nonetheless, sulfide rapidly disappears in the water column since it reacts with seawater, other fluid constituents and chemoautotrophic bacteria (Mottl and McConachy 1990, Zhang and Millero 1993), and is thus likely to be detectable only close (few meters) to the fluid emissions. In contrast, methane (Charlou and Donval 1993, de Angelis et al. 1993), iron (German et al. 1993, Waeles et al. 2017) and manganese (Aumond 2013) can disperse far (up to several kilometers) in the hydrothermal plumes. Methane and iron have been proposed as other potential attractants for vent shrimp (Segonzac et al. 1993, Renninger et al. 1995) but there is to date no experimental evidence of their detection by vent animals.

5.3. Other sensory modalities

Segonzac et al. (1993) proposed several additional hypotheses for the mechanisms that could permit the orientation of vent shrimp in their habitat:

- Vent shrimp could detect thermal gradients occurring around active chimneys and use them as an orientation cue. The authors reported *in situ* observations of shrimp that abruptly swim downwards when encountering ascending warm fluid. More recently, attraction to higher temperature (11°C in a 3°C seawater background) was demonstrated in *R. exoculata* (Ravaux et al. 2009). Temperature could also be considered as a long-distance stimulus, since temperature anomalies of one tenth degree occur in the spreading hydrothermal plumes (Baker et al. 2016, Tao et al. 2017), which could fit to the thermosensitivity of crustaceans (Jury and Watson 2000).
- Vent shrimp could detect the acoustic vibrations triggered by the continuous emission of hydrothermal fluid. This “hearing” hypothesis is worth considering since crustaceans possess antennal mechanoreceptors that are sensitive to hydrodynamic stimuli (Bleckman 1991, Lovell et al. 2005, Tidau and Briffa 2016), and the acoustic signal of active vents might be slightly superior to the sea background noise (Little 1988).
- Vent shrimp could memorize the vents topography by recording spatial microvariations of the local magnetic field. Interestingly, the rhodopsin visual pigment identified in vent shrimp retina is also sensitive to magnetic stimuli in migratory birds (Semm and Beason 1990).

III. Isobaric recovery and maintenance for *in vivo* studies of vent fauna

The knowledge on the biology and ecology of deep vent fauna is limited by difficult and costly access to the hydrothermal environment for scientific research. In addition, deep animals must cope with an important and eventually lethal stress due to the decompression effects during sampling by submersible (Childress et al. 1978), especially from depths exceeding 2000 m (Shillito et al. 2008). Although *in situ* observations can be conducted (e.g. Bailey et al. 2007, Sarrazin et al. 2007, Cuvelier et al. 2009), laboratory studies on live animals are more suitable to investigate physiology issues under controlled conditions (Van Dover and Lutz 2004, Pradillon and Gaill 2007, Shillito et al. 2008, 2014).

Despite the constraints associated to sampling from depths, it is possible to maintain vent animals alive at the surface with devices that keep or restore the *in situ* pressure. The development of isobaric recovery devices now allows *in vivo* experiments with organisms that would not survive the trauma of decompression, by minimizing the physical stress associated to sampling and by significantly enhancing survival rates (Le Bris and Gaill 2007, Pradillon and Gaill 2007, Shillito et al. 2008). Pressurized aquaria allow the maintenance of deep live specimens under controlled conditions, for instance for direct observations or to investigate physiological and behavioral responses to environmental perturbations (Pradillon et al. 2004, Kadar and Powell 2006, Miyake et al. 2007, Shillito et al. 2014).

1. Isobaric recovery and transfer with PERISCOP and BALIST

The PERISCOP (Projet d'Enceinte de Récupération Isobare Servant à la Collecte d'Organismes Profonds) (Shillito et al. 2008) device allows the recovery of deep animals at their *in situ* pressure, to bring the specimens to the surface in a good physiological state. The system is composed of a stainless-steel pressurized recovery device (Figure 8A,B) with an internal volume of 6.6 L, and an *in situ* PVC sampling cell ("Periscopette", Figure 8B). Once the fauna has been confined inside the sampling cell (with the suction device of the submersible), the latter is stored inside the pressurized recovery device (Figure 8B) which is then sealed. To maintain the pressure prevailing inside the cell (which can be reduced by 30% during ascent by the metal expansion), the system also comprises a pressure compensation unit (Figure 8A) which minimizes the pressure loss to 15%.

The PERISCOP aperture is adapted to connect to an 8-L ship-based aquarium, BALIST (Biology of Alvinella Isobaric Sampling and Transfer), which allows the transfer of freshly caught animals without decompression and direct observation through a porthole (Figure 8C). BALIST can function at up to 300 bars, from 2 to 100 °C with a continuous renew of the seawater.

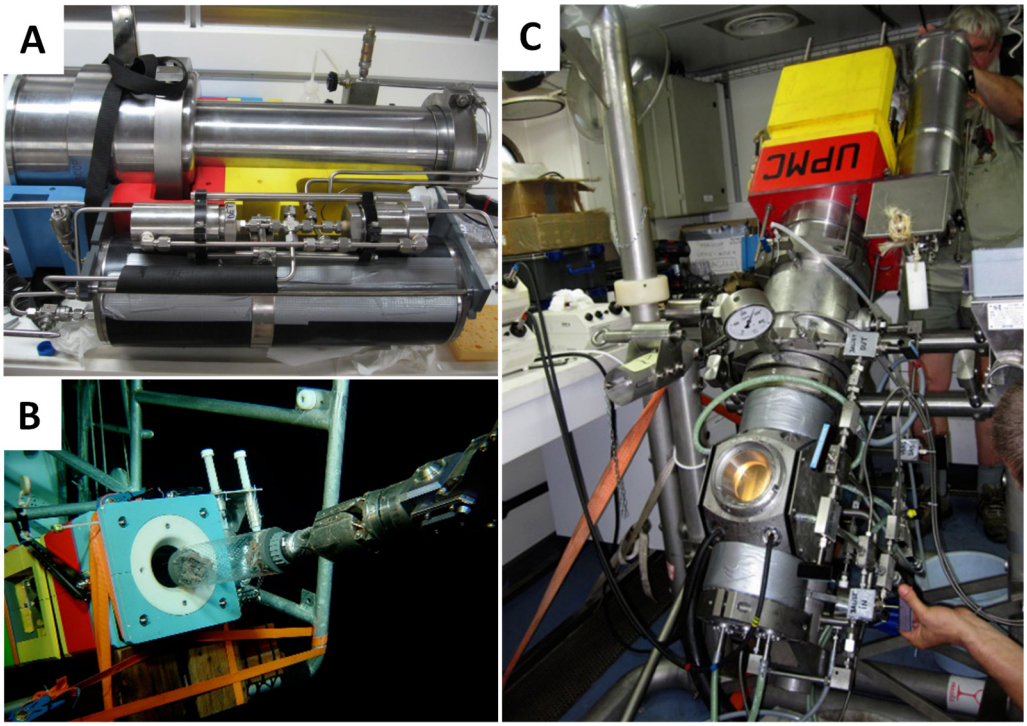

Figure 8 The isobaric recovery device PERISCOP and the pressure aquarium BALIST

A. Isobaric recovery device PERISCOP with its pressure compensator (foreground) (Credits: G. Hamel).
B. Remotely operated arm inserting the Periscopette sampling cell inside the PERISCOP device (Credits: Ifremer).
C. Isobaric transfer from the PERISCOP to the pressure aquarium BALIST (Credits: AMEX).

2. Maintenance at *in situ* pressure in the IPOCAMP and VISIOCAMP aquaria

The IPOCAMP™ (Incubateur Pressurisé pour l'Observation et la Culture d'Animaux Marins Profonds) (Shillito et al., 2014) aquarium allows to maintain vent fauna in a 18-L volume, at up to 300 bars, in close or open (20 L/h) circuit, ship-board or in a laboratory (

Figure 9A). The animal behavior can be video recorded with an endoscope through a small porthole (

Figure 9B). This device was used for several studies on deep sea animals, including on their thermal biology (Ravaux et al. 2003, Cottin et al. 2010), their osmoregulatory (Martinez et al. 2001) and respiratory (Chausson et al. 2004) adaptations, larval development (Pradillon et al. 2001, 2005), symbiotic relationships (De Cian et al. 2003, Zbinden et al. 2008, Ponsard et al. 2013, Duperron and Gros 2016), exotoxicology (Dixon et al. 2002, Company et al. 2004, 2006, Auguste et al. 2016) and pressure tolerance of non-vent species (Thatje et al. 2010, Oliphant et al. 2011).

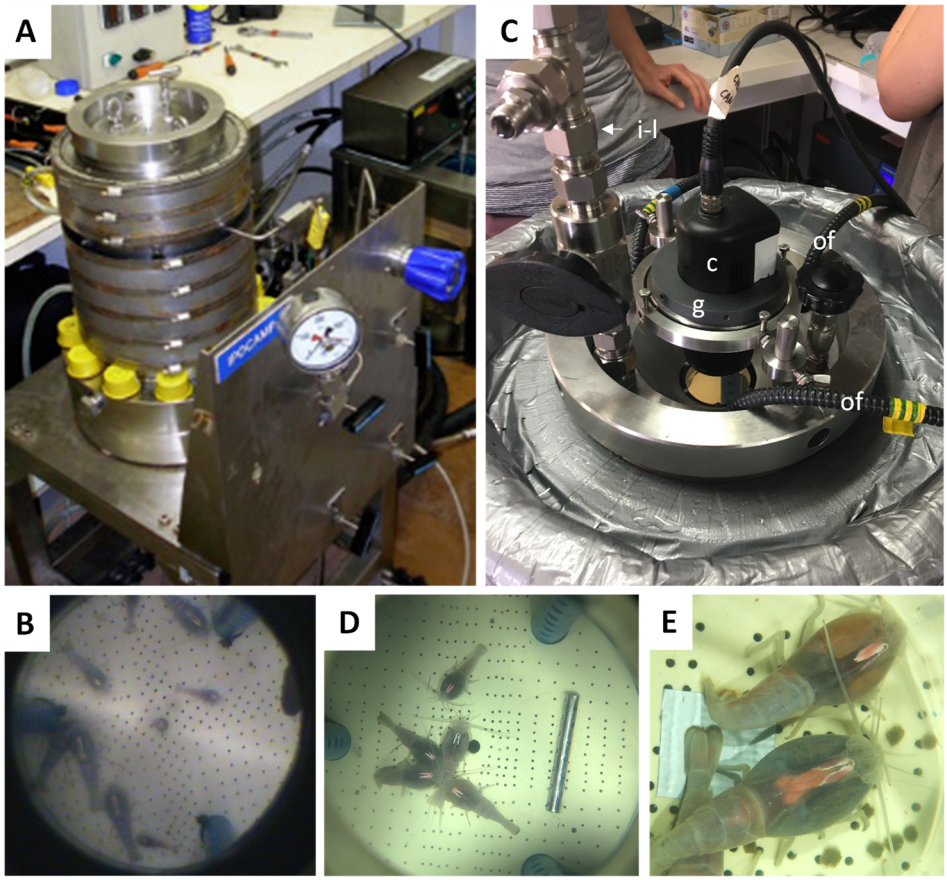

Figure 9 The pressure incubators IPOCAMP and VISIOCAMP

A. View of the 18 L IPOCAMP aquarium which allows to maintain vent animals at pressures up to 300 bars. The animal behavior can be recorded with an endoscope (**B**).
C. View of the lid of the VISIOCAMP aquarium which allows high quality video recordings of animal behavior (**D**) at several magnifications (**E**), as well as introduction of small elements (e.g. food) through an isobaric line.
c, camera; g, gyroscopic support for the camera; i-l, isobaric line; of, optical fibers.
(Credits: B. Shillito / AMEX).

VISIOCAMP is a recently upgraded IPOCAMP™, with a new lid that comprises a large porthole to allow direct observation as well as video recording with a high definition camera, which greatly enhances the image quality compared to an endoscope (

Figure 9C,D,E). In addition, the lid is equipped with an isobaric line that allows the introduction of small elements (e.g. food, stimulus) without disrupting the pressure inside the aquarium.

3. The AbyssBox project

The AbyssBox project is a collaboration between the AMEX team, the Ifremer and the Oceanopolis public aquarium (Brest, France), aiming to the long-term maintenance and the public exhibition of deep-sea hydrothermal fauna (Shillito et al. 2015). Since 2012, specimens of the vent shrimp *M. fortunata* and the vent crab *Segonzac mesatlantica* are maintained alive at their *in situ* pressure (180 bars, corresponding to the pressure at the Lucky Strike vent site) in the AbyssBox aquarium, as a part of a permanent public exhibition. AbyssBox (Figure 10A) is a pressurized 16.5 L aquarium designed to function permanently, with a flow-through system which circulates fresh seawater (background temperature 10°C), an isobaric feeding line (Figure 10B), a large conical viewport (Figure 10C) and a ring-shaped tube inside which circulates heated fluid (27°C) to create a "hotspot" for the animals (Figure 10C) with respect to the background temperature. The exhibition is sustained by a yearly sampling of specimens at the Lucky Strike vent site during the MOMARSAT cruises operated by the Ifremer.

The AbyssBox is also available to the scientific community. It provides one of the most useful tools for long-term maintenance and observation of vent species in conditions close to their natural habitat, giving information on lifespan (Shillito et al. 2015) or intra- and interspecies interactions (Matabos et al. 2015). Potential researches could also include studies of reproduction, larval development, responses and adaptations to heavy metal exposition, homeoviscous adaptations…

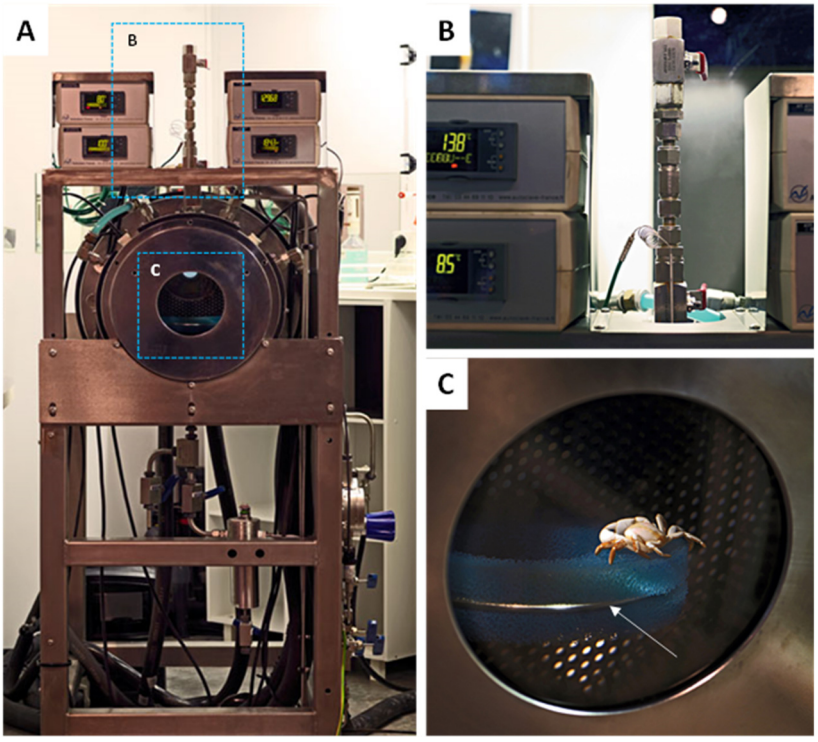

Figure 10 The pressure AbyssBox aquarium

A. Frontal view of the AbyssBox at the Oceanopolis public aquarium (Brest, France).
B. Isobaric line used to feed the animals without disrupting the pressure inside the aquarium.
C. View through the viewport of the AbyssBox. A crab *Segonzac mesatlantica* rests close to the warm spot (arrow) of the aquarium.
(Credits: V. Fournier)

IV. Chemo- and thermosensory mechanisms in marine crustaceans

In this section (and in the other chapters), the cited literature refers to various crustacean species. For better clarity, Crustacea classification is briefly presented hereafter.

Crustacea comprises almost 67 000 described species and forms a large and diverse arthropod taxon which includes animals as crab, lobster, crayfish and shrimp. Molecular studies showed that the crustacean group is paraphyletic: it comprises all animals other than hexapods in the Pancrustacea clade (Regier et al. 2010) (Figure 11). Phylogenetic relationships are still discussed, but the Remipedia and the Branchiopoda are more closely related to the Hexapoda than they are to Copepoda and Malacostraca.

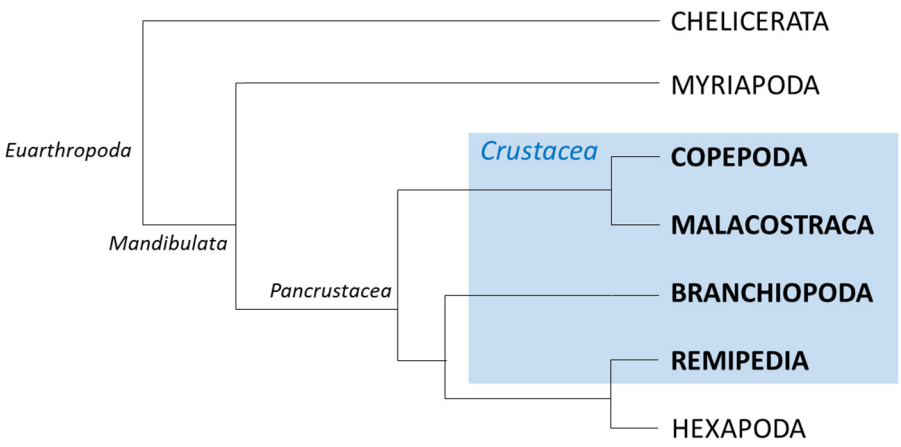

Figure 11 Classification of Crustacea among Euarthropoda

Simplified phylogeny of one hypothesis on the classification of Crustacea among Euarthropoda.

Remipedia is a class of blind crustaceans that live in coastal caves. Branchiopoda comprises several genera found in coastal regions, continental freshwater and salt lakes, and notably the model species *Daphnia pulex* which is the first crustacean to have its genome sequenced (Cristescu et al. 2006). Copepoda is a group of small crustaceans found in the sea and nearly every freshwater habitats. Malacostraca is the largest class of crustaceans, comprising about 40 000 living species that display a great diversity of body forms, are abundant in all marine environments and have colonized freshwater and terrestrial habitats. Among Malacostraca, Alvinocaridid vent shrimp are part of the Caridea, which is a basal taxon of the Decapoda order (Figure 12).

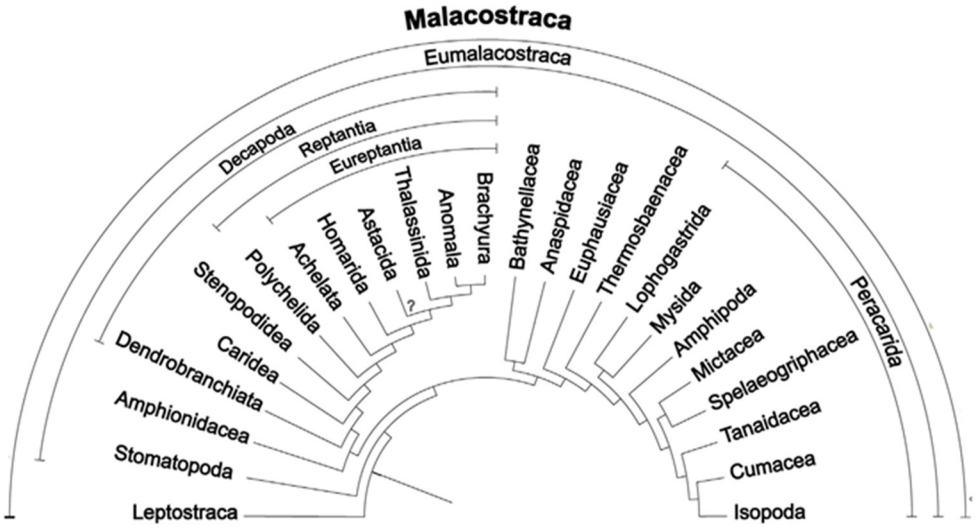

Figure 12 Phylogenetic relationships of malacostracan crustaceans
From Harzsch and Krieger 2018 (and references therein)

1. Chemodetection

Most functional studies on the chemosensory abilities of crustaceans focus on large Eureptantia decapod crustaceans (Figure 12) (Ache 2002, Schmidt and Mellon 2011, Derby and Weissburg 2014), including representatives of spiny lobster (Achelata), clawed lobster (Homarida), crayfish (Astacida) and crab (Brachyura). Chemodetection has also been explored in terms of diversity of lifestyles, habitats and morphology in other crustacean representatives such as hermit crab (Anomala), mantis shrimp (Stomatopoda), penaeid shrimp (Dendrobranchiata), amphipod and isopod (Peracarida). In contrast, studies on Caridea, which include Alvinocaridid vent shrimp, are scarce. Still, the following sections describe general chemosensory mechanisms believed to be common to all marine malacostracan, and possibly to all marine crustaceans. Adaptations linked to the colonization of freshwater and terrestrial habitats are not presented.

1.1. Context

For most crustaceans, chemodetection* is the dominant sensory modality (Schmidt and Mellon 2011). Marine crustaceans are surrounded by chemicals, and use their chemosensory senses for diverse biological processes, such as the detection and selection of food and habitat (Koehl 2011, Kamio and Derby 2017), the recognition of conspecifics (Thiel and Breithaup 2011), the localization of sexual partners (Wyatt 2014), and the detection of preys and predators (Derby and Zimmer 2012).

Chemodetection* is mediated by chemosensory sensilla present on all the body surface but particularly concentrated on chemosensory organs such as the antennules, the antennae, the mouthparts and the walking legs. The antennules (which comprises two flagella, one lateral and one medial) and the antennae (Figure 13) are considered as major sensory organs in crustaceans. The sensilla are innervated by chemosensory neurons that bear chemoreceptors on their dendrites. The binding of a chemical stimulus to its cognate chemoreceptor triggers a cascade of electrical and chemical events from the chemosensory neurons to the chemosensory centers within the brain, where the signal is processed and integrated.

*In the literature, chemosensory mechanisms are usually designed as “chemoreception”, with “chemoreceptive” organs, “chemoreceptive” sensilla, “chemoreceptor” neurons… Because of the confusion with the molecular chemoreceptors, I chose to use the terms “chemodetection” and “chemosensory […]” instead.

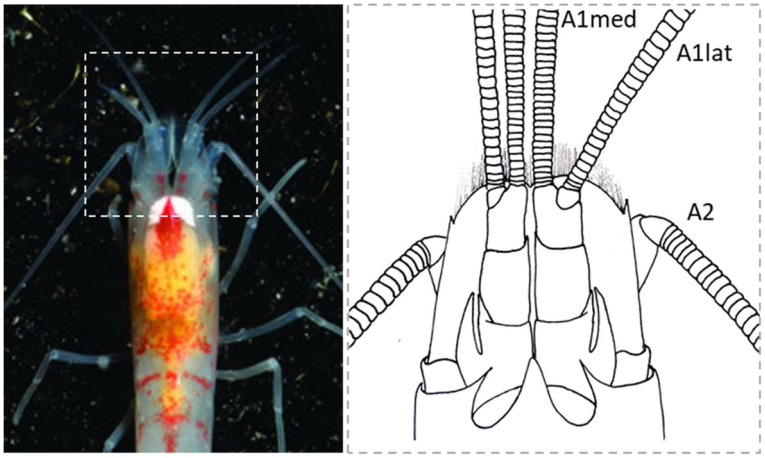

Figure 13 The antennules and the antennae

The antennules and the antennae are flagella composed of several annuli, associated to various sensory sensilla. A1lat, lateral antennule; A1 med, medial antennule; A2, antenna. (*M. fortunata*, credits: Océanopolis)

1.2. Two chemosensory pathways

Two different modes of chemodetection, linked to distinct chemosensory pathways, are processed by crustaceans: « olfaction(GLOSSARY) » and « distributed chemodetection(GLOSSARY) » (Schmidt and Mellon 2011, Derby and Weissburg 2014, Derby et al. 2016, Harzsch and Krieger 2018).

Olfaction, also called distance chemodetection, is mediated by the aesthetasc sensilla present only on the lateral flagella of the antennules (Figure 14A,B) and which detect soluble molecules (water-borne odors). These aesthetascs are innervated by olfactory sensory neurons(GLOSSARY) (OSNs) (see 1.3.) that project to the olfactory lobes(GLOSSARY) in the deutocerebrum region of the brain (see 1.4.).

Distributed chemodetection is mediated by bimodal[(GLOSSARY)] chemo- and mechanosensory sensilla present on the antennules and the antennae, and also on the mouthparts (Garm and Watling 2013), the walking legs (Schmidt and Gnatzy 1984) and the body surface (Figure 14A,B). Bimodal sensilla on the antennules project to the lateral antennular neuropils[(GLOSSARY)] in the deutocerebrum region of the brain, and those on the antennae project to the antennal neuropils[(GLOSSARY)] in the tritocerebrum region (see 1.4.). Their chemosensory neurons may primarily function as contact chemo-mechanoreceptors (e.g. for taste; Mellon 2012, 2014) but certain types of bimodal sensilla may also function as distance chemoreceptors (Steullet et al. 2001, 2002, Schmidt and Mellon 2011).

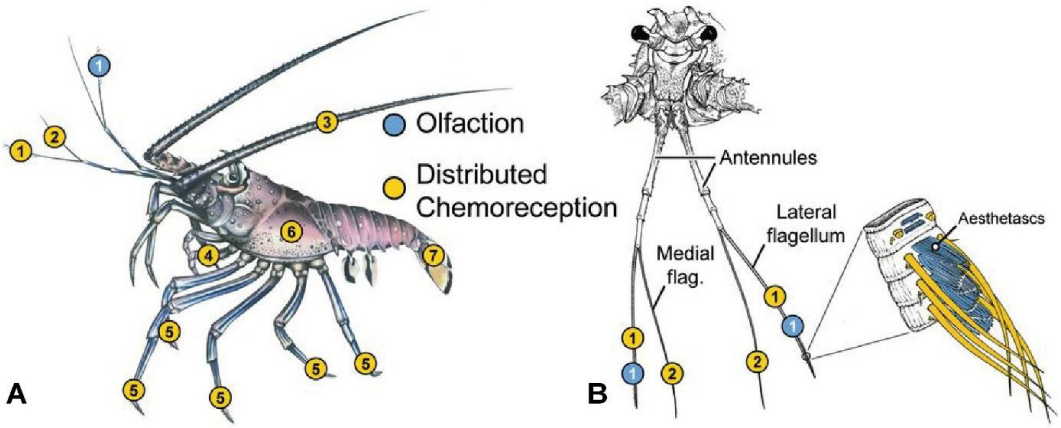

Figure 14 Two modes of crustacean chemodetection
From Derby et al. 2016 (and references therein).

A-B. Location of aesthetascs (blue dots) mediating olfaction and bimodal chemo-/mechanosensory sensilla (yellow dots) mediating distributed chemodetection on different body parts and appendages of the spiny lobster, *Panulirus argus*. 1, lateral flagellum of the antennule; 2, medial flagellum of the antennule; 3, antenna; 4, mouthpart appendages; 5, walking legs; 6, cephalothorax; 7, tail fan.

The functional difference between these two chemosensory pathways was hypothesized by Schmidt and Mellon (2011) as follows: olfaction is linked to a detailed representation of the chemical environment, by integrating various chemical signals of potential interest, with no reference to the location of the stimuli and without generating any motor response. In contrast, distributed chemodetection is linked to the representation of key chemical compounds (e.g. food odor sources, pheromones) in a somatotopic context, through the coupling with mechanosensory neurons which allows the spatial localization of chemical stimuli and the triggering of target motor responses. Although each of these pathways is sufficient to locate food odor sources, they are complementary for odor discrimination in a chemical background (Steullet et al. 2000, 2002).

1.3. Detection of chemicals

1.3.1. Chemoreceptors

Chemodetection is primarily mediated by proteins expressed in the membranes of the chemosensory neurons (i.e. chemoreceptors) or around them. Evolution has resulted in unique expansions of specific genes families and repurposing of them for chemodetection in various clades, including crustaceans (Derby et al. 2016). Chemosensory-related genes have been barely explored in crustaceans, especially in comparison to insects, mainly because few crustacean species have their genome sequenced. However, transcriptomics technologies have yield to a partial identification of proteins involved in crustacean chemodetection. Chemosensory-related proteins known to be expressed in Crustacea and Arthropoda are indicated in Figure 15A. The sequenced genome of the branchiopod *Daphnia pulex* contains several genes coding for chemosensory protein families also present in insects (Penalva-Arana et al. 2009): Ionotropic Receptors (IRs), Gustatory Receptors (GRs) and Chemosensory Proteins (CSPs). Eyun et al. (2017) identified IRs, GRs and CSPs in several copepod species, and CSPs in two dendrobranchiata and peracarida species. In decapods, only IRs were identified, in Achelata (Corey et al. 2013), Astacidea (McGrath et al. 2006, McClintock et al. 2006) and Anomura (Groh et al. 2014, Groh-Lunow et al. 2015). In insects, IRs, GRs and CSPs are known to be involved in chemodetection, but another class of chemoreceptors mediates olfaction: the Olfactory Receptors (ORs). ORs have never been reported in non-insect taxa, which suggests that olfaction in other groups, such as Crustacea, might be mediated by different mechanisms and other families of sensory proteins.

IRs are ion channels that are gated by ligands and represent an ancestral protostome chemosensory receptor family, evolving from ionotropic glutamate receptors (Croset et al. 2010). They function as heteromeric receptors, with co-receptor IR subunits that associate with other IR subunits that determine the specificity to the ligand (Croset et al. 2010) (Figure 15B). Corey et al. (2013) showed that the highly conserved subunits IR25a and IR93a are expressed in the antennules of *Panulirus argus*. So far, IRs are the only type of chemoreceptor molecules identified in the antennules (the main olfactory organs) of decapod crustaceans, and are considered as the putative crustacean olfactory receptors. In insects however, IRs also mediate other sensory modalities such as thermosensation and hygrosensation (Knecht et al. 2016). GRs are ionotropic 7-transmembrane receptors (Figure 15C). GRs are known to be expressed in gustatory neurons in the legs, mouthparts, wing margins, ovipositor and antennae of insects (Benton 2015, Robertson 2015). GRs have not been identified in decapod crustaceans yet but evidence from myriapods and chelicerates suggest that the presence of GRs is an ancestral arthropod trait (Derby et al. 2016, Eyun et al. 2017). CSPs are proteins present in the lymph

surrounding the chemoreceptors where they serve as carrier molecules for the ligands (Pelosi et al. 2014). Transient Receptor Potential (TRP) channels have also been reported to play a role in chemodetection in insects (Kang et al. 2010, Kim et al. 2010, Zhang et al. 2013) and might be expressed in crustaceans. Even if TRP genes have not yet been identified for crustacean chemodetection, OSNs of spiny lobster express channels that have some physiological properties in common with TRP channels (Bobkov et al. 2010).

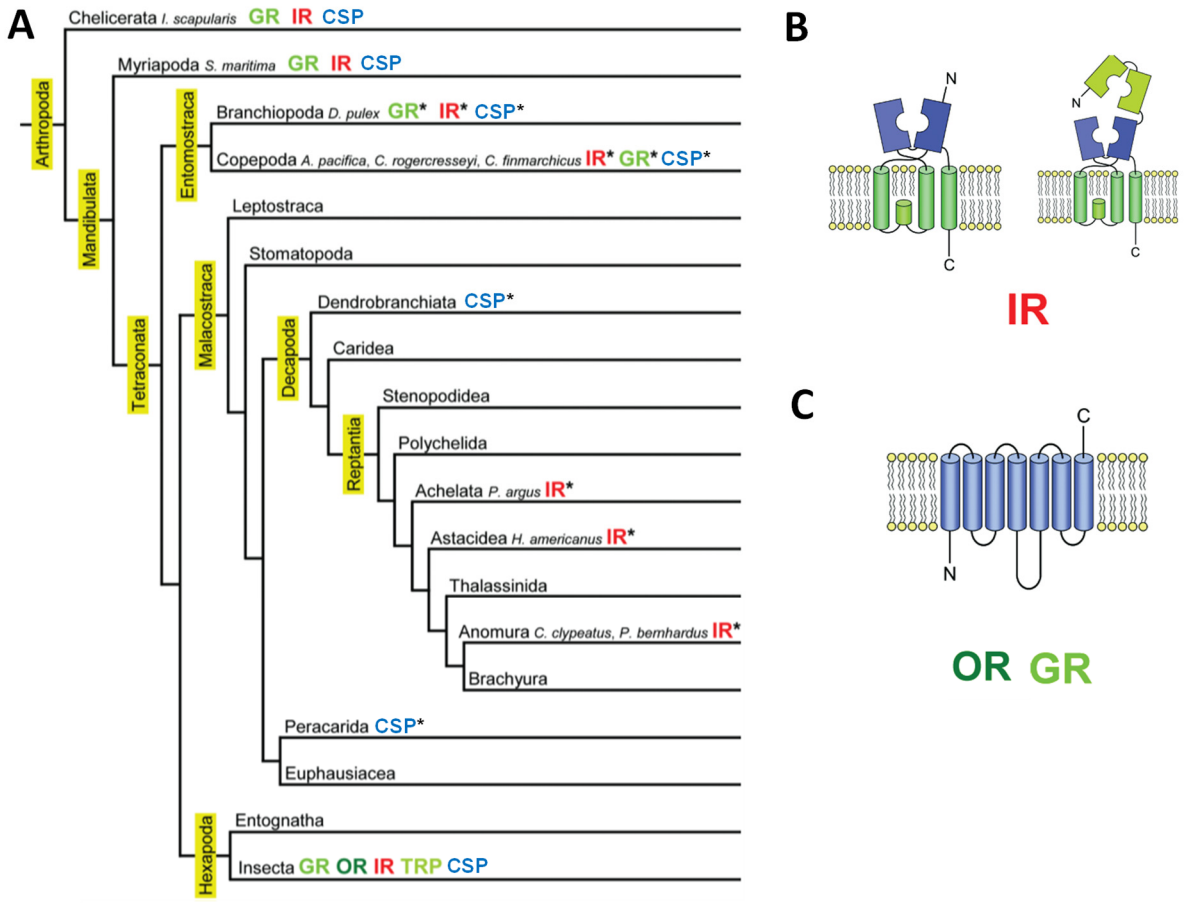

Figure 15 State of knowledge on chemosensory proteins in Crustacea and beyond
Modified from Derby et al. 2016, with additional data from Eyun et al. 2017 for CSPs.

A. Arthropod phylogeny and the chemosensory proteins known to be expressed in each clade. CSP, chemosensory protein; GR, gustatory receptor; IR, ionotropic receptor; OR, odorant receptor; TRP, transient receptor potential channel. Asterisks indicate proteins identified in Crustacea.
B. Schematized molecular structure of IRs. IRs derive from iGluRs that form heterotetrameric ion channels, with each monomer having 3 major domains: amino terminal domain, ligand binding domain, and ion channel domain. IR25a and IR8a are the only IRs that possess all 3 major domains (right sketch), whereas the other IRs only have the ligand binding domain and the ion channel domain (left sketch). A functional IR is a heteromeric complex with an IR co-receptor (e.g. IR25a, IR8a) associated with another, ligand specific IR subunit.
C. Schematized molecular structure of ORs and GRs. ORs and GRs are 7-transmembrane chemoreceptors, with an extracellular carboxyl terminal and an intracellular amino terminal.

1.3.2. Chemosensory sensilla and neurons

As previously described, two chemosensory pathways are associated to two types of chemosensory sensilla in crustaceans: the unimodal olfactory aesthetasc sensilla, and the bimodal chemo- and mechanosensory sensilla.

The aesthetasc sensilla are specialized in olfaction. They are exclusively present on the lateral flagella of the antennules (Figure 14B) and are characterized by a thin permeable cuticle. They are innervated by OSNs, for which the somata are arranged in cluster beneath the aesthetascs. The number of OSNs associated with individual aesthetasc display taxon-specific variation across the Malacostraca over a range of about 100-400 (Harzsch and Krieger 2018). Each OSN dendrite is divided into one inner dendritic segment (IDS) that project into the aesthetasc sensillum, where it divides dichotomously in outer dendritic sgments (ODS), which bear the olfactory receptors. The region where the IDSs divide into ODSs is called the transitional zone (Figure 16). Every aesthetasc is associated with an identical set of heterogeneous OSNs (i.e. characterized by different olfactory receptors) representing the entire odor range the animal can detect (Steullet et al. 2000, Mellon 2007).

Bimodal sensilla are innervated by both chemo- and mechanosensory neurons. They are present on the antennal appendages, the mouthparts, the walking legs, and all the body surface (Garm et al. 2003, 2005, Garm and Watling 2013, Ache 1982, Altner et al. 1983, Schmidt and Gnatzy 1984) (Figure 14A,B). Unlike aesthetascs, these sensilla display at least one terminal pore in their cuticle (Mellon 2012, 2014), through which chemicals must penetrate to reach the dendrites of the chemosensory neurons. Bimodal sensilla display a variety of morphology and innervation configurations, and overall their precise respective functions are not well understood. They are considered primary to mediate chemodetection by contact (Mellon 2007, 2012) and specific behaviors such as grooming[(GLOSSARY)] (Schmidt and Derby 2005). Studies on lobster suggest that some bimodal sensilla could also detect distant chemical sources (Steullet et al. 2001, 2002, Schmidt and Mellon 2011).

1.3.3. Flicking of the antennules

In crustaceans, chemical ligands must cross the aesthetasc cuticle or penetrate the pore of bimodal sensilla to bind their cognate receptors. This occurs by slow molecular diffusion (Atema and Steinbach 2007, Koehl 2011, Mellon and Reidenbach 2012) but is greatly enhanced by the flicking[(GLOSSARY)] of the antennules. Flicking corresponds to the quick depression of the lateral antennules from their normal posture, and they return at slower speed (Mellon 2007). The slow return

stroke traps the water in the aesthetasc arrays, and the downward stroke replaces the water sample. Each flick thus represents a sniff probing the odor plume by taking discrete samples, giving spatiotemporal information critical for orientation (Koehl 2011, Mead 2002). The frequency of antennules flicking and the resultant intermittent odor sampling might determine the temporal resolution with which the olfactory system extracts information from the environment (Harzsch and Krieger 2018).

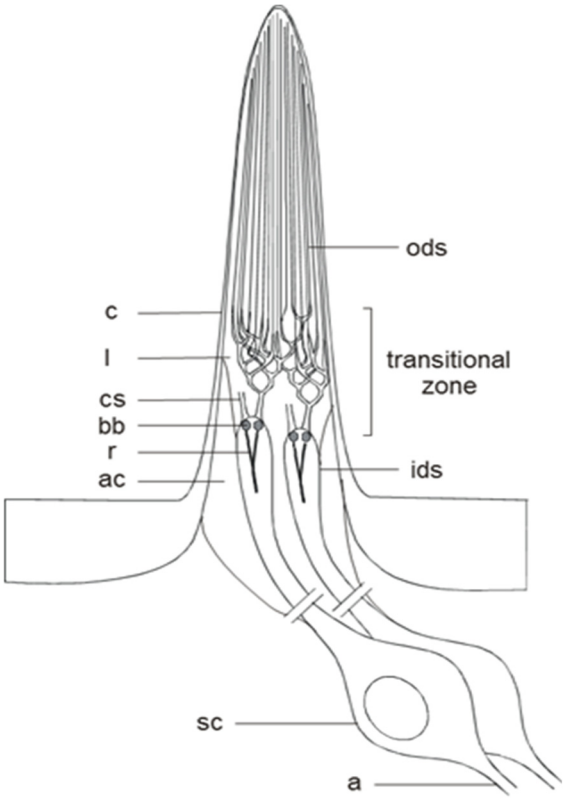

Figure 16 Sketch of an aesthetasc sensilla innervated by olfactory sensory neurons

Only two out of approximately 100 to 400 bipolar olfactory sensory neurons that innervate each aesthetasc are shown, and for each neuron only one cilium branching is shown. The transitional zone refers to the zone where the inner dendritic segments give rise to two ciliary segments, each starting to divide dichotomously in outer dendritic segments. Axon (a); accessory cell (ac); basal bodies (bb); cuticle (c); ciliary segment (cs); inner dendritic segment (ids); outer dendritic segment (ods); ciliary rootlet (r); lumen (l); sensory cell somata (sc). Not to scale.

1.4. Central integration of the chemical stimulus

1.4.1. Overview of the central nervous system

The brain of crustaceans contains several neuropils categorized in three regions, the proto-, deuto- and tritocerebrum, in addition to the optic neuropils. The ground pattern of malacostracan brain is sketched in Figure 17.

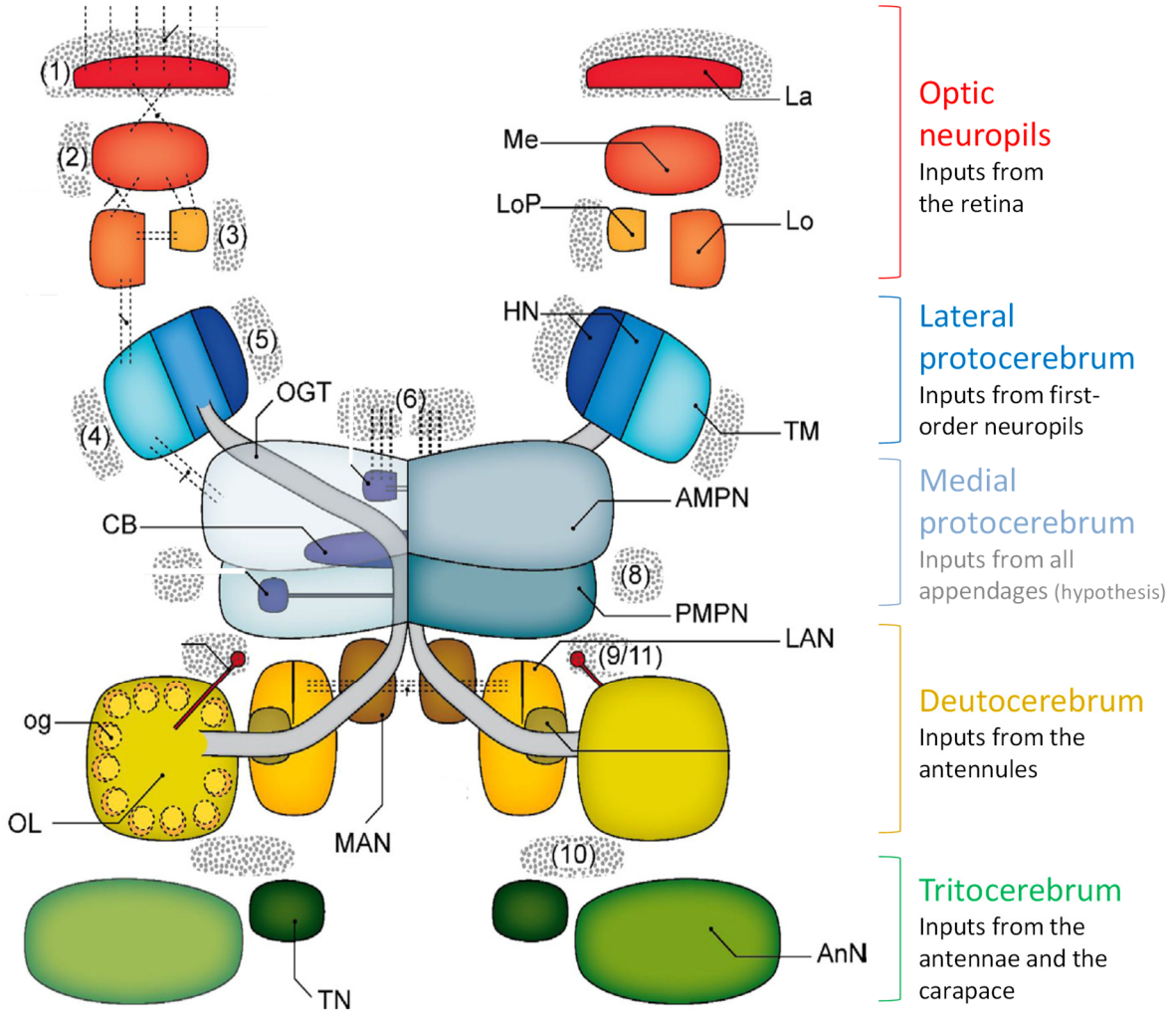

Figure 17 Ground pattern of the malacostracan brain

Modified from Harzsch and Krieger 2018, therein modified after Kenning et al. 2013.

Silhouette of the brain and antennal nerves are omitted.

Abbreviations: (1)–(11), cell clusters 1–10; AMPN, anterior medial protocerebral neuropil; AnN, antenna 2 neuropil; CB, central body; HN, hemiellipsoid body neuropils; La, lamina; LAN, lateral antenna l neuropil; LoP, lobula plate; MAN, median antenna 1 neuropil; Me, medulla; MT, medulla terminalis; og, olfactory glomerulus; OGT, olfactory globular tract; OL, olfactory lobe; PMPN, posterior medial protocerebral neuropil; TN, tegumentary neuropil.

A neuropil is a region of dense synaptic contact, in which information enters via afferent fibers (input) and leaves via efferent fibers (ouput). The first-order neuropils receive direct inputs from the sensory neurons in the peripheral nervous system(GLOSSARY) (e.g. the sensory organs, like the antennal appendages). They are associated to local interneurons that make connections within the neuropil, and to projection neurons that make connections with higher-order sensory neuropils (see Figure 18). The higher-order neuropils receive information from the first-order neuropils but not directly from the peripheral nervous system. For example, the olfactory lobes, the antennal and lateral antennular

neuropils (see descriptions hereafter) are first-order neuropils, since they receive direct inputs from the sensilla located on the antennal appendages. The hemiellipsoid bodies(GLOSSARY) and the medulla terminalis(GLOSSARY) (see descriptions hereafter) are higher-order neuropils, because they receive only inputs from other neuropils and are so called higher-integrative centers.

The optic neuropils, in which the visual inputs from the eyes are processed, consist in a series of nested columnar neuropils named the lamina, the medulla, the lobula and the lobula plate. They are located under the retina in the eyestalks (when present).

The protocerebrum is subdivided in lateral and medial protocerebrum. The lateral protocerebrum comprises two neuropils, the hemiellipsoid bodies and the medulla terminalis, both closely associated, sometimes barely demarcated, and usually located in the eyestalks close to the optic neuropils. They are centers of multimodal integration, further detailed below (see section 1.4.3.). The medial protocerebrum comprises neuropils referred as the central complex. The central position of these neuropils suggests a role in coordination of sensory inputs (Kenning et al. 2013), and functions in motor control of the appendages have also been proposed (Strausfeld and Andrew 2011).

The deutocerebrum comprises several neuropils that process the mechanosensory, olfactory and non-olfactory chemosensory information delivered by the antennules: the lateral antennular neuropils (LANs), the median antennular neuropils (MANs) and the olfactory lobes (OLs). The LANs receive afferents from the mechano- and chemosensory neurons innervating the bimodal sensilla (Blaustein et al. 1988, Schmidt and Ache 1996). They are hemispheric neuropils connected by a commissure. The MANs are diffusely organized neuropils located between the LANs, and receive primary afferents from the statocysts(GLOSSARY) (Yoshino et al. 1983). The OLs are paired, roundish neuropils that receive afferents from the OSNs that innervate the aesthetascs, and are further detailed below (see section 1.4.2.).

The input that enters into the OLs is relayed to different groups of local inter- and projection neurons, the latter comprising the olfactory globular tract that carries the information to the higher-order neuropils, i.e. the hemiellipsoid bodies and the medulla terminalis in the lateral protocerebrum (Sandeman et al. 1992, Krieger et al. 2012).

The tritocerebrum flanks the oesophagus and comprises the antennal neuropils (AnNs) and the tegumentary neuropils, both processing mechanosensory information delivered by the antennal nerves and the tegumentary nerves (Sandeman et al. 1992). The tegumentary nerves carry mechanosensory information from the carapace. The antennal nerves carry mechano- and chemosensory information from the neurons innervating the bimodal sensilla of the antennae.

1.4.2. First-order chemosensory centers (OLs, LANs, AnNs)

The OLs are the site of first order processing of aesthetasc chemosensory information (Mellon et al. 1992, Sandeman et al. 1992, Schachtner et al. 2005, Schmidt and Mellon 2011). They comprise multiple and distinct synaptic fields called the olfactory glomeruli, which seem to function as the fundamental processing units of the olfactory system where the afferents, local interneurons and projection neurons make synaptic contacts (Harzsch and Krieger 2018). These glomeruli are radially arranged around the periphery of a core of non-synaptic fibers, and are subdivided into a cap and a base region (and eventually a subcap region), resulting of a regionalized arrangement of local olfactory inter- and projection neuron synapses (Schachtner et al. 2005). These subdivisions of olfactory glomeruli are most likely functionally relevant (Schmidt and Ache 1996, 1997). Each glomerulus shares the same architecture, and possible functional differences between them have not yet been recognized (Harzsch and Krieger 2018). The axons of the OSNs innervating one aesthetasc target most if not all olfactory glomeruli (Sandeman and Denburg 1976, Schmidt and Ache 1996, Tuchina et al. 2015). The LANs and the AnNs are also first-order chemosensory centers that receive direct inputs from the bimodal sensilla on the antennules and the antennae respectively. The OLs are considered to code the odor quality, while the LANs and the AnNs contribute to odor tracking (Harzsch and Krieger 2018).

1.4.3. Higher-order integrative centers (hemiellipsoid bodies and medulla terminalis)

The hemiellipsoid bodies and the medulla terminalis are two neuropils located in the lateral protocerebrum, usually in the eyestalks. They are higher integrative centers that process information from various sensory modalities, receiving inputs from first-order neurons but not from any peripheral sensory afferents (Sandeman et al. 2014). Sandeman and collaborators (2014) suggested that in light of their high level of complexity and the large amount of brain space devoted to them, these neuropils functions go beyond simple reflexive behavior and may involve more sophisticated processes, for instance related to orientation within the environment during homing or migration, recognition of suitable mating partners, and social interactions. There is not much information available on the morphology and the functional significance of the medulla terminalis, in contrast to the hemiellipsoid bodies that have been described and thoroughly investigated in various malacostracan crustaceans.

The hemiellipsoid bodies vary greatly in both size and anatomy (Blaustein et al. 1988, Sandeman et al. 1993, Strausfeld 1998), with a common subdivision in distinct layers (at least a peripheral cap and a central core region) (Sullivan and Beltz 2001a, 2005). They receive inputs from the olfactory lobes via the olfactory globular tract and from the optic neuropils, for which the

information is relayed in the dense multilayered network (Brown and Wolff 2012, Strausfeld and Andrew 2011, Wolff et al. 2012). These inputs suggest a higher order integration of the corresponding stimuli. In addition, these neuropils might play an important role in olfactoryy learning (Mellon and Alones 1997) and general memory processes (Maza et al. 2016).

1.5. Assumptions on olfactory abilities from comparative studies

The behavioral response to a stimulus is the most integrated response and the most representative evidence of the sensory abilities of an animal. However, behavior experiments are delicate to conduct, and results can be complex to interpret since many uncontrolled factors may affect animal behaviors (Amdam and Hovland 2011). In crustaceans, a bioassay designed for one species is not necessarily ecologically suitable for another species (Kenning et al. 2015), and direct comparisons may be not relevant. Nonetheless, investigations at other levels (e.g. structural, molecular, and physiological) can provide cues on sensory abilities in a comparative context. In crustaceans olfaction has been extensively studied in various taxa, with functional studies but also with structural descriptions of the olfactory systems and comparison of numerical aspects that may be linked to olfactory efficiency, lifestyle or habitat. A non-exhaustive list of parameters frequently used in the literature to infer on crustacean olfactory abilities is presented hereafter. They will be examined in the following chapters to discuss on the olfactory abilities of the vent shrimp *M. fortunata* compared to the shallow-water species *Palaemon elegans*.

- The aesthetasc dimensions and cuticle thickness may influence the sampling efficiency of an odor plume. Longer and larger aesthetascs are associated to a larger chemoreceptive surface (Nelson et al. 2013), and the thinner portion of the aesthetasc cuticle likely defines the portion of the sensillum permeable to soluble odorants (Tierney et al. 1986, Derby et al. 1997). The distribution of the aesthetascs may also impact the spatial resolution of the chemical environment, e.g. crustaceans with small aesthetasc spans may be unable to detect asymmetries in odor concentrations as a source of navigational information, as crustaceans with a large array of aesthetascs do (Koehl 2011).

- The number of aesthetascs is linked to the sensitivity, whereas the number of OSNs and ODSs are associated to both sensitivity and discrimination of the chemical environment. Since each individual aesthetasc houses identical sets of OSNs (Steullet et al. 2000), a multiplication of aesthetascs raises primarily the sensitivity but does not promote the diversity of detectable odorants (Beltz et al. 2003). Similarly, an increasing number of identical OSNs (associated to the olfactory receptors) increases the sensitivity, while the number of OSNs expressing different olfactory receptors is linked

to the odorant discrimination potential (Derby and Weissburg 2014). The number of ODSs is representative of to the total area of dendritic membranes within are expressed olfactory receptors.

- The diversity of chemoreceptors and their levels and patterns of expression are the basis of the chemosensory abilities. The repertoire of chemoreceptors reflects the diversity of molecules perceived by the animal, and a higher density of receptors that detect the same stimulus may reduce noise while maintaining the resolution of the system (Galizia 2014).

- Modifications of the central nervous system occur in connection with the lifestyle of a species. There is a balance between the performance and the energetic costs associated to a sensory system, meaning that one system will be reduced during evolution if there is no need to maintain its performance. This is for example the case for the visual sensory system that is greatly reduced in cave species (Niven and Laughlin 2008). Also, the reduction of one sensory modality can be balanced by the preponderance of another modality (Sandeman et al. 2014). For instance, in blind crustacean Remipedia cave species, the eyes and optic neuropils are absent whereas the central olfactory system is greatly developed (Fanenbruck et al. 2004, Fanenbruck and Harzsch 2005, Stemme and Harzsch 2016). Another example are shrimp of the genus *Penaeus* for which the olfactory system is poorly developed, in contrast to sophisticated antennal neuropils that process mechanosensory input from the antennae, which may play a role in efficient predator avoidance via the detection of hydrodynamic stimuli (Meth et al. 2017, Sandeman et al. 1993). Hence, noticeable size dissimilarities between different neuropils and different species might be linked to their ecology and lifestyle.

- The volume of the olfactory lobes and the organization of the olfactory glomeruli might be linked to the power of odor discrimination and quality coding. The volume of the olfactory lobes is correlated to the amount of olfactory input and thus the repertoire of chemicals detected by the animal (Beltz et al. 2003). The level of subdivision of the olfactory glomeruli (i.e. cap and base versus cap, subcap and base) may be linked to the integration performance of the olfactory system (Harzsch and Krieger 2018). Also, the number of olfactory glomeruli exhibits great variation among species and is not correlated to the olfactory neuropils volume, the habitat or the lifestyle (Beltz et al. 2003) but is one of the numerical aspects commonly used to describe the chemosensory systems of crustaceans.

- At functional level, electrophysiology allows to test the detection of chemicals and to determine parameters such as response spectra and thresholds, which can vary between single neurons, or species. Typically, the functionality of OSNs is studied with patch-clamp(GLOSSARY) recording from single OSNs to obtain a representative response of one cell (Doolin et al. 2001, Ukhanov et al. 2011), but this method is inefficient to obtain population cell data. In insects, odor response patterns can be obtained from single sensilla (using single sensillum recording(GLOSSARY)) or from whole olfactory

organs (using electroantennography [EAG]). Odorant activation can also be monitored using calcium imaging(GLOSSARY) both at the central and peripheral levels, which Ukhanov et al. (2011) successfully performed on lobster OSNs. Such methods (except EAG, see Chapter IV) are still to be optimized for small crustaceans.

As a synthesis, the trajectory of a chemical stimulus integration via the olfactory pathway is sketched in Figure 18.

2. Thermodetection

The physiological basis of thermodetection is one of the least investigated areas of crustacean neurobiology. Barber (1961) indicated that crustaceans are behaviorally competent to detect thermal discontinuities, select preferred thermal zones in their environment and exhibit temperature acclimation, implying that thermosensory mechanisms must mediate such responses. In their review of thermal behavior of crustaceans, Lagerspetz and Vainio (2006) indicated that crustaceans seem to detect fine temperature variations, in the range 0.2-2°C, and that thermosensitivity is mediated by the peripheral nervous system. Puri and Faulkes (2015) demonstrated that crayfish antennae are responsive to high temperature (42,8°C) and suggested that the antennae might contain sensory neurons specialized in nociception rather than in general thermodetection.

Specific thermoreceptors, or putative multimodal thermoreceptors, have not been identified in crustacean yet (Lagerspetz and Vainio 2006). In insects, thermodetection is known to be mediated in part by TRP channels, especially by proteins from the TRPA subfamily (e.g. TRPA1, painless and pyrexia) that each detect different ranges of temperature (Lee et al. 2005, Sokabe and Tominaga 2009). Several insect species have four or five TRPA genes, but the crustacean *D. pulex* has only one TRPA gene (Matsuura et al. 2009). In *Drosophila melanogaster*, one part of the antennae, the arista, contains thermosensory neurons expressing TRP channels (Gallio et al. 2011), but neurons expressing pyrexia are distributed throughout the fly body (Lee et al. 2005), indicating that temperature may serve not only as a stimulus for specific end organs but is likely widely detected.

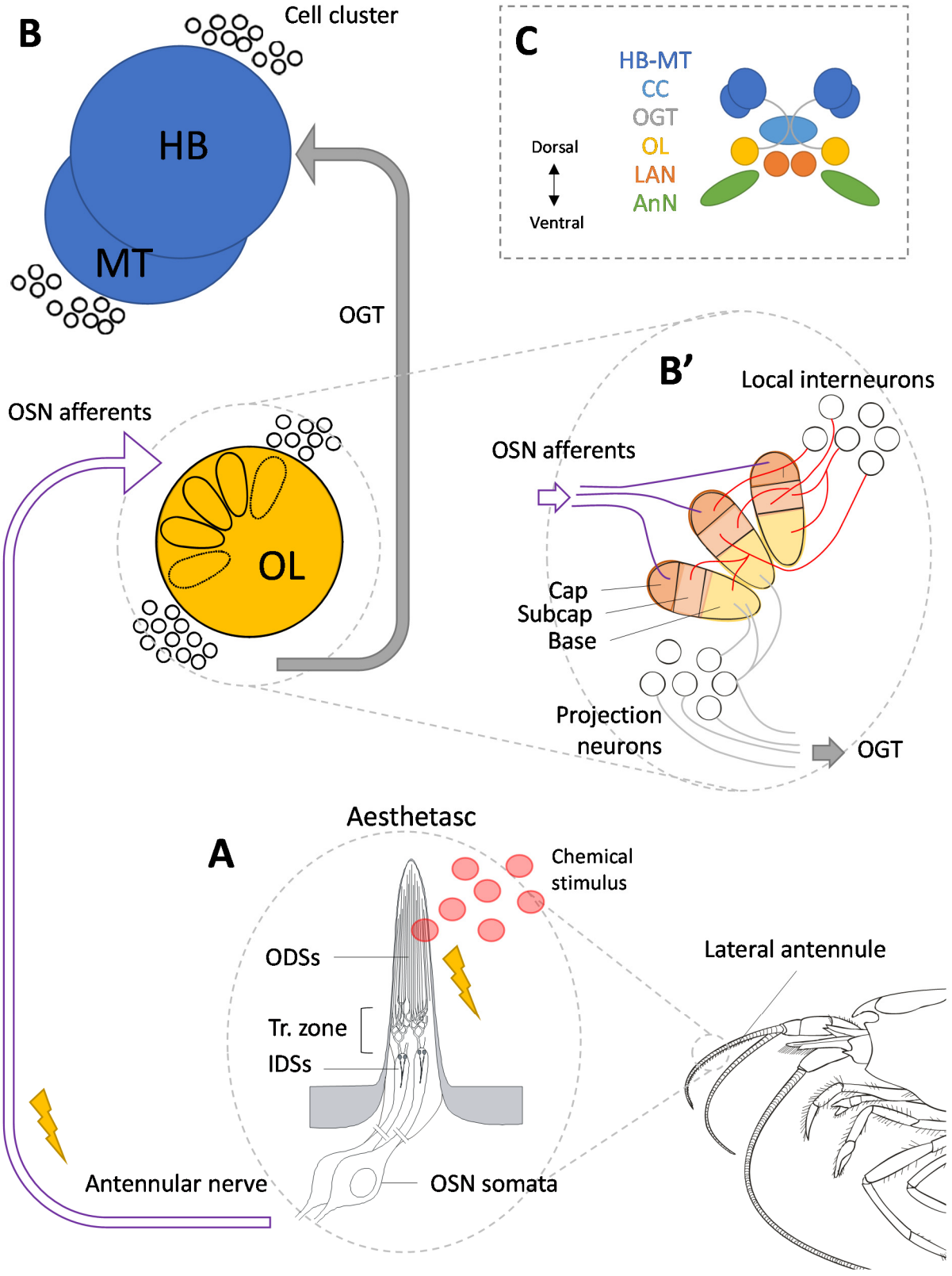

Figure 18 Diagram of the olfactory pathway
Legend next page.

A. Chemical stimuli are detected by OSNs housed in the aesthetasc sensilla located on the lateral flagellum of the antennules. Odor molecules cross the thin aesthetasc cuticle to bind to their cognate chemoreceptors located within the membranes of ODSs. This binding generates an electrical signal (the receptor potential) transmitted to the OSN somata, where it triggers the firing of action potentials that propagate within the OSN axons.
B. OSN axons gather to form the antennular nerve, and project into the brain in the OLs, organized in olfactory glomeruli (**B'**. Within the glomeruli, regionalized in cap, [subcap] and base regions, synapses from local interneurons make various connections between glomeruli and regions to process the olfactory information. Efferent fibers from projection neurons, connected to the base region of the glomeruli, bundle into the OGT). The OGT emanates from the OLs and projects to the HB and the MT, where the olfactory signal is processed likely in respect with signals from other sensory modalities.
C. Schematic view of neuropils organization in a crustacean brain (optic neuropils omitted).
AnN, antennal neuropil; CC, central complex; HB, hemiellipsoid bodies; IDSs, inner dendritic segments; LAN, lateral antennular neuropil; MT, medulla terminalis; OGT, olfactory globular tract; OL, olfactory lobes; OSNs, olfactory sensory neurons; Tr, transitional zone.

V. Models used in the present study

1. The vent species *Mirocaris fortunata*

1.1. Selection criteria

M. fortunata (Martin and Christiansen 1995) (**Figure 5**F) was selected as a hydrothermal species model for this thesis project. First, this species is widely distributed along the Mid-Atlantic Ridge (MAR), from the shallowest vent sites (e.g. Menez Gwen, 850 m depth) to the deepest ones (e.g. Ashadze, 4080 m depth). Next, *M. fortunata* presents the considerable advantage to survive at atmospheric pressure when sampled at depths that do not exceed 2000 m, as the Menez Gwen and Lucky Strike sites (Gebruk et al. 2000, Shillito et al. 2015). This species can thus be maintained at atmospheric pressure in classic aquaria and be used for *in vivo* experiments such as electrophysiology and behavioral tests in the same conditions as a shallow-water species. Because this species is a secondary consumer, it can be fed with mussels or shrimp food products and hence be maintained for several months in the laboratory. Thanks to a collaboration with the Oceanopolis aquarium, specimens of *M. fortunata* are yearly collected during the MOMARSAT cruises to sustain the AbyssBox exhibition (Shillito et al. 2015 and see section III.3.) and are available for experiments conducted by the AMEX team.

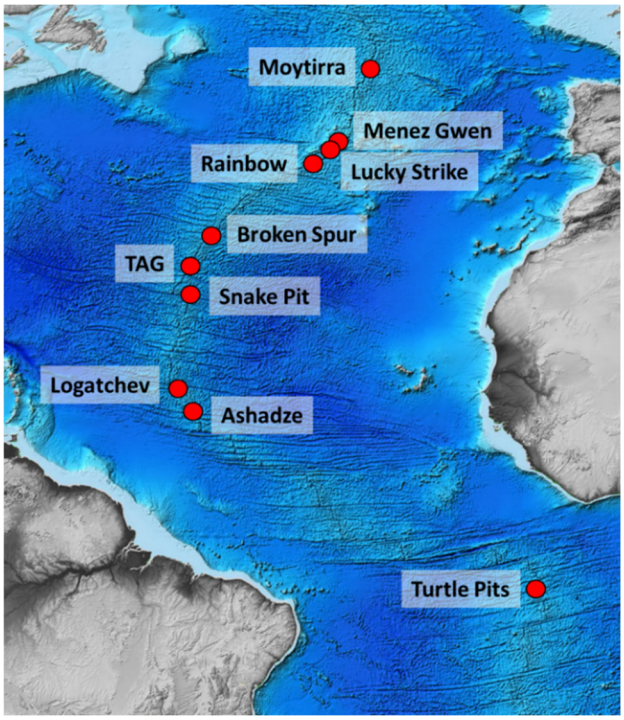

Site	Coordinates	Depth (m)
Moytirra	45°28.998'N, 27°51.000'W	3000
Menez Gwen	37°50.502'N, 31°31.500'W	840-865
Lucky Strike	37°17.598'N, 32°16.398'W	1600-1740
Rainbow	36°13.800'N, 33°54.120'W	2270-2320
Broken Spur	29°10.200'N, 43°10.302'W	3044-3100
TAG	26°8.202'N, 44°49.602'W	3436-3670
Snake Pit	23°22.098'N, 44°57.000'W	3044-3100
Logatchev	14°45.120'N, 44°58.710'W	2925-3050
Ashadze	12°58.398'N, 44°51.798'W	4080
Turtle Pits	04°48.57'S, 12°22.41'W	2922-2998

Figure 19 Distribution of *M. fortunata* along the Mid-Atlantic Ridge

1.2. Distribution

M. fortunata is an endemic species of vents at the MAR, where it occurs both on north and south portions, from 840 to 4000 m depth, and was reported at ten vent sites, thus having the widest geographic distribution among Alvinocarididae (Komai and Segonzac 2003, Lunina and Vereshchaka 2014) (Figure 19). It is the dominant Alvinocaridid species at the Lucky Strike and the Menez Gwen sites, and is found in variable abundances (50-2800 individuals per square meter) at the Rainbow site (Desbruyères et al. 2000). Only few specimens are reported at vent sites exceeding 3000 m depth.

1.3. Gross morphology

M. fortunata is part of the clade Mirocaridinae (which comprises two genera: *Nautilocaris* and *Mirocaris* [Figure 4B]) supported by the following synapomorphies: strap-like epipods terminating in a hook occur on the fourth pereopod (walking appendages), and the appendix interna is much reduced in second to fourth pleopods (swimming appendages) (Vereshchaka et al. 2015). The size of adult specimens of *M. fortunata* ranges from 1.2 to 3.3 cm in total length (Martin and Christiansen 1995). As species of the genus *Rimicaris* and *Chorocaris*, *M. fortunata* has a degenerated rostrum, reduced external spines and a dorsal organ homologous to the "dorsal eye" found in *R. exoculata* but smaller and restricted to postorbital region (Figure 20). In addition, *M. fortunata* is distinguishable from other Alvinocardidae species by its completely toothless rostrum (Komai and Segonzac 2003).

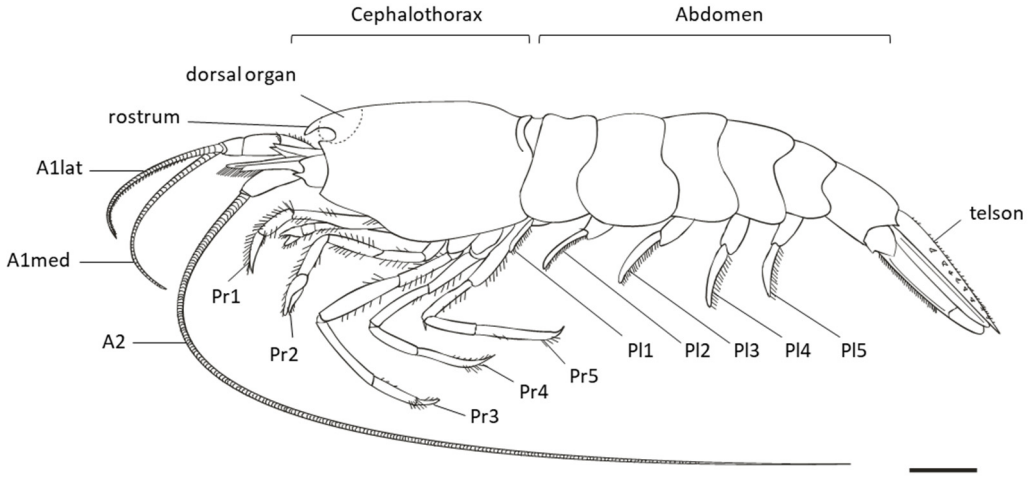

Figure 20 Morphology of *M. fortunata*

The mouthparts maxillipeds, maxillae and mandibles are not shown. The antennule and the antenna are not to scale. A1lat, lateral antennule; A1med, medial antennule; A2, antennae; Mxp, maxillipeds; Pl1-5, pleopods 1-5; Pr1-5, pereopods 1-5. Scale bar = 3 mm.

1.4. Trophic behavior

M. fortunata is mainly a secondary consumer, scavenging on tissues of mussels, shrimp and other invertebrates when available, and it also grazes on bacterial mats (Gebruk et al. 2000, Desbruyères et al. 2001).

1.5. Habitat and chemical and thermal environment

M. fortunata has a broad distribution across the vent-fluid dilution gradient (Desbruyères et al. 2001, Ravaux et al. 2007), but is usually found at the periphery of the main chimneys, in zones of high biomass such as mussel assemblages (Vinogradov and Vereshchaka 1995, Gebruk et al. 1997, 2000, Desbruyères et al. 2001). Mean values from *in situ* measurements of temperature, pH and chemical concentrations in the habitats of *M. fortunata* were previously given in Table 2. A more detailed data set is presented in Table 3 with measurements *in M. fortunata* habitats and close diffuse vents at the Rainbow and the Lucky Strike vent sites. Overall, the habitat of *M. fortunata* is relatively warm (from 6.8 to 13.7 °C) and slightly acid (pH range 6.01 to 7.3), with large variations of sulfide (2.4 to 38.1 µmol.L^{-1}) and methane (0 to 6.5 µmol.L^{-1}) concentrations.

Table 3 Temperature, pH and chemical concentrations in *M. fortunata* habitats and close diffusers

Results are given as mean ± SD (*n* number of replicates).

Site	Sample	Temp. (°C)	pH	S (µM)	CH_4 (µM)	Fe (µM)	Cu (µM)	References
Rainbow (PP29)	Diffuser	47.5 ± 3.5 (2)	5.8 ± 0.4 (2)	12.8 ± 13.4 (2)	112.4 ± 31.4 (2)	-	-	Desbruyères et al. 2001
	Mirocaris	11.2 ± 4 (5)	7.1 ± 0.3 (5)	7.2 ± 8.7 (5)	6.5 ± 4.3 (5)	-	-	Desbruyères et al. 2001
Lucky Strike (Eiffel Tower)	Diffuser	29.3 ± 29.9 (5)	6.4 ± 1 (5)	18.8 ± 30.6 (5)	61.9 ± 115.2 (5)	-	-	Desbruyères et al. 2001
	Mirocaris	6.8 ± 1.3 (11)	7.3 ± 0.4 (11)	2.4 ± 2.4 (11)	0.8 ± 1 (11)	-	-	Desbruyères et al. 2001
		7.49 ± 1.54 (13-19)	6.01 ± 0.22 (2-4)	38.31 ± 11.94 (13-19)		3.53 ± 2.67 (13-19)	1.62 ± 1.96 (2-4)	Sarrazin et al. 2015
Lucky Strike (Bairro Alto)	Diffuser	9.2 ± 4 (2)	6.6 ± 0.6 (2)	2.3 ± 3.1 (2)	0.3 ± 0.3 (2)	-	-	Desbruyères et al. 2001
	Mirocaris	9.5 ± 3.4 (6)	6.9 ± 0.4 (6)	19.9 ± 14.7 (6)	0.2 ± 0.2 (6)	-	-	Desbruyères et al. 2001
Lucky Strike (Elisabeth PP24)	Diffuser	85.0 ± 63.6 (2)	5.3 ± 1.1 (2)	155.7 ± 147.5 (2)	4.8 ± 6.4 (2)	-	-	Desbruyères et al. 2001
	Mirocaris	13.7 (1)	6.31 (1)	2.78 (1)	0 (1)	-	-	Desbruyères et al. 2001

2. The shallow-water species *Palaemon elegans*

2.1. Selection criteria

Palaemon elegans (Rathke 1837) was selected as a comparative shallow-water species model. The Palaemonidae family has a close taxonomic relationship to the vent Alvinocarididae (Figure 4A) (Tokuda et al. 2006, Sun et al. 2018), they are approximatively in the same size range (adults are slightly larger than *M. fortunata*), easily breed and maintained in laboratory, and they tolerate a similar thermal range as vent species, with daily thermal fluctuations ranging from 8 to 25°C in intertidal environments (Bates et al. 2010) and temperatures superior to 30°C in summer during low tide (Ravaux et al. 2016). Both environments display an unstable temperature regime, although changes in the intertidal habitat are not as acute as in the vent environment (Bates et al. 2010). For these reasons, physiological comparisons between Palaemonidae and Alvinocarididae appear relevant, and the palaemonid species *Palaemonetes varians* has previously been used as a model species for comparison with deep hydrothermal vent shrimp (Gonzalez-Rey et al. 2007, 2008, Cottin et al. 2010, Oliphant et al. 2011, Ravaux et al. 2012, Smith et al. 2013). For this thesis project, specimens of *P. elegans* were kindly sampled twice a year and provided to the AMEX team by Nicolas Rabet (UMR 7208 BOREA).

2.2. Distribution, feeding habits and gross morphology

P. elegans is commonly found on the rocky foreshore of the French coast, and is more generally present on the coastal regions of the Atlantic, the Baltic, the Mediterranean, the Black Sea, the Caspian Sea and the Azores (Neal 2008). It inhabits intertidal areas, lagoons and estuaries, forming abundant populations in vegetated places (Dalla Via 1985). This species is an opportunist feeder, omnivorous and necrophageous, feeding on algae, small invertebrates, organic detritus and dead animals. *P. elegans* has the typical morphology of a benthic caridean shrimp, with an elongated and serrated rostrum and stalked eyes (Figure 21A,B). It can reach 6.3 cm in total length and its carapace is transparent with variable pigmentation (Figure 21B) as a camouflage strategy. Notably, the lateral antennule is divided into a long, thin external ramus and a short internal ramus, the latter bearing the olfactory aesthetasc sensilla.

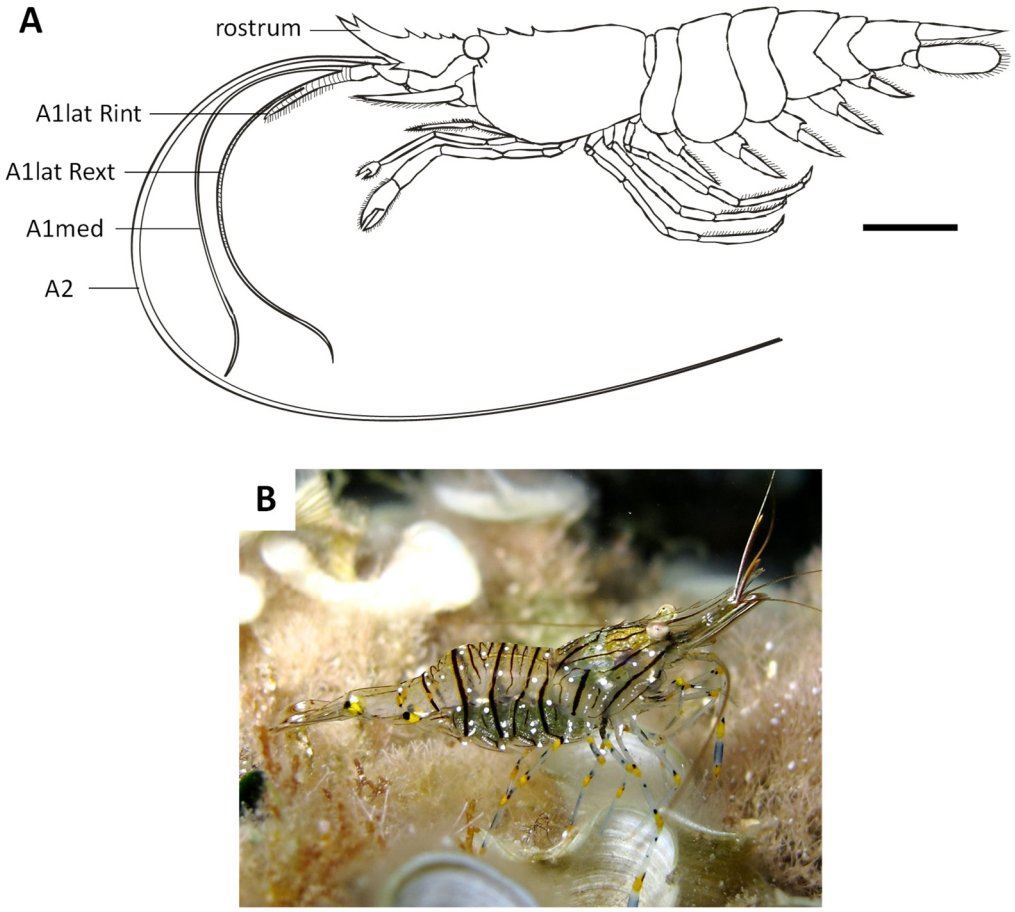

Figure 21 Morphology of *P. elegans*

A. Left view sketch. Antennules and antennae are not to scale. A1lat Rint, intern ramus of the lateral antennule; A1lat Rext, extern ramus of the lateral antennule; A1med, medial antennule; A2, antenna. Scale bar = 1cm.
B. Right view photography (Credits: R. Pillon).

Chapter II

Materials and Methods

I. Sampling, acclimatization and maintenance

1. Hydrothermal shrimp
2. Coastal shrimp

II. Imaging approaches

1. Photonic microscopy
2. Scanning Electron Microscopy
3. Transmission Electron Microscopy
4. Epifluorescent and confocal microscopy
5. X-ray micro-computed tomography

III. Experiments on live animals

1. Electroantennography
   - 1.1. Specimens
   - 1.2. Biological preparation
   - 1.3. Recordings, stimulus delivery and analysis
   - 1.4. Chemicals
     - Positive and negative controls
     - Food odor stimuli
     - Hydrothermal fluid chemical stimuli and pH controls
   - 1.5. Statistical analysis
2. Behavior experiments
   - 2.1. Experiments at atmospheric pressure on *P. elegans* and *M. fortunata*
     - 2.1.1. Attraction tests to food odor sources and sulfide
     - Two-choice experiments on single individual…
     - Multiple-choice experiments on single individual…
     - Two-choice experiments on multiple individuals…
     - 2.1.2. Attraction test to warm temperature
   - 2.2. Experiments at *in situ* pressure on *M. fortunata* and *R. exoculata*
     - Preliminary experiment in the IPOCAMP…
     - Experiments in the VISIOCAMP…

IV. Molecular biology

1. RNA extraction and reverse transcription
2. Sequencing and mRNA expression using RT-PCR

I. Sampling, acclimatization and maintenance

1. Hydrothermal shrimp

Vent shrimp were sampled with a vacuum device controlled by the hydraulics arms of the Victor 6000 (Remote Operated Vehicle [ROV]) or Nautile 6000 (Human Operated Vehicle [HOV]) submersibles. Cruises and sites from the Mid-Atlantic Ridge where specimens of *Mirocaris fortunata*, *Rimicaris exoculata*, *Rimicaris chacei* and *Alvinocaris markensis* were sampled are summarized in Table 4.

Table 4 Cruises and sampling origin of vent shrimp used for the experiments

Cruise, year	Vessel /Submersible	Chief scientist	Sites*	Species	Experiments
MOMARSAT 2011	Pourquoi Pas? / ROV Victor	M. Cannat	Lucky Strike	*M. fortunata*	Imaging (A) Molecular biology
MOMARSAT 2012	Thalassa / ROV Victor	M. Cannat and P-M. Sarradin	Lucky Strike	*M. fortunata*	Imaging (A) Molecular biology
BIOBAZ 2013	Pourquoi Pas? / ROV Victor	F. Lallier	Lucky Strike	*M. fortunata*	Imaging (A) Molecular biology
			Menez Gwen	*M. fortunata*	Behavior Molecular biology
			Rainbow	*R. exoculata, R. chacei, A. markensis*	Molecular biology
MOMARSAT 2014	Pourquoi Pas? / ROV Victor	M. Cannat	Lucky Strike	*M. fortunata*	Behavior
BICOSE 2014	Pourquoi Pas? / ROV Victor	M-A. Cambon-Bonavita	TAG, Snake Pit	*M. fortunata, R. exoculata, R. chacei, A. markensis*	Molecular biology
MOMARSAT 2016	Pourquoi Pas? / ROV Victor	M. Cannat	Lucky Strike	*M. fortunata*	EAG Behavior
MOMARSAT 2017	Pourquoi Pas? / ROV Victor	M. Cannat	Lucky Strike	*M. fortunata*	Behavior
BICOSE 2018	Pourquoi Pas? / HOV Nautile	M-A. Cambon-Bonavita	TAG	*R. exoculata*	Behavior
			Snake Pit	*M. fortunata*	Behavior Imaging (B)

A, antennal appendages; B, brain; EAG, electroantennography.
*Lucky Strike (37°18'N,32°16'W) 1700 m depth; Menez Gwen (37°85'N,31°51'W) 800 m depth; Rainbow (36°13'N,33°54'W) 2260 m depth; TAG (26°8'N,44°49'W) 3600 m depth; Snake Pit (23°22'N,44°57'W) 3500 m depth.

For *in vivo* studies, isobaric recovery with the PERISCOP device (see Chapter I – section III.1.) was used during the BICOSE 2018 cruise to sample *M. fortunata* and *R. exoculata* specimens from the TAG (3600 m depth) and Snake Pit (3500 m depth) sites, prior to behavior experiments in the VISIOCAMP aquarium (see Chapter I – section III.2.). For behavior and electrophysiology experiments at atmospheric pressure (see this chapter, section III.), specimens of *M. fortunata* were collected from the Lucky Strike site (1700 m depth) without isobaric recovery and maintained on board in 5 to 10 L seawater aquaria at 5-9 °C, at atmospheric pressure. This species tolerates relatively well the variations of pressure and temperature during the ascent, from sites that do not exceed 2000 m depth (Shillito et al. 2015). At the end of the cruise, surviving specimens were transferred to the Oceanopolis aquarium (Brest, France) and acclimated for at least two weeks in 80 L open circuit aquaria with oxygenated seawater at 9°C, in dark conditions (except during feeding). Each aquarium contained up to ~50 individuals. Shrimps were fed first with mussels, and progressively with a nutritive powder for crustaceans (LiptoAqua, Madrid, Spain).

After acclimatization, shrimps were maintained in their rearing tanks for behavior experiments at the Oceanopolis aquarium, or transferred to the AMEX laboratory (Paris, France) in a 175-L aquarium containing up to 40 individuals, with artificial oxygenated seawater (Red Sea Salt, Red Sea, Houston, TX, USA) at 9°C, in dark conditions, and fed twice a week. For both locations, a 50 W thermostat heater set to 25°C was placed in each aquarium to serve as a hot spot for the shrimps.

2. Coastal shrimp

Specimens of *Palaemon elegans* were collected from Saint-Malo Bay, France, by Nicolas Rabet (UMR 7208 BOREA) in 2016, 2017 and 2018 using a shrimp hand net. They were acclimated at the AMEX laboratory for at least two weeks and housed communally in a 175-L aquarium with oxygenated artificial seawater at room temperature (20±1°C) under a 12:12 light:dark cycle, and fed three times a week with shrimp food pellets (Novo Prawn, JBL, Neuhofen, Germany).

II. Imaging approaches

Procedures, species and origin of the samples used for the imaging are summarized in Table 5. Samples preparation, protocols and equipment configurations are detailed hereinafter into table format.

Table 5 Summary of procedures, species and origin of the samples used for imaging

Samples	Procedures	Species	Sites	Sampling
Lateral antennule, antenna	SEM, TEM	*M. fortunata*	Lucky Strike (37°18'N,32°16'W)	Momarsat 2011, 2012; Biobaz 2013
		P. elegans	Baie de St Malo (48°38'N,2°0'W)	2012
		R. exoculata	Rainbow (36°14'N,33°54'W)	Biobaz 2013
Brain	Immunohisto-chemistry, X-ray micro-computed tomography	*M. fortunata*	Snake Pit (23°22'N,44°57'W)	Bicose 2018
		P. elegans	Baie de St Malo (48°38'N,2°0'W)	2017
			Baie de St Coulomb (48°41'N,1°57'W)	2018

1. Photonic microscopy

SAMPLES PREPARATION	
Fixation	
Fixative	Glutaraldehyde 2.5 % 35 mL filtered seawater (0.2 µm) + 10 mL distilled water + 5 mL glutaraldehyde 25%
Rinsing solution	Seawater / Sodium azide NaN_3 50 mL filtered seawater (0.2 µm) + 0.04 NaN_3
Samples were fixed for 4-16 h at 4°C. The fixative was then replaced by rinsing solution until the post-fixation step.	
Post-fixation	
Post-fixative solution	1 volume osmium 4% : 3 volumes distilled water
3 rinses with distilled water – 3x 10 min 1 bath in post-fixative solution at ambient temperature – 45 min 3 rinses with distilled water – 3x 10 min	
Dehydration	
Successive baths in ethanol (50°-70°-95°-100°-100°) - 10 min each 1 bath in ethanol 99% / propylene oxide – 10 min 1 bath in propylene oxide – 10 min	
Embedding	
Epoxy resin	Epon812 6 g + Dodecenyl succinic anydride DDSA 2.25 g + Methyl nadic anhydre MNA 3.75 g + Benzyldimethylamine BDMA 0.35 g
1 bath in ¼ epon / ¾ propylene oxide – ½ day 1 bath in ½ epon / ½ propylene oxide – ½ day 1 bath in ¾ epon / ¼ propylene oxide – ½ day 1 bath in pure epon -1 h à 50°C under vacuum Embedding in pure epon – 48 h at 60°C	

SECTIONING
Embedded samples were cross-sectioned (500-600 nm) with an ultramicrotome (Leica, Ultracut R). Sections were dropped off on glass slides.

STAINING	
Staining solution	Toluidine blue 1 g + azur blue 1 g + saccharose 1 g + sodium borate 1 g
Sections were stained on glass sides over a heating plate.	

OBSERVATION
Sections were observed under a photonic microscope Olympus BX61 and images were recorded with ImagePro Plus software, with the help of Muriel Jager at the IBPS, Paris, France.

2. Scanning Electron Microscopy (SEM)

SAMPLES PREPARATION	
Fixation	
Fixative	Glutaraldehyde 2.5 % 35 mL filtered seawater (0.2 µm) + 10 mL distilled water + 5 mL glutaraldehyde 25%
Rinsing solution	Seawater / Sodium azide NaN_3 50 mL filtered seawater (0.2 µm) + 0.04 NaN_3
Samples were fixed for 4-16 h at 4°C. The fixative was then replaced by rinsing solution until the post-fixation step.	
Post-fixation	
Post-fixative solution	1 volume osmium 4% : 3 volumes distilled water
3 rinses with distilled water – 3x 10 min 1 bath in post-fixative solution at ambient temperature – 45 min 3 rinses with distilled water – 3x 10 min	
Dehydration	
Successive baths in ethanol (50°-70°-95°-99°-99°) - 10 min each	
Critical Point Drying	
Samples dehydration was completed with critical point drying (CPD7501, Quorum Technologies)	

METALLIZATION
Samples were metallized with platinum in a Scancoat six Edwards sputter-unit and carbonated (to evacuate charges that could accumulate in non-conductive samples that would consequently be destroyed)

OBSERVATION
Samples were viewed with a scanning electron microscope Hitachi SU3500 operating at 20 kV, with the help of Geraldine Toutirais at the MNHN, Paris, France.

3. Transmission Electron Microscopy (TEM)

SAMPLES PREPARATION	
Fixation	
Fixative	Glutaraldehyde 2.5 % 35 mL filtered seawater (0.2 µm) + 10 mL distilled water + 5 mL glutaraldehyde 25%
Rinsing solution	Seawater / Sodium azide NaN_3 50 mL filtered seawater (0.2 µm) + 0.04 NaN_3
Samples were fixed for 4-16 h at 4°C. The fixative was then replaced by rinsing solution until the post-fixation step.	
Post-fixation	
Post-fixative solution	1 volume osmium 4% : 3 volumes distilled water
3 rinses with distilled water – 3x 10 min 1 bath in post-fixative solution at ambient temperature – 45 min 3 rinses with distilled water – 3x 10 min	
Dehydration	
Successive baths in ethanol (50°-70°-95°-99°-99°) - 10 min each 1 bath in ethanol 99% / propylene oxide – 10 min 1 bath in propylene oxide – 10 min	
Embedding	
Epoxy resin	Epon812 6 g + Dodecenyl succinic anydride DDSA 2.25 g + Methyl nadic anhydre MNA 3.75 g + BDMA 0.35 g
1 bath in ¼ epon / ¾ propylene oxide – ½ day 1 bath in ½ epon / ½ propylene oxide – ½ day 1 bath in ¾ epon / ¼ propylene oxide – ½ day 1 bath in pure epon -1 h à 50°C under vacuum Embedding in pure epon – 48 h at 60°C	

SECTIONING
Embedded samples were sectionned (70-80 nm) with an ultramicrotome (Leica, Ultracut R). Sections were dropped on copper grids (150, 200 or 300 mesh) eventually covered with formvar (Agar Scientific and Athene)

CONTRAST	
Contrasting agent	Saturated uranyl acetate (filtered 0.2 µm)
Grids were dropped off (sample side) on the contrasting agent on a heating device at 60°C for 15-20 min protected from the light (uranyl acetate solutions are photolabile). Grids were than washed by 20 consecutive immersions in 3 beakers of distilled water (filtered 0.2 µm), and dried on filter paper (blank side)	

OBSERVATION
Grids were viewed with a transmission electron microscope Hitachi H7100 operating at 75 kV, with the help of Chakib Djebiat at the MNHN, Paris, France.

4. Epifluorescent and confocal microscopy

SAMPLES PREPARATION	
Fixation	
Fixative	Formaldehyde 4% prepared with Phosphate Buffered Saline (PBS) 0.1 M
Rinsing solution	PBS 0.1 M pH 7.4
Samples were fixed for 24-48 h at 4°C. The fixative was then replaced by rinsing solution until the dissection step.	
Dissection	
Brains were dissected in PBS under a binocular microscope	
Embedding	
Dissected brains were embedded in low-gelling agarose 3 %	

SECTIONING
Brains were sectioned (100 µm) in the horizontal plane with a vibratome (Zeiss Hyrax V-50)

ANTIBODY STAINING	
Pre-incubation	
Brain sections were pre-incubated for 2x30 min in PBT (PBS + 0.3 % Triton-X100 + 1 % bovine serum albumin) to improve antibody penetration. Sections were then washed in PBS 0.1 M 6x30 min.	
Primary antibody incubation	
Primary antisera*	Monoclonal anti-SYNORF1 synapsin antibody (DSHB, 3C1 1; from mouse) Polyclonal anti-A-allatostatin antiserum (A-type Dip-Allatostatin I; Jena Bioscience, abd-062; from rabbit)
Brain sections were incubated overnight in the primary antisera at room temperature. Sections were then washed in PBS 0.1 M 6x30min.	
Secondary antibody incubation	
Secondary antisera	Alexa Flour 488 (goat, anti-rabbit) Cy3 (goat, anti-mouse) + HOECHST 33258 (Sigma, 14530) as nuclear marker
Brain sections were incubated overnight in the secondary antisera at room temperature. Sections were then washed in PBS 0.1 M 6x30min.	

*Antibody specificity is detailed below.

OBSERVATION
Sections were mounted in Mowiol 4-88 (Roth, No. 0713.2) and viewed with a Nikon Eclipse 90i epifluorescent microscope and with a Leica TCS SP5II confocal laser-scanning microscope equipped with DPSS, Diode- and Argon-lasers and operated by Leica "Application Suite Advanced Fluorescence" software package (LASAF), with the help of Rebecca Meth at the Zoological Institute and Museum, Greifswald, Germany. Digital images were processed with LIF and Fiji softwares. Only the global picture enhancement features (brightness and contrast) were used.

Antibody specificity (from Meth et al. 2017)

Synapsin[(GLOSSARY)]

The monoclonal anti-SYNORF1 synapsin antibody (DSHB Hybridoma Product 3C11; anti SYNORF1 as deposited to the DSHB by E. Buchner) was raised against a *Drosophila melanogaster* GST-synapsin fusion protein and recognizes at least four synapsin isoforms (70, 74, 80 and 143 kDa) in western blots of *D. melanogaster* head homogenates (Klagges et al. 1996). Similar to the fruit fly, the antibody consistently labels brain structures in major subgroups of the malacostracan crustaceans (e.g. Beltz et al. 2003; Harzsch et al. 1998, 1999; Krieger et al. 2012) in a pattern that is consistent with the assumption that this antibody labels synaptic neuropils in crustaceans.

A-type Dip-allatostatin I

The A-type allatostatins[(GLOSSARY)] represent a large family of neuropeptides that were first identified from the cockroach *Diploptera punctate*. The polyclonal rabbit allatostatin antiserum was raised against the *D. punctata* A-type Dip-allatostatin I, APSGAQRLYGFGL amide, coupled to bovine thyroglobulin using glutaraldehyde (Vitzthum et al. 1996). It has previously been used to localize A-type allatostatin-like peptides in crustacean and insect nervous systems (e.g. Kreissl et al. 2010, Polanska et al. 2012). In the text, the term allatostatin immunoreactivity is used to indicate that the antibody most likely binds to various related peptides within this peptide family.

5. X-ray micro-computed tomography

SAMPLES PREPARATION	
Fixation	
Fixative	Bouin (Sigma)
Full samples remained in the fixative until the rinsing and dehydration step.	
Rinsing and dehydration	
Successive baths in ethanol (30°-50°-60°-70°-80°-90°-96°-99°-99°) – 30 min each	

CONTRAST
Full samples were contrasted in iodine, rinsed in ethanol 99° 2x30 min and critical point dried to enhance the contrast

OBSERVATION
Full samples were scanned dry (scan medium air) using a XRadia XCT-200 that use a 90 kV/8 W tungsten x-ray source and switchable scintillator-objective lens units, with the help of Jakob Krieger, Marie Hörnig and Andy Sombke at the Cytology and Evolutionary Biology department, Greisfwald, Germany.
3D reconstruction
Tomography projections were reconstituted using the reconstruction software provided by Xradia, resulting in image stacks (DICOM format). The 3D volume reconstructions of the image stacks were performed using the software AMIRA (VSG), with the help of Jakob Krieger at the Cytology and Evolutionary Biology department, Greisfwald, Germany.

III. Experiments on live animals

1. Electroantennography (EAG)

1.1. Specimens

Specimens of *M. fortunata* and *P. elegans* were transferred to the INRA laboratory (Neuro-Ethology of Olfaction team, Sensory Ecology department, iEES institute, Saint-Cyr, France) for the electrophysiological experiments. Each species was housed communally in a 80 L-aquarium with oxygenated artificial sea water (Red Sea Salt, Red Sea, Houston, TX, USA) under a natural light:dark cycle. *P. elegans* specimens were kept at room temperature (21±1°C). *M. fortunata* specimens were kept at 9±1°C with a 50 W thermostat heater (set to 25°C) to serve as a hot spot. The shrimps were starved for at least 48 h to prevent any potential adaptation of their chemosensory neurons to food odors. During starvation, *P. elegans* were isolated individually in 18 L-aquaria to prevent cannibalism.

➔

A. Sketch of the biological preparation used to record EAG responses from antennal appendages. The shrimp is held in a pipette cone, ventral face to the top, with the anterior region immerged in PS solution. PS is also continuously perfused over the branchial cavity, while a second perfusion allows the evacuation of solution from the bath. The recording electrode is inserted in the antennal appendage, and the reference electrode is inserted between the abdomen and the telson. The stimulation device is inclined in order to stimulate the overall length of the recorded organ. Not to scale. PS, *Panulirus* saline.
B. Perspective sketch of the lateral antennule (here of *P. elegans*), showing the insertion of the recording electrode through the cuticle, between two rows of aesthetascs. When a chemical solution stimulates the sensilla, it activates the innervating chemosensory neurons, which produce an electrical field potential, recorded by the electrode. The neuron and axon clusters representation is speculative. Not to scale.
C. Functional diagram of the EAG set up. The stimulation protocol, defined under the Clampex software, is transmitted by the acquisition board to the electrovalves. According to the procedure selected, an electrovalve opens, which allows the passage of the stimulus from a pressurized reservoir to the biological preparation, via the manifold. The biological electrical signal is recorded by the electrodes, amplified and digitized by the acquisition board and the computer.

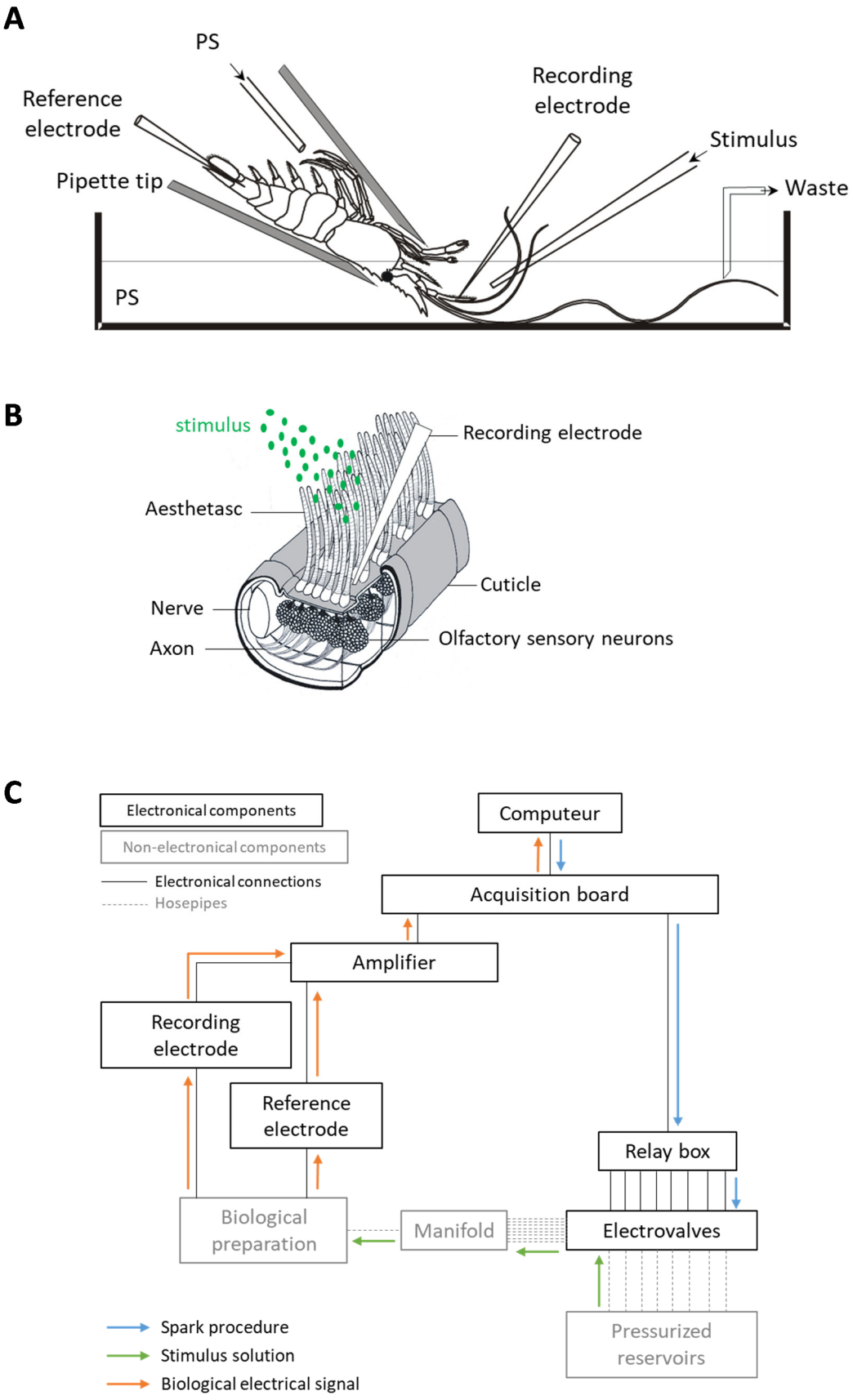

Figure 22 Sketches of biological preparation, recording electrode connection and EAG set up

Legend previous page.

1.2. Biological preparation

The EAG experimental design is sketched in Figure 22A and Figure 23. The shrimp was restrained in a 1 mL or 5 mL pipette tip cut according to the shrimp size with the antennal appendages and the posterior part of the abdomen out at each extremity of the cone. The shrimp was placed ventral face to the top to have direct access to the ventral side of the antennule bearing the aethetascs. The preparation was attached to a UM-3C micromanipulator (Narishige, London, UK) and angled at approximately 45° so that the anterior part of the animal (i.e. antennal appendages) was submerged in a Petri dish filled with *Panulirus* saline (PS, see composition in section 1.4) and the posterior part (i.e. telson and abdomen) remained in air. A gravity-fed PS perfusion was inserted in the pipette tip just over the cephalothorax, to irrigate the branchial cavity and keep the animal alive, and to renew the PS bath solution. The antennules were immobilized with U shape tungsten hooks on a piece of Styrofoam stuck on the bottom of the Petri dish. The preparation was visualized under a dissecting microscope (M165C, Leica, Nanterre, France). For *P. elegans*, experiments were done at room temperature (21±1°C). For *M. fortunata*, the PS perfusion was cooled to 9±1°C using frozen blocks.

➔

A. Global view of the EAG apparatus within a Faraday cage. b, biological preparation; f, Faraday cage; m, micromanipulateur (m_1, recording electrode; m_2, shrimp holder; m_3, stimulator; m_4, reference electrode); t, magnetic table.

B. Devices around the biological preparation. a, amplifier headstage; b, biological preparation; m', manifold (two entries connected to the stimulation device); of, optic fibers.

C. Biological preparation and electrodes connection. a, amplifier headstage; cp, pipette cone; E_{rec}, recording electrode; E_{ref}, reference electrode; m', manifold exit; of, optic fibers; PS, *Panulirus* saline solution; p, PS perfusion over the branchial cavity; s, shrimp; w, waste perfusion.

D. Pressurized stimulation device with 8 channels. Ev, electrovalves; g, gaz entry (air or nitrogen); m'', manometer; R, pressurized reservoirs.

E. Immobilization of the lateral antennule of *P. elegans* for EAG recordings. E_{rec}, recording electrode; th, tungsten hook; r_{int}, intern ramus of the lateral flagellum of the antennule; r_{ext}, extern ramus of the lateral flagellum of the antennule; sty, styrofoam; sc, scaphocerite.

F. Connection of the recording electrode within the internal ramus of the lateral antennule of *P. elegans*. aes, aesthetascs; E_{rec}, recording electrode; r_{int}, internal ramus of the lateral flagellum of the antennule; r_{ext}, external ramus of the lateral flagellum of the antennule; sty, Styrofoam.

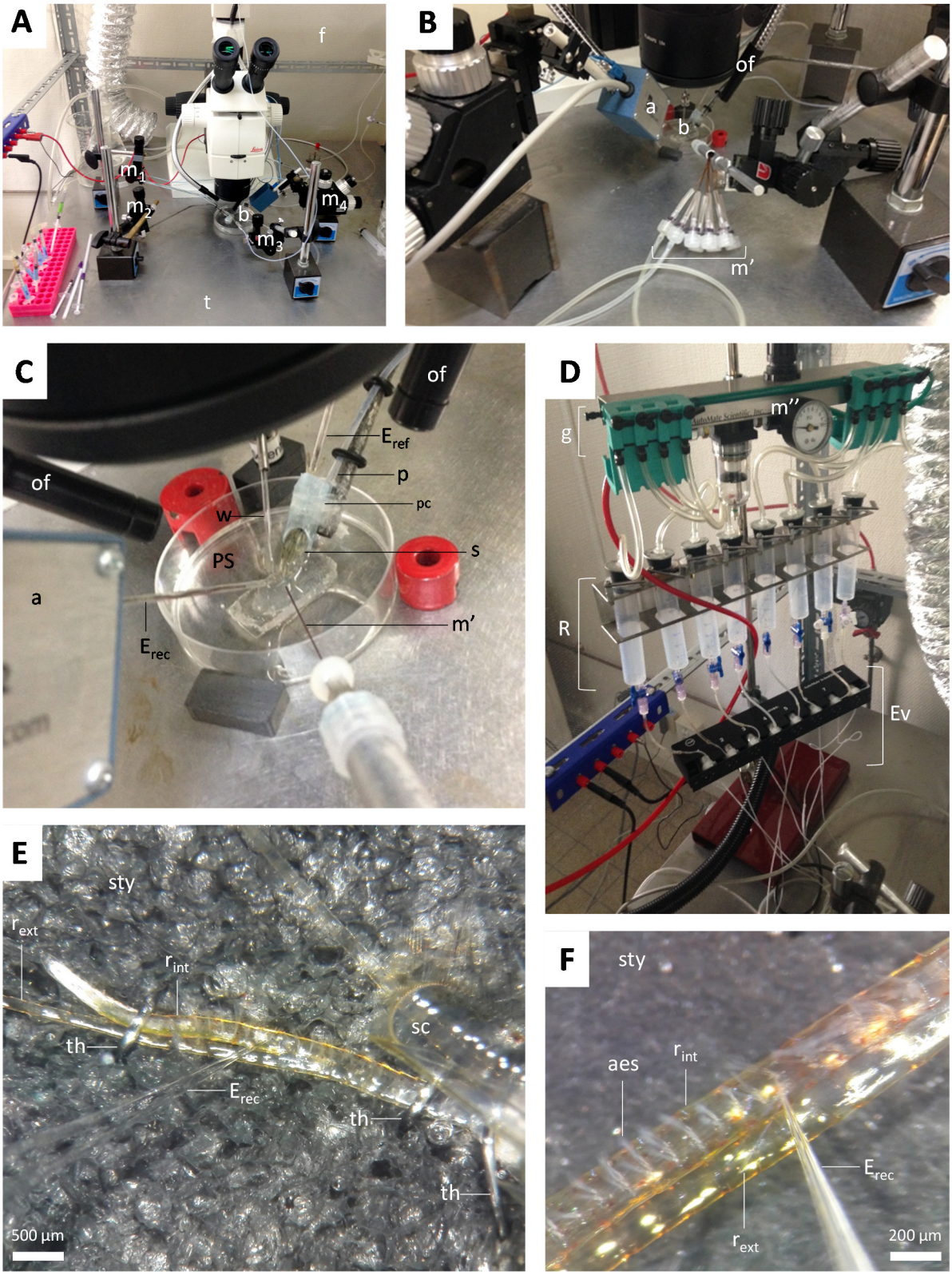

Figure 23 EAG set up illustrations

Legend previous page.

1.3. Recordings, stimulus delivery and analysis

Electrodes were pulled from GB150F-8P glass capillaries (Science Products, Hofheim, Germany) using a P-97 puller (Sutter Instrument, USA). They had a tip diameter of 1 to 2.5 µm and were filled with PS. The reference electrode was introduced through the soft articular membrane between the telson and the abdomen. The recording electrode was inserted with a NMM-25 micromanipulator (Narishige, London, UK) in the base, middle or apex region of the antennule bearing the aesthetascs, between two aesthetasc rows (Figure 22B; Figure 23E,F), or in the proximal region of the antenna. Signals were amplified (x100) and filtered (0.1-1000 Hz) using an EX1 amplifier with a 4002 headstage (Dagan, Minneapolis, USA), and digitized at 2 kHz by a 16-bit acquisition board (Digidata 1440A) under Clampex 10.3 (Molecular Devices, Union City, USA) (Figure 22C). Data were analyzed using Clampfit (Molecular Devices). Signals were low-pass filtered offline at 20 Hz with a Gaussian low-pass filter. Data are given as mean ± s.e.m.

To deliver chemical stimuli, a pressurized perfusion system with 8 channels (AutoMate Scientific, Berkeley, CA) was used (Figure 23D). For stimulations with hydrothermal fluid compounds, the perfusion system was pressurized with nitrogen gas to prevent the oxidation of the solutions within the reservoirs. Each reservoir was connected to one entry of a MPP-8 multi-barrel manifold**(GLOSSARY)** (Harvard Apparatus, Les Ulis, France). A segment (60 mm) of deactivated gas chromatography (GC) column (0.25 mm internal diameter) was glued to the manifold exit. The manifold was mounted onto a UM-3C micromanipulator and the tip of the stimulus GC column was positioned approximately 1.5 mm from the recorded flagellum in its longitudinal axis.

Stimuli were applied for 1 s at 5 psi (1.1 $mL.min^{-1}$). Consecutive stimuli were delivered with at least 2 min intervals to prevent chemosensory adaptation. To establish the dose-response relationship for a food odor stimulus (positive control, see section 1.4), stimuli were applied in increasing concentrations. To analyze the local and global response patterns, glass capillaries with two diameters were used to stimulate wide and narrow portions of the antennule (0.86 mm and 100 µm internal diameter, respectively) perpendicular to the antennule axis. Responses to the positive control were measured at the beginning and at the end of each stimulation series to ensure that the quality of recording remained constant throughout the experiment. Recordings of low quality (i.e. amplitude of responses to the positive control inferior to 0.3 and 0.08 mV for the antennule and the antenna, respectively) were excluded from the analysis. When responses to the negative control had different amplitudes at the beginning and at the end of an experiment, the average of the two values was used.

1.4. Chemicals

Stimuli, concentrations and controls used for EAG are given in Table 6.

Table 6 Stimuli and concentrations tested with EAG on *M. fortunata* and *P. elegans*

Stimulus	Concentrations, dilutions	Use
Shrimp food extract	0.2 $g.mL^{-1}$	Positive control
Panulirus saline (PS)	-	Negative control
PS pH 6	-	pH control for $FeCl_2$
PS pH 11	-	pH control for Na_2S 14 $mmol.L^{-1}$
Mussel extract	0.5 $g.mL^{-1}$	Food odor stimulus
Crab extract	0.1 $g.mL^{-1}$	Food odor stimulus
Dead shrimp extract	non diluted (75 $mg.mL^{-1}$); 1:10; 1:100	Food odor stimulus
Na_2S	0.04, 0.1, 0.4, 1, 4, 40, 300, 2000, 14000 $\mu mol.L^{-1}$	Hydrothermal fluid stimulus
$FeCl_2$	0.05, 0.1, 0.5, 1, 5, 60, 900, 10000 $\mu mol.L^{-1}$	Hydrothermal fluid stimulus
$MnCl_2$	0.05, 0.1, 0.5, 1, 5, 50, 500, 3500 $\mu mol.L^{-1}$	Hydrothermal fluid stimulus

- **Positive and negative controls**

A *Panulirus saline* (PS) solution (composition in $mmol.L^{-1}$: 486 NaCl, 5 KCl, 13.6 $CaCl_2$, 9.8 $MgCl_2$ and 10 Hepes, pH 7.8-7.9; Hamilton and Ache, 1983) was used as a negative control, and for the preparation of stimuli. The osmotic pressure was adjusted to 1050 $mOsm.L^{-1}$ with mannitol.

An aqueous extract of shrimp food pellets (Novo Prawn [NP]) was used as positive control in all experiments, and for the determination of recording parameters. The pellets were dissolved for 48 h at room temperature at 0.1 or 0.2 $g.mL^{-1}$ in PS. The extracts were then centrifuged at 5900 g for 10, 15 and 20 min and the supernatants were collected after each centrifugation and filtered (0.45 µm), aliquoted and stored at -20°C until use.

- **Food odor stimuli**

Aqueous extracts of dead *M. fortunata* and *P. elegans* individuals were prepared, from dead specimens kept in PS for 48 h at room temperature at approximately 75 $mg.mL^{-1}$. Extracts were then centrifuged at 2000 g and the supernatant was filtered (0.45 µm), aliquoted and stored at -20°C. Before use, pH was adjusted to 7.8-7.9 and solutions were diluted 10 and 100 times. Aqueous extracts of green crab *Carcinus maenas* and blue mussel *Mytilus edulis* individuals were prepared from fresh

material at approximately 0.1 and 0.5 g.mL^{-1} in PS, respectively, using the same protocol as described above. Osmolarity (1050 mOsm.L^{-1} with mannitol) and pH (7.85 with NaOH) were adjusted for all solutions.

- **Hydrothermal fluid chemical stimuli and pH controls**

For common chemical stimuli of the hydrothermal fluid (sulfide, iron and manganese), dose-response relationships were established with concentrations (Figure 24) in the range of those that *M. fortunata* is likely to encounter it its environment (sulfide, 5-38 µmol.L^{-1}; iron, 0.2-2.5 µmol.L^{-1} [Sarrazin et al. 2015]; manganese, 0.004-4.8 µmol.L^{-1} [Aumond 2013]) to concentrations in the range of those of the hydrothermal fluid at the Lucky Strike site (sulfide, 2-15 mmol.L^{-1} [Renninger et al. 1995]; iron, 30-863 µmol.L^{-1}; manganese, 50-450 µmol.L^{-1} [Charlou et al. 2000]). To minimize oxidation, all solutions were prepared under a funnel connected to a nitrogen gas cylinder, with PS previously deoxygenated by bubbling nitrogen for 5-10 min. All dilutions were made the day of use.

For the concentrations of *M. fortunata* close environment, stock solutions were prepared at 2 mmol.L^{-1} in deoxygenated PS, with pH adjusted to 2 for $FeCl_2$ (reference 372870, Sigma-Aldrich) and $MnCl_2$ (reference M8054, Sigma-Aldrich) solutions, and to 9 for Na_2S (reference 208043, Sigma-Aldrich) solution. Stock solutions were diluted with deoxygenated PS. The concentrations 40 µmol.L^{-1} for Na_2S and 5 µmol.L^{-1} for $FeCl_2$ and $MnCl_2$ correspond to the estimated concentrations in the environment of *M. fortunata* (Sarrazin et al. 2015 for iron and sulfide, Aumond 2013 for manganese). For higher concentrations, 4 concentrations were chosen on a logarithmic scale, the lowest corresponding to the estimated concentration in the environment of *M. fortunata*, and the second highest corresponding to the concentration measured in the pure fluid at the Lucky Strike vent site (Charlou et al. 2000). Solutions were prepared in deoxygenated PS with serial dilutions from the highest concentration. For $FeCl_2$ solutions, pH was adjusted to 6 to avoid iron precipitation. PS adjusted to pH 6 was used as a pH control for $FeCl_2$ stimulation, and PS adjusted to pH 11 was used as a pH control for Na_2S stimulation series, to match the pH of the highest concentrated Na_2S solution (14 mmol.L^{-1}).

1.5. Statistical analysis

One-way ANOVA with permutation test was used to test differences among amplitudes of EAG responses to concentrations of each stimulus. For significant results, two-sided one-sample or two-sample permutation test using Welsh t test was performed to investigate the difference with reference values (0 or 1) or with the negative control for each condition/concentration. Data are given as means ± s.e.m. Data analyses were carried out using RStudio v.1.0.136 software.

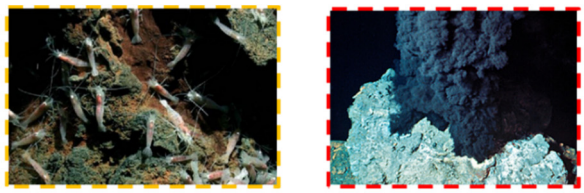

$FeCl_2$	0,05	0,1	0,5		1	5	63	900	10000
$MnCl_2$	0,05	0,1	0,5		1	5	45	500	3500
Na_2S	0,04	0,1	0,4	4	1	40	282	2000	14000

µmol.L^{-1}

Figure 24 Concentrations of hydrothermal fluid compounds tested with EAG

Concentrations of $FeCl_2$, $MnCl_2$ and Na_2S tested on *M. fortunata* and *P. elegans* with the EAG. Concentrations include those measured in the habitat of *M fortunata* (yellow boxed numbers) and the the pure fluid at the Lucky Strike site (red boxed numbers).

2. Behavior experiments

Species and origin of the samples used for behavior experiments are summarized in Table 7.

Table 7 Summary of behavior experiments, species and sampling origin

Pressure condition	Stimuli	Species	Sites	Sampling
Atmospheric	Food odor sources, sulfide	*M. fortunata*	Lucky Strike (37°18'N,32°16'W)	MOMARSAT 2014, 2017
		P. elegans	Baie de St Malo (48°38'N,2°0'W)	2015, 2016, 2017
	Temperature	*M. fortunata*	Lucky Strike (37°18'N,32°16'W)	MOMARSAT 2016
		P. elegans	Baie de St Malo (48°38'N,2°0'W)	2016, 2017
*In situ**	Food odor sources, sulfide	*M. fortunata*	Snake Pit (23°22'N,44°57'W) ;	BICOSE 2018
		R. exoculata	TAG (26°8'N,44°49'W)	BICOSE 2018
		M. fortunata	Menez Gwen (37°85'N,31°51'W)	BIOBAZ 2013

*Experiments at *in situ* pressure on *M. fortunata* and *R. exoculata* were conducted on the vessel "Pourquoi Pas?" (Ifremer) during the BICOSE 2018 cruise, for which the AMEX team (including Bruce Shillito, Magali Zbinden, Louis Amand and I) was part of the scientific crew. The pressure devices VISIOCAMP, PERISCOP and BALIST were used and are presented in Chapter I, section III. Preliminary experiments on *M. fortunata* were conducted during the BIOBAZ 2013 cruise by Juliette Ravaux, Magali Zbinden and Bruce Shillito.

2.1. Experiments at atmospheric pressure on *P. elegans* and *M. fortunata*

2.1.1. Attraction tests to food odor sources and sulfide

- **Two-choice experiments on single individual of *P. elegans* and *M. fortunata***

For *P. elegans*, two-choice experiments were conducted in a plastic tank (32x18x18 cm). The shrimps were starved at least for 48 h before the experiment. A shrimp was placed in the tank filled with 8 L seawater at room temperature, and allowed to explore for 5 min before the beginning of the trial. Two little bags made of compress tissue were then introduced just below the water surface, one containing mussels without shell (food source) and the other only compress tissue (lure) (Figure 25A). The shrimp was further observed for 10 min. After each trial, the tank was cleaned and refilled with fresh seawater.

To examine the role of the antennules in food localization behavior, two ablations were tested: lateral antennule or both medial and lateral antennule (Figure 25B). Ablated shrimps recovered for one week prior to being tested. 20 shrimps were tested for each condition. Preliminary tests were conducted under red light and dim light to reduce the visual cues, but the behavior was similar to that observed under room light (fluorescent tube) (data not shown).

For *M. fortunata*, the same experiments were conducted at the Oceanopolis in a glass tank (30x20x20 cm) filled with 8 L seawater at 10°C, as described above. No ablations were tested for *M. fortunata* since no attraction to food-related odor was observed for non-ablated specimens (see Chapter V).

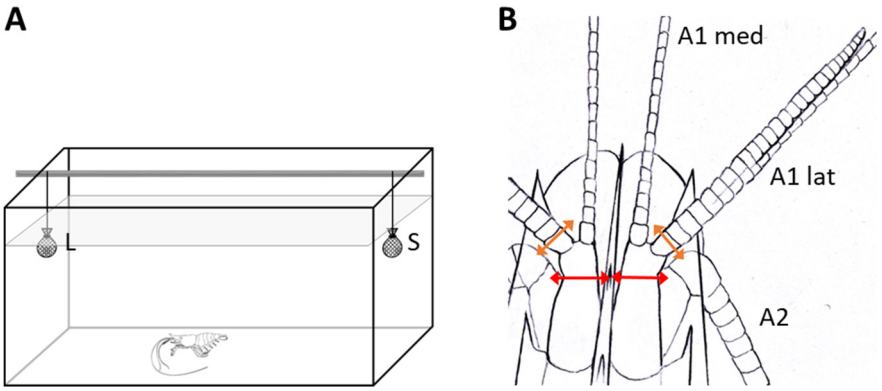

Figure 25 Setup for two-choice experiments on single *P. elegans* and *M. fortunata*

A. Experimental setup. The shrimp was first placed in the tank for 5 min (*P. elegans*, room temperature; *M. fortunata*, 10°C). The stimulus (S, food odor source) and the lure (L) were then immersed under the water surface and the shrimp was observed for 10 min. **B.** Antennules ablations in *P. elegans*. Orange arrows, ablation of lateral antennules; red arrows, ablation of both medial and lateral antennules. A1 lat, lateral antennule; A1 med, medial antennule; A2, antenna.

- **Multiple-choice experiments on single individual of *P. elegans* and *M. fortunata***

For *P. elegans*, multiple-choice experiments were conducted in a glass tank (50x30x35 cm) filled with 8 L seawater at room temperature. 0.5 % Agarose gels were prepared with either seawater (control gel), mussel extract (0.1 $g.mL^{-1}$) (food-related odor gel), Na_2S (2 $mmol.L^{-1}$) (sulfide gel) or a mixture of mussel extract and sulfide at the same concentrations (food-sulfide gel). 20 mL gels were casted in the bottom of 50 mL black tubes (Falcon). For each trial, three control gel tubes and one stimulus gel tube were introduced in the bottom of the tank at each corner, the opening of the tube facing the center of the tank (Figure 26). The position of the stimulus was randomized in each trial. A shrimp was placed in the tank and its behavior was video recorded from above with a camera (Canon Legria camescope) for 30 min. After each trial, the tank was cleaned and refilled with fresh seawater.

For *M. fortunata*, the same experiments were conducted at the Oceanopolis aquarium in a plastic tank (32.5x17.5x19 cm) filled with 8 L seawater at 10°C. The food-related odor gel was prepared with shrimp food (0.1 $g.mL^{-1}$; Liptoaqua food pelets, Liptosa, Madrid, Spain). The two species were starved for at least 48 h before the experiment.

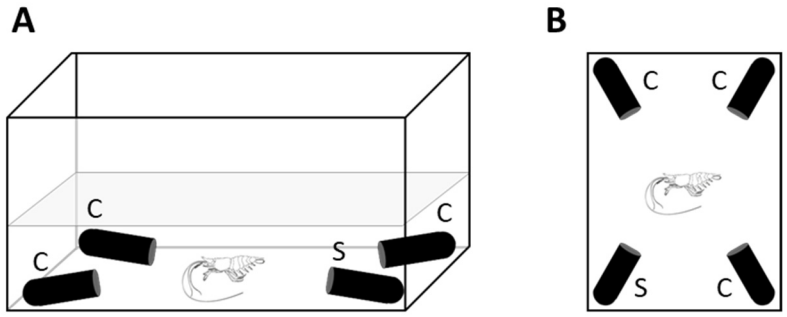

Figure 26 Setup for multiple-choice experiments on single *P. elegans* and *M. fortunata*

Perspective (**A**) and from above (**B**) views of the experimental setup. The shrimp was placed in the tank (*P. elegans*, room temperature; *M. fortunata*, 10°C) after the introduction of four tubes containing agarose gels (three controls [C], one stimulus [S]) in each corner of the tank. The shrimp behavior was video recorded for 30 min from above.

- **Two-choice experiments on multiple individuals of *M. fortunata***

Two-choice experiments were conducted at the Oceanopolis aquarium in rearing glass tanks (40x40x40 cm) filled with 80 L seawater at 10°C and containing an aquaria heater set to 25°C. Each tank contained several *M. fortunata*. 0.5 % Agarose gels were prepared with either seawater (control gel), shrimp food extract (0.1 $g.mL^{-1}$; Liptoaqua food pelets, Liptosa, Madrid, Spain) (food-related odor gel), Na_2S (2 $mmol.L^{-1}$) (sulfide gel) or a mixture of food extract and sulfide at the same concentrations (food-sulfide gel). The gels were casted in 20 mL cubic molds. For each replica, a control gel and a

stimulus gel were introduced on each side of the tank (Figure 27). The position of the stimulus was randomized for each replica. The heater used for rearing was left ON. The shrimp behavior was observed for 30 min.

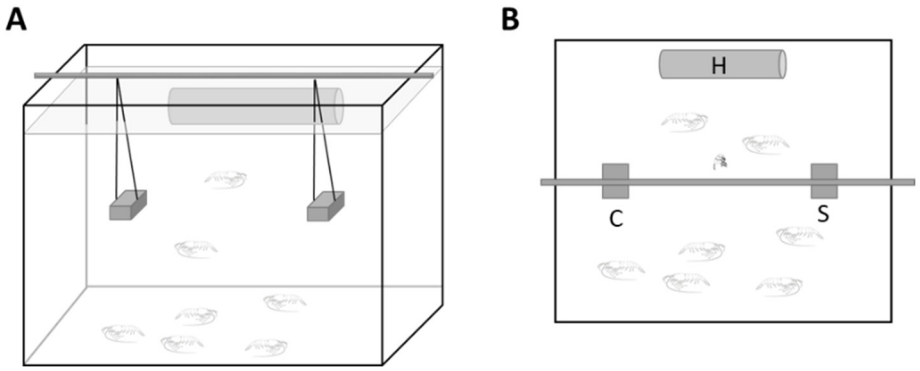

Figure 27 Setup for two-choice experiments on multiple *M. fortunata*

Perspective (**A**) and from above (**B**) views of the experimental setup. The experiments were conducted in 9°C rearing tanks containing several individuals of *M. fortunata* with one thermostat heater (H). Two gels (one control [C], one stimulus [S]) were introduced on each side of the tank. The shrimp were observed for 30 min.

2.1.2. Attraction test to warm temperatures

- **Choice experiments between ON and OFF heaters on multiple individuals of *P. elegans* and *M. fortunata***

Choice experiments were conducted in glass tanks (40x40x40 cm) filled with 80 L seawater at 9°C containing several *M. fortunata* and *P. elegans*, at the Oceanopolis aquarium. Seawater was continuously renewed. Thermostat heaters were used as a hot spot stimulus. Each heater was covered with foam fixed with 3 plastic collars, the position of which defined four zones (1-4) along the heater (Figure 28A,C). Thermal gradient along the heater in the tank was measured with a temperature probe at 20 points along the foam surface (Figure 28A). Positioning of the heaters close to the entrance of new seawater or to the opposite side of the tank did not modified the thermal gradient (not shown). Temperature gradient as well as mean temperature per zone is presented in Figure 28D.

For *P. elegans*, a batch of shrimps was placed in a tank and acclimated for 1 h with no heater. Two heaters (one turned ON, one turned OFF) were then introduced in the tank on each lateral side, in an upper position. The number of shrimps on each resistance was counted at different time intervals for 180 min. For each consecutive 180 min trial, the heaters were inverted. For *M. fortunata*, two batches of shrimps already present in their rearing tanks were tested, as described above. 6 and 4 trials were conducted on *M. fortunata* and *P. elegans* respectively, and repeated on a second batch for each species. Two trials were extended overnight.

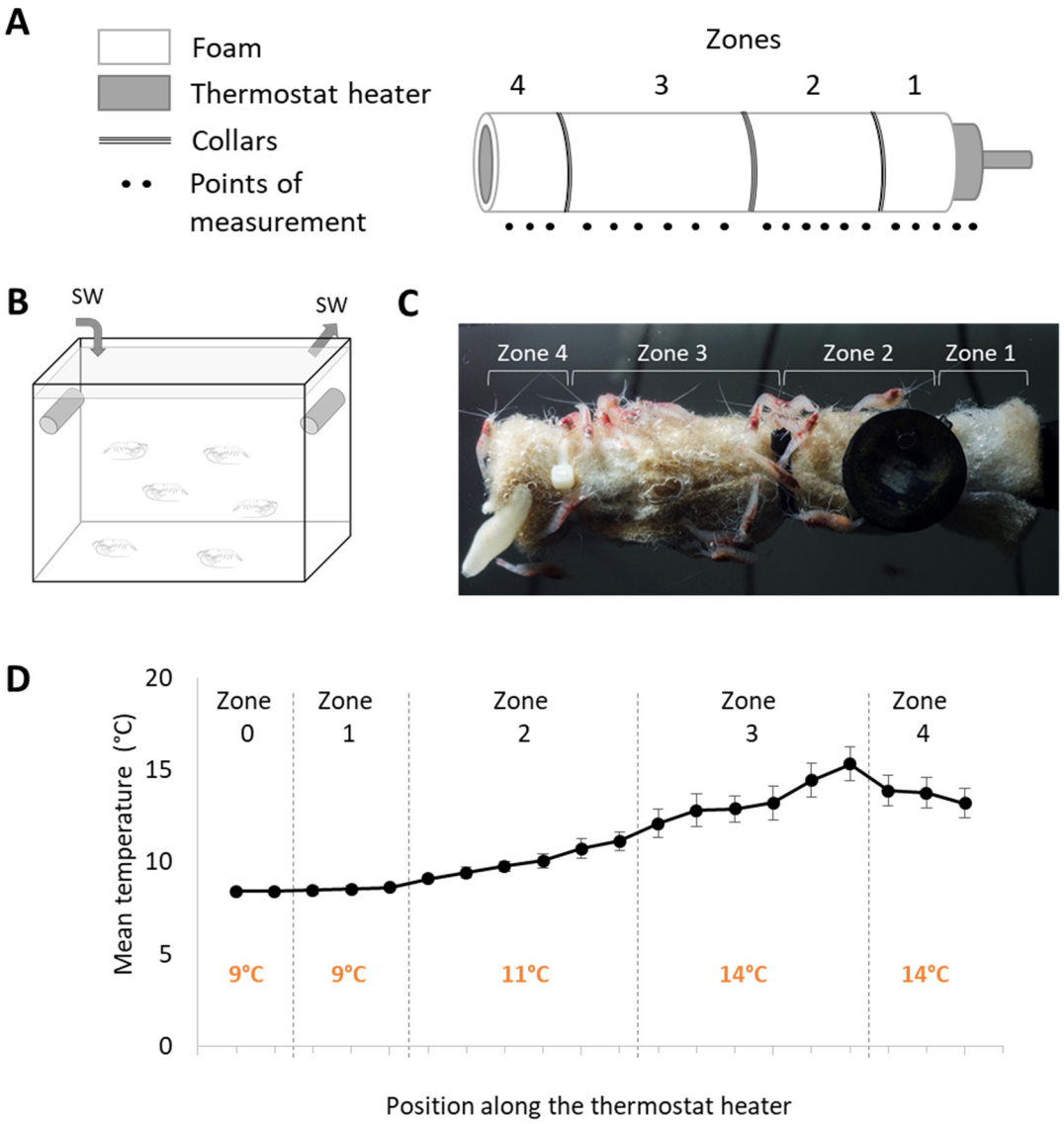

Figure 28 Setup for choice experiments between ON and OFF thermostat heaters on multiple *P. elegans* and *M. fortunata*

A. Sketch of a thermostat heater covered by foam fixed with plastic collars that define 4 zones along the heater, and points of measurements for establishing the thermal gradient.
B. Experimental setup. The experiments were conducted in 9°C rearing tanks containing several individuals of *P. elegans* or *M. fortunata.* Two heaters (one turned ON, one turned OFF) were introduced and positioned on the lateral sides of the upper region of the tank. Shrimp position over each heater was measured for 180 min and eventually overnight. Arrows indicate the entrance and the exit of the renewing seawater system. SW, seawater.
C. View of a heater turned ON, with several individuals of *M. fortunata*. (Credits: D. Barthelemy / Océanopolis).
D. Thermal gradient along the foam surface, with mean (± s.e.m.) temperature at each point of measurement (indicated in A), and mean temperature (orange) for each zone.

2.2. Experiments at *in situ* pressure on *M. fortunata* and *R. exoculata*

- **Experiment in the IPOCAMP aquarium with multiple individuals of *M. fortunata***

An experiment at *in situ* pressure was conducted during the BIOBAZ (2013) cruise, in the IPOCAMP aquarium, to test the attraction to sulfide. The shrimps were sampled from the Menez Gwen site (800 m depth) and recovered in the IPOCAMP aquarium at 70 bars, 9°C for 1 h. Three successive pulses of increasing concentrations of sulfide were applied by injecting 3 L of Na2S solutions at 25, 50 and 100 µmol.L-1 via the recirculating seawater system entrance, with one hour interval between each pulse (Figure 29). The shrimp behavior was video recorded during the whole experiment. The number of shrimps in a 6 cm² surface around the pulse entrance was counted for 5 min prior and 10 min after the beginning of each pulse.

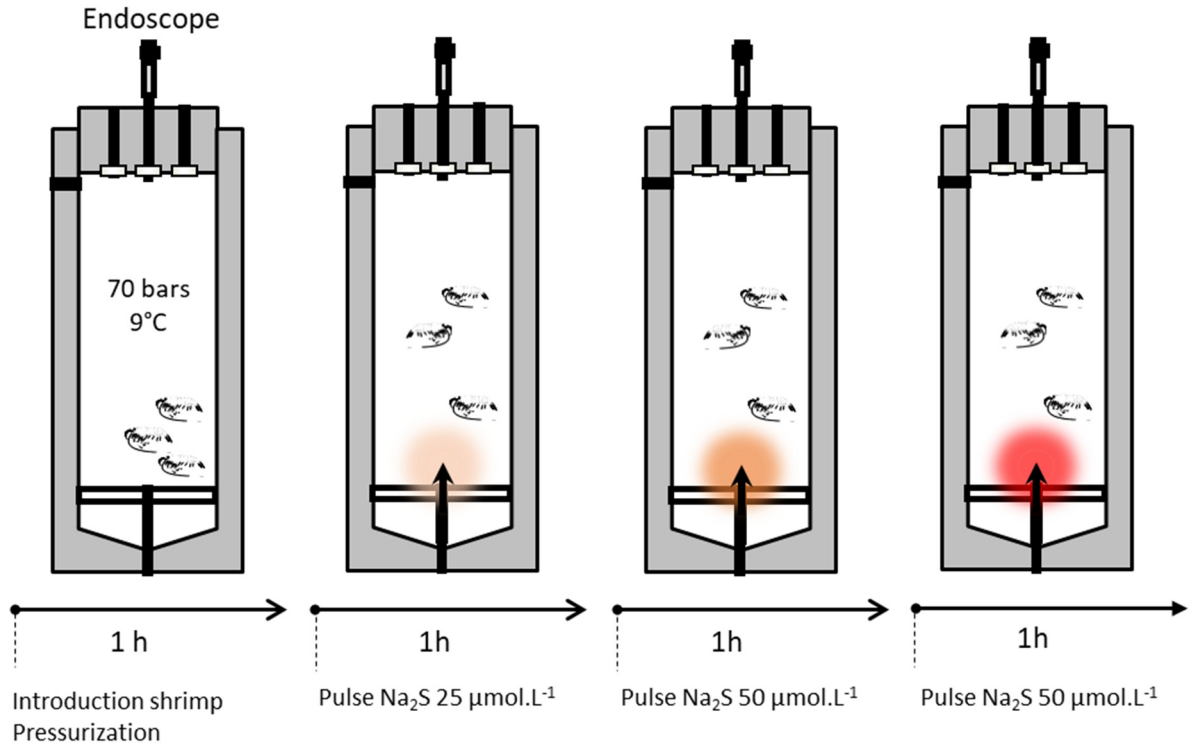

Figure 29 Setup for preliminary experiment at *in situ* pressure on multiple *M. fortunata*

Experimental setup. Just after sampling, a batch of shrimps was placed in the IPOCAMP aquarium and maintained at 70 bars, 9°C for 1 h before the beginning of the experiment. Pulses of increasing concentrations of sulfide were injected from the bottom of the tank with 1 h interval. The shrimp behavior was video-recorded during the whole experiment.

- **Experiments in the VISIOCAMP aquarium with multiple individuals of *M. fortunata* and *R. exoculata***

Behavior experiments at *in situ* pressure were conducted during the BICOSE (2018) cruise, with diverse stimuli: 0.3% agarose gels were prepared with either seawater (control gel), mussel extract (food-related odor gel), or Na_2S (2 mmol.L^{-1}) (sulfide gel). When prepared with no pH adjustement, sulfide solutions are extremely basic (e.g. pH 11 for Na_2S 2 mmol.L^{-1}) and the main sulfide species under these pH conditions is bisulfide S^{2-}, which is poorly released. The release of sulfide under the Na_2S form (and H_2S form in the vent habitat) is greatly enhanced when the pH is forced below the dissociation constant (for H_2S, pKA = 7.05), for example using acid. To test the release of sulfide in conditions closer to the vent shrimp habitat, a gel was prepared with Na_2S (2 mmol.L^{-1}) at pH 4 (acid sulfide gel), and another prepared with seawater adjusted to pH 4 (pH control gel), using HCl.

The gels were casted in metal tubes (to be heavy enough to sink) previously drilled in 50 positions (to allow the diffusion of chemicals outside the gel). The shrimps were sampled from the vent sites (TAG, 3600 m depth; Snake Pit, 3500 m depth) with the PERISCOP device. On board, the PERISCOP was opened, and the shrimps were separated in three batches. One batch was placed at 300 bars, 10°C in the VISIOCAMP aquarium for the first replica experiment, and the two other batches were stored at 300 bars, 10°C in the BALIST aquarium for the second and third replica experiments. Two hours of recovery followed the re-pressurization step. Then, using an isobaric line on the VISIOCAMP lid (which allow the introduction of small elements without pressure variation [Shillito et al. 2015]), three agarose gels (two controls, one stimulus) were introduced in the tank consecutively with 45 min interval (Figure 30). The two control gels were always introduced first. The shrimp behavior was video recorded using a high-definition camera (AG-HCK10G HD camera head, AG-HMR10 portable recorded, Panasonic) during the whole experiment.

The diffusion of sulfide from the gel was measured on board with the help of Christophe Brandily (Ifremer). Briefly, one metal tube containing a sulfide gel prepared at 2 mmol.L^{-1} was placed in seawater in a 50 mL falcon tube. Sulfide concentration was measured in the surrounding seawater 2 and 3 hours after the gel introduction and was respectively 35 and 20 µmol.L^{-1}. There is a decrease of released sulfide overtime, consistent with its oxidation by seawater. In our behavior experiment, the sulfide gel diffuses during 45 min; it is likely that in the tank, close to the gel, sulfide do not exceed concentrations in the micromolar range.

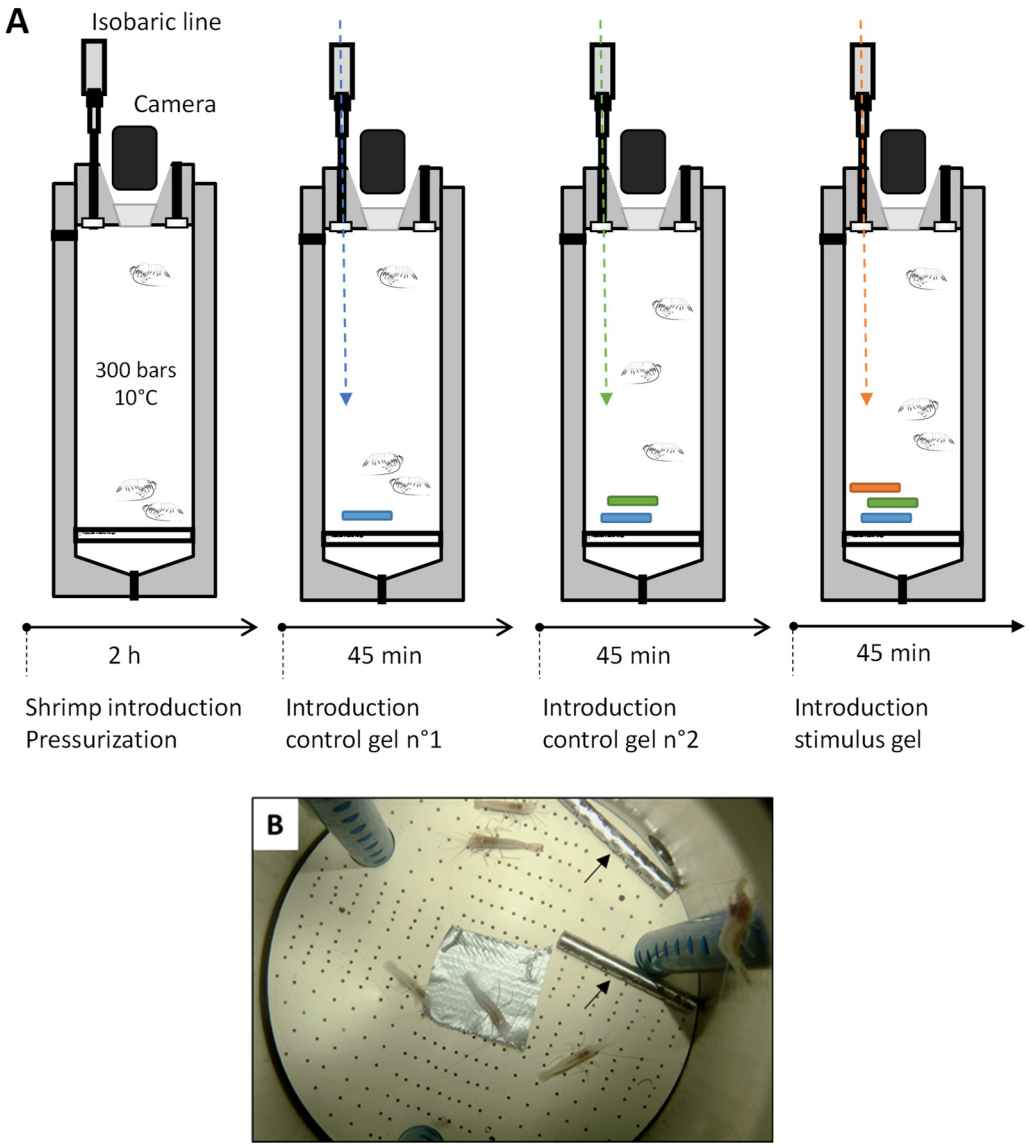

Figure 30 Setup for experiments at *in situ* pressure on multiple *M. fortunata* and *R. exoculata*

A. Experimental setup. Just after sampling, a batch of shrimps was placed in the VISIOCAMP aquarium and maintained at 300 bars, 10°C for 2 h before the beginning of the experiment. Two control gels and one stimulus gel were then introduced in the tank through an isobaric line at 45 min interval. The shrimp behavior was video-recorded during the whole experiment.
B. View inside the VISIOCAMP aquarium during the experiment, with several individuals of *M. fortunata* and two control gels inside drilled metal tubes (arrows).

IV. Molecular biology

1. RNA extraction and reverse transcription

Four hydrothermal species were used for molecular biology experiments (*Rimicaris exoculata, Rimicaris chacei, Mirocaris fortunata and Alvinocaris markensis*). Cruises and sampling sites are indicated in Table 8. The following organs were dissected: antennular medial and lateral flagella, the antennae and abdominal muscles. The coastal species *P. elegans* was also included in the analysis, for which the dissection included the following organs: antennular medial and lateral flagella (internal and external ramus separated), the antennae, the mouthparts (mandibles and 2 pairs of maxillae), the first and second walking legs and the eyestalks. All tissues were frozen in liquid nitrogen.

Table 8 Cruises and sites origin of the samples used for molecular biology

Sites	Latitude	Longitude	Depth (m)	Cruise, year	Ship/submersible	Chief scientist
Menez Gwen	37°51'N	31°31'W	840	Biobaz, 2013	Pourquoi Pas? / ROV Victor	F. Lallier
Lucky Strike	37°51'N	32°16'W	1700	Biobaz, 2013	Pourquoi Pas? / ROV Victor	F. Lallier
				Momarsat, 2011	Pourquoi Pas? / ROV Victor	M. Cannat
				Momarsat, 2012	Thalassa / ROV Victor	M. Cannat and P. M. Sarradin
Rainbow	36°13'N	33°54'W	2260	Biobaz, 2013	Pourquoi Pas? / ROV Victor	F. Lallier
TAG	26°08'N	44°49'W	3600	Bicose, 2014	Pourquoi Pas? / ROV Victor	M. A. Cambon-Bonavita
Snake Pit	23°23'N	44°58'W	3480	Bicose, 2014	Pourquoi Pas? / ROV Victor	M. A. Cambon-Bonavita

Frozen tissues were ground in TRIzol Reagent (Thermo Fisher Scientific) with a Minilys homogenizer (Bertin Corp.). Total RNA was isolated according to the manufacturer's protocol, and quantified by spectrophotometry and electrophoresis in a 1.2% agarose gel under denaturing conditions. RNA (500 ng) was DNAse treated to remove contamination using the TURBO DNAse kit (Thermo Fisher Scientific) and then reverse transcribed to cDNA with the Superscript II reverse transcriptase kit (Thermo Fisher Scientific) using a oligo$(DT)_{18}$ primer according to the manufacturer's instructions.

2. Sequencing and mRNA expression using RT-PCR

The cDNA fragments encoding IR25a were amplified by 2 rounds of polymerase chain reaction (PCR). Oligonucleotide primers were designed from a multiple-sequence aligment of IR25a sequences of crustaceans (*Daphnia pulex*, Croset et al. 2010; *H. americanus* AY098942, Hollins et al. 2003, *Lepeophtheirus salmonis* PRJNA280127, genome sequencing project), insects (*Acyrthosiphon pisum*, *Aedes aegypti*, *Anopheles gambiae*, *Apis mellifera*, *Bombyx mori*, *Culex quinquefasciatus*, *D. melanogaster*, *Nasonia vitripennis*, *Pediculus humanus*, *Tribolium castaneum*, Croset et al. 2010), gastropod molluscs (*Aplysia californica*, *Lottia gigantea*, Croset et al. 2010), nematods (*Caenorhabditis briggsae* XM_002643827, Stein et al. 2003, *Caenorhabditis elegans* NM_076040, The *C. elegans* Sequencing Consortium) and an annelid (*Capitella capitata*, Croset et al. 2010). The nucleotide sequences of generalist and specific primers, used for IR25a sequencing and localization in tissues respectively, are listed in Table 9. The corresponding primers used for each species are listed in Table 10.

Table 9 Nucleotide sequences and specificity of primers used for IR25a sequencing and localization in tissues

Primer	Specificity	Sequence
Fw-IR25a-1	generalist	TGGAACGGCATGATYAARSA
Fw-IR25a-2	generalist	GAYTTCACSGTGCCTTACTA
Rv-IR25a-3	generalist	TCCACCATCKCTCYTTSAGCG
Rv-IR25a-4	generalist	ACGATRAASACACCACCGATGT
Fw-IR25a-5	*Rimicaris exoculata*	TGACTGTACTAGAGCCTGAGGTGT
Rv-IR25a-8	*Rimicaris exoculata*	AGCTTCCTCTGGTTCAAGAGCTTC
Fw-PE-IR25a-2	*Palaemon elegans*	GAATGCCTCTGGTTCTGCATGACA
Rv-PE-IR25a-3	*Palaemon elegans*	TCGAGAATTCCTCACCTACCATCTGC

R=A/G, Y=C/T, N=A/T/G/C, S=G/C, Fw, forward ; Rv, reverse

Table 10 Primers used for IR25a sequencing and localization in tissues of each shrimp species

Species	IR25a sequencing (PCR)	Localization in tissues (RT-PCR)
Rimicaris exoculata	Fw-IR25a-1 / Rv-IR25a-4 Fw-IR25a-2 / Rv-IR25a-3	Fw-IR25a-5 / Rv-IR25a-8
Rimicaris chacei	Fw-IR25a-5 / Rv-IR25a-8	Fw-IR25a-5 / Rv-IR25a-8
Mirocaris fortunata	Fw-IR25a-5 / Rv-IR25a-8	Fw-IR25a-5 / Rv-IR25a-8
Alvinocaris markensis	Fw-IR25a-5 / Rv-IR25a-8	Fw-IR25a-5 / Rv-IR25a-8
Palaemon elegans	Fw-IR25a-1 / Rv-IR25a-4 Fw-IR25a-2 / Rv-IR25a-3	Fw-PE-IR25a-2 / Rv-PE-IR25a-3

PCR amplification reactions were performed in a 20 µL volume containing 1 µL of cDNA template, 2 µl of each primer [10 µM], 11.7 µL of H_2O, 2 µL of PCR buffer [10x], 0.8 µL of $MgCl_2$ [50 mM], 0.4 µL of dNTP [10 mM] and 0.1 µL of BIOTAQ polymerase [5 U/µL] (Eurobio AbCys). The thermal profile consisted of an initial denaturation (94°C, 3 min), followed by 35 cycles of denaturation (94 °C, 30 s), annealing (45 to 55°C, 45 s) and extension (72°C, 2 min), and a final extension (72°C, 10 min) step. The PCR products were separated on a 1.5% agarose gel, purified with the GeneClean kit (MP Biomedicals), and cloned into a pBluescript KS plasmid vector using the T4 DNA ligase (Thermo Fisher Scientific). The ligation product was introduced in competent *Escherichia coli* cells (DH5alpha) that were cultured at 37 °C overnight. The clone screening was performed through PstI/HindIII (Thermo Fisher Scientific) digestion of plasmid DNA after plasmid extraction. Positive clones were sequenced on both strands (GATC Biotech). The resulting nucleotide sequences were deposited in the GenBank database under the accession numbers KU726988 (*M. fortunata* IR25a; consensus sequence from 6 clones), KU726987 (*R. exoculata* IR25a; consensus sequence from 3 clones), KU726989 (*R. chacei* IR25a; consensus sequence from 4 clones), KU726990 (*A. markensis* IR25a; consensus sequence from 4 clones) and KU726984 (*P. elegans* IR25a; consensus sequence from 11 clones). Specific primers were further designed to amplify IR25a sequences in diverse tissues of the 4 alvinocaridid species and the palaemonid *P. elegans* (Table 10). PCR amplifications were performed using BIOTAQ polymerase (Eurobio, AbCys) in a thermocycler (Eppendorf, Hamburg, Germany) with the following program: 94 °C for 3 min, 35 cycles of (94 °C for 30 s, 55 °C for 45 s, 72 °C for 2 min), and 72 °C for 10 min, with minor modifications of annealing temperature for different primer pairs.

Chapter III

Structure of chemosensory systems in *M. fortunata* and *P. elegans*

I. Introduction

II. Results and discussion

1. Description of antennal appendages morphology and anatomy
   - General morphology of the antennal appendages
   - Distribution of the aesthetascs on the lateral antennules
   - Number of aesthetascs
   - Dimensions of aesthetascs
   - Diversity of non-aesthetasc setae
   - Bacterial coverage on the antennal appendages of vent species
   - Gross anatomy of the lateral antennules and the antennae
2. Ultrastructural analysis of aesthetasc cuticle and innervation
   - Aesthetasc cuticle structure and thickness
   - Pore-like structures in the aesthetasc cuticle of vent shrimp
   - Number of olfactory sensory neurons
3. Structure of the chemosensory centers
   - Brain general description
   - Olfactory lobes and glomeruli subdivision
   - Olfactory lobes volume and number of olfactory glomeruli
   - Antennal and lateral antennular neuropils
   - Hemiellipsoid bodies – Medulla terminalis complex

III. Conclusions

I. Introduction

The adaptive and functional relation of an organism to its habitat, environment and behavior can be reflected in the structure of its sensory organs. For instance, shrimp that inhabit dark hydrothermal vents present major transformations of their visual system to detect faint sources of light, including a highly sensitive retina, loss of the eyestalks and image-forming optics (Van Dover et al. 1989, Pelli and Chamberlain 1989, O'Neill et al. 1995, Nuckley et al. 1996, Lakin et al. 1997, Jinks et al. 1998, Chamberlain 2000) and migration of the optic neuropils in a dorso-posterior position in the brain (Charmantier-Daures and Segonzac 1998, Gaten et al. 1998b). In contrast to the visual system, the chemosensory system in vent shrimp has been poorly studied (Renninger et al. 1995), even though their environment is characterized by particular chemical conditions. As adaptations to detect their habitat, vent shrimp may present structural specificities of their chemosensory system both at peripheral and central levels, perhaps linked to highly efficient chemosensory abilities to take advantage of the hydrothermal chemical scape.

The detection of chemicals starts at the peripheral level, for which the antennal appendages are considered as major chemosensory organs. The lateral antennules bear olfactory aesthetasc sensilla innervated by olfactory sensory neurons (OSNs) (Laverack 1964, Ache 1982, Grünert and Ache 1988, Hallberg et al. 1992, Mellon 2007, Hallberg and Skog 2011, Schmidt and Mellon 2011, Derby and Weissburg 2014). Dendrites of OSNs from decapods exhibit a similar structure, with inner dendritic segments (IDSs) that emanate from the somata, and divide into the aesthetasc shaft in outer dendritic segments (ODSs) that bear the chemoreceptors (Ghiradella et al. 1968, Grünert and Ache 1988, Hallberg et al. 1992, Mellon 2007, Hallberg and Skog 2011, Schmidt and Mellon 2011, Derby and Weissburg 2014) (see Chapter I, Figure 16). Aesthetascs are also characterized by the absence of a terminal pore, resulting in a necessarily thin cuticle to allow the passing of soluble odorant molecules that must bind their cognate receptors located on the dendritic membranes of the OSNs (Blaustein et al. 1993, Derby et al. 1997). Many structural features of the aesthetascs are associated to the olfactory abilities of a species. The dimensions of the aesthetascs are likely to influence the sampling of an odor plume, with longer aesthetascs associated to a larger chemoreceptive surface (Nelson et al. 2013). Similarly, the aesthetasc cuticle thickness defines the portion of the sensillum permeable to odor molecules (Derby et al. 1997). Because aesthetascs are associated to identical clusters of OSNs (Steullet et al. 2000), a multiplication of these sensilla might raises the sensitivity to odorants (Beltz et al. 2003). The number of IDSs and ODSs, subsequent to the number of olfactory receptors, could be linked to the odorant discrimination performance (Ghiradella et al. 1968, Grünert and Ache 1988, Chittka and Niven 2009). Determination of these parameters (dimensions, number and cuticle thickness of aesthetascs,

number of IDSs and ODSs) for vent shrimp could reveal potential hints for their olfactory abilities when compared to a shallow-water shrimp species. Also, non-aesthetasc sensilla are located both on antennular and antennal flagella, mouthparts, walking legs and on the body surface (Ache 1982, Garm et al. 2003, Garm and Walting 2013). They are bimodal sensilla innervated by mecano- and chemosensory neurons (Schmidt and Ache 1996, Cate and Derby 2001, Schmidt and Mellon 2011), and exhibit a wide diversity of shapes, maybe linked to diverse chemosensory functions (Derby and Steullet 2001, Steullet et al. 2002, Horner et al. 2004, Schmidt and Derby 2005). Most of the knowledge on the aesthetascs and bimodal sensilla results from studies on members of the Eureptantia (lobster, crayfish and crab) (e.g. Tierney et al. 1986, Hallberg et al. 1992, Mellon 2007, Hallberg and Skog 2011, Schmidt and Mellon 2011, Derby and Weissburg 2014), whereas only few studies are available on representatives of caridean shrimp for which only the aesthetasc external morphology has been described for few species (Hallberg et al. 1992, Mead 1998, Obermeier and Schmitz 2004, Zhang et al. 2008, Zhu et al. 2011, Solari et al. 2017).

The chemosensory neurons associated with the aesthetascs or bimodal sensilla innervate distinct regions in the brain (Schachtner et al. 2005, Schmidt and Mellon 2011, Strausfeld and Andrew 2011, Loesel et al. 2013, Derby and Weissburg 2014, Harzsch and Krieger 2018) (see Chapter I, section IV.1.4. and Figure 17). The axons of the OSNs target the olfactory lobes, whereas the axons of the chemosensory neurons innervating non-aesthetasc sensilla target the lateral antennular neuropils. The olfactory pathway is sketched in Figure 18 (Chapter I). The olfactory lobes consist in radially arranged functional subunits called glomeruli. Central neurons connect the olfactory glomeruli with higher-order neuropils, namely the hemiellipsoid bodies – medulla terminalis complex, which are multi-modality integrative centers. During evolution, specific brain regions may have expanded relatively to the rest of the brain, in correspondence with ecological specialization (Chittka and Niven 2009, Harzsch and Krieger 2018). For instance, in blind cavernous crustaceans the olfactory lobes are well-developed, whereas the optic neuropils are considerably reduced, suggesting an important role of olfaction for these species (Stegner et al. 2015, Ramm and Scholtz 2017). Furthermore, changes in the organization of a neuropil, e.g. an increased volume of the olfactory lobes, could indicate a varying ability to discriminate the sensory input (Beltz et al. 2003). Few studies report the brain structure of Caridea species (two Palaemonidae *Macrobrachium* species [Sandeman et al. 1993, Ammar et al. 2008] and two Antarctic *Pleyocyemata* species [Bluhm et al. 2002]), which is close to the original decapod brain ground plan. The brain of the hydrothermal shrimp *Rimicaris exoculata* and *Rimicaris chacei* have been examined with regards to their optic neuropils (Charmantier-Daures and Segonzac 1998), but poor attention has been devoted to their chemosensory centers.

Morphometric quantifications of chemosensory structures, especially the olfactory system (e.g. number and dimensions of aesthetascs, number of IDSs and ODSs, aesthetasc cuticle thickness, volume of olfactory lobes, number of olfactory glomeruli), are used as rough estimates to infer on the chemosensory performance of a species, and comparative data can be used as a basis to infer on differences in chemosensory abilities between two species, as specific adaptations to habitat and lifestyle (Ghiradella et al. 1968, Beltz et al. 2003, Sandeman et al. 2014, Krieger et al. 2015, Harzsch and Krieger 2018). In this context, Magali Zbinden, Juliette Ravaux and I conducted a comparative multi-level description of the antennal appendages, with a special attention given to the olfactory system, in the vent shrimp *Mirocaris fortunata* and the coastal shrimp *Palaemon elegans*, to search for structural differences between the two species. The morphology of the antennules, the antennae and the associated sensilla was studied with Scanning Electron Microscopy. The aesthetascs cuticle structure and innervation by OSNs was investigated with Transmission Electron Microscopy. I analyzed brain architecture using immunohistochemistry and X-ray microcomputed tomography, with the help of Steffen Harzsch[1] and Jakob Krieger[1] during a one month stay at their laboratory. Altogether, these approaches aim at providing a first global description of the chemosensory system, especially the olfactory system, in the vent shrimp *M. fortunata*, for which anatomical dissimilarities with the shallow-water shrimp *P. elegans* could suggest highly efficient or particular chemosensory abilities to detect the hydrothermal chemical environment.

[1] Greifswald University (Germany), Zoological Institute and Museum, Cytology and Evolutionary Department

II. Results and discussion

Measurements and estimations of aesthetascs and olfactory lobes characteristics we conducted on *M. fortunata* and *P. elegans* are summarized in Table 11, in comparison with data for other marine decapod species.

➔

Rough animal lengths are given for comparison. Total length is given for lobsters, hermit crabs and shrimp, carapace width for crabs.

[1] Measurements were made from SEM images. Aesthetasc diameter was measured on n = 21 (*M. fortunata*) and n = 14 (*P. elegans*) aesthetascs. Aesthetasc length was measured on n = 46 (*M. fortunata*) and n = 10 (*P. elegans*) aesthetascs.

[2] Measurements of cuticle thickness were made from TEM sections at various levels of n = 20 and n = 30 aesthetascs for *M. fortunata* (5 individuals) and *P. elegans* (4 individuals), respectively. Data are given as maximum (for the "thick" cuticle") and minimum (for the "thin" cuticle) values.

[3] The number of IDSs per aesthetasc was estimated from counts in several 25 to 150 µm² portions of TEM sections from the base of the sensilla, on n = 11 (*M. fortunata*, 3 individuals) and n = 13 (*P. elegans*, 2 individuals) aesthetascs. Data are given as range.

[4] The number of ODSs per aesthetasc was estimated from counts in several 4 to 30 µm² portions of TEM sections of the sensilla judged to contain the highest number of ODS containing single microtubules, on n = 7 (*M. fortunata*, 4 individuals) and n = 28 (*P. elegans*, 4 individuals) aesthetascs. Data are given as range.

[5] Measurements were made as explained in Beltz et al. 2003. To determine the volume of the olfactory neuropil from the immunohistochemistry sections, the area of the synaptic signal in the olfactory lobes was measured with Fiji software, and the areas for the serial sections were then added and multiplied by the section thickness (100 µm) to provide a total volume of the glomerular neuropil. Next, a mean value was obtained for the volume of a single glomerulus. Because the glomeruli are neither conical nor cylindrical but a combination of these, the volume was derived from calculating the average of the cylindrical and the conical volumes. The length and cross-sectional areas of the glomeruli were measured directly on the synapsin-labelled tissue of n = 10 glomeruli for each olfactory lobe. Finally, an estimate of the glomerular number for each olfactory lobe was obtained by dividing the total glomerular volume by the volume of a single glomerulus. Measurements were made on n = 5 (*M. fortunata*, 3 individuals) and n = 4 (*P. elegans*, 2 individuals) olfactory lobes. Data are given as range, for olfactory neuropils on both sides of the brain.

Taxon	Species	Aesthetascs						Olfactory lobes			References
		Total number	Dimensions (diameter x length, µm)	Thickness of "thick" cuticle (µm)	Thickness of "thin" cuticle (µm)	Number of IDSs	Number of ODSs	Neuropil total volume ($x10^6$ μm^3)	Mean glomerular volume ($x10^3$ μm^3)	Glomerular number	
Brachyura (crabs)											
	Cancer productus (10-20 cm)	-	-	2.1	1.1	100	-	-	-	-	Ghiradella et al. 1968
	Cancer borealis (10-20 cm)	540	-	-	-	-	-	166	230	733	Beltz et al. 2003
	Callinectes sapidus (23 cm)	-	-	-	-	105	1420	-	-	-	Gleeson et al. 1996
	Carcinus maenas (9 cm)	100-300	13 x 750	-	-	-	-	-	247	-	Fontaine et al. 1982, Hallberg and Skog 2011
Anomura (hermit crabs)											
	Pagurus hirsutiusculus (1-7 cm)	-	-	1.3	0.4	400	6000-8000	-	-	-	Ghiradella et al. 1968
	Pagurus bernhardus (3 cm)	673	-	-	-	-	-	-	171	536	Tuchina et al. 2015
	Petrolisthes coccineus (2 cm)	328	-	-	-	-	-	12	19	655	Beltz et al. 2003
Achelata (spiny lobsters)											
	Panulirus interruptus (20-60 cm)	1786	-	4	1	300	-	345	288	1202	Spencer and Linberg 1986, Beltz et al. 2003
	Panulirus argus (20-60 cm)	2000-4000	40 x 1000	3	0.8	300-350	8000-10000	154	118	1332	Grünert and Ache 1988, Beltz et al. 2003
	Jasus edwardii (20-60 cm)	1537	-	-	-	-	-	592	616	961	Beltz et al. 2003
Homarida (lobsters)											
	Homarus americanus (20-60 cm)	2000	20 x 600	-	-	-	-	141	592	249	Guenther and Atema 1998
Stenopoidea (shrimps)											
	Stenopus hispidus (6 cm)	85	-	-	-	-	-	11	123	89	Krieger et al. (unpublished)
Thalassinida (shrimps)											
	Callianassa australiensis (4 cm)	22	-	-	-	-	-	7	28	235	Beltz et al. 2003
Caridea (shrimps)											
	Lysmata (5-7 cm)	210-460	20 x 800	-	-	-	-	-	-	-	Zhang et al. 2008
	Palaemon adspersus (7 cm)	-	-	1	0.4	-	-	-	-	-	Solari et al. 2017
	Palaemon elegans (7 cm)	280	14 x 230[1]	1.3[2]	0.14[2]	177-519[3]	1568-10637[4]	145-190[5]	426-600[5]	320-340[5]	This study
	Mirocaris fortunata (3 cm)	120	16 x 234[1]	1.5[2]	0.15[2]	90.223[3]	1568-10638[4]	63-147[5]	218-380[5]	195-560[5]	This study

Table 11 Comparative table of aesthetascs and olfactory lobes characteristics in different marine decapods

Legend previous page.

1. Description of antennal appendages morphology and anatomy

[Results for morphology published in Zbinden et al. 2017]

The aim of this section is to provide a comparative overview of the morphology and the anatomy of major chemosensory organs, the antennules and the antennae, in *M. fortunata* and *P. elegans*. We focus mainly on the lateral antennules that bear the aesthetascs to discuss on the olfactory abilities of each species. The antennae that bear only bimodal sensilla are described as a non-olfactory chemosensory organ for comparison.

- **General morphology of the antennal appendages**

In both *M. fortunata* and *P. elegans*, antennae and antennules consist of a peduncle and segmented flagella (one for the antennae and two for the antennules: a lateral and a medial [Figure 31A,G]). In the three flagella, the diameter and the length of the annuli vary, being large and short at the base and becoming thinner and longer towards the apex. In *P. elegans*, the lateral antennule is divided in two rami after a short fused basal part: a long external one and a shorter internal one (1/3 of the long one).

- **Distribution of the aesthetascs on the lateral antennules**

In the most studied large decapods like lobster and crayfish, the aesthetascs are localized in tufts on the distal part of the ventral side of the lateral antennules (Cate and Derby 2001, Guenther and Atema 1998, McCall and Mead 2008, Tierney et al. 1986, Mellon 2012). This location at the tip of the antennules may increase the spatial resolution of the chemical environment, but could also increase the risk of damage during encounters with the environment or other animals. On the contrary, we observed that the aesthetascs are localized on the basal two-third of the lateral antennules in *M. fortunata* (latero-ventral position, Figure 31B,C), and on the basal part of the shorter rami of the lateral antennules in *P. elegans* (in a ventral furrow [Figure 31G,H] as in other palaemonid species like *P. serratus* and *Macrobrachium rosenbergii* [Hallberg et al. 1992]). The aesthetascs are thus less likely to be lost or damaged, but this arrangement may decrease spatial resolution.

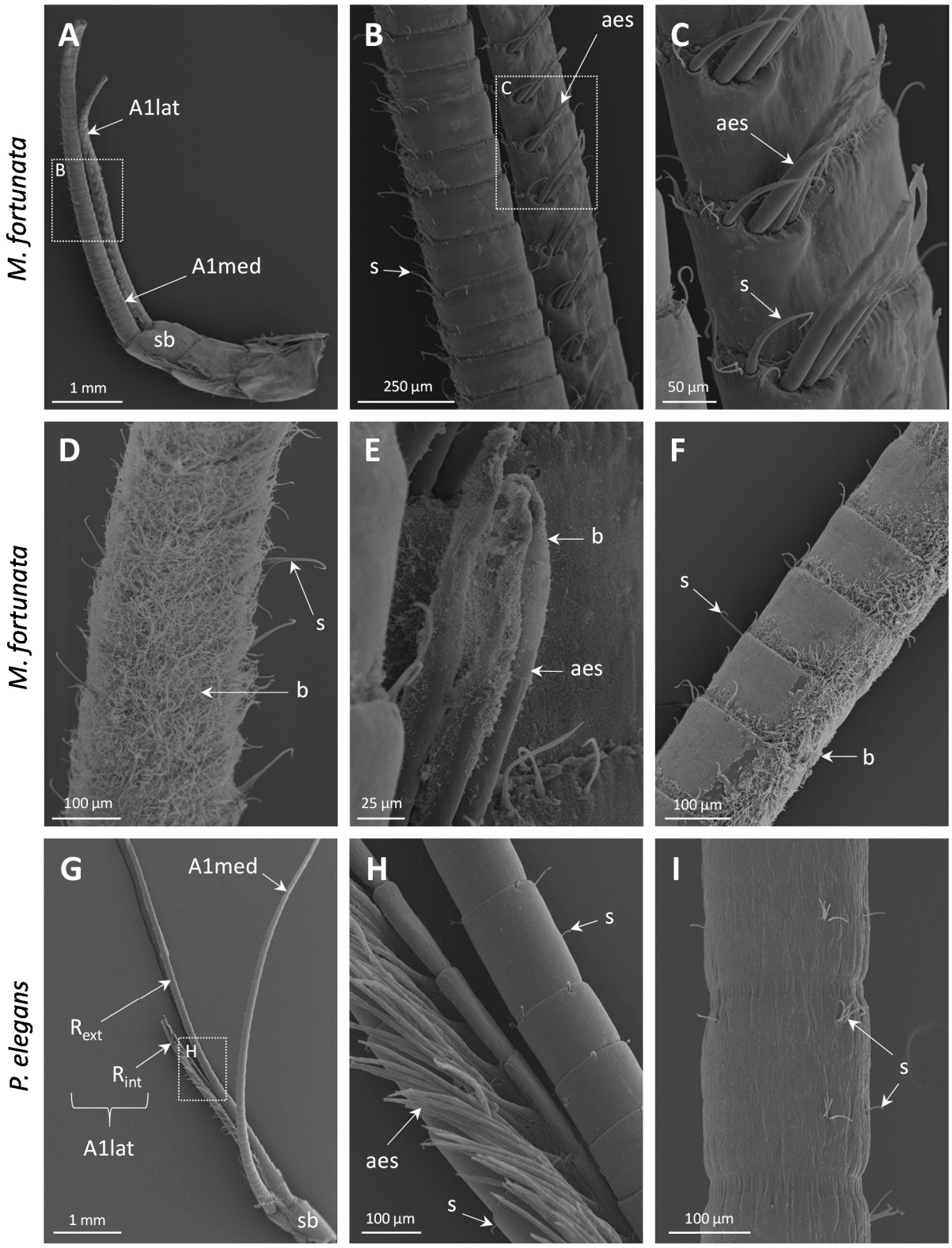

Figure 31 Morphology of the antennal appendages of *M. fortunata* and *P. elegans*
Legend next page.

A-C. *M. fortunata* antennule comprises two flagella, a lateral and a medial one (**A**), associated to several non-aesthetasc setae (**B,C**), and the lateral flagellum bears the aesthetascs (**C**).
D-F. The lateral antennule (**D**), aesthetascs (**E**) and antenna (**F**) of *M. fortunata* are often covered by bacteria. Non-aesthetasc setae also occur on the antenna (**F**).
G-H. *P. elegans* antennule comprises two flagella, a medial and a lateral one, the latter being divided into an internal and an external rami (**G**). Each flagellum bears several non-aesthetasc setae, and the internal ramus of the lateral flagellum bears the aeshteascs (**H**).
I. *P. elegans* antenna is also associated to several non-aesthetasc setae.
A1lat, lateral flagellum of the antennule; A1med, medial flagellum of the antennule; aes, aesthetasc sensilla; b, bacteria; R_{int}, intern ramus of the lateral antennule; R_{ext}, extern ramus of the lateral antennule; s, non-aesthetasc setae; sb, basal segment of the antennule.

- **Number of aesthetascs**

Each aesthetasc is associated to functionally identical OSNs clusters (Steullet et al. 2000), meaning that an increase of the aesthetasc number raises primarily the sensitivity to detectable odorants (Beltz et al. 2003). We observed in *M. fortunata* one row of 3 to 4 aesthetascs on the distal part of each annulus (Figure 31C), leading to a total number of approximately 60 aesthetascs per ramus, or 120 aesthetascs per individual. In *P. elegans* we found two rows of 5 to 6 aesthetascs on each annulus (one row at the distal part of the annulus and the other at the middle part) (Figure 31H), except for the two or three basal and apical annuli which have a smaller number of aesthetascs, giving a total number of approximatively 140 aesthetascs per ramus, or 280 aesthetascs per individual (Table 11). In other decapod species, the aesthetascs are usually organized in 2 successive rows (in the different lobsters and crayfish cited above and also in *Lysmata* shrimp, Zhang et al. 2008) or in 2 juxtaposed rows in the short antennules of the crab *Carcinus maenas* (Fontaine et al. 1982). Surprisingly, we observed only one row of aesthetascs on each annulus in *M. fortunata*. Nevertheless, comparisons of the total number of aesthetascs in our shrimp models and in diverse decapod species (Table 11) relative to the animal size indicated that this number is relatively similar among the shrimp group and other decapods of similar size range (e.g. the crab *C. maenas*) (Table 11). Hence, *M. fortunata* sensitivity to odorants is not likely to be enhanced regarding the number of aesthetascs.

- **Dimensions of aesthetascs**

Dimensions of aesthetascs might be linked the sampling efficiency of an odor plume, since elongated and large aesthetascs present a large chemoreceptive surface, which improves the odor capture (Nelson et al. 2013). We found that the dimensions of *M. fortunata* aesthetascs (up to 18.3 µm in diameter and 290.3 µm in length) are similar to those of *P. elegans* (up to 20.3 µm in diameter and 393 µm in length) and rather small compared to other decapod species (Table 11). This, added to

our previous observations of aesthetascs distribution, suggests that *M. fortunata* does not present morphological features to promote an enhanced sampling of the odorant environment.

- **Diversity of non-aesthetasc setae[(GLOSSARY)] (presumably bimodal sensilla)**

Most studies on chemodetection in crustaceans focus on the aesthetascs, however several lines of evidence suggest that non-aesthetasc bimodal sensilla (innervated by mecano- and chemo-sensory neurons [Schmidt and Mellon 2011]) also play a major role in chemosensory-driven behaviors (Guenther and Atema 1998, Cate and Derby 2001, Schmidt and Mellon 2011). The wide variety of morphologies of the bimodal sensilla may correspond to a multiplicity of perceived stimuli (Cate and Derby 2001, Derby and Steullet 2001). We observed several types of non-aesthetasc setae on the two flagella of the antennules and on the antennae in *M. fortunata* (Figure 31B,C,D,F, Figure 32A-C) and *P. elegans* (Figure 31H,I, Figure 32D-G). Without evidence for their innervation by neurons, we cannot strictly define these sensilla as bimodal sensilla, but it is probable they are, as shown for other decapod species (Schmidt and Gnatzy 1984, Cate and Derby 2001, Schmidt and Mellon 2011, Garm and Watling 2013). We identified a higher diversity in setal types in *P. elegans* (5 setal types) than in *M. fortunata* (3 setal types), but at this point of our knowledge it is difficult to explain the observed differences and even more to speculate on the functions of these setae.

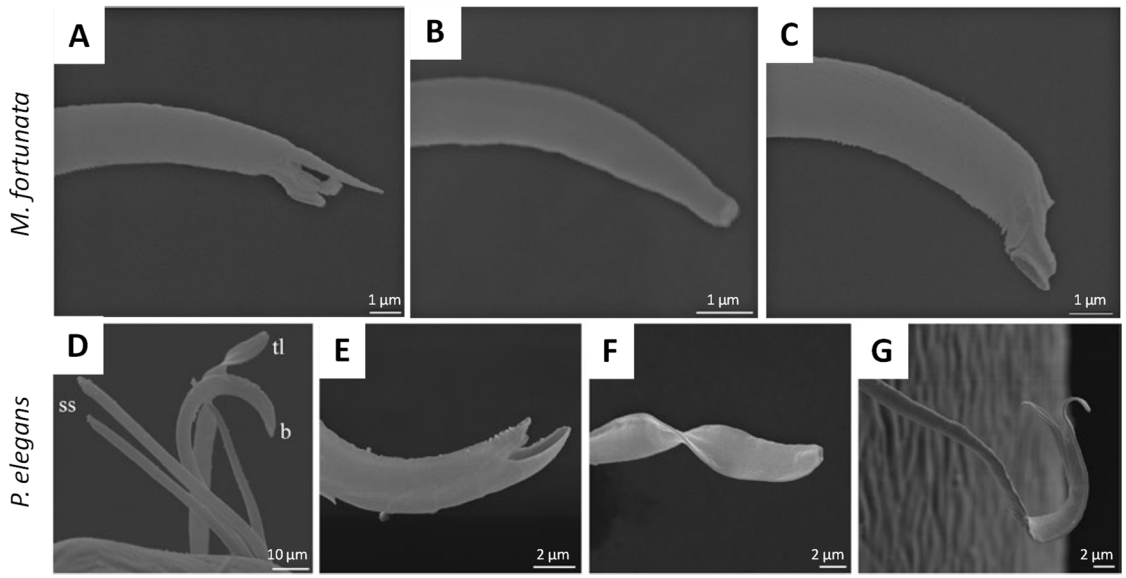

Figure 32 Morphology of the non-aesthetasc setal types of *M. fortunata* and *P. elegans*

A-C. Apex of the three types of non-aesthetasc setae observed in *M. fortunata*.
D-G. Five types of non-aesthetasc setae observed in *P. elegans.* b, beaked scaly seta; s, simple short seta; tf, twisted flat seta.

- **Bacterial coverage on the antennal appendages of vent species**

We observed in *M. fortunata* a thick layer of bacteria often covering the antennal appendages, and sometimes the whole surface of the aesthetascs (Figure 31D,E,F), as well as in other vent shrimp species (more results in Zbinden et al. 2017, and Figure 5B for *R. exoculata*). Any bacterial coverage has been observed for *P. elegans*. The presence of such a thick layer of bacteria over the antennal appendages is thus likely a feature specific to hydrothermal shrimp.

Crustaceans living in aquatic environments are under constant exposure to a wide variety of microbial fouling organisms, and are known to frequently groom their antennules in order to remove the material that have accumulated on their surface (Bauer 1989, Barbato and Daniel. 1997). Barbato and Daniel. (1997) stated that anything enhancing the level of microbial fouling is presumably detrimental to the functional role of the antennules as a chemosensory organ. Experiments preventing shrimp from grooming their antennules indeed lead to extensive structural damage of the aesthetascs (Bauer 1978). In the vent species, we did not observe any structural damage that could be caused by this fouling. If the bacterial colonization really impairs their chemosensory system, the occurrence of the bacterial coverage can plead for a secondary role of this sense. We can also raise the hypothesis that the bacteria have specific role for the shrimp, which could cultivate them in purpose. At hydrothermal vents, bacteria associated to the local fauna are involved in their nutrition through chemosynthesis, but also in detoxification (Zbinden et al. 2004, 2008, Durand et al. 2009, Jan et al. 2014). Identification of the different bacterial functional types present on each species is needed to discuss on their potential role or impact on shrimp sensory detection.

- **Gross anatomy of the lateral antennules and the antennae**

In *M. fortunata* and *P. elegans*, the lumen of the lateral antennules and the antennae is mainly filled with internal fluid, and contains the somata of sensory neurons, the axons of which group into bundles to form the antennular or antennal nerves (Figure 33) that project to specific neuropils in the brain. The somata of the sensory neurons that presumably innervate non-aesthetasc seate are located on the inner side of the flagellum cuticle. In the lateral antennules, the somata of the OSNs that are packed in clusters –one per aesthetasc– that occupy a large area of the extracellular space (Figure 33A,B). From our observation of a high abundance of OSNs in the lateral antennule, we expect that this flagellum plays the main role in chemoreception rather than the antenna. Nonetheless, Voigt and Atema (1992) demonstrated in *Homarus americanus* that, physiologically, the antenna is a major chemosensory organ, with chemosensory neurons having a similar tuning spectrum to those of the antennules. Therefore, the antenna had to be considered as the antennule for further electrophysiology experiments (see Chapter IV).

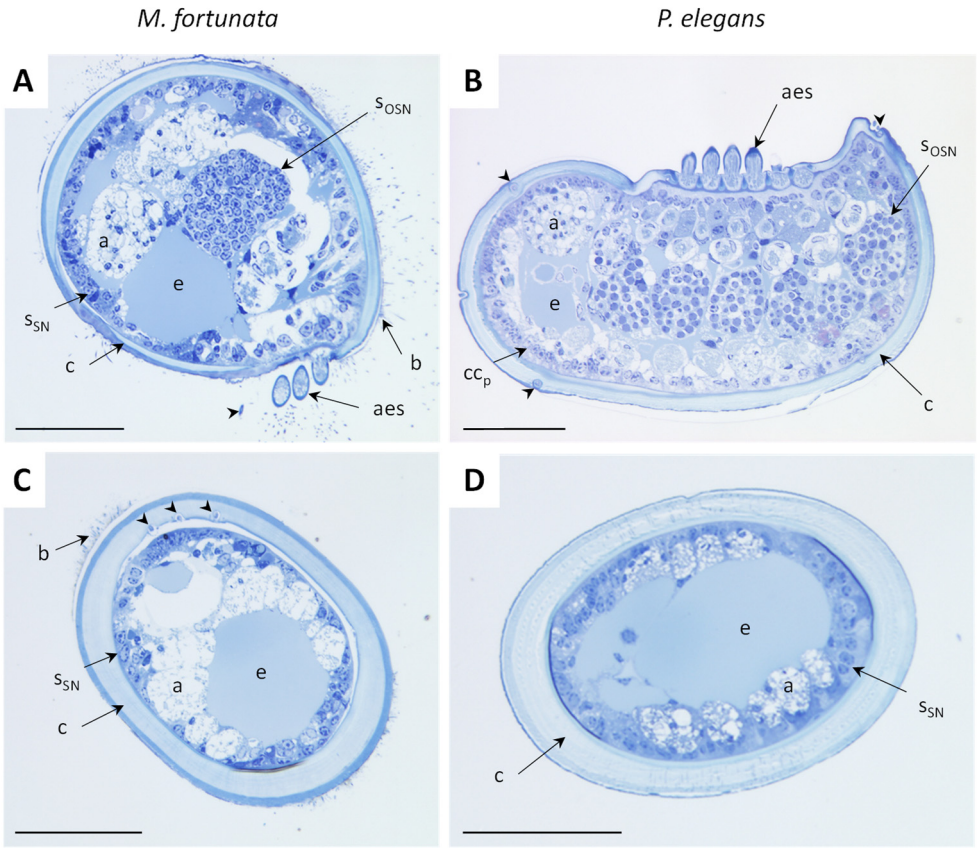

Figure 33 Anatomy of the lateral antennule and antenna in *M. fortunata* and *P. elegans*

A-B. Cross sections of the lateral antennule of *M. fortunata* (**A**) and *P. elegans* (**B**).
C-D. Cross sections of the antenna of *M. fortunata* (**C**) and *P. elegans* (**D**).
Scale bars = 100 µm. a, axons bundles; aes, aesthetasc; b, bacteria; c, cuticle; e, extracellular space; s_{SN}, somata of sensory neurons innervating non-aesthetasc sensilla; s_{OSN}, somata of olfactory sensory neurons innervating the aesthetascs. Arrowheads, non-aesthetasc setae.

2. Ultrastructural analysis of aesthetasc cuticle and innervation

[Results published in Machon et al. 2018]

Although the general organization of aesthetascs and OSNs is analogous between decapod species (see Chapter I, Figure 16), the aesthetasc cuticle thickness and the numbers of IDSs and ODSs can vary (Ghiradella et al. 1968, Hallberg et al. 1992, Beltz et al. 2003, Mellon 2007). The cuticle thickness relates to the permeability of the aesthetasc, and accordingly is linked to the ability to detect soluble odorants (Derby et al. 1997). IDSs and ODSs refer respectively to the number of OSNs and dendritic branches innervating a single aesthetasc, and are likely to be linked to odorant discrimination

performance (Derby and Weissburg 2014). In the present approach, we investigated potential specificities of *M. fortunata* chemosensory system regarding the aesthetasc cuticle structure and innervation in comparison with the shallow-water species *P. elegans* and the existing data on other crustacean species.

- **Aesthetasc cuticle structure and thickness**

Aesthetascs of marine decapods are characterized by a thin (0.4 to 4 µm thick, Table 11), poreless cuticle, unlike bimodal sensilla that have a pore at their tip (Garm et al. 2003) and a thick cuticle (for example from 2 to 7 µm thick for the distal part of an antennular bimodal sensilla in *R. exoculata*; not shown). The aesthetasc cuticle, especially in the distal part, possibly functions as a molecular sieve through which appropriate odorants move quickly to activate OSNs, as reported in spiny lobster (Derby et al. 1997) and crayfish (Tierney et al. 1986). Therefore, the cuticle thickness and structure along an aesthetasc might define the portion of the sensillum permeable to soluble odorants.

A sketch of an aesthetasc sensilla is presented in Figure 16 (Chapter I). The region of the sensillum where the IDSs divide into ODSs is called the transitional zone. From the base to the transitional zone, the aesthetasc cuticle is thick, from 0.8 to 1.8 µm in *M. fortunata* and from 0.6 to 1.3 µm in *P. elegans*. Just distal to the transitional zone, in *P. elegans* the cuticle becomes thin (0.6 to 0.3 µm) on almost all the distal part of the sensilla (80% of the length), with the cuticle at the tip of the aesthetasc thinning to 0.15 µm. In *M. fortunata* the cuticle remains thick on the first half of the aesthetasc length, and becomes thin on the distal half of the sensilla, from 0.8 to 0.15 µm. For each species, the thick cuticle has a lamellar structure (Figure 34A,B,F), which gradually becomes loose (transitional cuticle, Figure 34C,G) when thinning, until becoming spongy (Figure 34D,E,H,I,J).

Comparison of aesthetascs from *M. fortunata* and *P. elegans* with other marine decapod species reveals similarities in cuticle thickness in the basal region of aesthetascs among the caridean shrimp group, marine crab and hermit crab (Table 11), as well as in its lamellar structure (Ghiradella et al. 1968, Grünert and Ache 1988, Gleeson et al. 1996). In our shrimp species, the distal region of aesthetascs has a thinner cuticle than described for other decapod species (Table 11), but similar to the thickness of *Daphnia* aesthetasc cuticle (Hallberg et al. 1992), and identical between *M. fortunata* and *P. elegans*. It is likely that the thin cuticle thickness is similar between species of similar size (e.g. *M. fortunata*, *P. elegans* and *P. adspersus*). The differences in thin cuticle thickness observed between our shrimp models and other species from the literature may results from different zones used for the measurements (we present minimum values from measurements from the very tip of the sensilla, whereas in the literature authors may have measured the distal part of the sensilla but not the very

tip of the sensilla). Regarding the cuticle structure, the spongy non-lamellar cuticle most likely corresponds to the odorant-permeable region. We found that a portion of 50 and 80 % of the aesthetasc length has a thin and spongy cuticle in *M. fortunata* and *P. elegans*, respectively. Since the two species have a similar aesthetasc length (Table 11), *P. elegans* aesthetascs appear to have a larger surface area permeable to odorants than *M. fortunata*, suggesting a better sampling efficiency of the environment for the coastal species.

➔

Figure 34 Structure of aesthetasc cuticule in *M. fortunata* and *P. elegans*

Cross sections of aesthetasc cuticle of *M. fortunata* (**A-E**) and *P. elegans* (**F-J**) at different levels along the sensillum, indicated on the central sketch (not to scale). For the two species, the cuticle is lamellar in the proximal region of the aesthetasc (**A,B,F**), and is spongy in the apical region (**D,E,H,I,J**). The transition between the lamellar and the spongy cuticle is gradual, and named transitional structure (**C,G**). The relative length of each structure along the aesthetasc is illustrated on the side of the central sketch, as well as the relative thickness of the cuticle and the occurrence of pore-like structures in *M. fortunata*.
Scale bars = 1 µm. b, bacterium; c_l, lamellar cuticle; c_s, spongy cuticle; c_t, transitional cuticle; p, pore-like structure.

- **Pore-like structures in the aesthetasc cuticle of vent shrimp**

In *M. fortunata*, we observed pore-like structures occurring in the lamellar cuticle (Figure 34B,C and Figure 35). They can reach approximatively 0.2 µm in diameter, open to the inner side of the aesthetasc and are separated from the outside by a cuticle layer that thins from 0.4 to 0.06 µm. They are present from the transitional zone to approximately 50 % of the aesthetasc length, when the cuticle starts to thin, and are no longer present in the spongy part of the cuticle (Figure 34B). We also observed these pore-like structures in the same region of the aesthetascs in the hydrothermal shrimp *R. exoculata* (Figure 35), with a diameter slightly larger (up to 0.4 µm). We did not observed any pore-like structures in the aesthetascs of *P. elegans*.

Other types of pore-like structures have been described in the basal region of the aesthetasc for some marine decapods. Pore canals perforate the lamellar cuticle of the basal tenth of the aesthetascs in the hermit crab *Pagurus hirsutiusculus* (Ghiradella et al. 1968), proximal to the ciliary segments of the transitional zone, and pore-like structures occur from the base to the transitional zone in the lobster *Panulirus argus*, and contain extensions of the auxiliary cells (Grünert and Ache 1988). However, in *M. fortunata* the pore-like structures only appear from and beyond the transitional zone,

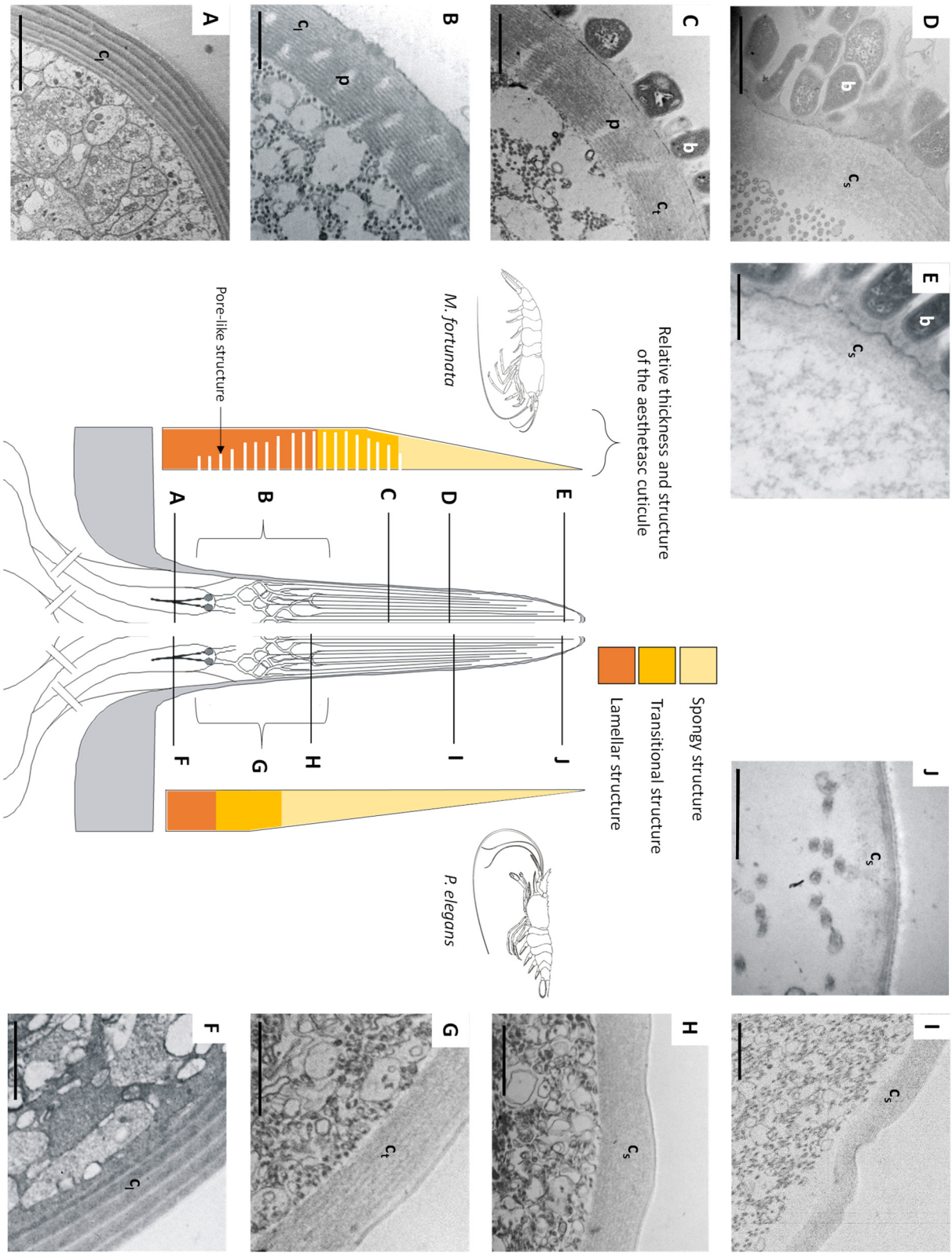

Legend previous page.

where the auxiliary cells end. In addition these pore-like structures are much more abundant than those described in *P. hirsutiusculus* and *P. argus*, and are longer, crossing almost the entire thickness of the cuticle. We propose these pore-like structures as a feature specific to hydrothermal shrimp. Their function is unknown. Since the cuticle layer separating the inner side of the pore-like structures with the outside is extremely thin, they could facilitate the passage of different odorant molecules (e.g. with a higher molecular mass) that cannot cross normally the aesthetasc cuticle and thus enhance the sampling of the environment in *M. fortunata*.

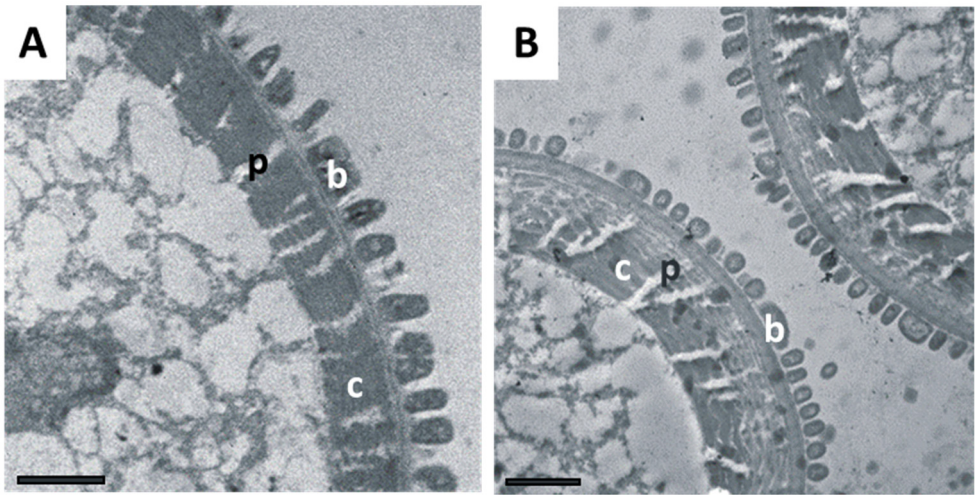

Figure 35 Pore-like structures in the cuticle of *M. fortunata* and *R. exoculata* aesthetascs

Cross sections of the aesthetascs middle region in *M. fortunata* (**A**) and *R. exoculata* (**B**), showing the lamellar cuticle and bacterial coverage.
Scale bars = 1 µm. b, bacterium; c, cuticle; p, pore-like structure.

➔

Figure 36 Inner and outer dendritic segments of olfactory sensory neurons in *M. fortunata* and *P. elegans*

Cross sections of aesthetascs of *M. fortunata* (**A-D**) and *P. elegans* (**E-H**), from the base region (**A,E**), the transitional zone (**B,F**), the medium region (**C,G**) and the apex region (**D,H**) of the sensilla. The central sketch indicates the position of each section along the aesthetasc (not to scale). Scale bars = 1 µm. ac, accessory cell; b, bacterium; c, cuticle; cr, ciliary rootlet; IDS, inner dendritic segment; m, mitochondrium; ODS, outer dendritic segment; ODS_{unb}, unbranched outer dendritic segment. Arrowheads, swelling of the outer dendritic segments.

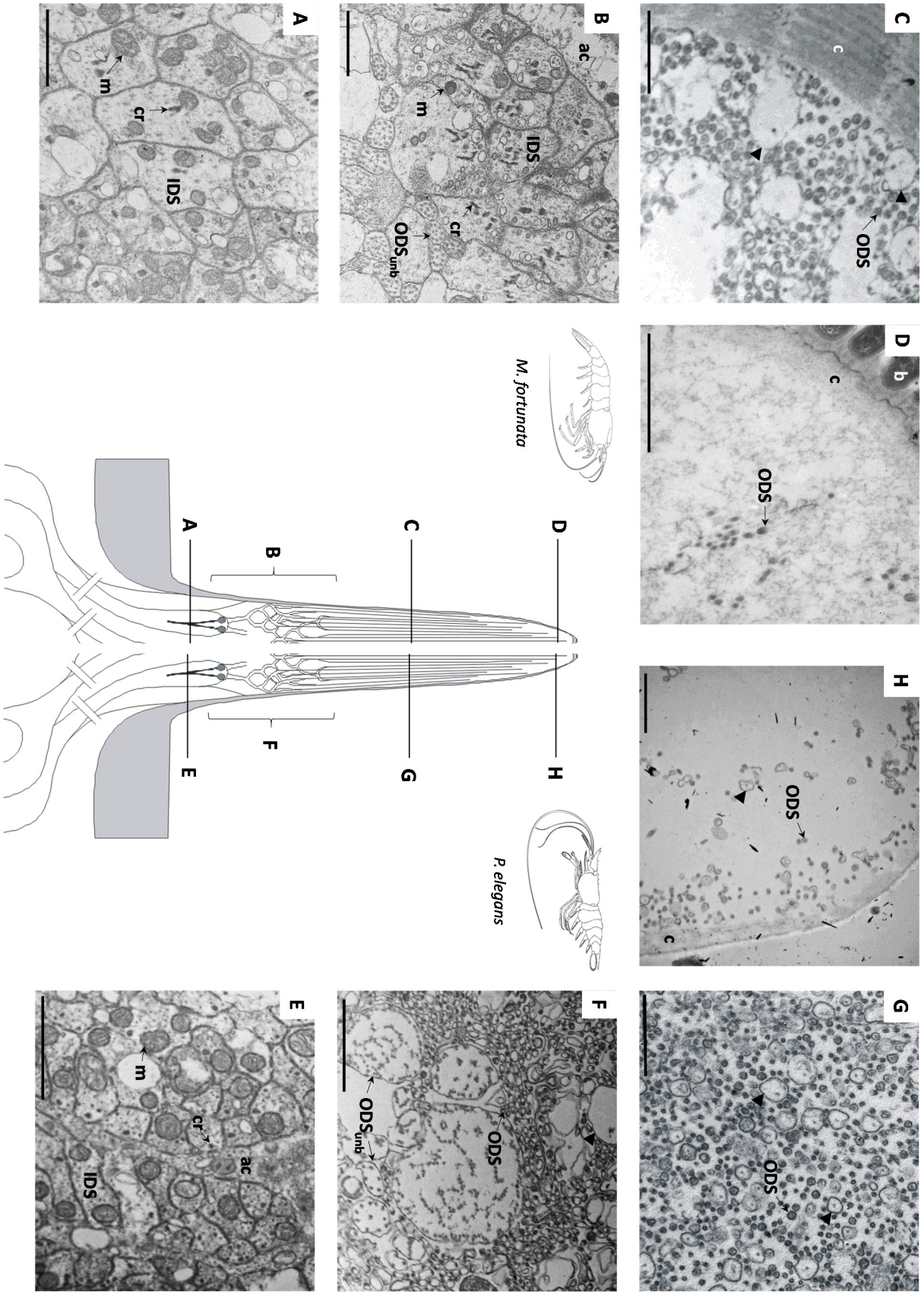

Legend previous page.

- **Number of OSNs innervating the aesthetascs**

We observed in *M. fortunata* and *P. elegans* the classical structural features of aesthetasc innervation by OSNs (sketched in Figure 16, Chapter I). IDSs, which emanate from the OSNs somata, are surrounded by auxiliary cells (Figure 6E) and extend into the lumen of the aesthetasc, where they terminate at various levels within the transitional zone (Figure 36B,F). They contain mitochondria, microtubules, vesicles and a ciliary rootlet (Figure 36A,E). Each aesthetasc contains approximatively from 90 to 223 and from 177 to 519 IDSs for *M. fortunata* and *P. elegans*, respectively, meaning it is innervated by approximatively 90 to 223 and 177 to 519 OSNs for each species (Table 11). In the transitional zone, the IDSs divide into ODSs surrounded only by lymph (Figure 36C,G). Swellings occur along the entire length of the outer dendritic segments (Figure 36C,D,F,G,H), and have been previously associated to chemosensory function (Grünert and Ache 1988). Only few ODSs extend to the tip of the aesthetasc (Figure 36D,H). There is approximatively from 2545 to 5383 ODSs per aethetasc for *M. fortunata* and from 1568 to 10637 ODSs per aesthetasc for *P. elegans* (Table 11).

An increased number of IDSs and ODSs may be associated to a higher sensitivity and a better discrimination of the chemical environment (Derby and Weissburg 2014). The animal's entire olfactory range of detection is represented by the OSNs housed in each individual aesthetasc (Steullet et al. 2000, Beltz et al. 2003), each OSN having a specific odor response spectrum. The olfactory receptors are most likely located on the membranes of the ODSs (Blaustein et al. 1993), for which a higher number might reflects a larger chemoreceptive membrane surface. Our results show that the estimated numbers of IDSs (reflecting the number of OSNs) per aesthetasc for *M. fortunata* and *P. elegans* fit within the range of about 100-400 displayed by several Malacostracan taxons (Table 11; Harzsch and Krieger 2018). The ranges number of OSNs and ODSs per aesthetascs of *M. fortunata* overlap those of *P. elegans*, suggesting that the vent species is not likely to have an enhanced chemosensitivity regarding this character. However, these data need to be completed by identifying and quantifying the receptor proteins expressed by OSNs for each species.

3. Structure of the chemosensory centers

Most of the knowledge on the basic structure of the central chemosensory systems comes from studies on lobster and crayfish (e.g. Blaustein et al. 1988, Sandeman et al. 1992, 2014). But as pointed by Eberhard and Wcislo (2011), "a significant limitation to understanding brain-behavior relations is the dearth of comparative data resulting from the collective blinders imposed by the "model system" approach…". In the following, the brain architecture of *M. fortunata* and *P. elegans* was investigated to complement the current knowledge on crustacean brain architecture, and to eventually find neuroanatomic dissimilarities that could reflect a dominance of chemosensory inputs processed in the brain of the vent species.

- **Brain general description**

The ground pattern of a crustacean brain is presented in Chapter I, section IV.1.3. and Figure 17. The brains of *M. fortunata* and *P. elegans* are sub-divided into three successive regions, the proto-, deuto- and tritocerebrum, in addition to the optic neuropils (Figure 37), as in other Malacostracan crustaceans (Harzsch et al. 2012, Sandeman et al. 2014, Harzsch and Krieger 2018). The lateral protocerebrum comprises the medulla terminalis and the hemiellipsoid bodies (both shown as a complex). Usually, these neuropils and the optic neuropils are located in the eyestalks at distance from the main brain. This is the case in the eyestalked species *P. elegans* (Figure 37B). In *M. fortunata*, the eyestalks are absent, the medulla terminalis and the hemiellipsoid bodies are fused to the medial protocerebrum, and the visual neuropils are located on a dorso-posterior position (Figure 37A), as previously described in *R. exoculata* by Charmentier-Daures and Segonzac (1998). The antennular nerve connects the antennules to the deutocerebrum, which comprises the olfactory lobes, the lateral antennular neuropils and the medial antennular neuropils (the latter is not shown because we did not identified it in our two species) (Figure 37). The axons of the aesthetasc OSNs project to the olfactory lobes, whereas the axons of the sensory neurons innervating the bimodal sensilla on the antennules project to the lateral antennular neuropils. The tritocerebrum is associated with the antennae, whose nerves project to the antennal neuropil (Figure 37).

The present study focuses on the neuropils involved in chemodetection: the olfactory lobes, the lateral antennular neuropils, the antennal neuropils and the higher integrative centers hemiellipsoid bodies and medulla terminalis. Otherwise specified, the following descriptions apply for both *M. fortunata* and *P. elegans*.

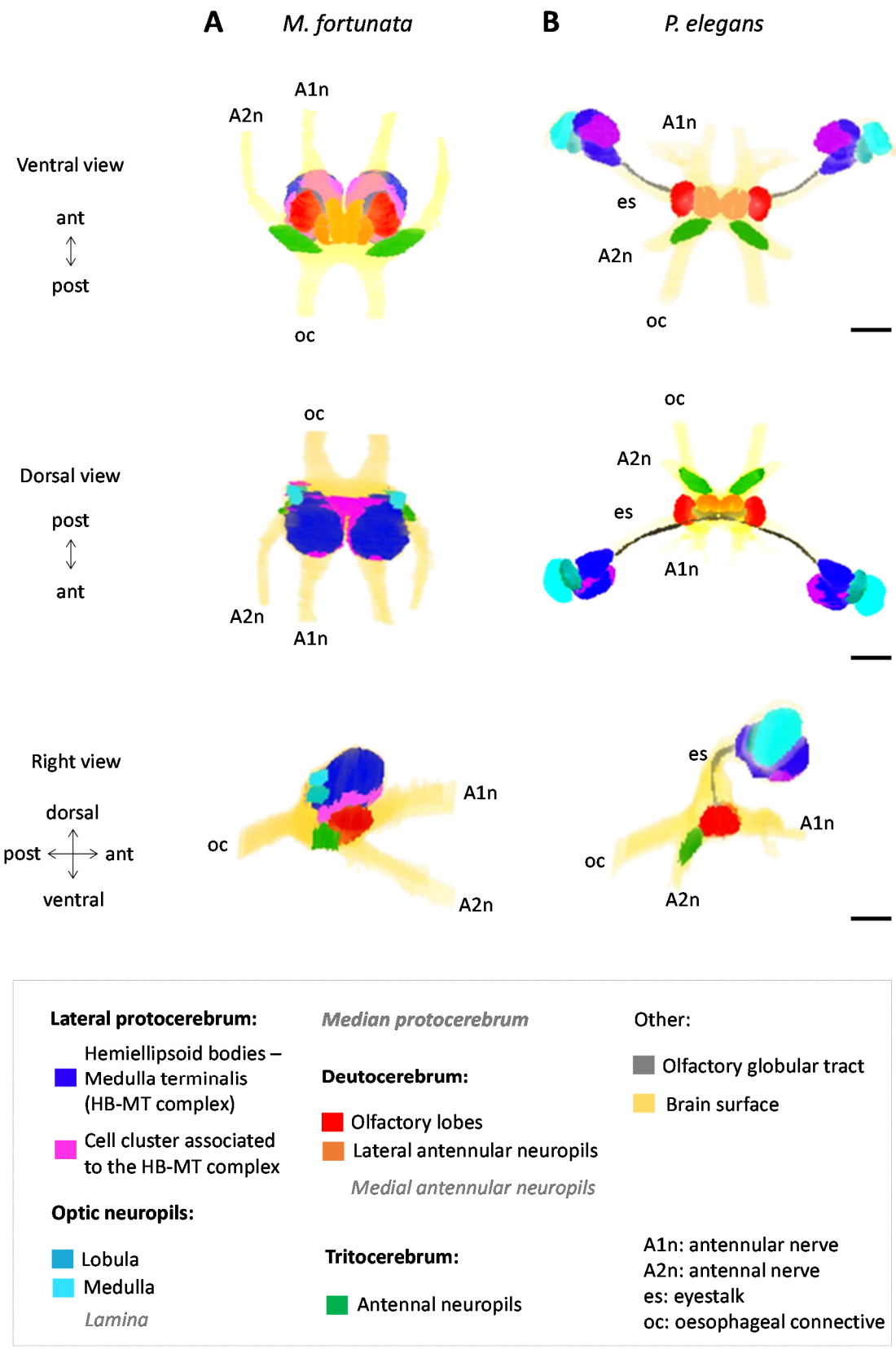

Figure 37 Brain organization in *M. fortunata* and *P. elegans*

3D reconstituted brain and selected neuropils of *M. fortunata* (**A**) and *P. elegans* (**B**) from X-ray micro-computed tomography scans, in ventral, dorsal and right views. In the legend box, non-represented neuropils are indicated in grey and italic. Scale bars = 0.5 mm (approximative).

- **Olfactory lobes and glomeruli subdivision**

The olfactory lobes are located laterally in the deutocerebrum (Figure 37 and Figure 38A,B). Each olfactory lobe is composed of olfactory glomeruli arranged radially around its periphery (Figure 38C,D). They show a strong synapsin immunoreactivity, reflecting a high synaptic density, and are innervated by local interneurons from an adjacent cell cluster that displays allatostatin immunoreactivity (Figure 38), confirming their peptidergic nature. In addition, the allatostatin immunoreactivity reveals a regionalization of the olfactory glomeruli along their long axis, with a cap, a subcap (with allatostatin signal) and a base regions. Although the subdivision in cap and base regions is well documented in most crustacean taxa (Schachtner et al. 2005, Schmidt and Mellon 2011, Polanska et al. 2012, Harzsch and Krieger 2018), the occurrence of a subcap region was previously observed only in "higher" Eureptantia decapods with elaborated olfactory systems (e.g. spiny lobster, Wachowiak et al. 1997; hermit crab, Krieger et al. 2010; crayfish, Sandeman and Luff, 1973). Thus, the subdivision of the olfactory glomeruli we observed in *M. fortunata* and in *P. elegans* might reflects an efficient computing performance of the olfactory system as seen in some Eureptantia.

- **Olfactory lobes volume and number of olfactory glomeruli**

Harzsch and Krieger (2018) pointed out that comparative studies across the Malacostraca reveal a significant divergence of the glomerular volume, which is linked to the computational power of the olfactory system. Because morphometric analysis of neuronal structures have been considered as rough estimates to infer one the sensory processing performance of a species (Krieger et al. 2015), we estimated in *M. fortunata* and *P. elegans* the total olfactory neuropil volume, the mean glomerular volume and the number of olfactory glomeruli (Table 11). Relative to the size of the two species, our results show similar volumes for the total olfactory neuropil and mean glomerulus in *M. fortunata* and *P. elegans.* The large range of glomerulus number obtained for *M. fortunata* does not allow comparison between the two species for this parameter. Compared to other marine decapods species, the values we obtained for the olfactory lobe volume in *P. elegans* and *M. fortunata* are high, especially regarding the rough size of the animals. For example, our values are 5 to 10 times higher than for the shrimp species *Stenopus hispidus* (Krieger et al. unpublished) of similar size, but are in the range of those obtained for the big *Homarus americanus* (Guenther and Atema, 1988). Considering the number of olfactory glomeruli, there is no correlation with the size of the animal, for example the small hermit crabs *Pagurus bernhardus* and *Petrolisthes coccineus* possess several hundreds of olfactory glomeruli (Tuchina et al. 2015, Beltz et al. 2003), in the range of the crab *Cancer borealis* (Beltz et al. 2003) which is 10 times larger. Beltz and collaborators (2003) included in their analysis 17 crustacean species from different habitats, and in general their study did not reveal any clear correlation between the

glomerular number and the olfactory neuropil volume, the body size or the habitat. Nonetheless, the authors suggested that animals with OSNs converging onto relatively few glomeruli can detect only relatively few odors. Hence, our shrimp models exhibit a seemingly performant central olfactory system, likely able to perceive a broad range of odorants. Overall, at this structural level, *M. fortunata* does not present any differences that could reflect adaptations to the hydrothermal environment when compared to *P. elegans*.

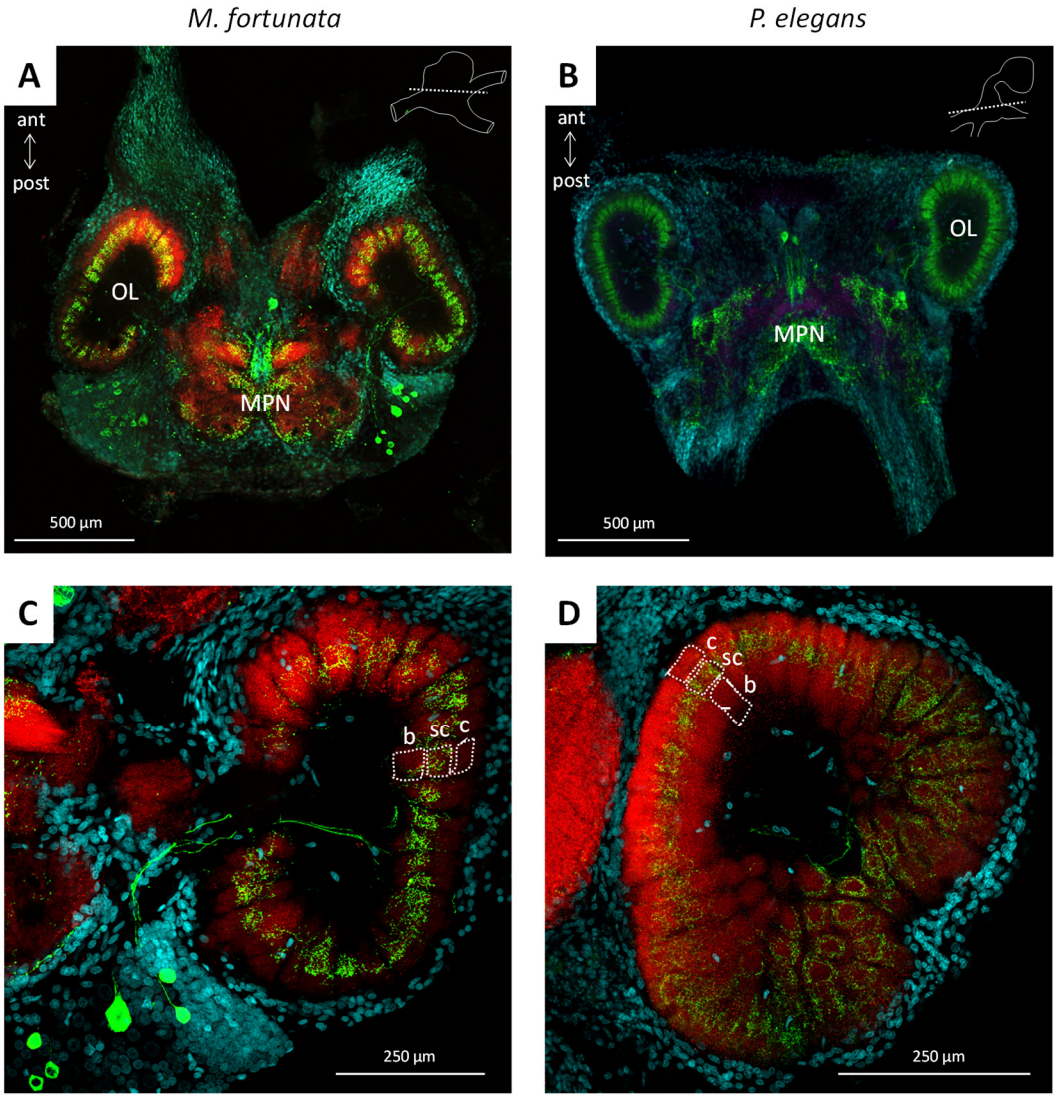

Figure 38 Olfactory lobes in *M. fortunata* and *P. elegans*

A-B. Horizontal sections of the median brain of *M. fortunata* (**A**) and *P. elegans* (**B**), showing the paired lateral olfactory lobes (OL) and part of the median protocerebrum neuropil (MPN). The position of the sections is indicated by right view sketches of the brains.
C-D. Higher magnification of the olfactory lobes of *M. fortunata* (**C**) and *P. elegans* (**D**), showing the subdivision of the olfactory glomeruli in cap (c), subcap (sc) and base (b) regions.
Brains are triple-labeled for synapsin-immunoreactivity (*red* and *purple*), allatostatin-immunoreactivity (*green*) and nuclear marker (*blue*).

- **Antennal and lateral antennular neuropils**

The lateral antennular neuropils are U-shaped (Figure 37 and Figure 39A,B) and the antennal neuropils have a cylindrical shape (Figure 37 and Figure 39B). Both the lateral antennular and antennal neuropils show a strong synapsin immunoreactivity, as well as allatostatin immunoreactivity in a transversely stratified pattern (Figure 39). This striation perpendicular to the long axis suggests a somato- or spatiotopic representation of the chemo- and mechanosensory inputs from these appendages (Sandeman et al. 2014), meaning that the sensilla array on each flagellum is represented like a map along its length. Accordingly, the two species must rely on processing the combined mechano- and chemosensory inputs provided by the antennules and the antennae to extract spatial and temporal information from a chemical signal (Harzsch and Krieger 2018).

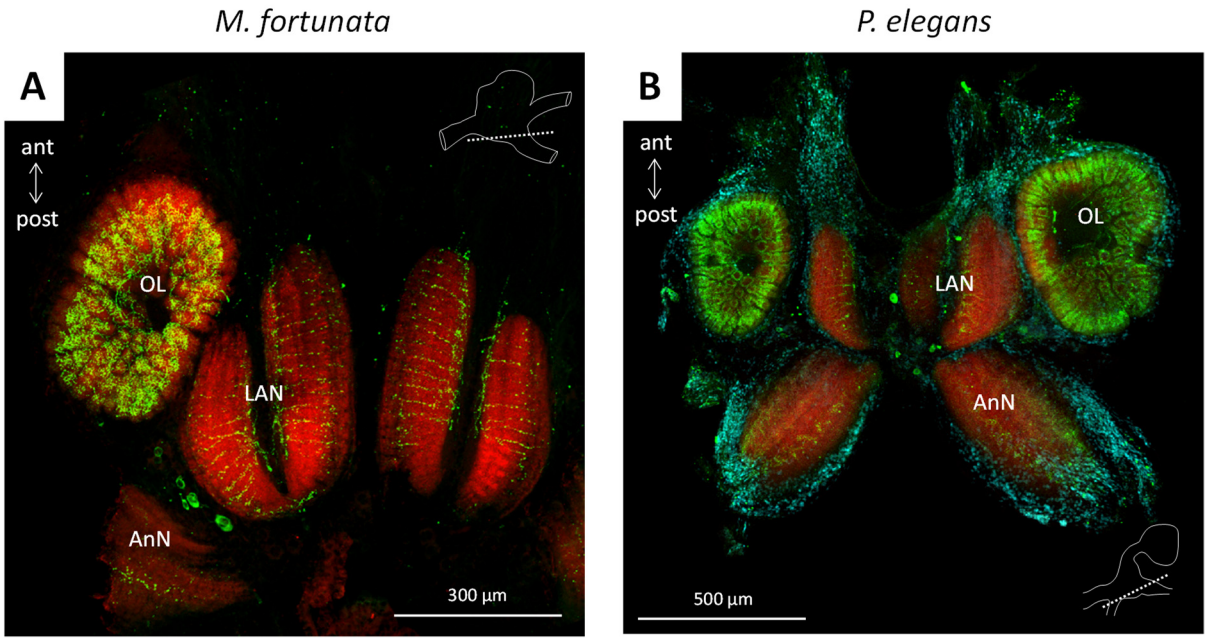

Figure 39 Antennal and lateral antennular neuropils in *M. fortunata* and *P. elegans*

Horizontal sections at the ventral level of the brain of *M. fortunata* (**A**) and *P. elegans* (**B**), showing the olfactory lobes (OL), lateral antennular neuropil (LAN) and the antennal neuropil (AnN). The position of the sections is indicated on right view sketches of the brains.
Brains are triple-labeled for synapsin-immunoreactivity (*red*), allatostatin-immunoreactivity (*green*) and nuclear marker (*blue*).

- **Hemiellipsoid bodies – Medulla terminalis complex (HB-MT complex)**

The hemiellipsoid bodies and the medulla terminalis are located in the lateral protocerebrum close to the visual neuropils (Figure 37 and Figure 40). They receive the output pathway of the olfactory lobes via the olfactory globular tract (Figure 37B, not shown for *M. fortunata*). Both the size of the HB-MT complex and the amount of cells projecting into it might be related to the processing power of sensory inputs in these higher integrative centers (Sandeman et al. 2014). For our specimens, in *M. fortunata*, the hemiellipsoid bodies and the medulla terminalis complex (HB-MT complex) appears well developed (Figure 37A and Figure 40A) and associated to massive cell clusters (Figure 37A and Figure 40C) compared to *P. elegans* (Figure 37B and Figure 40D). I obtained from tridimensional reconstructions of the brain of *M. fortunata* and *P. elegans* the volumes of the HB-MT complex and the associated cell clusters, for one specimen of each species. In *M. fortunata*, the volume of the HB-MT complex was $32x10^9$ μm^3, and the volume of the associated cell clusters was $8x10^9$ μm^3. In *P. elegans*, the volume of the HB-MT complex was $17x10^9$ μm^3, and the volume of the associated cell clusters was $3x10^9$ μm^3. Relative to the size of each specimen used (cephalothorax length: 7.6 mm for *M. fortunata*, 8 mm for *P. elegans*), the HB-MT complex and the associated cell clusters are respectively two and three times more voluminous in *M. fortunata* than in *P. elegans*. In addition, in *P. elegans* the structure of the HB-MT complex is less conspicuous than in *M. fortunata* (Figure 40), for which preliminary observations from paraffin sections indicate a high degree of complexity in the architecture of the HB-MT complex (not shown). These results and observations –although preliminary– suggest that sensory processing in *M. fortunata* is more sophisticated than in *P. elegans*.

In terrestrial hermit crab, the hemiellipsoid bodies display an extremely complex organization, reflecting a massive input from their sophisticated olfactory system (Harzsch and Hansson 2008, Wolff et al. 2012). In contrast, in basal eumalacostracan taxa the hemiellipsoid bodies and the medulla terminalis are unstructured and poorly developed neuropils, such as in Dendrobrachiata (Meth et al. 2017). Thus, size and complexity of these regions can reflect the level of olfactory input received. Nonetheless, I previously showed that the olfactory lobes of *M. fortunata* are similar in structure to those of *P. elegans*, hence it is not likely that the elaborated HB-MT complex is mainly devoted to olfaction in the vent species. Because the HB-MT complex receives inputs from other neuropils than the olfactory lobes, other sensory modalities are likely to be predominantly integrated therein. Regarding the hydrothermal habitat, the evaluation of temperature gradients seems crucial for the endemic vent species, and must be integrated somewhere, maybe in the higher integrative centers. But the mechanisms of thermodetection are poorly known, especially in crustaceans, for which neither specific receptors nor sensory center areas have been identified yet (Lagerspetz and Vainio 2006).

Furthermore, the hemiellipsoid bodies of some crustacean species are frequently assimiled to particular neuropils present in Hexapoda, namely the mushroom bodies, which are well-known as learning and memory centers (Wolff et al. 2012, 2017, Kenning et al. 2013, Harzsch and Krieger 2018). Wolff and collaborators (2017) pointed out that large hemiellipsoid bodies are found in eumalacostracan groups that evidence memory of exact locations (cleaner shrimp [Limbaugh et al. 1961], land hermit crabs [Rotjan et al. 2010]) and eusociality (pistol shrimp [Duffy 1996]). The well-developed hemiellipsoid bodies in *M. fortunata* could thus eventually be involved in memory processes, particular navigational skills or social interactions.

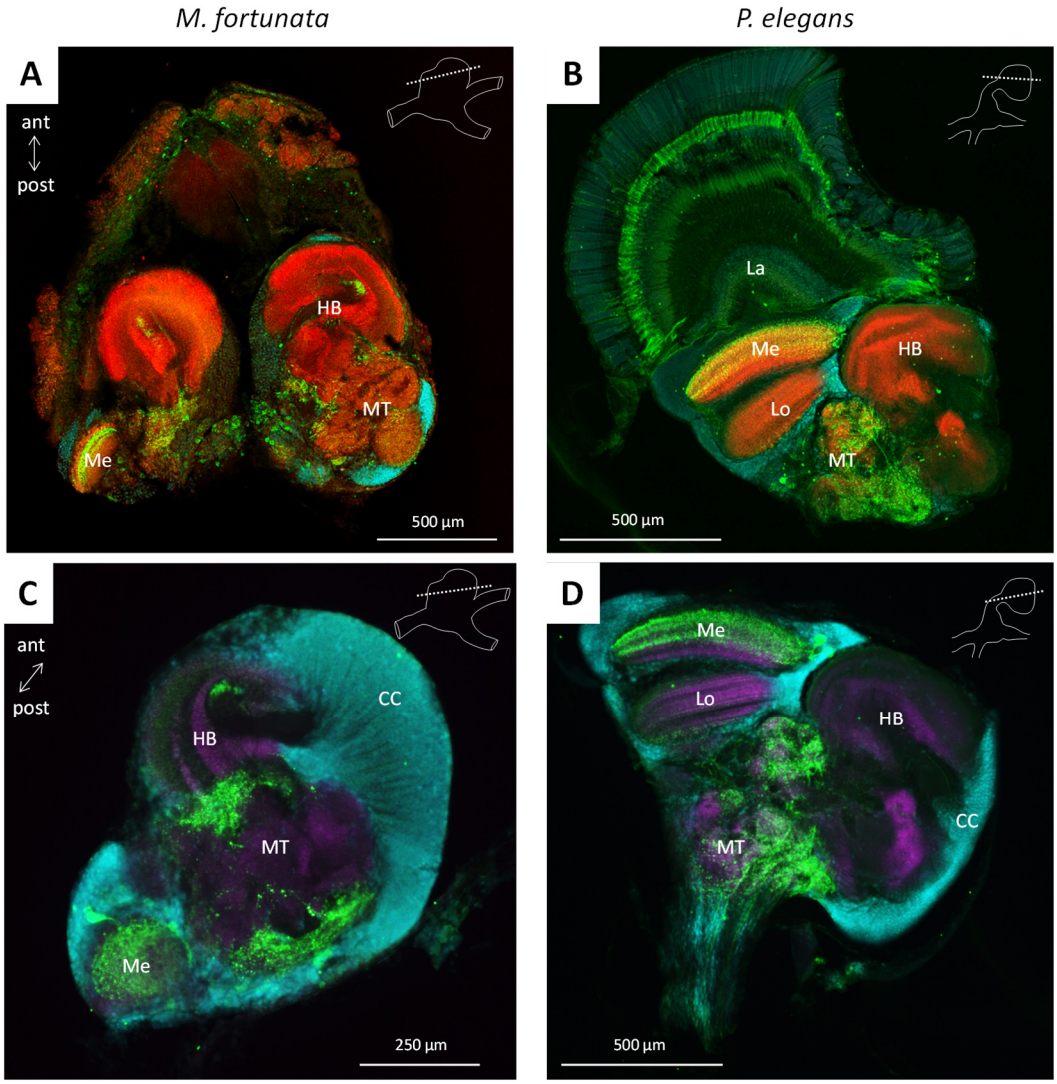

Figure 40 Hemiellipsoid bodies and medulla terminalis in *M. fortunata* and *P. elegans*

Horizontal sections of the lateral protocerebrum of *M. fortunata* (**A,C**) and *P. elegans* (**B,D**), showing the hemiellipsoid bodies neuropils (HB), the medulla terminalis (MT), the associated cell clusters (CC) and the visual neuropils lobula (Lo), medulla (Me) and lamina (La). The position of the sections is indicated on right view sketches of the brains. B, C and D show only one brain hemisphere.
Brains are triple-labeled for synapsin-immunoreactivity (*red* and *purple*), allatostatin-immunoreactivity (*green*) and nuclear marker (*blue*).

III. Conclusions

In this chapter, we described the structure of the chemosensory systems, with a strong focus on the olfactory system, in the vent shrimp *M. fortunata,* in comparison with the shallow-water species *P. elegans* to get insights into the vent species chemosensory abilities and potential adaptations of its chemosensory system reflected by anatomical features.

Our results indicate that *M. fortunata* is equipped with all elements that are part of a functional chemosensory system. Its antennules bear olfactory aesthetasc sensilla innervated by numerous olfactory sensory neurons that project to the olfactory lobes in the brain. The antennules and the antennae also bear presumably bimodal chemo- and mechanosensory sensilla of -yet- unknown functions. There is accordingly no doubts that chemodetection is used by this species.

To infer on the shrimps olfactory abilities, numerical aspects of aesthetascs and olfactory lobes characteristics in *M. fortunata* were measured and compared to the coastal shrimp *P. elegans*. We found that the dimensions and number of aesthetascs and innervating olfactory sensory neurons of *M. fortunata* fit within the ranges displayed by *P. elegans* and other marine decapod species, and that the olfactory lobes are similar in size and structure between *M. fortunata* and *P. elegans*. These results do not suggest any structural adaptation nor peculiar olfactory abilities of the vent species regarding these characters. Nonetheless, some differences were noticed between the vent and coastal species. At the peripheral level, we found that pore-like structures occurring in the aesthetasc cuticle and a dense bacterial coverage of the antennal appendages are likely specific to vent shrimp species. At this point of knowledge, the functional or adaptive significance of these features is unknown. Speculatively, the pore-like structures occurring in the aesthetasc cuticle could enhance the permeability of the cuticle to soluble odorants. The role of the bacterial coverage on the sensory appendages of vent shrimp could be hypothesized from the identification of the bacterial types. For example, sulfide-oxidizing bacteria are abundant in hydrothermal vent, and their occurrence on the antennal appendages could detoxify the hydrogen sulfide prior to reach the olfactory dendrites. At the central level, the higher integrative centers hemiellipsoid bodies and medulla terminalis are especially well-developed in *M. fortunata* compared to *P. elegans*. Because we did not found striking anatomical features in the olfactory system of *M. fortunata*, we can hypothesize that sensory modalities other than olfaction may be predominantly processed in the higher integrative centers. Alternatively, these elaborated neuropils could be involved in memory processes, navigation or social interactions in vent species.

Chapter IV

Chemodetection of ecologically-relevant stimuli by the antennal appendages of *M. fortunata* and *P. elegans*

I. Introduction

II. Development of an electroantennography (EAG) method on marine shrimp

1. Determination of recording parameters
    - Electrode placement and signal propagation
    - Stimulatory pressure
    - Time interval for consecutive stimulations
2. EAG recording of chemosensory responses

III. Results and discussion

1. Detection of food-related odors mixture
2. Detection of hydrothermal fluid chemicals
    - Responses to sulfide
    - Responses to basic pH
    - Responses to iron and manganese

IV. Conclusions

I. Introduction

Chemosensory abilities of vent shrimp have been poorly studied, despite their importance for understanding how they detect their habitat, food sources or congeners. Because the vent shrimp *M. fortunata* possesses aesthetascs innervated by olfactory sensory neurons (OSNs) and chemosensory centers seemingly functional (see Chapter III) as in shallow water decapods, this species must exploits its chemical environment. However, which chemicals are detected and used as orientation cues by *M. fortunata*, and vent shrimp in general, is largely unknown. As for all animals, food sources are obvious attractants (Gebruk et al. 2000). Regarding the hydrothermal environment, vent shrimp might be able to sense the chemicals that are extensively released by active vents (Segonzac et al. 1993, Renninger et al. 1995, Sarrazin et al. 1999). Vent shrimp might detect hydrothermal fluid chemicals in their microhabitat, and maybe also at distance from active sites, when the buoyant plumes spread in the water column.

In hydrothermal fluids, even if their composition varies from one site to another, sulfide, manganese and iron are among the compounds commonly encountered (Radford-Knoery et al. 1998, Charlou et al. 2000). Chemical gradients occur from the fluid emission point, and can be either steep or gradual depending on the chemicals (Klevenz et al. 2011). For example, around the chimneys, sulfide rapidly disappears from the water column after reacting with seawater and hydrothermal fluid constituents (Mottl and McConachy 1990, Zhang and Millero 1993). Manganese is more stable (Cowen et al. 1990) and can thus be detected at considerable distances from the fluid source (Radford-Knoery et al. 1998). Iron is also detected at several hundreds of kilometers from the source (Aumond 2013, Waeles et al. 2017) when partially stabilized by complexation with dissolved organic matter (Toner et al. 2009). Thus, sulfide might potentially be used by the shrimp as a short-distance stimulus, while manganese and iron could serve rather as long-distance stimuli. Only one study has so far addressed the chemosensory abilities of hydrothermal shrimp, i.e. that of Renninger and collaborators (1995) who recorded electrophysiological responses from the antenna of the vent shrimp *R. exoculata* upon exposure to sulfide, and reported preliminary behavioral observations suggesting attraction to sulfide. This would support the potential role of hydrothermal fluid components as orientation cues for vent shrimp, which still has to be investigated for other components than sulfide, and also extended to other vent species. Food sources are another potential attractant for vent shrimp, for example invertebrate tissues for scavenger species as *M. fortunata* (Gebruk et al. 2000).

To test whether *M. fortunata* can detect food sources and hydrothermal fluid chemicals (such as sulfide, manganese and iron) through its presumed main chemosensory organs, Phillipe Lucas[1], Magali Zbinden, Juliette Ravaux and I developed an electroantennography (EAG) method to record the

global responses of the antennal appendages neurons to stimulation with environmental stimuli. The coastal shrimp *P. elegans* was used for the development of the EAG, as well as for further comparison of the responses to selected chemicals with the vent shrimp *M. fortunata*.

[1] iEES Paris, Sensory Ecology department, Neuroethology of Olfaction team

II. Development of an electroantennography (EAG) method on marine shrimp

[Results published in Machon et al. 2016]

Responses of crustacean chemosensory neurons to odor stimuli are classically recorded either extracellularly from their axons (Derby, 1989; Kamio et al., 2005) or intracellularly with the patch-clamp method (Ache, 2002; Anderson and Ache, 1985; Bobkov et al., 2012). These methods are invasive, time-consuming to establish on a new model, and require many replicates to get an overview of an organ global sensitivity. Hydrothermal vent specimens are difficult to collect and maintain alive and therefore are available in low numbers for experiments. The objective here was to develop a method with a high rate of success, allowing the recording of global responses of the antennules and antennae in marine shrimp. In insects, such a technique called electroantennography (EAG; Schneider, 1957) is commonly used to measure the global responses of antennal OSNs to odors. This technique is for instance widely used for screening moth pheromones (Roelofs, 1984). In crustaceans, EAG measurements were performed in aerial conditions on two terrestrial crabs, i.e. the giant robber crab *Birgus latro* (Stensmyr et al., 2005) and the hermit crab *Coenobita clypeatus* (Krång et al., 2012), and on one the marine hermit crab *Pagurus berhnardus* (Stensmyr et al., 2005). Two papers reported very briefly EAG recordings, with no technical demonstration, from fresh water crustaceans: the branchiopoda *Daphnia spp.* (Simbeya et al., 2012) and the crayfish *Procambarus clarkii* (Ameyaw-Akumfi and Hazlett, 1975). Hence, an EAG method performed under natural (i.e. underwater) conditions has so far never been developed for aquatic crustaceans.

We implemented a new EAG technique on a marine decapod while keeping both its antennal appendages and the stimulus in its natural (marine) environment. This technique is derived from the EAG on insects. Insect antennae have different shapes which impacts the positioning of the recording electrode. In Lepidoptera, EAG is typically performed from whole insect preparations by cutting the tip of the antenna and inserting it in a glass electrode filled with electrolyte, with the reference electrode inserted in the insect body. Excised antennae can also be used but they have a shorter lifetime (Martinez et al., 2014). These recording methods were unsuitable for our model shrimp species, since sectioned tissues of the antennal appendages deteriorate in few minutes, and cutting the extremity of one antenna or antennule induces a prominent outflow of antennal fluid. In Coleoptera, the recording electrode is inserted in the antenna (Roelofs, 1984); this method is the less invasive and has consequently been selected for the EAG on shrimp. Next, the main constraint for EAG in aquatic species is the short circuit resulting from placing the two electrodes (reference and recording) in water. We

used the air-water interface to prevent this short circuit, by putting the anterior part of the shrimp (i.e. antennular appendages, one lateral flagellum being impaled by the recording electrode) in the bath solution and the posterior part (i.e. telson and abdomen, connected to the reference electrode) in the air.

1. Determination of recording parameters

We used a food odor stimulus (shrimp food extract) as a positive control (i.e. that is expected to trigger a chemosensory response) and *Panulirus* saline (PS) as a negative control (i.e. that triggers only a mechanosensory response), to determine the best conditions to record EAG responses on *P. elegans* (i.e. position for the recording electrode, stimulatory pressure, time interval between two consecutive stimulations).

- **Electrode placement and signal propagation**

To estimate if the electrode records responses from a large or small portion of the antennule (i.e. how global are the responses), different portions of the lateral antennule were stimulated with a food odor stimulus. Fast Green was used to visualize stimulated zones and it did not modified responses to the food odor stimulus. When narrow stimuli were applied along the antennule while recording from the basal region (Figure 41A,B), the electrode recorded responses from zones stimulated far from the electrode location. Then, increasing lengths of the antennule were stimulated by moving a larger stimulation capillary along the antennule while recording from the apex (Figure 41A,C) or the base regions (Figure 41A,D). For both electrode placements, the EAG amplitude increased with the size of the stimulated area. Thus, there is a good propagation of the electrical signal consecutive to the chemical stimulation, meaning that the activity from a large fraction of sensory neurons can be recorded. To maximize the amplitude of recorded responses (i.e. to record the activity of the largest number of sensory neurons), following experiments were done by stimulating the whole length of the flagellum and placing the recording electrode in the middle region of the antennule.

The EAG response is assumed to represent the summation of receptor potentials(GLOSSARY) of many synchronously activated chemosensory neurons (Schneider, 1957; Schneider, 1999; Nagai, 1983; Mayer et al., 1984). As slow electrical events (e.g. receptor potentials) travel better than action potentials due to low-pass filtering of the extracellular space (Bedard et al., 2004), our observation that odor-evoked signals travelled far within the antennule supports that we do record summed receptor potentials with our EAG method on shrimp.

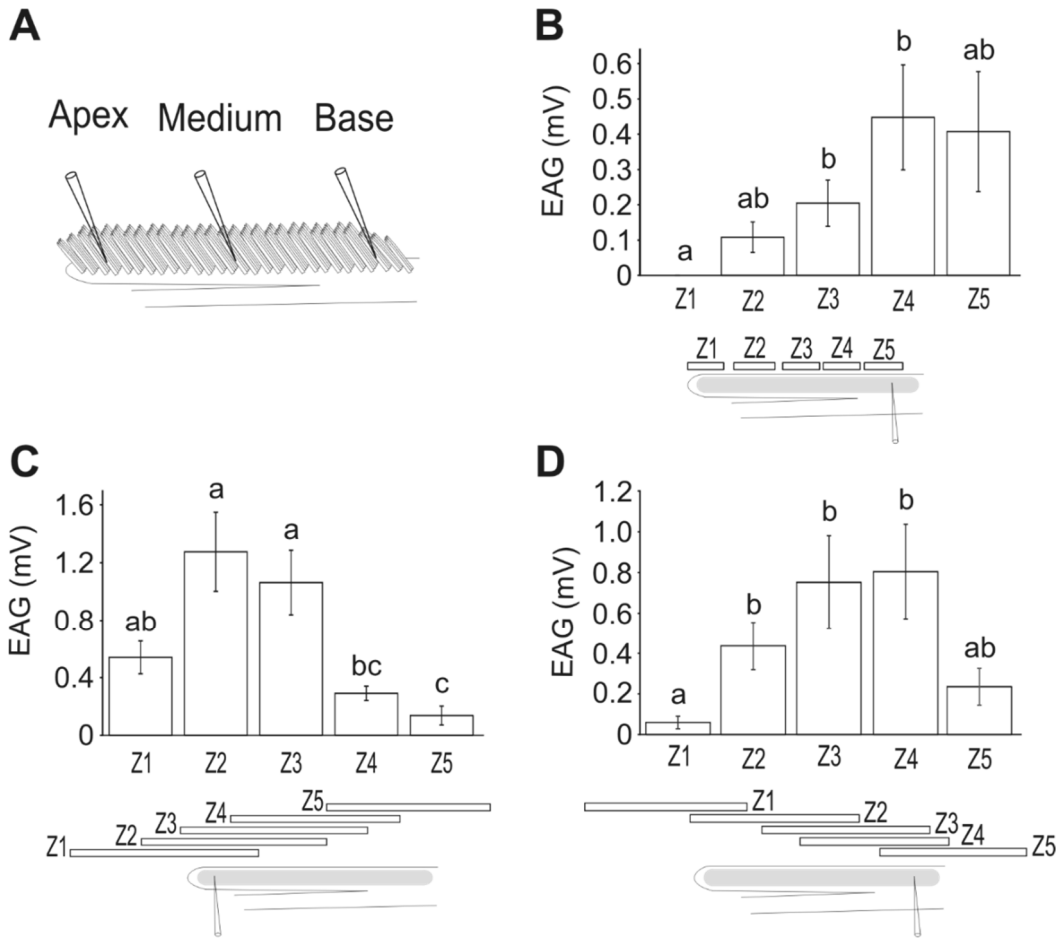

Figure 41 EAG recordings allow monitoring responses from a large fraction of sensory neurons

A. Sketch of *P. elegans* aesthetascs bearing antennular flagellum with the different electrode placements at the base, middle and apex regions. Not to scale.

B. EAG amplitudes recorded from the basal region to narrow stimuli at different zones along the antennule (Z1, Z2, Z5, n=4; Z3, Z4, n=5).

C. EAG amplitudes recorded from the apical region to wide stimuli at different zones along the antennule (Z1, Z4, Z5, n=5; Z2, n=7; Z3, n=6).

D. EAG amplitudes recorded from the basal region with wide stimuli at different zones along the antennule (Z1, Z2, Z3, n=7; Z4, n=6; Z5, n=4).

In B–D, EAGs were recorded in response to a food odor stimulus (0.2 g ml^{-1} of shrimp food extract for 1 s in B, 0.5 s in C and D). The gray zone on the antennule sketch represents the aesthetascs bearing area. Means ± s.e.m. were compared with a one-way ANOVA with permutation test (B, p=0.04; C, p=0.002; D, p=0.01) and by multiple comparisons with two-sample permutation t-tests; Benjamini–Hochberg corrections were applied. Means with different letters are significantly different (p<0.05).

- **Stimulatory pressure**

In decapods, the antennule is equipped with unimodal olfactory aesthetascs housing OSNs, and also with bimodal (chemo- and mechanosensory) non-aesthetasc sensilla, present in lower density than aesthetascs (Cate and Derby, 2001; Hallberg et al., 1997; Obermeier and Schmitz, 2004; Steullet et al., 2002). Hence, both neurons innervating the aesthetascs and the non-aesthetasc sensilla can contribute to the recorded signal, i.e. the EAG traces represent the summation of chemical and mechanical responses. To estimate the contribution of mechanosensory neurons in the responses obtained, negative control stimuli (PS) were applied at increasing pressures (2 to 10 psi) (Figure 42A). PS responses were pressure-dependent, with no significant response for the lowest pressure (2 psi) and significant response for pressure values of 4 psi and more (Figure 42A,B) indicating that a stimulus sent at these pressures on the flagellum can trigger the activation of mechanosensory neurons. The response increase from 4 (-0.17 ± 0.04 mV, n = 24) to 10 psi (-0.32 ± 0.09 mV, n = 25) was not significant (one-way ANOVA with permutation test, $p = 0.8$) due to a high variability of the amplitude of responses across recordings. We thus decided to adjust the pressure of all stimulations to 5 psi, to facilitate the stimulus access to aesthetascs through their dense packing and to bimodal sensilla without eliciting strong mechanical responses that would have impeded measuring correctly chemical responses.

- **Time interval for consecutive stimulations**

Responses of chemosensory neurons not only depend on the stimulus characteristics (quality, quantity) but also on previous chemosensory experience via the process of adaptation (Kaissling et al., 1987). When chemosensory neurons are adapted to a stimulus, responses to subsequent stimuli are reduced. The recovery from adaptation is time-dependent. To determine the recovery time necessary between consecutive stimuli to prevent measuring responses from adapted sensory neurons, we measured EAG responses to pairs of identical stimuli (food odor stimulus) with increasing the inter-stimulus time intervals (4 to 90 s) (Figure 42C,D). As the inter-stimulus interval was increased, the average amplitude of the responses to the second stimulation increased towards that of the first stimulation. Both amplitudes did not differ significantly when the time interval was at least 90 s. For safety, in the following, we kept an interval of at least 2 min between consecutive stimuli.

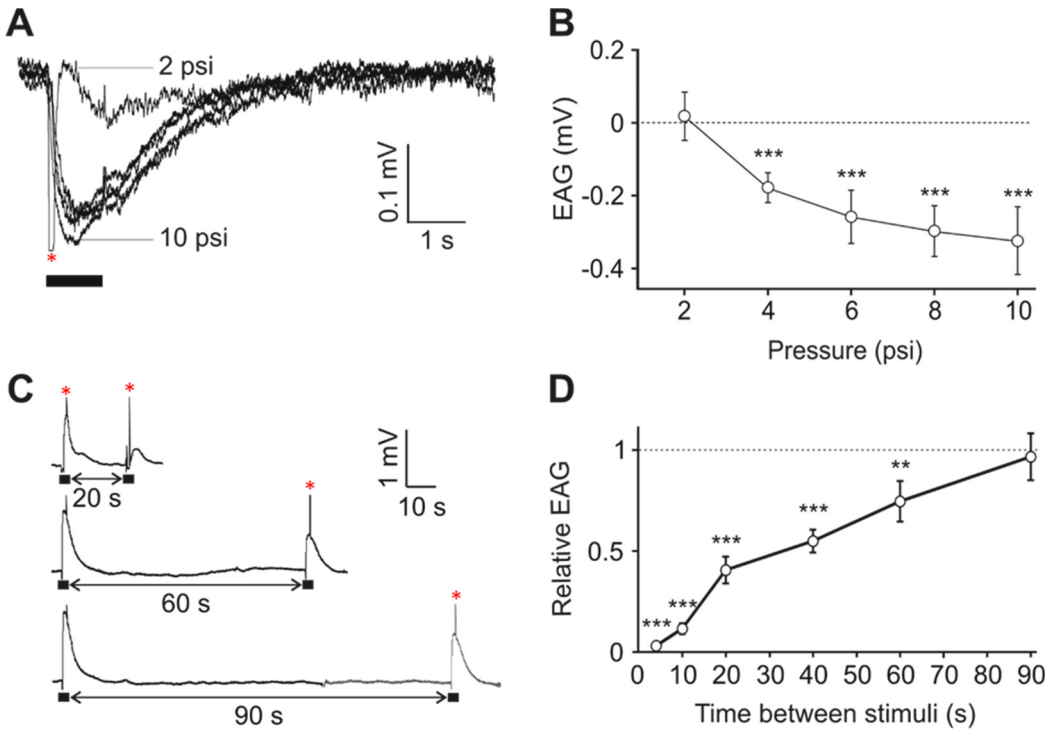

Figure 42 EAG responses to mechanical and consecutive chemical stimulations in *P. elegans*

A. Superimposed traces of EAG responses to *Panulirus* saline with increasing pressure, the upper trace corresponding to 2 psi, and the others to 4, 6, 8 and 10 psi.
B. EAG pressure-response curve to *Panulirus* saline (n = 21 for 2 psi; n = 24 for 4 psi; n = 25 for 6, 8 and 10 psi).
C. Examples of EAG responses to two consecutive stimulations with a food odor stimulus (0.1 $g.mL^{-1}$ of shrimp food extract for 1 s at 5 psi) separated by 20, 60 and 90 s.
D. Amplitude of EAG responses to a food odor stimulus (same as in C) relative to the amplitude of EAG response to a previous identical stimulation, as a function of the time between the two stimuli (n = 7 for 10, 60 and 90 s, n = 9 for 4 and 40 s; n = 11 for 20 s).
In A and C, bars indicate the stimulus delivery. Transient peaks (*) are valve opening artefacts. Means ± s.e.m. were compared with a one-way ANOVA with permutation test (B, p = 0.004; D, p < 10-15), and with one-sample permutation t-tests to reference values (0 in B, 1 in D). *: P<0.05; **: P<0.01; ***: P<0.001.

2. EAG recording of chemosensory responses

All the responses to a food odor stimulus were positive deviations of the baseline (Figure 43A). Increasing concentrations of the food odor stimulus (0.001 $g.mL^{-1}$ to 0.2 $g.mL^{-1}$) elicited dose-dependent responses with a threshold between 0.001 and 0.003 $g.mL^{-1}$ (Figure 43B) and amplitudes reaching 2.6 mV for the highest concentration (0.2 $g.mL^{-1}$). The delay between the electrovalve opening command and the beginning of the EAG response is 62 ± 3 ms (n = 20). Antennules were also stimulated with other food extracts made from green crabs, blue mussels and dead *P. elegans* individuals, and responses had the same polarity as those for the shrimp food extracts (Figure 43C). A similar response profile to dead shrimp extract was obtained for the hydrothermal species *M. fortunata* (Figure 43D).

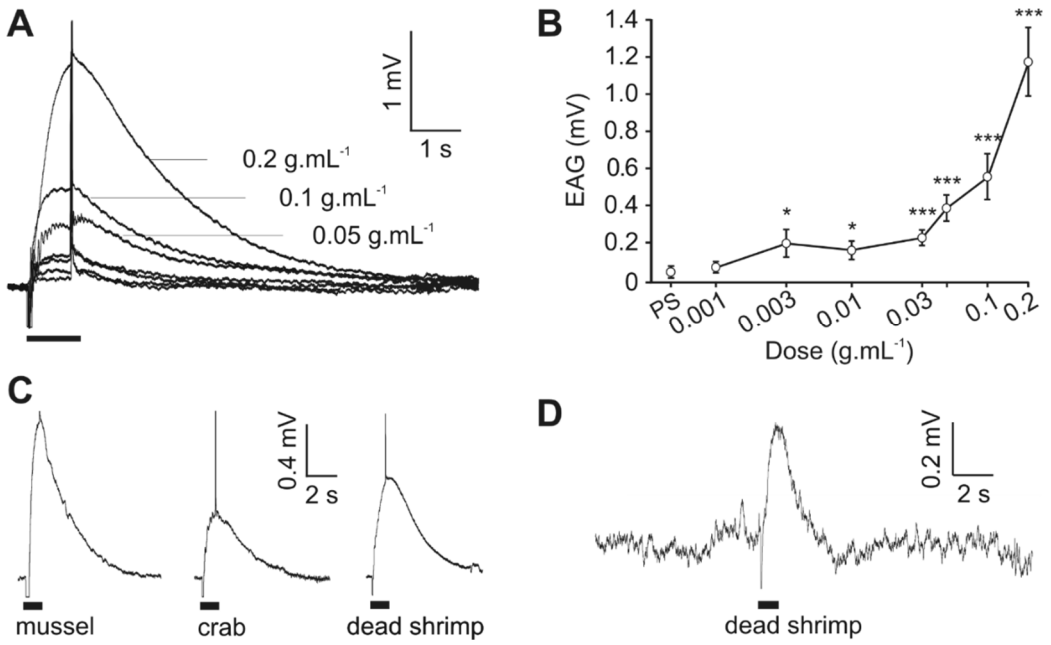

Figure 43 EAG responses to food odor stimuli in *P. elegans* and *M. fortunata*

A. Superimposed traces of EAG responses to dilutions of a shrimp food extract (0.001, 0.003, 0.01, 0.03, 0.05, 0.1 and 0.2 $g.mL^{-1}$).
B. EAG dose-response curve to dilutions of a shrimp food extract (n = 10 for 0.05 $g.mL^{-1}$; n = 11 for 0.001 and 0.003 $g.mL^{-1}$; n = 12 for control; n = 14 for 0.2 $g.mL^{-1}$; n = 16 for 0.01, 0.03 and 0.1 $g.mL^{-1}$). Means ± SEM were compared with a one-way ANOVA with permutation test ($p < 10\text{-}15$), and with two-sample permutation t-test to control stimuli (PS). *: P<0.05; **: P<0.01; ***: P<0.001.
C. EAG responses to fresh mussel extract, fresh crab green extract and extract of dead *P. elegans* individuals.
D. EAG response to dead shrimp extract from *M. fortunata*.
In A, C and D, bars indicate the stimulus delivery. Transient peaks are valve opening artefacts.

EAG responses to a food odor stimulus in *P. elegans* are reproducible, dose-dependent and exhibit sensory adaptation, characteristics that confirm we indeed recorded chemosensory responses. We could not reach the saturation level in the dose-response curve because we reached the saturating concentration of the food extract. All chemical stimuli we tested (shrimp food extract, crab, mussel and dead shrimp) elicited positive EAGs in *P. elegans* whereas insect EAGs are usually negative (Roelofs, 1984). In contrast, mechanical stimuli elicited negative EAGs. Recordings from single chemosensory neurons and single mechanoreceptor neurons could help clarifying why chemical and mechanical responses have opposite polarities.

EAG recordings from the antenna were also successful, on both *P. elegans* and *M. fortunata*. Figure 44 gives the mean amplitude of the responses of the antenna and the antennule to positive (Figure 44A) and negative (Figure 44B) controls. Antennular responses to a food odor stimulus have a significantly higher amplitude in *P. elegans* than in *M. fortunata*. By contrast, the amplitude of the antennal responses to a food odor stimulus were significantly higher in *M. fortunata* than in *P. elegans*. In both cases, it is not possible to distinguish between if one organ is more responsive for one species, or if the connection of the electrode is of superior quality (for example, in *P. elegans* the portion of the antennule bearing the aesthetascs is relatively soft, making the electrode connection easier and thus allowing frequent good quality –i.e. high amplitude– recordings). Same uncertainty takes place for antennules responses to mechanical stimulations with PS, for which the absolute amplitudes were significantly higher for *P. elegans* (-232±2 µV) than for *M. fortunata* (-80 ± 10 µV). Antennal EAG responses being always of smaller amplitude than those of the antennules might be explained by the quantity of sensory neurons innervating each organ, the antennule housing numerous clusters of chemosensory neurons that are absent in the antenna (see Chapter III – II.1. Figure 33).

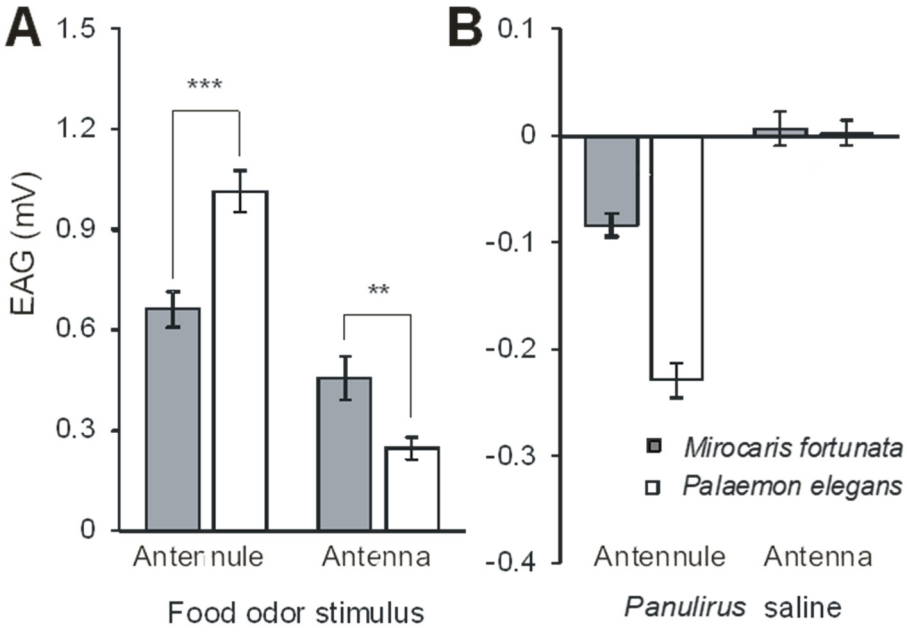

Figure 44 EAG responses to chemical and mechanical stimulations in *M. fortunata* and *P. elegans*

Responses to (**A**) a chemical stimulation (shrimp food extract 0.2 g.mL^{-1}**)** and to (**B**) a mechanical stimulation (*Panulirus* saline) recorded from the antennules and antennae (grey, *M. fortunata*; white, *P. elegans*), Antennule, *M. fortunata*: n = 44, *P. elegans*: n = 58; antenna, *M. fortunata*: n = 13, *P. elegans*: n = 27. Means (± s.e.m.) were compared between the two species for each organ and stimulus with a two-sample permutation *t*-test. ***P*<0.01, ****P*<0.005.

III. Results and discussion

[Results published in Machon et al. 2018]

1. Detection of food-related odor mixtures

M. fortunata exhibits an opportunistic feeding behavior, scavenging on tissues of mussel, shrimp and other invertebrates when available, as well as grazing bacteria on sulphide surfaces (Gebruk et al. 2000, Colaço et al. 2002, De Busserolles et al. 2009). An extract of dead *M. fortunata* was used as an environmental relevant food-odor stimulus to test whether the detection of food is mediated by the antennule for this species. This stimulus elicited dose-dependent responses from the antennule (Figure 46A), confirming its presumed role in food detection. An extract of dead *P. elegans* also stimulated the antennule of *P. elegans* (Figure 46A). The responses thresholds were between dilution 1:10 and non-diluted extract for *M. fortunata* and between dilutions 1:100 and 1:10 for *P. elegans*, with amplitudes reaching respectively 70 and 250 µV. These results are consistent since *P. elegans* and *M. fortunata* have a similar food profile, being secondary consumers. EAG responses toa food odor stimulus previously obtained from both the antennule and the antenna (Figure 44) suggest that the antenna is also involved in the chemodetection of food sources in both species.

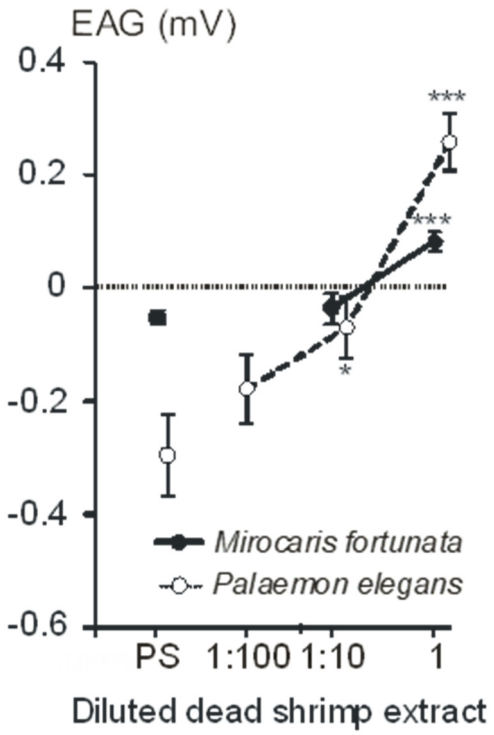

Figure 45 EAG responses to dead shrimp extracts in *M. fortunata* and *P. elegans*

Responses to dead shrimp extracts recorded from the antennules. *M. fortunata*: n = 7, *P. elegans*: n = 8. Means (± s.e.m.) were compared with a one-way ANOVA with permutation tests ($p<^{10^{-}}15$) and with two-sample permutation *t*-tests to control stimulus (*Panulirus* saline, PS). **p<0.01, ***p<0.005.

2. Detection of hydrothermal fluid chemicals

Chemicals and their concentrations were chosen regarding the chemical composition of the hydrothermal fluids (Radford-Knoery et al. 1998, Charlou et al. 2000) and in the shrimp vicinity (Aumond 2013, Sarrazin et al. 2015) at the Lucky Strike hydrothermal vent site, where *M. fortunata* specimens were sampled. Each chemical presents different removal rates, associated to reaction with seawater, other hydrothermal fluid constituents, dissolved organic matter, and to consumption by chemoautotrophic bacteria. Sulfide removal rate is high and sulfide is thus considered as a short-distance stimulus, detectable near hydrothermal fluid emission points, while manganese and iron are more stable, detectable far from the source, thus are considered as long-distance stimuli (Radford-Knoery et al. 1998, Aumond 2013, Waeles et al. 2017). To investigate if vent shrimp use such hydrothermal fluid compounds as orientation cues for both near-field and distant perception of the habitat, we tested the detection of selected chemicals by the antennular and antennal appendages of *M. fortunata*, as well as those of the coastal shrimp *P. elegans*, to check for potential hydrothermal shrimp specificity.

Each chemical was first tested on the antennules at concentrations that *M. fortunata* is likely to encounter in its environment. For all the stimuli tested (Na_2S: 0.04 to 40 µmol.L^{-1}; $FeCl_2$ and $MnCl_2$: 0.05 to 5 µmol.L^{-1}) responses from the antennule of *M. fortunata* and *P. elegans* did not depend on stimulus concentrations (Figure 46A,C,E), i.e. none elicited responses distinct from responses to the negative control. Higher concentrations were used afterwards, up and beyond to the concentrations measured in the pure fluid of the Lucky Strike site, for the antennules and antennae of both species.

➔

EAG responses to increasing concentrations for Na_2S, $FeCl_2$ and $MnCl_2$ in *M. fortunata* (black dots) and *P. elegans* (white dots).
A. Responses to Na_2S recorded from the antennules.
B. Responses to Na_2S recorded from the antennae.
For A and B, pH control is set to 11 and corresponds to the pH of the 14000 µmol.L^{-1} Na_2S solution.
C. Responses to $FeCl_2$ recorded from the antennules.
D. Responses to $FeCl_2$ recorded from the antennae.
For C and D, pH control is set to 6 and corresponds to the pH of the 5 to 10000 µmol.L^{-1} $FeCl_2$ solutions.
E. Responses to $MnCl_2$ recorded from the antennules.
F. Responses to $MnCl_2$ recorded from the antennae.
Under the x axis, white bars indicate concentrations that *M. fortunata* is likely to encounter in its environment, and black bars indicate concentrations measured in the pure fluid at the Lucky Strike vent field. Means (± s.e.m.) were compared with a one-way ANOVA with permutation test ($P<10^{-15}$ for sodium sulfide dose-responses) and with a two-sample permutation t-test to control stimuli (*Panulirus* saline, PS). *p<0.05, **p<0.01, ***p<0.001. The n numbers of antennules and antennae tested for each species and for each condition are presented in Table 12.

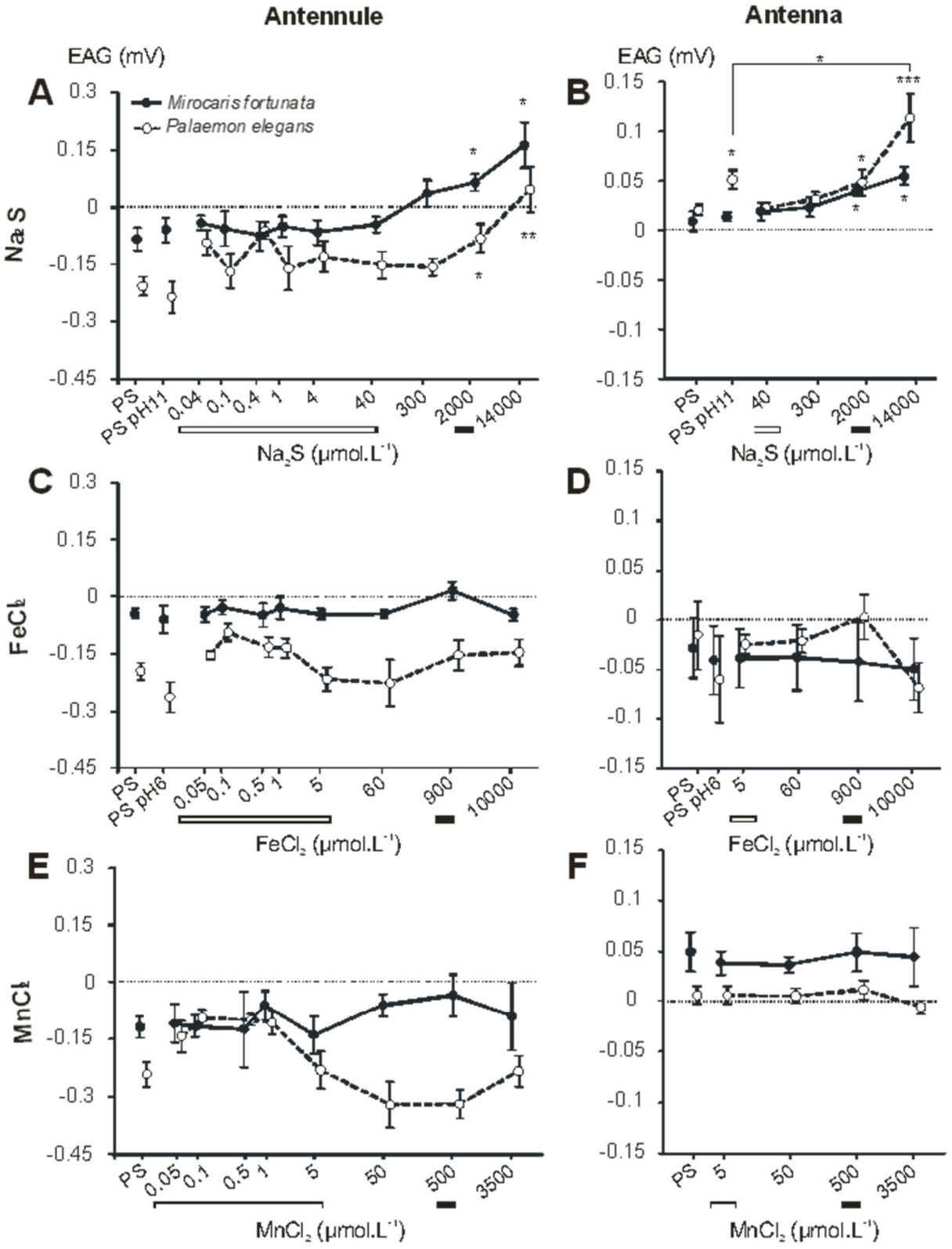

Figure 46 EAG responses to hydrothermal fluid compounds in *M. fortunata* and *P. elegans*

Legend previous page.

Table 12 *n* of antennules and antennae tested for sulfide, iron and manganese in EAG

Stimulus	Concentrations, controls	*n*			
		Antennules		Antennae	
		M. fortunata	*P. elegans*	*M. fortunata*	*P. elegans*
Na_2S	PS (negative control)	9	12	4	8
	PS pH 11 (pH control)	4	7	4	8
	0.04, 0.1, 0.4, 1, 4 µmol.L^{-1}	5	5	-	-
	40 µmol.L^{-1}	8	12	4	8
	300, 2000, 14000 µmol.L^{-1}	4	7	4	8
$FeCl_2$	PS (negative control)	11	15	5	9
	PS pH 6 (pH control)	6	10	5	9
	0.05, 0.1, 0.5, 1 µmol.L^{-1}	5	5	-	-
	5 µmol.L^{-1}	10	15	5	9
	60, 900, 10000 µmol.L^{-1}	6	10	5	9
$MnCl_2$	PS (negative control)	10	17	4	10
	0.05, 0.1, 0.5, 1 µmol.L^{-1}	5	6	-	-
	5 µmol.L^{-1}	9	17	4	10
	50, 500, 3500 µmol.L^{-1}	5	11	4	10

- **Responses to sulfide**

At higher concentrations, Na_2S elicited dose-dependent responses from the antennules and antennae of *M. fortunata* (Figure 46A,B and Figure 47). Thresholds were between 0.3 and 2 mmol.L^{-1} for both antennal appendages. Thus sulfide is detected by bimodal sensilla on the antennae, but for the antennules we cannot distinguish the role played by aesthetascs and bimodal sensilla in sulfide detection. Renninger et al. (1995) recorded trains of action potentials from nerve fibers of the three antennal appendages of the hydrothermal shrimp *R. exoculata*, and found that only the antennae respond in a dose-dependent way to sulfide. This absence of concentration-dependent responses for the antennule in *R. exoculata* might be due to technical limitations rather than no detection. Recording from nerve fibers implies that only a fraction of axons are connected to the electrode opening, and thus action potentials are recorded from only a minority of neurons. The EAG method overcomes this problem since the electrode records neuron activation from almost the whole length of the flagellum (as shown above, section II.1. and Figure 41). Hence at least two hydrothermal shrimp species are physiologically able to detect sulfide via their antennal appendages, supporting the hypothesis that sulfide could serve as an effective orientation cue in the close hydrothermal environment. Yet because the sulfide concentrations that triggered significant EAG responses were equivalent to those encountered in the pure fluid, there is some doubt about the ecological relevance of the responses obtained since *M. fortunata* inhabits diffuse vents with low sulfide concentrations (Cuvelier et al.

2011), and *R. exoculata* lives closer to vent chimneys but still in fluid-diluted areas. However, convergence of sensory inputs onto higher-level neurons occurs in the chemosensory pathway of crustaceans (Mellon 2000), as in vertebrates and insects (Van Drongelen et al. 1978). This convergence makes neurons in the central nervous system highly sensitive (Rospars et al. 2014). Hence, behavioral responses to chemical stimuli can potentially be observed at concentrations that do no trigger EAG responses, and questions regarding the relevance of the sulfide concentrations tested could be addressed with behavior experiments. Antennules and antennae of the coastal shrimp *P. elegans* were also responsive to sulfide, with thresholds between 0.3 and 2 mmol.L^{-1} for the antennules and 2 and 14 mmol.L^{-1} for the antennae. Sulfide detection is therefore not specific to vent species and is likely not an adaptation to the hydrothermal environment. Again, behavior experiments are needed to investigate if hydrothermal species present specific responses to sulfide, such as attraction behavior, compared to coastal species.

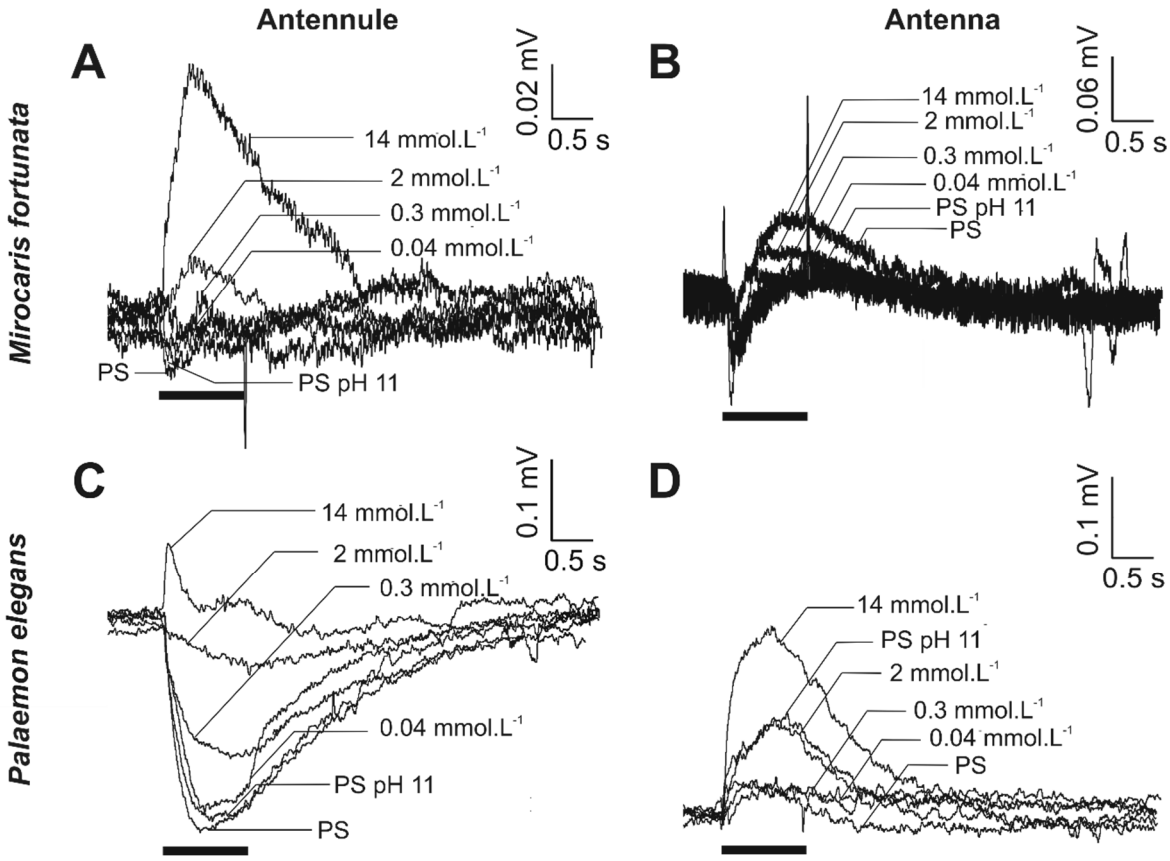

Figure 47 Dose-dependent EAG responses to sulfide in *M. fortunata* and *P. elegans*

Superimposed traces of EAG responses to *Panulirus* saline (PS) to increasing concentrations of Na_2S (0.04, 0.3, 2, 14 mmol.L^{-1}) and to pH control solution (PS at pH 11) from the antennule (A, C) and the antenna (B, D) in *M. fortunata* (A, B) and *P. elegans* (C, D). Horizontal bars indicate stimulus delivery. Transient peaks in A, B and D are valve opening artifacts.

- **Responses to basic pH**

P. elegans antenna was significantly responsive to a control pH 11 stimulus (Figure 46B), as observed by Renninger and collaborators (1995) for the coastal shrimp *Penaeus aztecus* antenna exposed to a pH 13 stimulus. But the response to pH 13 in *P. aztecus* was not significantly different from the response to a pH 13 sulfide solution (1300 mmol.L^{-1}). In the present study, response of the antenna in *P. elegans* to pH 11 significantly differs in amplitude from the response to pH 11 sulfide solution (Na_2S 14 mmol.L^{-1}), meaning there is detection of both sulfide and high pH by the antenna of *P. elegans*. The confounded responses to sulfide and pH 13 stimulus in *P. aztecus* (Renninger et al. 1995) might be due to the low number of specimens tested ($1<n<4$), insufficient to bring out a significant difference between these two stimuli. Responses to high pH stimuli could be specific to coastal species, since neither *M. fortunata* antenna (this study) nor *R. exoculata* antenna (Renninger et al. 1995) were significantly responsive to basic pH solutions. However, in shallow habitats extreme pH are rarely encountered and may appear as ecologically irrelevant stimuli that should not evoke any behavioral response (Puri and Faulkes 2010). Note that pH 11 stimulus was used in the present study as a control for the highest concentrated sulfide solution, not as a pH stimulus. To investigate the detection of pH variations as an orientation cue for hydrothermal shrimp, acid pH solutions should be tested since in the Lucky Strike vent site hydrothermal fluid pH range from 3.84 to 6.45 (Charlou et al. 2000), and from 6.1 to 7.3 in the shrimp habitat (Desbruyères et al. 2001).

- **Responses to iron and manganese**

Detection of manganese and iron by a vent and a costal shrimp was tested here for the first time, and the two stimuli did not trigger dose-dependent responses for the antennules and the antennae at any concentration tested (Figure 46C,D,E,F). This suggests but does not definitely proves that shrimp cannot detect these compounds since the sensitivity of the EAG method is limited. EAG represents the summation of receptor potentials generated by many sensory neurons responding simultaneously (Nagai 1985). Thus, if iron and manganese stimulate only a low number of chemosensory neurons, the sensitivity of the EAG method is most likely not sufficient to detect a response. However, the alternative that manganese and iron are actually not detectable by vent shrimp raises questioning about the relative importance of chemodetection for these animals. Manganese and iron are relevant stimuli for long-distance detection of hydrothermal fluids, which is a fundamental issue regarding vent shrimp lifestyle. Because hydrothermal vents are dynamic and ephemeral ecosystems, vent animals need to detect new venting sites to settle in, and the extremely high abundances of shrimp on MAR sites (Polz et al. 1998, Martin and Haney 2005) suggest that they are successful colonizers. Which fluid attractants are used for the long-distance detection of active

sites, and which stage of life are involved (Herring and Dixon 1998, Tyler and Young 2003), is still uncertain. Since sulfide, although emblematic of vent chemicals, is not a relevant stimulus in this context, the prospective that vent shrimp cannot detect manganese and iron makes the distant chemodetection of hydrothermal plume doubtful for adults. Detection of other long-distance relevant chemicals such as methane (de Angelis et al. 1993) should be tested, as well as other possible long-distance attractants like noise (Crone et al. 2006) or temperature (Baker et al. 2016). Chemodetection abilities of other life stages should also be investigated, since larval dispersal is thought to play a role in colonization processes (Lutz et al. 1984) and aesthetasc sensilla are present in Alvinocaridid first zoeal stages (Hernandez-Avila et al. 2015).

IV. Conclusions

We tested the detection of food related odors and hydrothermal fluid chemicals by the antennal appendages of the vent shrimp *M. fortunata* and the coastal shrimp *P. elegans* to investigate the ability of the vent species to detect its chemical environment, and to get insights into the potential chemotaxis role of the hydrothermal fluid for both short- and long-distance distance of the hydrothermal habitat. We found that the two species detect the short-distance stimulus sulfide, but not iron and manganese which are relevant for the long-distance detection of the hydrothermal plume.

To test the detection of various organic and chemical compounds by the antennal appendages in the shrimps *M. fortunata* and *P. elegans*, we developed the first EAG method in marine shrimp underwater. This technique is especially suitable for rare vent species since it does not require killing the specimens, who can recover and eventually be re-used for further experiments. Moreover, EAG gives the most general idea of the animal sensitivity compared to other classical electrophysiological methods (e.g. patch-clamp), and is thus relevant in an ecological approach. It allows the screening of several chemicals before testing potential odor-gated behavioral responses.

Food-related odors triggered significant EAG responses from the antennal appendages of *M. fortunata* and *P. elegans*. This result supports the ability of the vent species to locate food sources, and highlight that not only the lateral antennules (associated to the olfactory aesthetascs) are involved in such detection, but also the antennae which bear bimodal sensilla that mediate the distributed chemodetection pathway.

Sulfide was detected by both the antennule and the antenna of *M. fortunata*, and it has previously been demonstrated to be also detected by the antenna of *R. exoculata*. These results suggest that hydrothermal shrimp may sense sulfide in the near field of the vents. Hence, sulfide is a good candidate for subsequent behavior experiments to investigate if vent shrimp use this chemical signature of the hydrothermal fluid for orientation in their local environment. The coastal shrimp *P. elegans* also detected sulfide via the antennule and the antenna, meaning that sulfide detection is not specific to hydrothermal species. Behavior experiments have to be developed for this species too, as it is not likely to encounter sulfide in its natural environment and may respond differently to a sufide stimulation.

Iron and manganese did not trigger significant EAG responses neither for *M. fortunata* and *P. elegans*. These chemicals are transported in the hydrothermal plume far from the emission point, and could thus be used for the detection of distant active sites by vent shrimp. The eventuality that *M. fortunata* cannot detect iron manganese raises doubts on the relevance of long-distance

chemodetection of hydrothermal plumes at adult stages. However, the absence of detection through EAG should not be interpreted as conclusive. Iron and manganese may stimulate a low number of chemosensory neurons and prompt behavioral responses while not triggering perceptible EAG responses. Chemodetection abilities of other life stages should also be investigated, since dispersal and colonization processes are believed to occur at larval stages (Lutz et al. 1984), which are also equipped with aesthetascs and maybe are more sensitive to long-distance stimuli than adults. Furthermore, behavioral responses to both short and long-distance stimuli must be investigated for *M. fortunata* and other hydrothermal species using pressurized aquaria (Shillito et al. 2014). Shrimp species occupy distinct microhabitats around vent chimneys, thus they may not be sensitive to the same attractants and could exhibit different chemosensory abilities.

Chapter V

Insights into the behavioral responses to food odor sources, sulfide and temperature in *M. fortunata*, *R. exoculata* and *P. elegans*

I. Introduction

II. Results and discussion

1. Attraction to food-related odors
2. Attraction to sulfide
3. Attraction to warm temperatures

III. Conclusions

I. Introduction

Hydrothermal vents are dynamic ecosystems, with steep fluctuations of temperature and chemical concentrations created by cooling and dilution of the hydrothermal fluid when mixing with the surrounding seawater (Johnson et al. 1986, Coumou et al. 2006). Ecological studies often suggest that the distribution of vent fauna is linked to food availability or environmental features such as temperature and chemical conditions (Sarrazin et al. 1997, 2002, Gebruk et al. 2000, Desbruyères et al. 2001, Cuvelier et al. 2009). Nevertheless, how these parameters are actually detected by the animals and exploited to choose their microhabitat has not been demonstrated.

Vent shrimp are continuously exposed to the release of various chemicals in the hydrothermal habitat, and may use the chemical signature of diluted fluids as an orientation cue. It is unknown if the chemicals trigger specific behavioral responses such as attraction or repulsion. Among the chemical stimuli of the hydrothermal fluid potentially used by vent shrimp, sulfide is the only one that has been considered. Sulfide is known for its toxicity and triggers escape responses in the shallow water caridean species *Crangon crangon* (exposed to 20 µmol.L^{-1} H_2S, Vismann 1996) and *Palaemonetes vulgaris* (exposed to 0.08 mmol.L^{-1} H_2S, Sofranko and van Dover, unpublished data). In contrast, Renninger and collaborators (1995) noticed an orientation behavior in the vent shrimp *Rimicaris exoculata* to a piece of sulfidic rock removed from a chimney, and suggested an attraction guidance by sulfide, argued by sulfide chemodetection by the antenna.

Habitat selection by marine species is determined principally by thermal conditions (Williams and Morritt, 1995). Attraction to temperature has been observed with *in vivo* experiments for *R. exoculata* (attraction to 11°C in 3°C seawater background, Ravaux et al. 2009). For the vent shrimp *Mirocaris fortunata*, relation to temperature has been examined in terms of temperature preference (19,2±1.1°C, Smith et al. 2013) and observation of aggregation behavior on warm zones (27-27,8°C) in rearing aquaria equipped with heaters at *in situ* and atmospheric pressure (Matabos et al. 2015). Nonetheless, attraction to warm temperature as a behavior specific to vent shrimp has not been robustly characterized.

Behavior experiments on vent fauna are challenging to conduct primarily because animals suffer from decompression during sampling at depths and are difficult to maintain in good physiological conditions. *In situ* imagery has provided direct access to living species in their natural habitat (Cuvelier et al. 2009, 2011, 2012) and enabled to investigate species spatial and temporal distribution, as well as some behavioral aspects in polychaetes (Chevaldonné and Jollivet 1993, Grelon et al. 2006). However, observations under controlled conditions are needed to quantify behavior such

as attraction. Pressurized devices were appropriately developed (Shillito et al. 2008, 2014) and provide the unique opportunity to quantify peculiar behaviors on live deep vent shrimp. Also, *M. fortunata* presents the advantage to survive quite well to decompression when sampled at depths that do not exceed 2000 m, such as from the Lucky Strike (1700 m depth) and Menez Gwen (800 m depth) sites. *M. fortunata* can thus successfully be maintained at atmospheric pressure for several months (Shillito et al. 2015, Matabos et al. 2015) and being tested for behavioral responses in similar conditions than shallow water species.

To investigate if vent shrimp use the hydrothermal fluid chemicals and temperature as hints for orientation, we conducted attraction experiments on *M. fortunata* using various setups at *in situ* and atmospheric pressure. Responses were compared to those of the coastal shrimp *P. elegans* to get insights into the adaptive significance of vent shrimp behaviors. Food odor sources were used as a stimulus expected to trigger an attractive response. Sulfide was selected as a hydrothermal fluid chemical stimulus, because sulfide was proposed as a potential attractant for vent animals in the literature, and sulfide was detected by the antennal appendages of both *M. fortunata* and *P. elegans* using electroantennography (see Chapter IV). Attraction to sulfide was also tested on *R. exoculata* at *in situ* pressure to investigate potential differences with *M. fortunata* linked to their distinct lifestyles. We also tested attraction to warm temperature in *M. fortunata* and *P. elegans.*

II. Results and discussion

The stimuli tested for triggering behavioral responses and the corresponding results for each species tested are briefly summarized in Table 13.

Table 13 Stimuli tested in behavior experiments and corresponding results for *P. elegans*, *M. fortunata* and *R. exoculata*

Species	Food odor source	Food - sulfide	Sulfide	Warm temperature
P. elegans	+	+	-	-
M. fortunata	-	-	-	+
R. exoculata	nt	nt	-	+*

+, attraction; -, no attraction observed; nt, not tested. Food odor source can be either mussel extract or shrimp food extract. Sulfide (Na_2S) concentration is 2 $mmol.L^{-1}$. Temperature corresponds to ~17°C in a 9°C seawater background.

*attraction to warm temperature in *R. exoculata* was not tested in the present study but was previously demonstrated in Ravaux et al. 2009.

1. Attraction to food-related odors

An intrinsic challenge of animal behavior experiments is to define relevant indicators for behavior observations. For attraction experiments, position relative to a stimulus source can be tracked, and quantitative information can be extracted, such as the number and duration of contacts with a source. Another challenge is to find an experimental design that fits to the animal and efficiently triggers behavioral responses. This implies for example the material setup, the choice of stimuli quality and quantity, and beforehand preparation of the animals (e.g. acclimatization, starving period). To choose a relevant attraction experimental design, the logic way is to start with a stimulus that is known to trigger attraction response, usually food.

To test the attraction to a food odor source and the role of the antennules for this detection, we used first a two-choice experiment between a food odor source and a lure of identical aspect (Figure 48). The shrimps, starved for 48 h, were tested one by one for 15 min with the stimulus and the lure positioned beneath the surface. The percentage of first contact with the food source, the lure

or none revealed an attraction behavior to the food odor source in *P.elegans* (45% of first contact). The detection of the food odor source was worsen by the selective ablation of the lateral antennules (20% of first contact) or both the lateral and medial antennules (25% of first contact). The impaired attraction to a food odor source when the antennules of *P. elegans* are ablated confirms the chemosensory function of these organs to locate food sources, in consistency with the results of Steullet et al. (2001) on spiny lobster. However, other indicators measured such as the mean number and duration of contacts (not shown) were similar for the food source and the lure in the non-ablated group of *P. elegans*. This experimental design is thus not optimal to demonstrate attraction to a food odor source in *P. elegans*. The experiment was not conclusive for *M. fortunata* either, for which the majority of the intact specimens went to the lure first (65% of first contact), so we did not performed consecutive ablation experiments for the vent species.

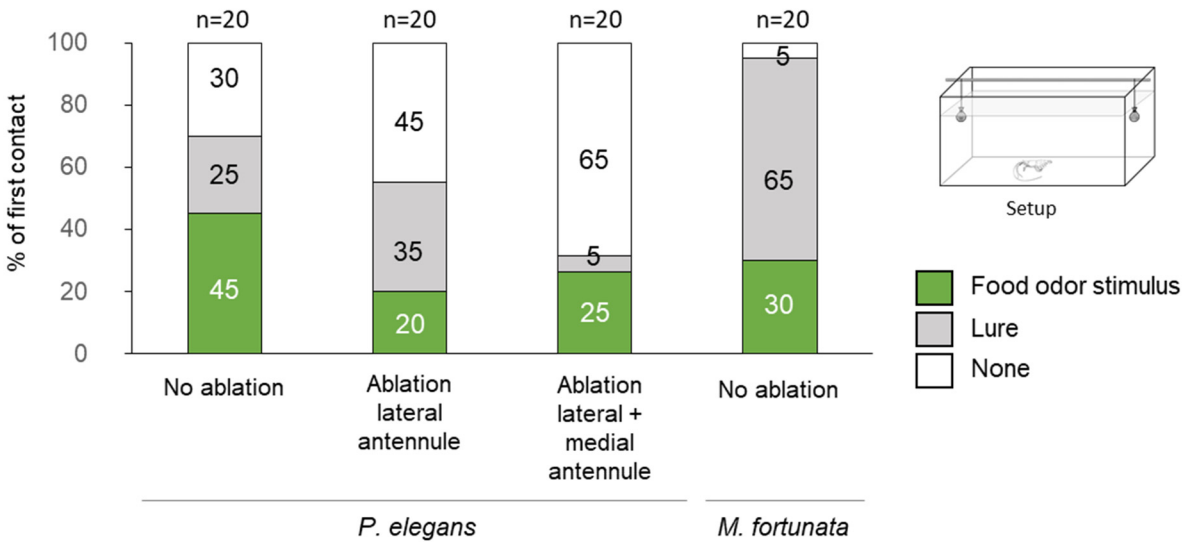

Figure 48 Responses to a food odor stimulus with two-choice experiments on single *P. elegans* and *M. fortunata*

Distribution of the shrimps according to the first contact they made, either with the food odor source, the lure or none. For *P. elegans*, both ablated groups significantly differed from the control intact group (Fisher exact test, two-sided, p = 0.0007 for lateral antennule ablated and p = 7.10^{-8} for whole antennule ablated).

Setup: The shrimps were starved for 48h and placed individually in the tank for 5 min. The food odor source and the lure were then immersed and the shrimp were observed for 10 min. Three groups of shrimps were tested for *P. elegans*: intact, lateral antennule ablated, and whole antennule ablated. One group of intact *M. fortunata* was tested. The whole experiment is detailed in Chapter II – section II.2.1.1.

For the second setup, we used a multiple choice experiment with three tubes containing control gels and one tube containing a stimulus (food odor) gel (Figure 49). The gels were casted in the bottom of black tubes in order to preclude any visual bias. The tubes were placed on the bottom corners of the tank prior to the shrimp introduction, and the number and duration of entrances in each tubes was measured during 30 min. With this setup, we observed a significant attraction behavior to a food odor source in *P. elegans* (Figure 49A,B): 61% of shrimps went first in the stimulus tube (Figure 49A), and the time spend in this tube compared to the control tubes was significantly higher (Figure 49B), as well as the number of entrances in the stimulus tube (not shown). In contrast, results for *M. fortunata* did not show any attraction to the food odor source (Figure 49C,D) although the shrimps explored the tank and the tubes (40% of first entrance in the control tubes).

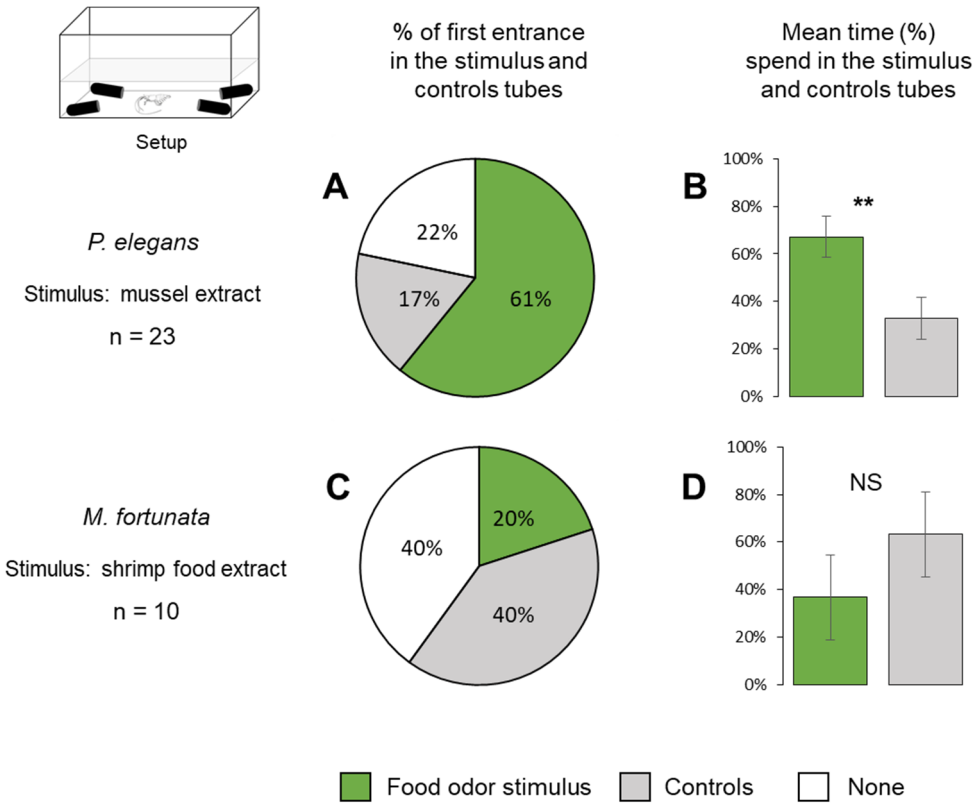

Figure 49 Responses to a food odor stimulus with multiple choice experiments on single *P. elegans* and *M. fortunata*

A,C. Distribution of the shrimps according to their first entrance in the tube containing a stimulus gel (food odor) or one of the tubes containing control gels, or none.
B,D. Mean (± s.e.m.) time spend in the tube containing a stimulus gel (food odor) or the three tubes containing control gels, relative to the total time spend in the four tubes (presented in percentage). Means were compared with a two-sample *t*-test, two sided (B, $p = 0.008$). **, $p < 0.01$.

Setup: The shrimp were starved for 48h and placed individually in the tank just after tubes introduction (3 containing control gels, 1 containing stimulus gel). The shrimp behavior was video recorded from above for 30 min. The whole experiment is detailed in Chapter II – section II.2.1.1.

These experiments to test attraction to a food odor source were not conclusive on *M. fortunata* individuals tested one by one. However, it is easily observable that they detect and locate a food source in their rearing tanks at atmospheric and *in situ* pressure (i.e. in the AbyssBox) when fed with mussels or shrimp food pellets (e.g. Matabos et al. 2015). The question was raised if the shrimps were heavily stressed when manipulated from one tank to another for the one by one experiments. Therefore, we tested a third setup directly in the rearing tanks containing several individuals of *M. fortunata*, at the Oceanopolis aquarium (Figure 50). The shrimps were not displaced from their rearing tanks, and the aquarium thermostat heaters were left ON. The shrimps were starved for one week. The water inlet and outlet were closed prior to insert one control gel and one stimulus (food odor) gel on each side of the aquaria. The number and duration of contacts with each gel were measured over 30 min. The results obtained for the two batches of *M. fortunata* tested were not pooled because the number of shrimps for each batch was too divergent (n=16 versus n=8), so we could not exclude a bias resulting from the shrimp density. Because each batch was tested only twice, we could not conduct statistical analysis, and results are presented as single observations (Figure 50). For the n=16 batch, the maximum number of shrimp on the stimulus gel compared to the control gel suggests a possible attraction to the food odor source (Figure 50A). By contrast, results between the stimulus and control gels are similar for the n=8 batch (Figure 50B). Thus, the density of shrimp in the tank might influence their behavior. For the two batches, the percentage of time the stimulus gel was occupied by shrimp did not differ from the control gel (Figure 50C,D). Altogether, these results for *M. fortunata* do not suggest an attraction behavior to the food odor source, which contrast with the observations of *M. fortunata* swimming to the food source when fed weekly during maintenance. In all instances, results presented in Figure 50 are observations that cannot be thoroughly interpreted since only two replicates were generated per batch.

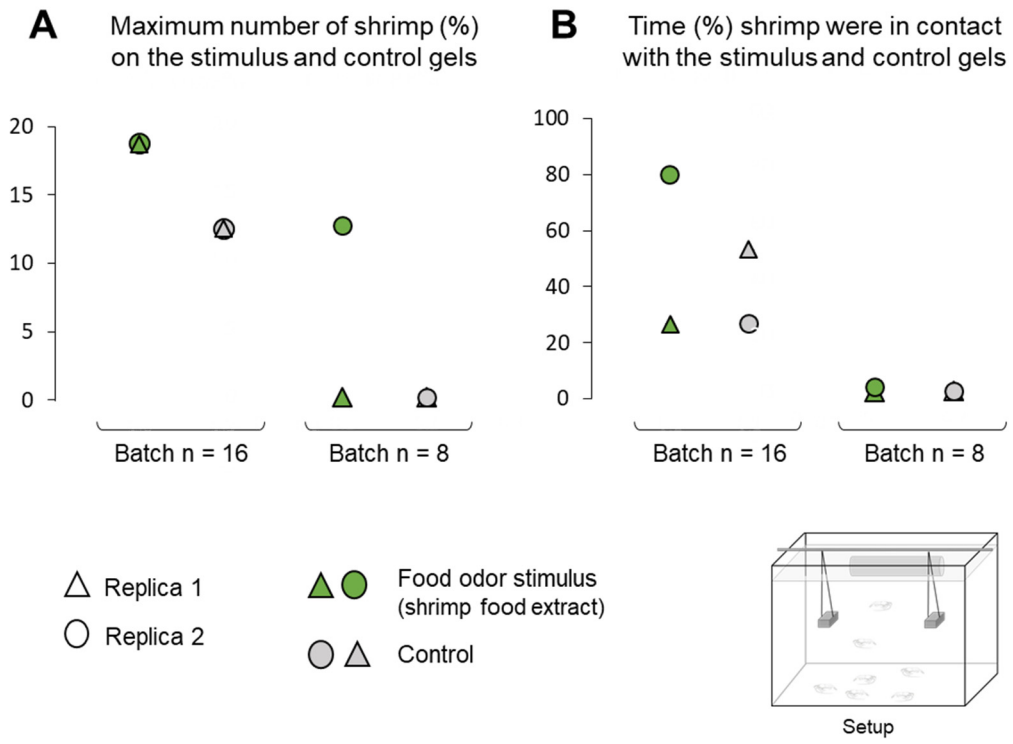

Figure 50 Responses to a food odor stimulus with two-choice experiments on multiple *M. fortunata*

A. Maximum percentage of shrimps on the stimulus (food odor) and control gels over the experiment duration (30 min).
B. Percentage of time shrimp (one or more) were in contact with the stimulus (food odor) and control gels.
Two batches (n=16 and n=8) of *M. fortunata* were tested twice. No statistical analysis could be conducted and results are presented as single observations for each replica.

Setup: The shrimps were tested in their rearing tank after a one-week starving period. Two gels (one control, one stimulus) were introduced on each side of the middle zone of the tank. The shrimps were observed for 30 min. The whole experiment is detailed in Chapter II 2.1.

To further investigate the attraction to a food odor source in conditions closer to the natural state of vent shrimp, we tested a fourth setup, at *in situ* pressure in the VISIOCAMP aquarium, on multiple *M. fortunata* during the BICOSE (2018) cruise on the Mid-Atlantic Ridge (Figure 51). The shrimps were sampled from the Snake Pit vent site (3500 m depth) at *in situ* pressure in the PERISCOP device, and were briefly bring to atmospheric pressure for transfer into the VISIOCAMP aquarium. After a 2 h shrimp recovery at 300 bars, 10°C, gels were introduced in the tank through an isobaric line with 45 min interval, and the number and duration of contact with the gels were measured. Two control gels and one stimulus (food odor) gel were used. Because there are only two replicas (two batches of shrimps tested), the results are presented as single observations. The results do not indicate a potential attraction behavior to the food odor source. The shrimps may simply not being attracted

to the stimulus (e.g. quality of the food, no starving period…). But the number of replicas does not allow a robust analysis. An additional batch should have been tested, but the shrimps from the third batch were in noticeable bad conditions and were not therefore tested.

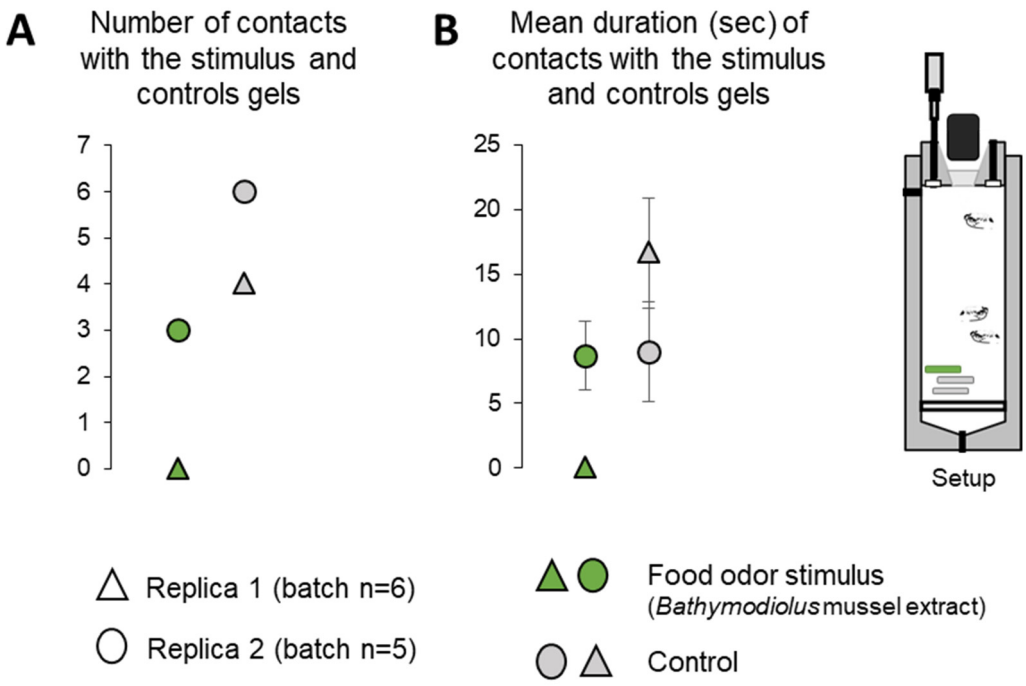

Figure 51 Responses to a food odor stimulus with experiments at *in situ* pressure on multiple *M. fortunata*

A. Number of contacts with the stimulus (food odor) and the control gels.
B. Mean (± s.e.m.) duration of contacts (sec) with the stimulus (food odor) and control gels.
Two batches of n=6 and n=5 *M. fortunata* were tested once. No statistical analysis could be conducted and results are presented as single observations.

Setup: Just after sampling, the shrimps were placed in the VISIOCAMP aquarium and recovered at 300 bars, 10°C for two hours. Three gels (two controls, one stimulus) were then consecutively introduced with 45 min of interval through an isobaric line. All the experiment was video recorded. The whole experiment is detailed in Chapter II – section II.2.2.

Several setups were experimented on *M. fortunata* and *P. elegans*. Attraction to a food odor source was significantly demonstrated in *P. elegans* using a multiple choice experiment, but no conclusive results were obtained for *M. fortunata* with the same setup (and also at *in situ* pressure), although a food odor was expected to trigger an attraction behavior for this species too. This failure raises several questions regarding the experimental conditions. A first unknown is the effective duration of starving for vent species to eliminate the bias due to satiety. *M. fortunata* were usually fed 2 times a week, and were starved up to one week before experiments at atmospheric pressure. A

starving period of two weeks could be tested but seems excessive. To starve the animals prior to experiments at *in situ* pressure on cruises is not an option due to time limitation and multiple uses of the pressurized systems. The physiological state of the shrimps is also of major importance to conduct behavior experiments, and can be suspicious for such vent specimens manipulated far from their habitat. However, *M. fortunata* specimens that are acclimatized to atmospheric pressure for several weeks seem healthy, exhibit features of fitness such as feeding and molting (Matabos et al. 2015), and several experiments have been previously conducted in the IPOCAMP aquarium with animals in a seemingly good physiological state after re-pressurization (Shillito et al. 2014). Finally, comparison of experiments between different species is hampered by behavioral differences towards search of food or response to chemicals. Various parameters influence the foraging like odor diffusion dynamics, water flow conditions or the quality and quantity of the stimuli (Kenning et al. 2015). It has been showed for example that flow velocities or stimulus concentrations below or above a certain threshold can impede or even prevent the successful localization of odor sources (Moore and Grills 1999). Thus, a setup designed and suited for one species is not necessarily ecologically relevant for another species (Kenning et al. 2015), as seen for *P. elegans* versus *M. fortunata*.

2. Attraction to sulfide

Sulfide is an obvious signature of the hydrothermal fluid, and has been previously proposed as a potential orientation cue for vent animals (Segonzac et al. 1993, Renninger et al. 1995, Rittschof et al. 1998). In addition, sulfide is detected by the antennae of *R. exoculata* (Renninger et al. 1995) and we demonstrated that sulfide is also detected by the antennal appendages of *M. fortunata* and *P. elegans* (see Chapter IV). For these reasons, we selected sulfide as a hydrothermal fluid chemical stimulus for behavior attraction experiments.

A preliminary experiment to test attraction to sulfide in *M. fortunata* was carried out by the AMEX team during the BIOBAZ (2013) cruise (Mid-Atlantic Ridge, Menez Gwen site, 850 m depth), at *in situ* pressure in the IPOCAMP aquarium (Figure 52). Injections of 25 to 100 µmol.L^{-1} Na_2S solutions did not trigger any particular reaction from the shrimps. The experiment was repeated only twice on one batch of shrimps, which precludes any robust statistical analysis. However it can be suspected that the concentrations of the injected solutions were not sufficient to trigger any response when diluted in the tank.

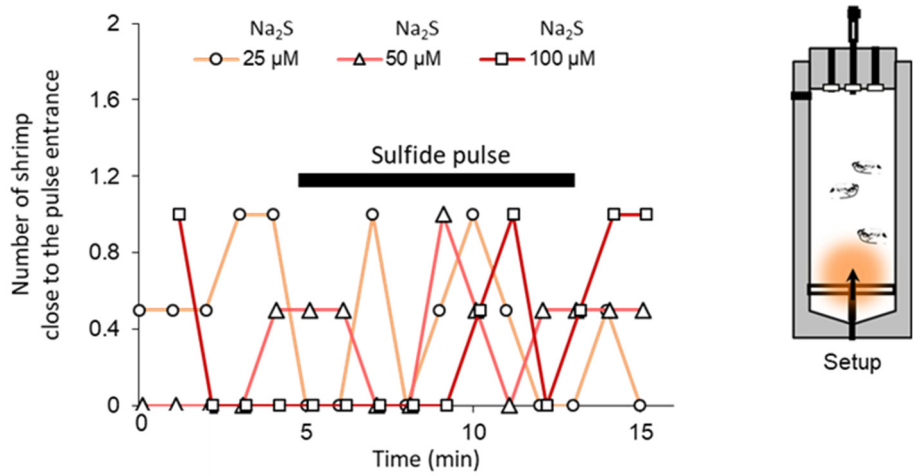

Figure 52 Responses to sulfide stimuli with preliminary experiment at *in situ* pressure on multiple *M. fortunata*

Number of shrimps in a 6 cm² surface around the entrance of the seawater renewing system, prior and after injection of increasing concentrations of sulfide solutions. The experiment was conducted twice on the same batch (n=20) of shrimps (i.e. each point represents the mean of two replica).

Setup: Just after sampling, the shrimps were placed in the IPOCAMP aquaria and recovered at 70 bars, 9°C for 1 hour. Pulses of sulfide solutions were injected with one hour interval. All the experiment was video recorded. The whole experiment is detailed in Chapter II – section II.2.2.

Using electroantennography, the sulfide concentration that triggered a significant response of *M. fortunata* antennal appendages was 2 mmol.L^{-1} (see Chapter IV). We consequently selected this concentration for further behavior experiments using agarose gels. Since sulfide diffuses from the gel and is thus highly diluted in the medium, the concentration perceived by the shrimp is lower than the gel concentration. We suppose that the sulfide concentration perceived by the shrimp is likely in the micromolar range, as measured in diffusion test within a 50 mL tube (Chapter II – section II.2.2.). Micromolar concentrations are relevant compared to sulfide concentrations in the habitat of *M. fortunata* (e.g. at the Lucky Strike site: 5.11-38.31 µmol.L^{-1}, Sarrazin et al. 2015) or *R. exoculata* (e.g. at the TAG site: 0.5-77 µmol.L^{-1}, Cathalot et al. 2018).

To test attraction to sulfide with another setup, we used the two-choice experiment on multiple individuals of *M. fortunata* at atmospheric pressure (Figure 53) previously described (see section II.1). Two batches of n=16 and n=8 *M. fortunata* were tested, and the number of shrimps on stimulus and control gels and the duration of contacts were measured. The number of replicas (2) per batch does not allows any robust statistical analysis, however the observations do not indicate any potential attraction to sulfide or a food-sulfide mixture compared to control gel.

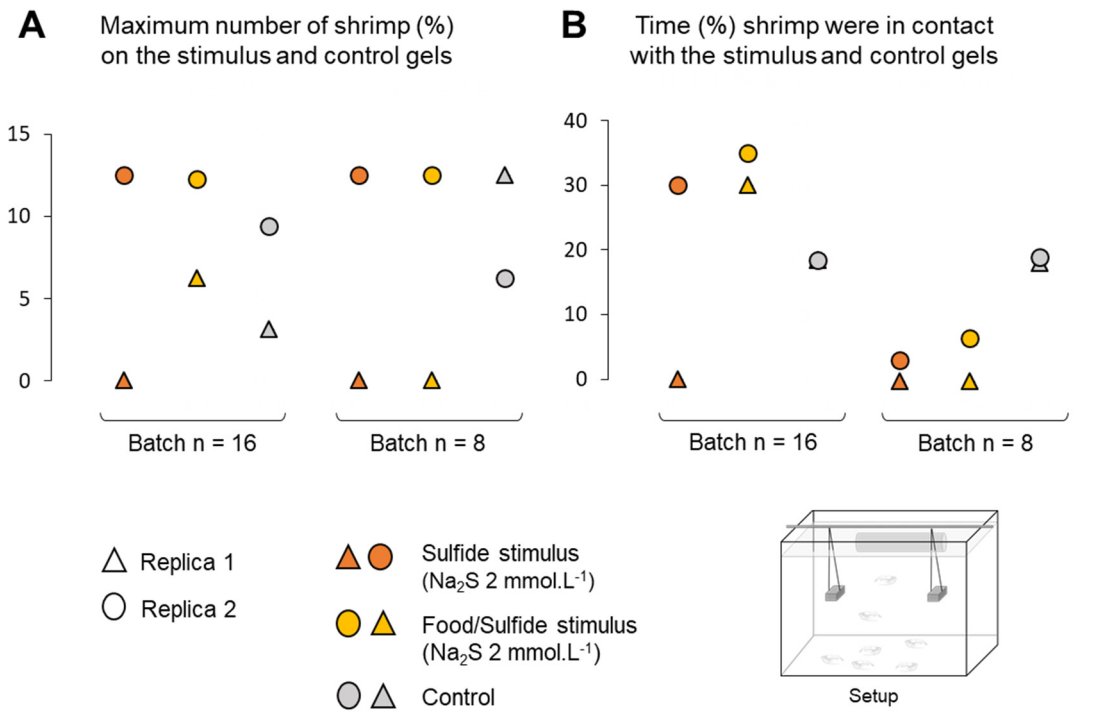

Figure 53 Responses to sulfide stimuli with two-choice experiments on multiple *M. fortunata*

A. Maximum percentage of shrimps on the stimulus (sulfide or food/sulfide mixture) and control gels over the experiment duration (30 min).
B. Percentage of time shrimp (one or more) were in contact with the stimulus (sulfide or food/sulfide mixture) and control gels.
Two batches (n=16 and n=8) of *M. fortunata* were tested twice. No statistical analysis could be conducted and results are presented as single observations for each replica.

Setup: The shrimps were tested in their rearing tank after a one week starving period. Two gels (one control, one stimulus) were introduced on each side of the middle zone of the tank. The shrimps were observed for 30 min. The whole experiment is detailed in Chapter II 2.1.

To discuss about adaptive behavior in relation with the habitat, we also tested behavioral responses to sulfide on single individuals of *P. elegans* (Figure 54) with the multiple-choice experiment previously presented in section II.1. Although no attraction to sulfide was observed compared to the controls (Figure 54A,B), *P. elegans* was significantly attracted to a mixture of food odor and sulfide (Figure 54C,D), suggesting that sulfide is not a strong repulsive for this species. This result was unexpected, since sulfide is well known for its toxicity. It has been shown to trigger escape behavior in the caridean shrimp *C. Crangon* after exposure to micromolar concentrations of H_2S (Vismann 1996), and avoidance response in the shrimp *Palaemonetes vulgaris* with concentrations inferior to 0.08 mmol.L^{-1} (Sofranko and Van Dover, unpublished data). The ecologically relevance of the non-repulsion to sulfide in *P. elegans* is unclear. It could be that a short exposure to high concentrations of sulfide is

not considered as harmful by this species, but this hypothesis is not supported by the literature cited above for other caridean species.

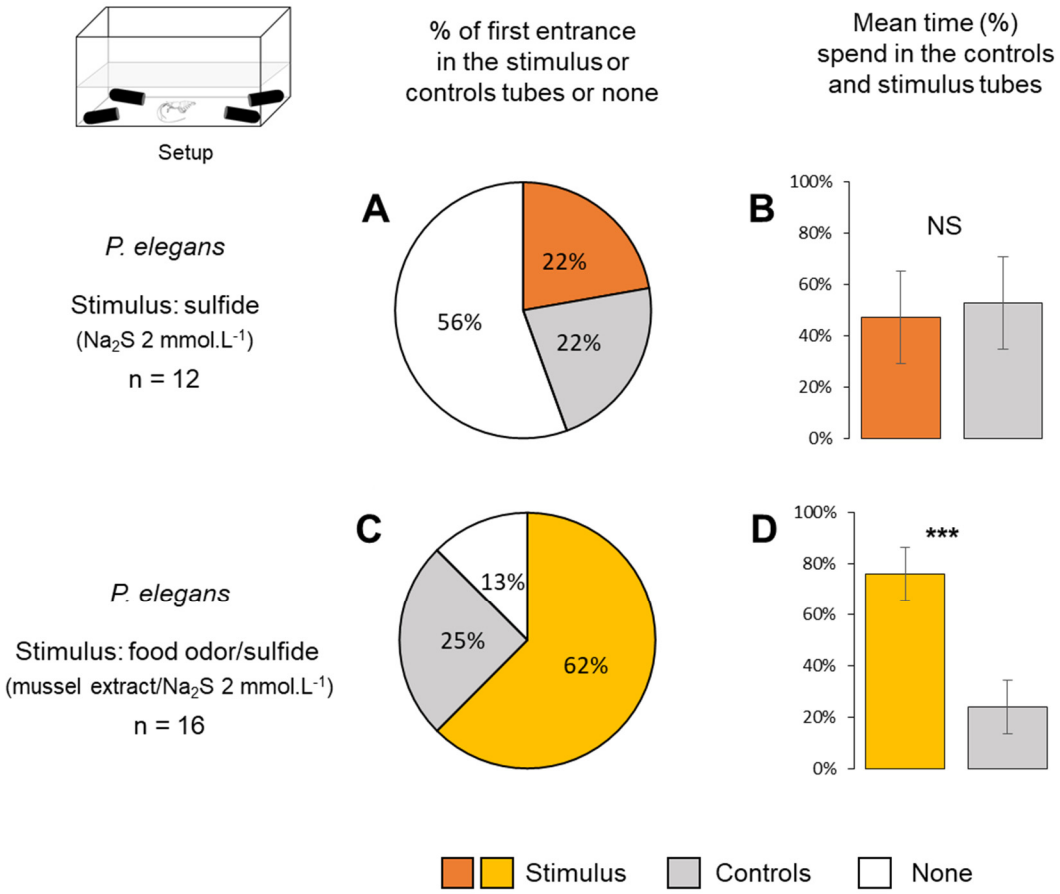

Figure 54 Responses to sulfide stimuli with multiple choice experiments on single *P. elegans*

A,C. Distribution of the shrimps according to their first entrance in the tube containing a stimulus gel (**A**, sulfide or **C**, food/sulfide mixture) or one of the tubes containing control gels, or none.
B,D. Mean (± s.e.m.) time spend in the tube containing a stimulus gel (**B**, sulfide or **D**, food/sulfide mixture) or the three tubes containing control gels, relative to the total time spend in the four tubes (presented in percentage). Means were compared with a two-sample *t*-test, two sided (D, $p = 0.001$). ***, $p < 0.005$.

Setup: The shrimps were starved for 48h and placed individually in the tank just after tubes introduction (3 containing control gels, 1 containing stimulus gel). The shrimp behavior was video recorded from above for 30 min. The whole experiment is detailed in Chapter II – section II.2.1.1.

Sulfide did not triggered noticeable attraction behavior in *M. fortunata* in our experiments. Nonetheless, relevance of sulfide as an orientation cue for this species can be debatable. *M. fortunata* lives at distance from chimneys exit, in a fluid-diluted zone where comes from diffuse emissions of fluid from cracks in the seafloor, at low concentrations (e.g. at the Lucky Strike site: 2.4-38 µmol.L^{-1} in diffusers and the habitat of *M. fortunata* [Desbruyères et al. 2001, Sarrazin et al. 2015], 2.5-3 mmol.L^{-1} in the pure fluid [Charlou et al. 2002]). Furthermore, *M. fortunata*, which does not exhibit any strong association to symbiotic bacteria, is rather an opportunistic feeder (Gebruk et al. 2000, Portail et al. 2018) and thus not depends directly on hydrothermal fluid emissions. In contrast, the hydrothermal species *R. exoculata* exhibits a strong dependence to the hydrothermal fluid to supplement its symbiotic bacteria in reduced compounds, such as hydrogen sulfide (Zbinden et al. 2004).

To investigate a possible link between trophic behavior and attraction to sulfide, we tested attraction to sulfide in *R. exoculata* with the experiment at *in situ* pressure in the VISIOCAMP aquarium (Figure 55) during the BICOSE (2018) cruise at the Mid-Atlantic Ridge. Two control gels and one stimulus (sulfide) gel were consecutively presented to three batches of 10 individuals of *R. exoculata*. A significant difference was observed between the mean number of contacts with the stimulus gel compared to the control gels (Figure 55A), suggesting an attraction to sulfide. When considering prolonged contacts (superior to 5 sec), which can be considered as more indicative of an attraction behavior, there was not significant difference between the two types of gels (Figure 55B). Mean duration of contacts and mean time before first contact were not conclusive either (not shown). In addition, the experiment was repeated with a pH 4 sulfide gel as a stimulus, since lowering the pH greatly enhances the release of sulfide. No difference with the control gel and a pH control gel was observed (Figure 55C). Attraction to sulfide in vent shrimp was proposed by Renninger and collaborators (1995), who reported a strong orientation behavior to a piece of sulfide removed from a chimney in *R. exoculata*, and proposed a chemical guidance to explain this observation. The results of our experiments do not support this hypothesis, since we did not demonstrate thoroughly attraction to sulfide in *R. exoculata*, and neither in *M. fortunata*. Nonetheless, we cannot affirm either that these species are not attracted to sulfide at all, because of the low number of replicas for each experiment, and the failure to find a setup that demonstrates robustly an attraction behavior in vent shrimp.

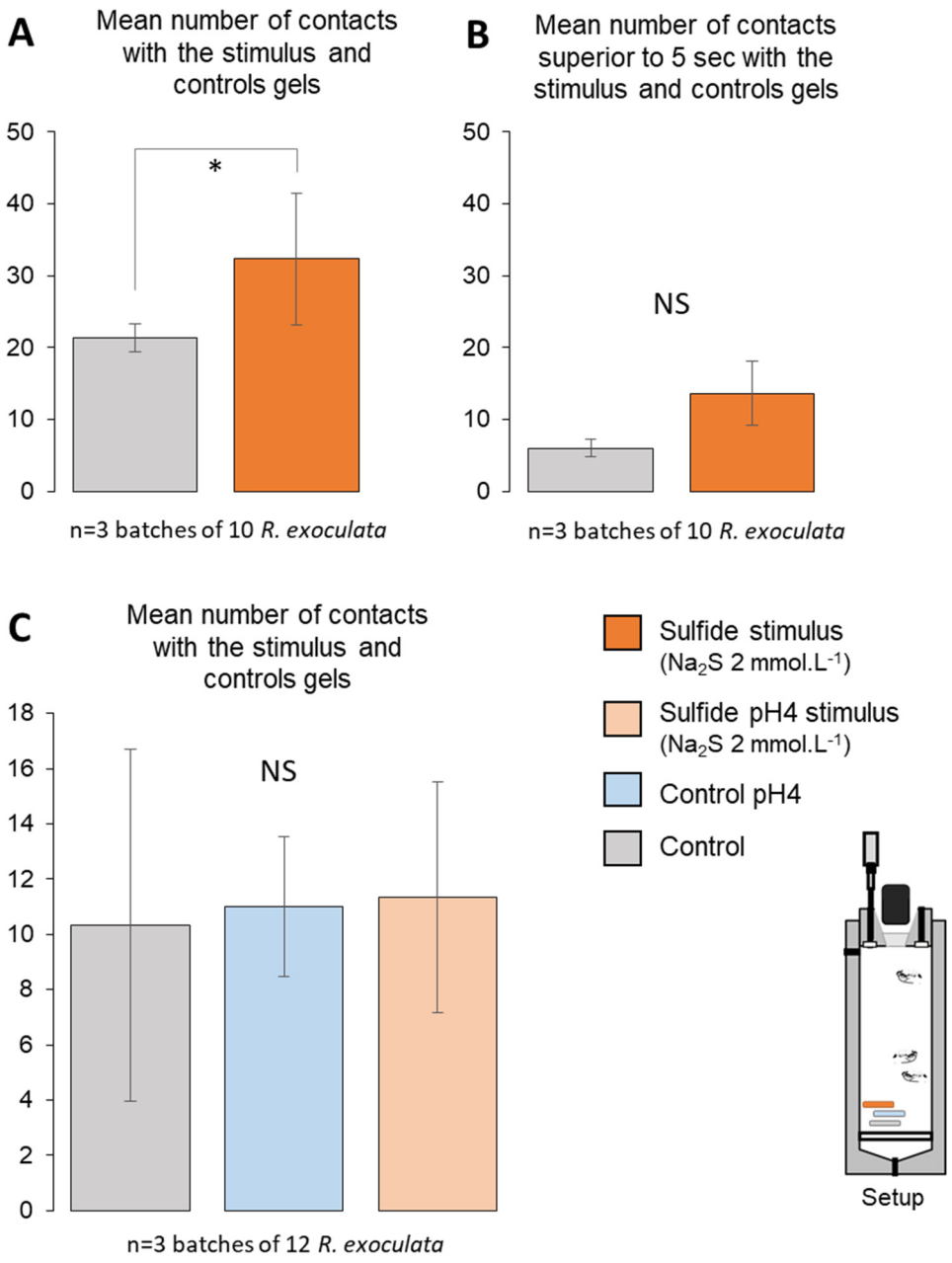

Figure 55 Responses to sulfide stimuli with experiments at *in situ* pressure on multiple *R. exoculata*

A,B. Mean (± s.e.m.) number of contacts (**A**) and contacts superior to 5 sec (**B**) with the control gels and the stimulus gel (sulfide).
C. Mean (± s.e.m.) number of contacts with the control gel, the pH control gel and the stimulus gel (sulfide pH 4).
Means were compared with a two sample permutation *t*-test (A, $p = 0.012$). * $p < 0.05$.

Setup: The shrimps were placed in the VISIOCAMP aquarium and recovered at 300 bars, 10°C for two hours. Gels were then consecutively introduced with 45 min of interval through an isobaric line. All the experiment was video recorded. The whole experiment is detailed in Chapter II – section II.2.2.

3. Attraction to warm temperatures

Temperature is likely a key factor influencing the positioning of the vent fauna around the active chimneys (Sarrazin et al. 1997, Lee 2003), where steep thermal gradients occur (Le Bris et al. 2005). Vent shrimp have developed molecular strategies to cope with short exposure to acute temperatures (Ravaux et al. 2003), but overall each vent species live in a relatively warm environment compared to the cold (2°C) abyssal seawater (e.g. *R. exoculata*: 4.7 to 25°C at the Rainbow site [Geret et al. 2002]; *M.fortunata*: 5.4 to 18°C at the Lucky Strike site [Sarrazin et al. 2015]). Hence, detection of temperature gradients might be involved in the selection of the habitat in vent shrimp, which may be attracted to these temperature ranges. To investigate if vent shrimp use the thermal signature of the hydrothermal fluid as an orientation cue, and if such behavior can have an adaptive significance, we conducted experiments on *M. fortunata* and *P. elegans* to test attraction to warm temperatures. Intertidal shallow-water species, as *P. elegans*, are also exposed in their natural habitat to fluctuating temperature conditions, although not as acute as in the vent environment (Bates et al. 2010).

We conducted choice experiments between two aquarium heaters (one turned ON set to 25°C, one turned OFF) on several batches of *M. fortunata* and *P. elegans* in their 9°C rearing tanks at the Oceanopolis aquarium (Figure 56). The number of shrimps on each heater was counted over time during 180 min, and overnight. During the whole experiment, for *P. elegans,* a maximum of 20 % of shrimps went on the ON and OFF heaters (Figure 56A). In contrast, for *M. fortunata*, 30% of shrimps went on the heater ON in 30 min, 50% in 180 min, and up to 80% after one night, whereas the number of shrimps never exceeds 5% on the heater OFF (Figure 56B). In addition, when examining the repartition of the shrimps on the heater ON, *M. fortunata* individuals aggregated on the warmer zones of the heater (Figure 56C), for which the temperature is approximatively 17°C. Thus, with this setup, the attraction to warm temperatures (~ 17°C) is clearly defined for the hydrothermal species, whereas no attraction is observed for the shallow-water species.

➔

A-B. Distribution of *P. elegans* (**A**) and *M. fortunata* (**B**) on the ON and OFF aquarium heaters over time.
C. Distribution of *M. fortunata* on each zone of the ON heater over time.
Two batches of 20 *P. elegans* were tested 4 times each (n=8 replicas per point, except overnight, n=4 replicas).
Two batches of 28 and 19 *M. fortunata* were tested 6 times each (n=12 replicas per point, except overnight, n=4 replicas).

Setup: ON (set to 25°C) and OFF heaters were introduced on each side of the rearing tank (9°C) in the upper region. The shrimps were observed for 30 min. Between consecutive trials, the heaters were inverted. The whole experiment is detailed in Chapter II – section 2.1.2.

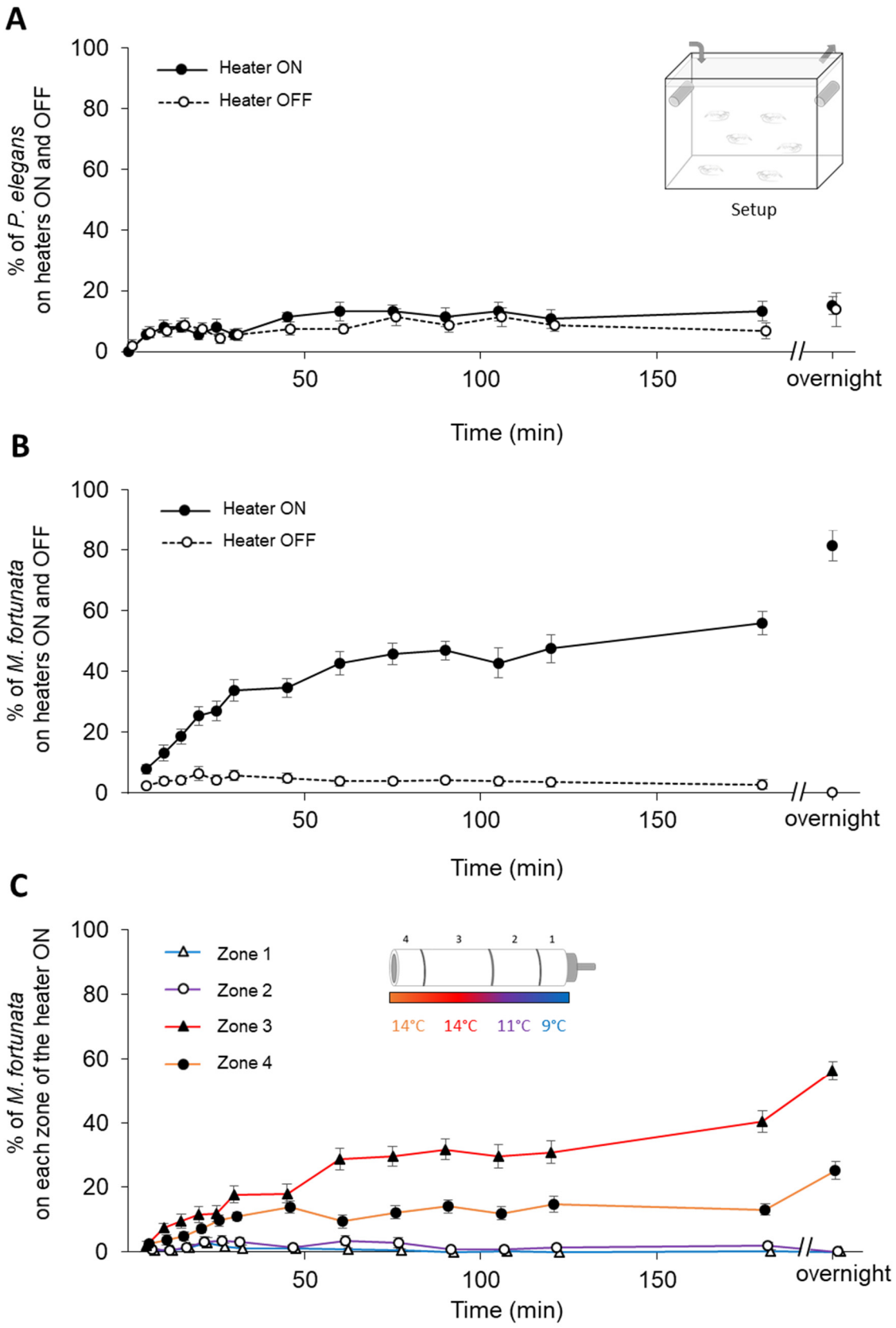

Figure 56 Distribution of multiple *P. elegans* and *M. fortunata* on ON and OFF thermostat heaters

Legend previous page.

The aggregation of *M. fortunata* shrimps on the warmer zone of the heater is consistent with the results from Smith and collaborators (2013), who established the temperature preference of *M. fortunata* to be 19.2°C. They also studied *Palaemonetes varians*, which selected a mean temperature of 18.3°C, contrasting with our results on *P. elegans* for which we did not observed any attraction to the heater. These differences could result from the acclimatization duration: *P. varians* were acclimated to 9°C for one week (Smith et al. 2013), whereas *P. elegans* were acclimated at least one month to 9°C (present study). It also must be pointed that the experimental setups are different, and consequently are the behaviors observed. Smith and collaborators (2013) demonstrated the temperature *preferendum* for each species, by exposing the shrimps to a thermal gradient. In the present study, we demonstrated that *M. fortunata* is attracted to a distant warm spot, in contrast to *P. elegans*. Furthermore, Ravaux and collaborators (2009) demonstrated that vent shrimps *R. exoculata* aggregate on a warm water source (injection of 11°C seawater in a 3°C background in the IPOCAMP aquarium). Taking together, our results with those from Ravaux and collaborators (2009) robustly support the statement of a key role of temperature in habitat selection as a specificity of hydrothermal species.

These behavioral responses of vent shrimp to warm sources suggest that they have sensing mechanisms to effectively exploit their thermal environment, as it is generally accepted for many crustaceans (Lagerspetz and Vainio 2006). Jury and Watson (2000) found that lobster can detect temperature changes of greater than 1°C, and probably as small as 0.15°C. In crab larvae (*Rhithropanopeus harrisii*), vertical migration in the water column is triggered by changes from 0.29 to 0.49°C (Forward 1990). The unknown is the thermosensitivity of vent shrimp, which could present particular abilities to detect fine temperature variationsIn the mixing zone of the hydrothermal fluid with the surrounding seawater, temperature can vary abruptly from 2°C to temperatures exceeding 30°C (Schmidt et al. 2008). In the periphery of the rising hydrothermal plume, and in the buoyant hydrothermal plumes spreading over 100 m, temperature differences with the seawater can be inferior to 0.03°C (Baker et al. 2016, Tao et al. 2017). To detect such small temperature anomalies could allow vent shrimp to orient towards an active site from distance.

III. Conclusions

We conducted behavior experiments on *M. fortunata*, *R. exoculata* and *P. elegans* to test attraction to factors relevant for the detection and orientation in the habitat of vent shrimp. Attraction to food odor sources and sulfide was not demonstrated for the vent species, but detection of temperature variations must be involved in the orientation within the vent habitat.

We investigated the responses to food odor sources as a stimulus expected to trigger an attraction behavior. Attraction to food odor sources was successfully demonstrated for *P. elegans* with choice experiments, but not for *M. fortunata* with experiments at both atmospheric and *in situ* pressure, suggesting that the experimental conditions were not appropriate for this species.

To get insights into the chemotaxis role of the hydrothermal fluid for vent shrimp, we used sulfide as a hydrothermal chemical stimulus, which has previously been proposed as an attractant for vent shrimp. Our results did not suggest an attraction to sulfide or a mixture of food and sulfide in *M. fortunata*. In *P. elegans*, we found that sulfide is not repulsive when mixed with a food odor, contrasting with avoidance responses observed for other caridean species in the literature. We also conducted an experiment at *in situ* pressure on *R. exoculata*, which relies much more on hydrothermal fluid emissions than *M. fortunata*, but again our results did not reveal any significant attraction to sulfide, or sulfide in acid conditions. Hence, we cannot discuss on the relevance of a chemical guidance for vent shrimp orientation.

We tested the attraction to warm temperature as a potential factor to guide vent shrimp in their habitat. Detection of temperature variations is relevant for the short-distance detection of the habitat, where steep thermal gradients occur, but also for the long-distance detection of an active site, with small temperature anomalies occurring between the hydrothermal plume and the ambient abyssal seawater. We found that *M. fortunata* is significantly attracted to warm temperatures (~17°C), as previously demonstrated in *R. exoculata*. In contrast, *P. elegans* does not exhibit such behavior. Therefore, temperature sensing is probably used to detect and choose the habitat around the chimneys, and has likely an adaptive significance. Thermosensitivity has not yet been investigated in vent shrimp, but could provide important insights into their adaptive relation to the thermal properties of their environment, as well as their ability to detect fine temperature variations for long-distance detection of an active vent. Another unknown is the expression of specific thermoreceptors in vent shrimp, but the mechanisms involved in thermodetection are poorly known in crustaceans yet.

Future bioassays could differ in setup, for example by testing aquaria equipped with choice-chambers (e.g. Lecchini et al. 2010, Santonja et al. 2018) on *M. fortunata* specimens acclimated to

atmospheric pressure. Other modes of stimulation should be explored too. Agarose gels were used to allow the slow diffusion of the stimuli, but it is not representative of what occurs in the vent habitat, where the shrimps are continuously exposed to steep chemical variations. Burst stimulations with stimulus solutions are a good option, but preliminary tests on *R. exoculata* were not conclusive (not shown). Also, other hydrothermal fluid chemicals should be tested for their potential to trigger attractive responses, such as iron, manganese and methane.

Chapter VI

Identification of chemo- and thermoreceptor candidates in vent and coastal species

---

I. Introduction

II. Results and discussion

1. Comparative expression of the olfactory co-receptor IR25a
2. Pre-identification of potential chemo- and thermosensory proteins from RNA-sequencing

III. Conclusions

I. Introduction

Sensory abilities are primarily defined by the proteins expressed by the sensory neurons. Vent shrimp could present adaptations at the molecular level, with the expression of specific sensory proteins, or different levels and patterns of expression in the sensory organs. Considering chemodetection, so far, only few chemoreceptor proteins have identified in crustaceans, and thermoreceptors have not been identified in crustaceans yet. This chapter provides very first insights into the molecular basis of chemo- and thermodetection in vent and coastal shrimp species, with the identification, and eventually the expression pattern, of chemo- and thermoreceptor candidates.

The nature of crustacean chemoreceptors has remained elusive until recently, since searches for the traditional insect olfactory receptors have been unsuccessful. The genome sequencing of the branchiopod *Daphnia pulex* revealed the presence of several Ionotropic Receptors (IRs), a family of receptors involved in odorant detection in insects and subsequently shown to be conserved in Protostomia (Benton et al. 2009, Croset et al. 2010). Several IRs were also identified from antennule transcriptomes in decapods: the spiny lobster *Panulirus argus* (Corey et al. 2013), the American lobster *Homarus americanus* (Hollins et al. 2003), and the hermit crabs *Pagurus bernhardus* (Groh et al. 2014) and *Coenobita clypeatus* (Groh-Lunow et al. 2015). IRs are hence considered as the putative crustacean olfactory receptors that mediate the odorant detection in the antennules (Derby et al. 2016). IRs function as heteromeric receptors, with IR25a, IR93a and IR8a being common subunits that associate with other IRs subunits that determine odor specificity in olfactory sensory neurons and likely in other chemosensory neurons (Abuin et al. 2011; Rytz et al. 2013). In addition, the genome of *D. pulex* revealed the presence of several Gustatory Receptors (GRs) and ChemoSensory Proteins (CSPs) (Eyun et al. 2017) that are also involved in chemodetection in insects (GRs: Scott et al. 2001, CSPs: Pelosi et al. 2014). GRs and CSPs were identified in transcriptomes from several species of copepods (Eyun et al. 2017), but they have never been reported in antennule transcriptomes of decapod species. So far, no chemoreceptors have been identified in Caridea, which comprises our shrimp models, the Alvinocarididae vent shrimp and the Palaemonidae shallow-water shrimp species.

Thermosensory mechanisms in crustaceans are unknown so far. In insects, thermoreceptors have been identified first in *Drosophila melanogaster*. They are mainly Transient Receptor Potential (TRP) channels, a family of receptors that are likely associated to every sensory modality (Fowler and Montell 2013). Several subfamilies of TRPs are believed to mediate thermodetection at different ranges of temperatures (Lee et al. 2005; Neely et al. 2011). Some IRs and GRs have also been proposed to mediate thermodetection in *D. melanogaster* (IRs: Ni et al. 2013; Knecht et al. 2016; GRs: Ni et al. 2013).

Juliette Ravaux, Magali Zbinden and I, in collaboration with Thomas Chertemps and Nicolas Montagné[1] (altogether referred in the text as “we”) investigated the expression of the olfactory candidate co-receptor IR25a in the antennal appendages of four vent shrimp species (*Rimicaris exoculata*, *Rimicaris chacei*, *Mirocaris fortunata* and *Alvinocaris markensis*). All the approaches were conducted in parallel on *Palaemon elegans*, to search for differences that could reflect molecular adaptation to the vent habitat. Comparisons within hydrothermal species were also conducted to examine possible specific adaptations related to their different microhabitats and lifestyles. In addition, I present in this chapter preliminary results from a transcriptome analysis we recently launched for the four vent shrimp species to further identify potential chemo- and thermoreceptors.

[1] Chimioréception et Adaptation (CREA) team, Sensory Ecology department, iEES

II. Results and discussion

1. Comparative expression of the olfactory co-receptor IR25a in hydrothermal vent and coastal shrimp

[Results published in Zbinden et al. 2017]

In order to identify organs putatively involved in olfaction, we investigated the expression pattern of the co-receptor IR25a. IR25a ancestor may have initially evolved to detect environmental glutamate and then it later acquired a co-receptor function after the IR repertoire duplicated and diversified (Croset et al. 2010; Rytz et al. 2013). L-glutamate is a major chemical stimulus for crustaceans, known to activate olfactory sensory neurons (OSNs) in the aesthetascs, and is linked to feeding behaviors (Ukhanov et al. 2011; Derby and Zimmer 2012). Corey and collaborators (2013) confirmed the olfactory function of IR25a in crustaceans by identifying and localizing IR25a in the dendritic membranes of lobster OSNs.

Using a homology-based PCR with primers designed from the alignment of IR25a sequences from diverse organisms, we obtained, for our 5 shrimp species, partial IR25a sequences of 903 bp for *R. exoculata* and *P. elegans*, and 763 bp for *M. fortunata*, *R. chacei*, and *A. markensis*. A phylogenetic analysis confirmed that these sequences group with IR25a sequences from other arthropods and form distinct clusters within the shrimp sequences, being congruent with the phylogeny of these groups (results in the thesis publication Zbinden et al. 2017). Our IR25a partial sequences are about 250 to 300 amino acids in length, which represents 25 to 30% of the total length expected for such sequences.

Then, using RT-PCR, we examined the expression pattern of IR25a in antennules, antennae, mouthparts and walking legs, as well as in non-chemosensory tissues (abdominal muscles, eye), from the 4 hydrothermal vent shrimp and the coastal shrimp *P. elegans* (Figure 57). In these 5 species, IR25a was predominantly expressed in the lateral antennular flagella (A1 lateral) that bear the aesthetascs (Figure 57). This result is consistent with the expression pattern of this IR subunit previously reported in *H. americanus* (iGluR1, Stepanyan et al. 2004), *P. argus* (Corey et al. 2013) and *C. clypeatus* (Groh-Lunow et al. 2015). In *P. elegans*, we observed a weaker expression in the external ramus than in the internal ramus of the lateral antennular flagella, the latter bearing the aesthetascs. IR25a expression in other chemosensory tissues than the lateral antennules varies amongst the species tested. We did not detect IR25a expression in the medial antennules and the antennae in *M. fortunata*, *A. markensis* and *P. elegans*, as results previously obtained for *H. americanus* (Stepanyan et al. 2004). In contrast,

we observed IR25a expression in the medial antennules in *R. exoculata* and *R. chacei*, and a weak expression was detected in the antennae of *R. exoculata*. IR25a expression was not detected in the eye, mouthparts and walking legs in *P. elegans* in the present study, although Corey et al. (2013) detected IR25a in the mouth and the two first walking legs in *P. argus*.

The occurrence of IR25a in tissues other than those bearing the aesthetascs suggested to Corey and collaborators (2013) that IR25a may play a more general role in decapod crustacean chemodetection than just mediating olfaction. In contrast, Keller et al. (2003) suggested that organs other than the aesthetasc bearing flagella can also have an olfactory role. Because our results show that IR25a is not only expressed in the lateral antennules, and that several recent reviews indicate that only the aesthetascs are considered as olfactory sensilla (Schmidt and Mellon 2011; Mellon 2014; Derby and Weissburg 2014; Derby et al. 2016), we rather support the hypothesis of Corey et al. (2013). All the antennal flagella, the mouthparts and the two first pairs of walking legs are associated to bimodal chemo- and mechanosensory sensilla, hence IR25a might not be involved only in the olfactory pathway mediated by the aesthetascs, but also in the distributed chemodetection pathway mediated by the bimodal sensilla.

Among hydrothermal species, the different patterns of IR25a expression we obtained for *R. exoculata* and *R. chacei* on one hand (detection in the lateral and medial antennules, and in the antennae for *R. exoculata*) and for *M. fortunata* and *A. markensis* on the other hand (detection in the lateral antennules only) would suggest different chemosensory mechanisms in these 2 shrimp groups. We propose that these differences may be related to their respective diets and thus to their distinct relations to the hydrothermal fluid. *R. exoculata* and *R. chacei* live in symbiosis with chemoautotrophic bacteria from which they derive all or part of their food (Gebruk et al. 2000; Ponsard et al. 2013), forcing them to stay permanently close to hydrothermal fluid emissions to supply their bacteria in reduced compounds necessary for chemosynthesis (Van Dover et al. 1988; Zbinden et al. 2004, 2008). This association with symbiotic bacteria is more extensive for *R. exoculata* than for *R. chacei* (Casanova et al. 1993; Apremont 2017), so the IR25a expression pattern in the antennae of *R. exoculata* could be reflective of its primary need to locate hydrothermal fluid chemicals, and consequently to have enhanced chemosensory abilities. On the other hand, *M. fortunata* and *A. markensis* are secondary consumers, scavenging on local organic matter and living at greater distances from the vent emissions (Gebruk et al. 2000; Desbruyères et al. 2006; De Busserolles et al. 2009; Husson et al. 2017). The coastal shrimp *P. elegans* has an IR25a expression pattern similar to hydrothermal secondary consumers *M. fortunata* and *A. markensis*, itself having an opportunistic omnivorous diet comprising invertebrate tissues (Janas and Baranska 2008).

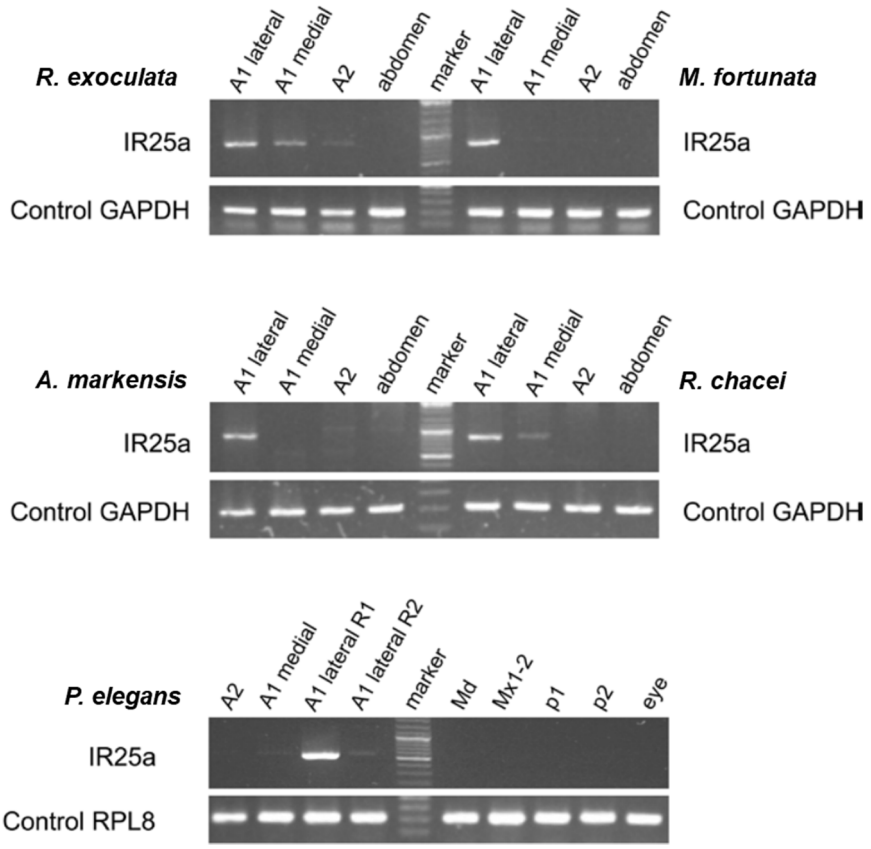

Figure 57 IR25a gene expression in hydrothermal and coastal shrimp species

Control RT-PCR products for comparative analysis of gene expression correspond to the glycolysis enzyme GAPDH for hydrothermal vent shrimp *R. exoculata*, *M. fortunata*, *A. markensis* and *R. chacei*, and to the ribosomal protein gene RPL8 for the coastal shrimp *P. elegans*. No amplification was detected in the absence of template (not shown).
A1, antennules; A2, second antennae; Md, mandibles; Mx1-2, maxillae; p1 and p2, first and second walking legs; R1, internal ramus of the lateral antennulles; R2, external ramus of the lateral antennules.

2. Pre-identification of potential chemo- and thermosensory proteins in vent shrimp from RNA sequencing

So far, IRs are the only family of chemoreceptors identified in decapod crustaceans (Derby et al. 2016, Eyun et al. 2017), but this statement is supported by transcriptomic data from the antennules of very few species. Other functional classes of chemosensory proteins are reported in the genome of *D. pulex* and the transcriptomes of several copepod species: the GRs and the CSPs, the latter being also identified in one Dendrobranchiata species (Eyun et al. 2017). To get a more exhaustive view of the sets of chemosensory proteins expressed in vent shrimp, as well as potential thermoreceptors, we recently launched a transcriptome analysis for main sensory organs in the vent species *R. exoculata*, *R. chacei*, *M. fortunata* and *A. markensis*.

RNAs were extracted (as detailed in Chapter II – IV. 1.) from 3 groups of organs for *R. chacei*, *M. fortunata* and *A. markensis*: the antennules (lateral and medial flagella pooled), the antennae and the abdomen muscles. For *R. exoculata*, RNAs were extracted from 6 groups of organs: the lateral antennules, the medial antennules, the antennae, the abdomen muscles, a pool of maxillipeds 2 and 3 and the first pair of walking legs, and the fifth pair of walking legs. Illumina RNA-sequencing was undertaken by the MGX Company (Montpellier, France), and the numbers of clustered sequences obtained are presented in Table 14.

Table 14 Results of Illumina RNA-sequencing for four hydrothermal shrimp species

Species	Samples	Total number of clusters*	Total number of clusters* per species
Rimicaris exoculata	Lateral antennules	23 586 189	229 172 327
	Medial antennules	20 226 159	
	Antennae	19 056 886	
	Abdomen muscles	67 313 780	
	Maxillipeds 2, 3 and first pair of walking legs	19 918 823	
	Fifth pair of walking legs	79 070 490	
Rimicaris chacei	Lateral and medial antennules	15 276 667	53 147 985
	Antennae	21 105 346	
	Abdomen muscles	16 756 972	
Mirocaris fortunata	Lateral and medial antennules	10 252 121	61 976 254
	Antennae	34 362 241	
	Abdomen muscles	17 361 892	
Alvinocaris markensis	Lateral and medial antennules	17 532 808	51 920 530
	Antennae	27 081 706	
	Abdomen muscles	7 306 016	

*Number of clusters after filtering the raw data to remove the clusters that present too much overlapping (i.e. to remove the least reliable data from the analysis)

Transcripts de novo assembly was carried out using Trinity. To identify receptor sequences, the first step is to establish a reference transcriptome by pooling, for each species, the transcripts from all the organs, and to annotate potential receptors by comparison with homologous sequences known in other species. Our preliminary results are presented in Table 15, in comparison with receptors previously identified in other marine crustaceans. From a first series of annotation, we identified several IRs, GRs, CSPs and TRPs in the pooled transcriptomes of each hydrothermal species.

Taxon	Species	Sequencing	Organs	Irs Antennal Irs	GRs	CSPs	TRPs	References
Branchiopoda								
	Daphnia pulex	Genome	Whole animal	IR25a, IR93a, IR76b (85 in total)	58	+	-	Penalva-Arana et al. 2009 ; Eyun et al. 2017
Copepoda								
	Eurytemora affinis	Transcriptome	Whole animal	IR93a, IR76b, IR21a, IR8a, IR25a (10 in total)	GR1-10	CSP1-4	-	Eyun et al. 2017
Decapoda								
	Pagurus bernhardus	Transcriptome	A1	IR25a, IR93a (20 in total)	nf	nf	nf	Groh et al. 2014
	Panulirus argus	Transcriptome	A1	IR25a, IR93a, IR8a, IR4,7,8,9,10,12,13, 14,18	nf	-	-	Corey et al. 2013
	Homarus americanus	cDNA	A1	IR25a, IR8a	-	-	-	Hollins et al. 2003
		Transcriptome	Brain, heart	-	-	-	TRPA1, pyrexia,painless, TRPM2, TRPM3	McGrath et al. 2016
	Penaeus monodon	Transcriptome	Whole animal	3	nf	2	-	Eyun et al. 2017
	Rimicaris exoculata	Transcriptome	A1, A2, abd	200-300	>2	>5	>8	This study
	Rimicaris chacei	Transcriptome	A1, A2, abd	>12	nf	>3	+	This study
	Mirocaris fortunata	Transcriptome	A1, A2, abd	>22	>3	>5	+	This study
	Alvinocaris markensis	Transcriptome	A1, A2, abd	>19	>1	>5	+	This study

Table 15 Identification of several classes of sensory proteins in vent shrimp species and comparison with other marine crustaceans

Results presented for the vent shrimp species are preliminary results from our ongoing reference transcriptome annotations. +, sensory proteins reported; -, sensory proteins not mentioned in the reference; nf, sensory proteins not found by the authors

The following paragraphs present general information on IRs, GRs, CSPs and TRPs families, regarding their previous reports in crustaceans, and their potential chemo- and thermosensory functions inferred from knowledge in insects. It must be reminded than any homology or similarity with insect receptors is highly speculative, since one receptor with an identified function in insect may have distinct roles in crustaceans. Hence, the following discussions must be considered as an introduction to the potential sensory functions that could be further explored from our transcriptome datasets, rather than interpretations. Also, at our current level of analysis, we cannot discuss on the different levels of expression of each sensory protein family in each organ used for the transcriptome analysis, since the presented results correspond to ongoing reference transcriptome annotations.

As explained previously, IRs are considered to play a general role in chemodetection in crustaceans (Corey et al. 2013). They are insect IR orthologs and are abundant in the genome of *Daphnia pulex* (Peñalva-Arana et al. 2009). From investigation of type and diversity of IRs in *D. melanogaster*, IRs were classified into two categories: antennal IRs, expressed in the antennae, and divergent IRs which are expressed in other chemosensory tissues (mouthparts, walking legs) (Croset et al. 2010; Koh et al. 2014; Groh et al. 2014). In crustaceans, IRs diversity has not yet been extensively explored, but the number of IRs appears to vary across species (Table 15 and Derby et al. 2016). For comparison, 66 IR genes were identified in *D. melanogaster* (Benton et al. 2009), 85 IR genes were identified in *D. pulex* (Peñalva-Arana et al. 2009), potentially 20 IRs were identified in the antennules transcriptome of the hermit crab *P. bernhardus* (Groh et al. 2014), 13 IRs were identified in the antennules transcriptome of the spiny lobster *P. argus* (Corey et al. 2013), and in the present study we found approximatively 200 to 300 IRs candidates in the transcriptome of *R. exoculata*. Comparison of these IRs RNAs expression within the transcriptome of each organ is needed to further discuss the proportion of antennal and divergent IRs in this vent species. IRs were also proposed to mediate thermodetection in *D. melanogaster* larvae, with IR21a mediating cool sensing together with IR25a (Ni et al. 2013), and IR93a being expressed in larval thermosensory neurons mediating cool avoidance (Knecht et al. 2016).

GRs are expressed in all arthropods and are ancestral to the Hexapod specific ORs (Eyun et al. 2017). In insects, GRs are expressed in antennae and other head and body appendages, and are involved for instance in the detection of sugar, bitter compounds (Sato et al. 2011; Scott et al. 2001; Ling et al. 2014) and also CO_2 (Kwon et al. 2007). GRs were identified in the *D. pulex* genome (Peñalva-Arana et al. 2009), in transcriptomes from several copepod species (Eyun et al. 2017) but not in the antennule transcriptomes of *P. bernhardus* (Groh et al. 2014) and *P. argus* (Corey et al. 2013) (Table 15). However, in the present study, we found GRs in the transcriptomes of *R. exoculata*, but also of *M. fortunata* and *A. markensis* for which only the antennules, antennae and abdomen muscles have been

sequenced. This expression in other structures than mouthparts suggests that GRs may be involved in sensory functions other than taste. For example, in *D. melanogaster*, one GR (GR28B) is involved in warm sensing (Ni et al. 2013). As pointed out by Eyun et al. (2017), the roles of GRs in non-insect arthropod taxa are poorly understood and require functional studies.

The molecular basis of chemodetection consists not only in chemoreceptors but also in the extracellular space surrounding them. In insects, processes that occur in the receptor environment before or after the chemical stimuli bind to their chemoreceptors involve olfactory binding proteins (OBPs) and chemosensory proteins (CSPs) (Pelosi et al. 2014). OBPs appear to be limited to terrestrial insect species and enhance chemodetection through their ability to increase the solubility of volatile odorants in the aqueous environment of the receptor. OBPs have never been identified in crustaceans, and we have not identified any OBP in the transcriptomes of our vent species either. In contrast, CSPs were reported in both insects and crustaceans. In crustaceans, CSPs were reported in *D. pulex*, several copepod species and one Dendrobranchiata species (Eyun et al. 2017) (Table 15). In insects, CSPs mediate the transport of ligands to the chemosensory receptors (Pelosi et al. 2014). Based on protein structure similarity, Eyun and collaborators (2017) suggested that copepod CSPs might have similar functions to those of insects. The sequencing of our transcriptomes revealed the presence of CSPs in the four vent species, hence being the second report of CSPs in decapods.

TRPs represent a large family of receptor genes that are key for multiple sensory modalities, including vision, hearing, chemodetection, thermodetection and mechanodetection (Fowler and Montell 2013). Consequently these channels are critical for sensing the external environment and for animal behaviors (Fowler and Montell 2013). The functions they mediate are extensively investigated in insects, but are fairly complex to define since some insect TRPs can be involved in the detection of multiple sensory stimuli (examples in Cattaneo et al. 2016). TRPs in insects have been divided into seven subfamilies, comprising at least four members (TRPC, TRPV, TRPA and TRPN) known to play roles in insect sensory systems (Fowler and Montell 2013). For thermodetection, in *D. melanogaster* several TRPA channels (TRPA1, Pyrexia, Painless) detect different ranges of temperature (Lee et al. 2005; Sokabe and Tominaga 2009) and contribute to the nociceptive responses (e.g. escape behavior) to excessively hot temperatures (40°C for Pyrexia, Lee et al. 2005; 46°C for TRPA1 and Painless, Neely et al. 2011). The isoforms of these receptors display different thresholds for temperature activation and unique expression patterns (Kwon et al. 2007; Zhong et al. 2012). For instance, Pyrexia-expressing neurons are widely distributed throughout the fly body (Lee et al. 2005). The arista (a large bristle attached to the front part of the antennae of *D. melanogaster*) contains thermosensory neurons and its heat-sensing function is thought to be mediated by TRP channels (Gallio et al. 2011). TRPA5 has also been reported to play a possible role in temperature sensing in antennae of the lepidoptera moth

Cydia pomonella (Cattaneo et al. 2016). In crustaceans, TRPA1, Painless and Pyrexia have been reported in transcriptomes from the brain and the heart of the lobster *H. americanus* but never from the antennal appendages (Table 15) (McGrath et al. 2016). In the present study, our transcriptome analysis revealed the presence of several TRPs, among which TRPA1 and Painless. These genes should be considered first for future localization in sensory organs, especially in the antennal appendages, to investigate a possible thermosensory function.

III. Conclusions

We investigated the molecular basis of chemo- and thermodetection in four vent shrimp species. They express in their antennal appendages the common IR25a known to be expressed in crustacean chemosensory neurons, and they also express several families of sensory proteins potentially involved in chemo- and thermodetection.

We identified partial sequences of the olfactory candidate co-receptors IR25a in the antennal appendages of four vent shrimp species (*R. exoculata*, *R. chacei*, *M. fortunata* and *A. markensis*) and of the coastal shrimp *P. elegans*. We showed that IR25a presents different patterns of expression in the antennal appendages of these species, maybe reflecting differences in lifestyle and consequent chemosensory abilities. In contrast to other species, *R. exoculata* express IR25a in all its antennal appendages, which could reflects its need to efficiently detect the hydrothermal fluids in order to supplement its symbiotic bacteria in chemicals. The different levels of expression of IR25a in the antennal appendages need to be quantified with qPCR.

Preliminary results of transcriptome sequencing from a pool of several sensory organs of the four vent species were also presented. They reveal the occurrence of several IRs, GRs, CSPs and TRPs, with GRs and TRPs being reported for the first time in decapod sensory organs. The further exploitation of these transcriptome datasets is very promising for the understanding of the molecular basis of chemodetection in Alvinocarididae and Crustacea. Regarding vent shrimp sensory biology, all these protein families are likely to be involved in chemodetection, and possibly in thermodetection for IRs, TRPs and GRs. Differential analyses of the transcriptomes will further provide information about the levels of expression of the corresponding RNAs in the antennules and the antennae of all species, as well as in the mouthparts and walking legs for *R. exoculata*. Relevant sensory receptors will be selected to search for their expression in the antennal appendages with RT-PCR, and within the neurons of the sensory organs, through *in situ* hybridization.

Conclusions and perspectives

For this thesis project, my supervisors[1], collaborators[2] and I investigated the abilities of deep vent alvinocaridid shrimp to detect their environment and to exploit hydrothermal fluid factors as orientation cues. We focused on the chemosensory abilities and, to a lesser extent, thermosensory abilities of vent shrimp, with *Mirocaris fortunata* as the main model, compared to those of a closely-related shallow-water species, *Palaemon elegans*, to discuss on potential sensory adaptations of the vent species. The main objectives of this work were:

- to describe the structure of *M. fortunata* chemosensory system and especially the olfactory system, from the morphology and the ultrastructure of the peripheral chemosensory sensilla to the inputs of the chemosensory neurons in the central nervous system. The chemosensory structures were compared with those of *P. elegans,* in order to reveal potential dissimilarities that may reflect adaptive traits;

- to identify and locate chemoreceptors in the main chemosensory organs of several vent shrimp species and *P. elegans*, for which distinct expression pattern may reflect functional differences in relation with the lifestyle of each species;

- to test the detection of relevant chemical stimuli by major chemosensory organs (i.e. the antennal appendages) using electrophysiology, in order to identify which hydrothermal fluid chemicals are perceived by *M. fortunata,* and if this species presents specific response profiles compared to *P. elegans*;

- to investigate the attraction to chemical and thermal cues in *M. fortunata*, with behavior experiments conducted in parallel on *P. elegans,* and a posteriori on the vent species *Rimicaris exoculata* to eventually highlight adaptive behavioral responses associated to vent shrimp lifestyle.

Overall, our results provide conclusions, insights and additional considerations for each issue, discussed hereafter with perspectives for future researches.

[1] Juliette Ravaux and Magali Zbinden (UMR 7208 BOREA, team Adaptations to Extreme Environments)

[2] Philippe Lucas, Thomas Chertemps, Nicolas Montagné (iEES, Sensory Ecology department); Steffen Harzsch, Jakob Krieger (Greisfwald University, Cytology and Evolutionary Biology department)

The olfactory system of the vent species *M. fortunata* is similar to that of the coastal species *P. elegans*

We investigated in *M. fortunata* and *P. elegans* the structural and molecular features of the olfactory pathway, mediated by the aesthetasc sensilla. We used morphometric measurements of structural characteristics of the olfactory system to infer on its performance. The distribution, dimensions and cuticle thickness of the aesthetascs are linked to the olfactory receptive surface. An enhanced number of aesthetascs, each associated to identical neuron clusters, raises the sensitivity to odorants. The number of OSNs, which bear different sets of olfactory receptors, and the related volume of the olfactory neuropils are linked to the odors discrimination abilities. We found that all these parameters are similar between *M. fortunata* and *P. elegans* (Zbinden et al. 2017, Machon et al. 2018). In addition, we analyzed the expression pattern of the co-receptor IR25a known to be involved in crustacean olfaction, and broadly expressed in chemosensory neurons. In both *M. fortunata* and *P. elegans*, IR25a is expressed only in the lateral antennules (Zbinden et al. 2017), which again suggests that both species possess similar olfactory systems.

Overall, at these levels of investigation, we did not observed striking differences that could suggest a different efficiency of the olfactory pathway in the vent species *M. fortunata* compared to the coastal shrimp *P. elegans*.

Distributed chemodetection, rather than olfaction, may be prevailing for the detection of the chemical environment by vent shrimp

For the structural analysis, a special attention was given to the aesthetascs (mediating olfaction) located on the lateral antennules. However, several results and preliminary observations presented hereafter suggest that the distributed chemodetection pathway (mediated by the bimodal sensilla, located on all antennal appendages) plays an important role for vent shrimp.

We successfully developed the first electroantennography (EAG) method on a marine shrimp in water (Machon et al. 2016), to test the detection of chemicals by the antennal appendages of *M. fortunata* and *P. elegans*. We found that not only the lateral antennules (that bear the aesthetascs) but also the antennae detect food-related odors and sulfide (Machon et al. 2018), indicating that at least the bimodal sensilla mediate such detection.

Analysis of IR25a expression patterns in several vent shrimp species revealed that, in contrast to *M. fortunata* and *P. elegans*, IR25a is expressed not only in the lateral antennules but also in the medial antennules for *Rimicaris chacei*, and in addition in the antennae for *R. exoculata* (Zbinden et al.

2017). These differences indicate that specificities at the molecular level are not restrained to the olfactory receptors, but concern also chemoreceptors expressed by the chemosensory neurons innervating the bimodal sensilla. Also, these results suggest that vent species might present adaptations of their chemosensory system linked to their lifestyle, *R. exoculata* being the most specialized to the vent habitat and could hence possess particular chemosensory abilities to efficiently supply its symbionts in chemicals, whereas *M. fortunata* is a secondary consumer as *P. elegans*.

Preliminary observations in rearing tanks and in video-recordings of *M. fortunata* and *R. exoculata* at *in situ* pressure suggest that the antennae, rather than the antennules, may be predominantly used to sense the environment. The two species use extensively their antennae while exploring (as previously observed by Matabos et al. 2015), whereas the antennules are not very mobile. Future investigation will quantify the flicking frequency of the antennules (mode of active chemodetection –sniffing– in crustaceans) in the vent species, in comparison with *P. elegans*.

The exploitation of our transcriptomic datasets will give precious information regarding the specialization of vent species chemosensory systems. We preliminary identified various chemoreceptor candidates in *R. exoculata*, *R. chacei*, *M. fortunata* and *Alvinocaris markensis*, including several Ionotropic Receptors (IRs), Gustatory Receptors (GRs) and Transient Receptor Potential channels (TRPs). Quantitative comparison for their expression levels in the antennules versus the antennae will give insights into their respective sensory functions, and differences in receptors diversity could have an adaptive significance regarding the lifestyle of each species. An additional RNA sequencing of the antennal appendages of *P. elegans* is needed to discuss on molecular adaptations to the hydrothermal environment.

The role of the hydrothermal fluid components in vent shrimp chemotaxis is uncertain, but thermodetection is likely a key sensory modality for the selection of the habitat

We conducted *in vivo* studies to investigate if the detection of active vents and selection of the habitat by shrimp is guided by chemical and thermal cues.

With the EAG method, we demonstrated that *M. fortunata* detects sulfide with both its lateral antennules and its antennae (Machon et al. 2018), supporting the statement of Renninger and collaborators (1995) on the chemodetection of the hydrothermal fluid. However, similar response profiles were obtained for *P. elegans*, indicating that sulfide detection is not specific to vent species.

Behavioural experiments at atmospheric and *in situ* pressure were not conclusive to discuss on the attraction to sulfide neither in *M. fortunata* nor in *R. exoculata*. We were not able to

demonstrate attraction to food-related odors in *M. fortunata* either, whereas we know this species locate food sources when fed in rearing tanks at atmospheric pressure, or at *in situ* pressure in the AbyssBox. Accordingly, our behavioural setups might not be appropriate to characterize an attraction behavior to chemicals, and other experiments should be conceived.

In contrast, we observed a significant attraction to warm temperatures (~17°C in a 9°C background) for *M. fortunata*, consistent with previous results obtained for *R. exoculata* (Ravaux et al. 2009). In our experimental conditions, we did not observed such behavior for *P. elegans*, suggesting that detection and attraction to temperature may have an adaptive significance in the vent habitat. The mechanisms for thermodetection are not known in crustaceans yet, but our transcriptomic analysis revealed that vent shrimp express several TRPs known to be activated each by specific temperatures in insects. Localization of these thermoreceptor candidates by *in situ* hybridization could provide for instance hints for the occurrence of sensilla specifically involved in thermodetection in vent shrimp.

The long-distance detection of active vents is still enigmatic

The long-term occurrence of shrimps at vents and evidence for high connectivity between different sites along the Mid-Atlantic Ridge (Teixeira et al. 2013) suggest that vent shrimp must have developed propagation strategies, including detection mechanisms to locate a distant active vent to settle in. Such processes are believed to occur at the larval stages, but their sensory abilities are unknown yet. However, it is not rare to observe from submersibles isolated shrimp adults swimming in the water column at tens of meters from the vent field, suggesting that they might be able to detect the vent activity from distance to return to their habitat.

Temperature is a potential factor for the long-distance detection of vents, since the spreading hydrothermal plumes can be warmer than the ambient seawater by tenth of degrees. Such range of temperature anomalies fits to the thermosensitivity estimated for some crustaceans, but remains to be determined for vent shrimp.

Sulfide is restrained in location to the close environment of a vent field, hence it is not likely a relevant cue for the long-distance detection of active vents. Iron and manganese were tested as stimuli relevant for long-distance detection of the hydrothermal plume, but no EAG responses were elicited by these compounds, which prevents any conclusion on their detection. Calcium imaging of the OSNs activation, although challenging to develop on small shrimp, could be used to further test the detection of iron and manganese.

Sensory modalities other than chemo- and thermodetection may be involved in the long-distance detection of active vents. Future research could examine sound detection as a sensory modality potentially used by vent shrimp to detect active vents. Acoustic vibrations are emitted at vents by the turbulent expulsion of the hydrothermal fluid through black smokers (Little 1988, Crone et al. 2006). Crustaceans can detect acoustic vibrations with particular mechanosensory organs, the statocysts, located in the basal segment of the antennules (Lovell et al. 2005). The hearing abilities of *M. fortunata* could be investigated, in comparison with *P. elegans*, with anatomical description of these organs and electrophysiology, using the Auditory Brainstem Response recording technique, previously used in the shallow-water shrimp *P. serratus* (Lovell et al. 2005). Furthermore, in our description of the central nervous system, we found that, compared to *P. elegans*, *M. fortunata* exhibits prominent hemiellipsoid bodies and medulla terminalis. These higher integrative centers process various sensory modalities and might be involved in learning, memory, or navigation skills in crustaceans. Although for now we can not speculate on their functions, these elaborated neuropils might have a functional significance for vent shrimp lifestyle.

Association with chemoautotrophic bacteria may be inherent to vent shrimp chemosensory abilities

The antennal appendages of vent shrimp, and sometimes even their sensilla, are often covered by a thick layer of bacteria, which was never observed on *P. elegans* (Zbinden et al. 2017, Machon et al. 2018, Zbinden et al. submitted). Most crustaceans groom their antennules to remove the microbial fouling, considered as detrimental to the chemosensory function of these organs (Barbato et al. 1997). Our preliminary observations indicate that *M. fortunata* grooms its antennules, but this behavior needs to be quantified and compared to *P. elegans.* However, the frequent occurrence of bacteria on the antennal appendages of vent shrimp is questioning. This bacterial coverage could impair the chemosensory abilities of vent shrimp, or alternatively may have a functional role. We recently identified these bacterial communities as *Epsilon-* and *Gammaproteobacteria* (Zbinden et al. submitted), which are sulfide and hydrogen oxidizers. One hypothesis is that they could have a detoxification role, for example by converting sulfide into less toxic sulphate, prior to the entrance of chemicals within the sensilla.

General conclusion

Together with a wide range of adaptations to the hydrothermal habitat, the sensory abilities are fundamental features to explain the long-term evolution of Alvinocarididae shrimp at deep hydrothermal vents. The chemical composition and the temperature of the hydrothermal fluid are among the potential attractants that had been proposed but poorly investigated. In this work, we demonstrated that vent shrimp use temperature as an orientation cue, and detect sulfide in the hydrothermal fluid, but we could not resolve the behaviors triggered by this chemodetection. The vent shrimp *Mirocaris fortunata* does not present striking specificities of its olfactory system compared to the coastal species *Palaemon elegans*. Chemosensory adaptations might be linked to the trophic behaviors of vent shrimp rather than to hydrothermal habitat itself. Comparison between Alvinocarididae species with different lifestyle, the use of other sensory modalities, the role of epibiotic bacteria, and the identification and localization of chemo- and thermoreceptors are promising areas of investigation for future advances on the sensory biology and adaptations of deep hydrothermal vent shrimp.

References

A

Abuin, L., Bargeton, B., Ulbrich, M.H., Isacoff, E.Y., Kellenberger, S., and Benton, R. **2011**. Functional architecture of olfactory ionotropic glutamate receptors. *Neuron*. 69:44–60.

Ache, B.W. **1982**. Chemoreception and thermoreception. In: Atwood, H.L., Sandeman, D.C. (Eds.), *The Biology of Crustacea, vol. 3: Neurobiology, Structure and Function*. Academic Press, New York. pp. 369–398.

Ache, B.W. **2002**. Crustaceans as animal models for olfactory research. In: Wiese, K. (Ed.), *Crustacean Experimental Systems in Neurobiology*. Springer, Berlin, Heidelberg. pp. 189–199.

Airriess, C.N., and Childress, J.J. **1994**. Homeoviscous properties implicated by the interactive effects of pressure and temperature on the hydrothermal vent crab *Bythograea thermydron*. *The Biological Bulletin*. 187:208–214.

Alayse-Danet, A.M., Desbruyeres, D., and Gaill, F. **1987**. The possible nutritional or detoxification role of the epibiotic bacteria of Alvinellid polychaetes: review of current data. *Symbiosis*. 4:51–61.

Altner, I., Hatt, H., and Altner, H. **1983**. Structural properties of bimodal chemo- and mechanosensitive setae on the pereiopod chelae of the crayfish *Austropotamobius torrentium*. *Cell and Tissue Research*. 228:357–374.

Amdam, G.V., and Hovland, A.L. **2012**. Measuring animal preferences and choice behavior *Nature Education Knowledge*. 3:74.

Ameyaw-Akumfi, C., and Hazlett, B.A. **1975**. Sex recognition in the crayfish *Procambarus clarkii*. *Science*. 190:1225–1226.

Ammar, D., Nazari, E.M., Müller, Y.M.R., and Allodi, S. **2008**. New insights on the olfactory lobe of decapod crustaceans. *Brain, Behavior and Evolution*. 72:27–36.

Anderson, P.A., and Ache, B.W. **1985**. Voltage-and current-clamp recordings of the receptor potential in olfactory receptor cells *in situ*. *Brain Research*. 338:273–280.

Apremont, V. **2017**. Description de la diversité microbienne associée à la crevette *Rimicaris chacei*: une possible double symbiose. PhD Thesis. Ifremer, Brest.

Atema, J., and Steinbach, M.A. **2007**. Chemical communication and social behavior of the lobster *Homarus americanus* and other decapod Crustacea. In: Duffy, J.E., Thiel, M. (Eds.), *Evolutionary Ecology of Social and Sexual Systems: Crustaceans as Model Organisms*. Oxford University Press, New York. pp. 115–144.

Auguste, M., Mestre, N.C., Rocha, T.L., Cardoso, C., Cueff-Gauchard, V., Le Bloa, S., Cambon-Bonavita, M.A., Shillito, B., Zbinden, M., Ravaux, J., and Bebianno, M.J. **2016**. Development of an ecotoxicological protocol for the deep-sea fauna using the hydrothermal vent shrimp *Rimicaris exoculata*. *Aquatic Toxicology*. 175:277–285.

Aumond, V. 2013. Spéciation du cuivre en milieu hydrothermal profond et dans les zones de suintements froids. PhD Thesis. Université de Bretagne occidentale, Brest.

Aznar-Cormano, L., Brisset, J., Chan, T.-Y., Corbari, L., Puillandre, N., Utge, J., Zbinden, M., Zuccon, D., and Samadi, S. **2015**. An improved taxonomic sampling is a necessary but not sufficient condition for resolving inter-families relationships in Caridean decapods. *Genetica*. 143:195–205.

B

Bailey, D.M., King, N.J., and Priede, I.G. **2007**. Cameras and carcasses: historical and current methods for using artificial food falls to study deep-water animals. *Marine Ecology Progress Series*. 350:179–192.

Baker, E.T., Resing, J.A., Haymon, R.M., Tunnicliffe, V., Lavelle, J.W., Martinez, F., Ferrini, V., Walker, S.L., and Nakamura, K. **2016**. How many vent fields? New estimates of vent field populations on ocean ridges from precise mapping of hydrothermal discharge locations. *Earth and Planetary Science Letters*. 449:186–196.

Barbato, J.C., and Daniel, P.C. **1997**. Chemosensory activation of an antennular grooming behavior in the spiny lobster, *Panulirus argus*, is tuned narrowly to L-glutamate. *The Biological Bulletin*. 193:107–115.

Barber, S.B. **1961**. Chemoreception and thermoreception. In: Waterman, T.H. (Ed.), *Physiology of Crustacea, vol. 2: Sense organs, Integration and Behavior*. Academic Press, New York. pp. 109–131.

Bates, A.E., Lee, R.W., Tunnicliffe, V., and Lamare, M.D. **2010**. Deep-sea hydrothermal vent animals seek cool fluids in a highly variable thermal environment. *Nature Communications*. 1:14.

Bauer, R.T. **1978**. Antifouling adaptations of caridean shrimps: Cleaning of the antennal flagellum and general body grooming. *Marine Biology*. 49:69–82.

Bauer, R.T. **1989**. Decapod crustacean grooming: functional morphology, adaptive value, and phylogenetic significance. *Crustacean Issues*. 6:49–73.

Beaulieu, S.E., Baker, E.T., German, C.R., and Maffei, A. **2013**. An authoritative global database for active submarine hydrothermal vent fields. *Geochemistry, Geophysics, Geosystems*. 14:4892–4905.

Beaulieu, S.E., Baker, E.T., and German, C.R. **2015**. Where are the undiscovered hydrothermal vents on oceanic spreading ridges? *Deep Sea Research Part II: Topical Studies in Oceanography*. 121:202–212.

Beltz, B.S., Kordas, K., Lee, M.M., Long, J.B., Benton, J.L., and Sandeman, D.C. **2003**. Ecological, evolutionary, and functional correlates of sensilla number and glomerular density in the olfactory system of decapod crustaceans. *Journal of Comparative Neurology*. 455:260–269.

Benton, R., Vannice, K.S., Gomez-Diaz, C., and Vosshall, L.B. **2009**. Variant ionotropic glutamate receptors as chemosensory receptors in *Drosophila*. *Cell*. 136:149–162.

Benton, R. **2015**. Multigene family evolution: Perspectives from insect chemoreceptors. *Trends in Ecology & Evolution*. 30:590–600.

Bergquist, D.C., Eckner, J.T., Urcuyo, I.A., Cordes, E.E., Hourdez, S., Macko, S.A., and Fisher, C.R. **2007**. Using stable isotopes and quantitative community characteristics to determine a local hydrothermal vent food web. *Marine Ecology Progress Series*. 330:49–65.

Blaustein, D.N., Derby, C.D., Simmons, R.B., and Beall, A.C. **1988**. Structure of the brain and medulla terminalis of the spiny lobster *Panulirus Argus* and the crayfish *Procambarus clarkii*, with an emphasis on olfactory centers. *Journal of Crustacean Biology*. 8:493–519.

Blaustein, D.N., Simmons, R.B., Burgess, M.F., Derby, C.D., Nishikawa, M., and Olson, K.S. **1993**. Ultrastructural localization of 5'AMP odorant receptor sites on the dendrites of olfactory receptor neurons of the spiny lobster. *Journal of Neuroscience*. 13:2821–2828.

Bleckmann, H., Breithaupt, T., Blickhan, R., and Tautz, J. **1991**. The time course and frequency content of hydrodynamic events caused by moving fish, frogs, and crustaceans. *Journal of Comparative Physiology A*. 168:749–757.

Bluhm, B.A., Beyer, K., and Niehoff, B. **2002**. Brain structure and histological features of lipofuscin in two antarctic Caridea (Decapoda). *Crustaceana*. 75:61–76.

Bobkov, Y.V., and Ache, B.W. **2005**. Pharmacological properties and functional role of a TRP-related ion channel in lobster olfactory receptor neurons. *Journal of Neurophysiology*. 93:1372–1380.

Bobkov, Y.V., Pezier, A., Corey, E.A., and Ache, B.W. **2010**. Phosphatidylinositol 4,5-bisphosphate-dependent regulation of the output in lobster olfactory receptor neurons. *Journal of Experimental Biology*. 213:1417–1424.

Bobkov, Y., Park, I., Ukhanov, K., Principe, J., and Ache, B. **2012**. Cellular basis for response diversity in the olfactory periphery. *PLoS One*. 7:e34843.

Brown, S., and Wolff, G. **2012**. Fine structural organization of the hemiellipsoid body of the land hermit crab, *Coenobita clypeatus*. *Journal of Comparative Neurology*. 520:2847–2863.

C

Casanova, B., Brunet, M., and Segonzac, M. **1993**. L'impact d'une épibiose bactérienne sur la morphologie fonctionnelle de crevettes associées à l'hydrothermalisme médio-atlantique = Bacterian epibiosis impact on the morphology of shrimps associated with hydrothermalism in the Mid-Atlantic. *Cahiers de Biologie Marine*. 34:573–588.

Cate, H.S., and Derby, C.D. **2001**. Morphology and distribution of setae on the antennules of the Caribbean spiny lobster *Panulirus argus* reveal new types of bimodal chemo-mechanosensilla. *Cell and Tissue Research*. 304:439–454.

Cathalot, C., Rouxel, O., et al. **2018**. Rapport de mission BICOSE2 - partie géochimie / Scientifique et Instrumentation. http://dx.doi.org/10.17600/18000004

Cattaneo, A.M., Bengtsson, J.M., Montagné, N., Jacquin-Joly, E., Rota-Stabelli, O., Salvagnin, U., Bassoli, A., Witzgall, P., and Anfora, G. **2016**. TRPA5, an ankyrin subfamily insect TRP channel, is expressed in antennae of *Cydia pomonella* (Lepidoptera: Tortricidae) in multiple splice variants. Journal of Insect Science. 16:83.

Chamberlain, S.C. **2000**. Vision in hydrothermal vent shrimp. *Philosophical Transactions of the Royal Society of London B: Biological Sciences*. 355:1151–1154.

Charlou, J.L., Donval, J.P., Douville, E., Jean-Baptiste, P., Radford-Knoery, J., Fouquet, Y., Dapoigny, A., and Stievenard, M. **2000**. Compared geochemical signatures and the evolution of Menez Gwen (37°50'N) and Lucky Strike (37°17'N) hydrothermal fluids, south of the Azores Triple Junction on the Mid-Atlantic Ridge. *Chemical Geology*. 171:49–75.

Charlou, J.L., Donval, J.P., Fouquet, Y., Jean-Baptiste, P., and Holm, N. **2002**. Geochemistry of high H_2 and CH_4 vent fluids issuing from ultramafic rocks at the Rainbow hydrothermal field (36°14'N, MAR). *Chemical Geology*. 191:345–359.

Charlou, J.L., Donval, J.P., Konn, C., Ondréas, H., Fouquet, Y., Jean-Baptiste, P., and Fourré, E. **2010**. High production and fluxes of H_2 and CH_4 and evidence of abiotic hydrocarbon synthesis by serpentinization in ultramafic-hosted hydrothermal systems on the Mid-Atlantic Ridge. In: Rona, P., Devey, C., Dyment, J., Murton, B. (Eds.), *Diversity Of Hydrothermal Systems On Slow Spreading Ocean Ridges*. American Geophysical Union, Washington DC. pp. 265–296.

Charmantier-Daures, M., and Segonzac, M. **1998**. Organ of Bellonci and sinus gland in three decapods from Atlantic hydrothermal vents: *Rimicaris Exoculata*, *Chorocaris Chacei*, and *Segonzacia Mesatlantica*. *Journal of Crustacean Biology*. 18:213–223.

Chausson, F., Bridges, C.R., Sarradin, P.-M., Green, B.N., Riso, R., Caprais, J.-C., and Lallier, F.H. **2001**. Structural and functional properties of hemocyanin from *Cyanagraea praedator,* a deep-sea hydrothermal vent crab. *Proteins: Structure, Function, and Bioinformatics*. 45:351–359.

Chausson, F., Sanglier, S., Leize, E., Hagège, A., Bridges, C.R., Sarradin, P.-M., Shillito, B., Lallier, F.H., and Zal, F. **2004**. Respiratory adaptations to the deep-sea hydrothermal vent environment: the case of *Segonzacia mesatlantica*, a crab from the Mid-Atlantic Ridge. *Micron*. 35:31–41.

Childress, J.J., Barnes, A.T., Quetin, L.B., and Robison, B.H. **1978**. Thermally protecting cod ends for the recovery of living deep-sea animals. *Deep Sea Research*. 25:419–422.

Childress, J.J., and Fisher, C.R. **1992**. The biology of hydrothermal vent animals: physiology, biochemistry, and autotrophic symbioses. *Oceanography and Marine Biology: An Annual Review*. 30:337-441.

Chittka, L., and Niven, J. **2009**. Are Bigger Brains Better? *Current Biology*. 19:R995–R1008.

Christoffersen, M.L. **1986**. Phylogenetic relationships between Oplophoridae, Atyidae, Pasiphaeidae, Alvinocarididae Fam. N., Bresiliidae, Psalidopodidae and Disciadidae (Crustacea caridea atyoidea). *Boletim de Zoologia*. 10:273–281.

Colaço, A., Dehairs, F., and Desbruyères, D. **2002**. Nutritional relations of deep-sea hydrothermal fields at the Mid-Atlantic Ridge: a stable isotope approach. *Deep Sea Research Part I: Oceanographic Research Papers*. 49:395–412.

Company, R., Serafim, A., Bebianno, M.J., Cosson, R., Shillito, B., and Fiala-Médioni, A. **2004**. Effect of cadmium, copper and mercury on antioxidant enzyme activities and lipid peroxidation in the gills of the hydrothermal vent mussel *Bathymodiolus azoricus*. *Marine Environmental Research*. 58:377–381.

Company, R., Serafim, A., Cosson, R., Camus, L., Shillito, B., Fiala-Médioni, A., and Bebianno, M.J. **2006**. The effect of cadmium on antioxidant responses and the susceptibility to oxidative stress in the hydrothermal vent mussel *Bathymodiolus azoricus*. *Marine Biology*. 148:817–825.

Corey, E.A., Bobkov, Y., Ukhanov, K., and Ache, B.W. **2013**. Ionotropic crustacean olfactory receptors. *PloS One*. 8:e60551.

Corliss, J.B., Dymond, J., Gordon, L.I., Edmond, J.M., Herzen, R.P. von, Ballard, R.D., Green, K., Williams, D., Bainbridge, A., Crane, K., Van Andel, T.H. **1979**. Submarine thermal springs on the Galápagos Rift. *Science*. 203:1073–1083.

Cottin, D., Shillito, B., Chertemps, T., Thatje, S., Léger, N., and Ravaux, J. **2010**. Comparison of heat-shock responses between the hydrothermal vent shrimp *Rimicaris exoculata* and the related coastal shrimp *Palaemonetes varians*. *Journal of Experimental Marine Biology and Ecology*. 393:9–16.

Cowen, J.P., Bertram, M.A., Wakeham, S.G., Thomson, R.E., William Lavelle, J., Baker, E.T., and Feely, R.A. **2001**. Ascending and descending particle flux from hydrothermal plumes at Endeavour

Segment, Juan de Fuca Ridge. *Deep Sea Research Part I: Oceanographic Research Papers*. 48:1093–1120.

Cristescu, M.E.A., Colbourne, J.K., Radivojac, J., and Lynch, M. **2006**. A microsatellite-based genetic linkage map of the waterflea, *Daphnia pulex*: On the prospect of crustacean genomics. *Genomics*. 88:415–430.

Croset, V., Rytz, R., Cummins, S.F., Budd, A., Brawand, D., Kaessmann, H., Gibson, T.J., and Benton, R. **2010**. Ancient protostome origin of chemosensory ionotropic glutamate receptors and the evolution of insect taste and olfaction. *PloS Genetics*. 6:e1001064.

Cuomo, M.C. **1985**. Sulphide as a larval settlement cue for *Capitella sp*. *Biogeochemistry*. 1:169–181.

Cuvelier, D., Sarrazin, J., Colaço, A., Copley, J., Desbruyères, D., Glover, A.G., Tyler, P., and Santos, R.S. **2009**. Distribution and spatial variation of hydrothermal faunal assemblages at Lucky Strike (Mid-Atlantic Ridge) revealed by high-resolution video image analysis. *Deep Sea Research Part I: Oceanographic Research Papers*. 56:2026–2040.

Cuvelier, D., Sarradin, P.-M., Sarrazin, J., Colaço, A., Copley, J.T., Desbruyères, D., Glover, A.G., Santos, R.S., and Tyler, P.A. **2011**. Hydrothermal faunal assemblages and habitat characterisation at the Eiffel Tower edifice (Lucky Strike, Mid-Atlantic Ridge). *Marine Ecology*. 32:243–255.

Cuvelier, D., De Busserolles, F., Lavaud, R., Floc'h, E., Fabri, M.-C., Sarradin, P.-M., and Sarrazin, J. **2012**. Biological data extraction from imagery–How far can we go? A case study from the Mid-Atlantic Ridge. *Marine Environmental Research*. 82:15–27.

D

De Angelis, M.A., Lilley, M.D., and Baross, J.A. **1993**. Methane oxidation in deep-sea hydrothermal plumes of the endeavour segment of the Juan de Fuca Ridge. *Deep Sea Research Part I: Oceanographic Research Papers*. 40:1169–1186.

De Busserolles, F., Sarrazin, J., Gauthier, O., Gélinas, Y., Fabri, M.-C., Sarradin, P.-M., and Desbruyeres, D. **2009**. Are spatial variations in the diets of hydrothermal fauna linked to local environmental conditions? *Deep Sea Research Part II: Topical Studies in Oceanography*. 56:1649–1664.

Derby, C.D. **1989**. Physiology of sensory neurons in morphologically identified cuticular sensilla of crustaceans. In: Felgenhauer, Thistle, A.B., Watling, L. (Eds.), *Functional Morphology of Feeding and Grooming in Crustacea*. CRC Press. pp. 27–47.

Derby, C.D., Cate, H.S., and Gentilcore, L.R. **1997**. Perireception in olfaction: molecular mass sieving by aesthetasc sensillar cuticle determines odorant access to receptor sites in the Caribbean spiny lobster *Panulirus argus*. *Journal of Experimental Biology*. 200:2073–2081.

Derby, C.D., and Steullet, P. **2001**. Why do animals have so many receptors? The role of multiple chemosensors in animal perception. *The Biological Bulletin*. 200:211–215.

Derby, C., and Zimmer, R. **2012**. Neuroecology of predator-prey interactions. In: Brönmark, C., Hansson, L.-A. (Eds.) *Chemical Ecology in Aquatic Systems*. Oxford University Press, London. pp. 158–171.

Derby, C., and Weissburg, M.J. **2014**. The chemical senses and chemosensory ecology of crustaceans. In: Derby, C., Thiel, M. (Eds.), *Nervous Systems and Control of Behavior.* Oxford University Press, New York. pp. 263–292.

Derby, C.D., Kozma, M.T., Senatore, A., and Schmidt, M. **2016**. Molecular mechanisms of reception and perireception in crustacean chemoreception: A comparative review. *Chemical Senses*. 41:381–398.

Desbruyeres, D., Almeida, A., Biscoito, M., Comtet, T., Khripounoff, A., Le Bris, N., Sarradin, P.-M., and Segonzac, M. **2000**. A review of the distribution of hydrothermal vent communities along the northern Mid-Atlantic Ridge: dispersal vs. environmental controls. *Hydrobiologia*. 440:201–216.

Desbruyères, D., Biscoito, M., Caprais, J.-C., Colaço, A., Comtet, T., Crassous, P., Fouquet, Y., Khripounoff, A., Le Bris, N., Olu, K., Riso, R., Sarradin, P.-M., Segonzac, M., and Vangriesheim, A.. **2001**. Variations in deep-sea hydrothermal vent communities on the Mid-Atlantic Ridge near the Azores plateau. *Deep Sea Research Part I: Oceanographic Research Papers*. 48:1325–1346.

Desbruyères, D., Hashimoto, J., and Fabri, M.-C. **2006**. Composition and biogeography of hydrothermal vent communities in Western Pacific back-arc basins. *Back-Arc Spreading Systems: Geological, Biological, Chemical, and Physical Interactions*. 215–234.

Dixon, D.R., Dixon, L.R.J., Shillito, B., and Gwynn, J. **2002**. Background and induced levels of DNA damage in Pacific deep-sea vent polychaetes: the case for avoidance. *Cahiers de Biologie Marine*. 43:333–336.

Doolin, R.E., Zhainazarov, A.B., and Ache, B.W. **2001**. An odorant-suppressed Cl^- conductance in lobster olfactory receptor cells. *Journal of Comparative Physiology A*. 187:477–487.

Douville, E., Charlou, J.L., Oelkers, E.H., Bienvenu, P., Jove Colon, C.F., Donval, J.P., Fouquet, Y., Prieur, D., and Appriou, P. **2002**. The rainbow vent fluids (36°14′N, MAR): the influence of ultramafic rocks and phase separation on trace metal content in Mid-Atlantic Ridge hydrothermal fluids. *Chemical Geology*. 184:37–48.

Duffy, J.E. **1996**. Eusociality in a coral-reef shrimp. *Nature*. 381:512–514.

Duperron, S., and Gros, O. **2016**. Colwellia and sulfur-oxidizing bacteria: An unusual dual symbiosis in a Terua mussel (Mytilidae: Bathymodiolinae) from whale falls in the Antilles arc. *Deep Sea Research Part I: Oceanographic Research Papers*. 115:112–122.

Durand, L., Zbinden, M., Cueff-Gauchard, V., Duperron, S., Roussel, E.G., Shillito, B., and Cambon-Bonavita, M.-A. **2009**. Microbial diversity associated with the hydrothermal shrimp Rimicaris exoculata gut and occurrence of a resident microbial community. *FEMS Microbiology Ecology*. 71:291–303.

E

Eberhard, W.G., and Wcislo, W.T. **2011**. Grade changes in brain–body allometry: Morphological and behavioral correlates of brain size in miniature spiders, insects and other invertebrates. *Advances in Insect Physiology*. 40:155–214.

Edmond, J.M. **1982**. The chemistry of ridge crest hot springs. *Marine Technology Society Journal*. 16:23–25.

Eyun, S., Soh, H.Y., Posavi, M., Munro, J.B., Hughes, D.S.T., Murali, S.C., Qu, J., Dugan, S., Lee, S.L., Chao, H., et al. **2017**. Evolutionary history of chemosensory-related gene families across the Arthropoda. *Molecular Biology and Evolution*. 34:1838–1862.

F

Fanenbruck, M., Harzsch, S., and Wägele, J.W. **2004**. The brain of the Remipedia (Crustacea) and an alternative hypothesis on their phylogenetic relationships. *Proceedings of the National Academy of Sciences*. 101:3868–3873.

Fanenbruck, M., and Harzsch, S. **2005**. A brain atlas of *Godzilliognomus frondosus* Yager, 1989 (Remipedia, Godzilliidae) and comparison with the brain of *Speleonectes tulumensis* Yager, 1987 (Remipedia, Speleonectidae): implications for arthropod relationships. *Arthropod Structure & Development.* 34:343–378.

Fisher, C.R., Kennicutt, M.C., and Brooks, J.M. **1990**. Stable carbon isotopic evidence for carbon limitation in hydrothermal vent vestimentiferans. *Science*. 247:1094–1096.

Fisher, C.R., Takai, K., and Le Bris, N. **2007**. Hydrothermal vent ecosystems. *Oceanography*. 20:14–23.

Fontaine, M.T., Passelecq-Gerin, E., and Bauchau, A.G. **1982**. Structures chemoreceptrices des antennules du crabe *Carcinus Maenas* (L.) (Decapoda Brachyura). *Crustaceana*. 43:271–283.

Forward Jr, R.B. **1990**. Behavioral responses of crustacean larvae to rates of temperature change. *The Biological Bulletin*. 178:195–204.

Fowler, M.A., and Montell, C. **2013**. Drosophila TRP channels and animal behavior. *Life Sciences*. 92:394–403.

Fustec, A., Desbruyeres, D., and Laubier, L. **1988**. Estimation de la biomasse des peuplements associés aux sources hydrothermales profondes de la dorsale du Pacifique oriental à 13 degrés Nord. *Oceanologica Acta*, Special issue (0399-1784).

G

Galizia, C.G. **2014**. Olfactory coding in the insect brain: data and conjectures. *European Journal of Neuroscience*. 39:1784–1795.

Galkin, S.V., and Sagalevich, A.M. **2017**. Endemism and biodiversity of hydrothermal vent fauna. In: Hermann, E. (Ed.), *Extreme Biomimetics*. Springer, Switzerland. pp. 97–118.

Gallio, M., Ofstad, T.A., Macpherson, L.J., Wang, J.W., and Zuker, C.S. **2011**. The coding of temperature in the Drosophila brain. *Cell*. 144:614–624.

Garm, A., Hallberg, E., and Høeg, J.T. **2003**. Role of maxilla 2 and its setae during feeding in the shrimp *Palaemon adspersus* (Crustacea: Decapoda). *The Biological Bulletin*. 204:126–137.

Garm, A., Shabani, S., Høeg, J.T., and Derby, C.D. **2005**. Chemosensory neurons in the mouthparts of the spiny lobsters *Panulirus argus* and *Panulirus interruptus* (Crustacea: Decapoda). *Journal of Experimental Marine Biology and Ecology*. 314:175–186.

Garm, A., and Watling, L. **2013**. The crustacean integument: setae, setules, and other ornamentation. *Functional Morphology Diversity*. 1:167–198.

Gaten, E., Herring, P.J., and Shelton, P.A. **1998a**. The development and evolution of the eyes of vent shrimps (Decapoda: Bresiliidae). *Cahiers de Biologie Marine*. 39:287-290.

Gaten, E., Herring, P.J., Shelton, P.M.J., and Johnson, M.L. **1998b**. Comparative morphology of the eyes of postlarval bresiliid shrimps from the region of hydrothermal vents. *The Biological Bulletin*. 194:267–280.

Gebruk, A.V., Pimenov, N.V., and Savvichev, A.S. **1993**. Feeding specialization of bresiliid shrimps in the TAG site hydrothermal community. *Marine Ecology Progress Series*. 98:247–253.

Gebruk, A.V., Galkin, S.V., Vereshchaka, A.L., Moskalev, L.I., and Southward, A.J. **1997**. Ecology and biogeography of the hydrothermal vent fauna of the Mid-Atlantic Ridge. *Advances in Marine Biology*. 32:93–144.

Gebruk, A.V., Southward, E.C., Kennedy, H., and Southward, A.J. **2000**. Food sources, behaviour, and distribution of hydrothermal vent shrimps at the Mid-Atlantic Ridge*. Journal of the Marine Biological Association of the United Kingdom*. 80:485–499.

Geret, F., Riso, R., Sarradin, P.-M., Caprais, J.-C., and Cosson, R.P. **2002**. Metal bioaccumulation and storage forms in the shrimp, *Rimicaris exoculata*, from the Rainbow hydrothermal field (Mid-Atlantic Ridge); preliminary approach to the fluid-organism relationship. *Cahiers de Biologie Marine*. 43:43–52.

German, C.R., Higgs, N.C., Thomson, J., Mills, R., Elderfield, H., Blusztajn, J., Fleer, A.P., and Bacon, M.P. **1993**. A geochemical study of metalliferous sediment from the TAG Hydrothermal Mound, 26° 08′ N, Mid-Atlantic Ridge. *Journal of Geophysical Research: Solid Earth*. 98:9683–9692.

Ghiradella, H.T., Case, J.F., and Cronshaw, J. **1968**. Structure of aesthetascs in selected marine and terrestrial decapods: Chemoreceptor morphology and environment. *Integrative and Comparative Biology*. 8:603–621.

Gleeson, R.A., McDowell, L.M., and Aldrich, H.C. **1996**. Structure of the aesthetasc (olfactory) sensilla of the blue crab, *Callinectes sapidus*: transformations as a function of salinity. *Cell and Tissue Research*. 284:279–288.

Gonzalez-Rey, M., Serafim, A., Company, R., and Bebianno, M.J. **2007**. Adaptation to metal toxicity: a comparison of hydrothermal vent and coastal shrimps. *Marine Ecology*. 28:100–107.

Gonzalez-Rey, M., Serafim, A., Company, R., Gomes, T., and Bebianno, M.J. **2008**. Detoxification mechanisms in shrimp: Comparative approach between hydrothermal vent fields and estuarine environments. *Marine Environmental Research*. 66:35–37.

Govenar, B. **2012**. Energy transfer through food webs at hydrothermal vents: linking the lithosphere to the biosphere. *Oceanography*. 25:246–255.

Govenar, B., Fisher, C.R., and Shank, T.M. **2015**. Variation in the diets of hydrothermal vent gastropods. *Deep Sea Research Part II: Topical Studies in Oceanography*. 121:193–201.

Grieshaber, M.K., and Völkel, S. **1998**. Animal adaptations for tolerance and exploitation of poisonous sulfide. *Annual Review of Physiology*. 60:33–53.

Groh, K.C., Vogel, H., Stensmyr, M.C., Grosse-Wilde, E., and Hansson, B.S. **2014**. The hermit crab's nose—antennal transcriptomics. *Frontiers in Neuroscience*. 7:266.

Groh-Lunow, K.C., Getahun, M.N., Grosse-Wilde, E., and Hansson, B.S. **2015**. Expression of ionotropic receptors in terrestrial hermit crab's olfactory sensory neurons. *Frontiers in Cellular Neuroscience*. 8:488.

Grünert, U., and Ache, B.W. **1988**. Ultrastructure of the aesthetasc (olfactory) sensilla of the spiny lobster, *Panulirus argus*. *Cell and Tissue Research*. 251:95–103.

Guenther, C.M., and Atema, J. **1998**. Distribution of setae on the *Homarus americanus* lateral antennular flagellum. *The Biological Bulletin*. 195:182–183.

H

Hallberg, E., Johansson, K.U.I., and Elofsson, R. **1992**. The aesthetasc concept: Structural variations of putative olfactory receptor cell complexes in crustacea. *Microscopy Research and Technique*. 22:325–335.

Hallberg, E., and Skog, M. **2011**. Chemosensory sensilla in crustaceans. In: Breithaupt, T., Thiel, M. (Eds.), *Chemical Communication in Crustaceans*. Springer, New York. pp. 103–121.

Harzsch, S., Miller, J., Benton, J., Dawirs, R.R., and Beltz, B. **1998**. Neurogenesis in the thoracic neuromeres of two crustaceans with different types of metamorphic development. *Journal of Experimental Biology*. 201:2465–2479.

Harzsch, S., Benton, J., Dawirs, R.R., and Beltz, B. **1999**. A new look at embryonic development of the visual system in decapod crustaceans: neuropil formation, neurogenesis, and apoptotic cell death. *Journal of Neurobiology*. 39:294.

Harzsch, S., and Hansson, B.S. **2008**. Brain architecture in the terrestrial hermit crab *Coenobita clypeatus*(Anomura, Coenobitidae), a crustacean with a good aerial sense of smell. *BMC Neuroscience*. 9:58.

Harzsch, S., Sandeman, D., and Chaigneau, J. **2012**. Morphology and development of the central nervous system. In: Forest, J., von Vaupel Klein (Eds.), *Treatise on Zoology: Anatomy, Taxonomy, Biology - The Crustacea, vol 3*. Brill, Leiden. pp. 9–236.

Harzsch, S., and Krieger, J. **2018**. Crustacean olfactory systems: A comparative review and a crustacean perspective on olfaction in insects. *Progress in Neurobiology*. 161:23–60.

Hauton, C., Brown, A., Thatje, S., Mestre, N.C., Bebianno, M.J., Martins, I., Bettencourt, R., Canals, M., Sanchez-Vidal, A., and Shillito, B. **2017**. Identifying toxic impacts of metals potentially released during deep-sea mining—A synthesis of the challenges to quantifying risk. *Frontiers in Marine Science*. 4:368.

Hernández-Ávila, I., Cambon-Bonavita, M.-A., and Pradillon, F. **2015**. Morphology of first zoeal stage of four genera of alvinocaridid shrimps from hydrothermal vents and cold seeps: Implications for ecology, larval biology and phylogeny. *PloS One*. 10:e0144657.

Herring, P.J., and Dixon, D.R. **1998**. Extensive deep-sea dispersal of postlarval shrimp from a hydrothermal vent. *Deep Sea Research Part I: Oceanographic Research Papers*. 45:2105–2118.

Hollins, B., Hardin, D., Gimelbrant, A.A., and McClintock, T.S. **2003**. Olfactory-enriched transcripts are cell-specific markers in the lobster olfactory organ. *Journal of Comparative Neurology*. 455:125–138.

Horner, A.J., Weissburg, M.J., and Derby, C.D. **2004**. Dual antennular chemosensory pathways can mediate orientation by Caribbean spiny lobsters in naturalistic flow conditions. *Journal of Experimental Biology*. 207:3785–3796.

Humphris, S.E., Zierenberg, R.A., Mullineaux, L.S., and Thomson, R.E. **1995**. Seafloor hydrothermal systems. *Physical, Chemical, Biological, and Geological Interactions American Geophysical Union*, Washington DC USA.

Husson, B., Sarradin, P.-M., Zeppilli, D., and Sarrazin, J. **2017**. Picturing thermal niches and biomass of hydrothermal vent species. *Deep Sea Research Part II: Topical Studies in Oceanography*. 137:6–25.

J

Jan, C., Petersen, J.M., Werner, J., Teeling, H., Huang, S., Glöckner, F.O., Golyshina, O.V., Dubilier, N., Golyshin, P.N., Jebbar, M., and Cambon-Bonavita, M. **2014**. The gill chamber epibiosis of deep-sea shrimp *Rimicaris exoculata*: an in-depth metagenomic investigation and discovery of Zetaproteobacteria. *Environmental Microbiology*. 16:2723–2738.

Jannasch, H.W., and Mottl, M.J. **1985**. Geomicrobiology of Deep-Sea Hydrothermal Vents. *Science*. 229:717–725.

Jinks, R.N., Battelle, B.-A., Herzog, E.D., Kass, L., Renninger, G.H., and Chamberlain, S.C. **1998**. Sensory adaptations in hydrothermal vent shrimps from the Mid-Atlantic Ridge. *Cahiers de Biologie Marine*. 39:309–312.

Johnson, K.S., Beehler, C.L., Sakamoto-Arnold, C.M., and Childress, J.J. **1986**. *In situ* measurements of chemical distributions in a deep-sea hydrothermal vent field. *Science*. 231:1139–1141.

Johnson, K.S., Childress, J.J., and Beehler, C.L. **1988**. Short-term temperature variability in the Rose Garden hydrothermal vent field: an unstable deep-sea environment. *Deep Sea Research Part A Oceanographic Research Papers*. 35:1711–1721.

K

Kadar, E., and Powell, J.J. **2006**. Post-capture investigations of hydrothermal vent macro-invertebrates to study adaptations to extreme environments. *Reviews in Environmental Science and Biotechnology*. 5:193–201.

Kadar, E., Costa, V., and Segonzac, M. **2007**. Trophic influences of metal accumulation in natural pollution laboratories at deep-sea hydrothermal vents of the Mid-Atlantic Ridge. *Science of the Total Environment*. 373:464–472.

Kamio, M., and Derby, C.D. **2017**. Finding food: how marine invertebrates use chemical cues to track and select food. *Natural Product Reports*. 34:514–528.

Kang, K., Pulver, S.R., Panzano, V.C., Chang, E.C., Griffith, L.C., Theobald, D.L., and Garrity, P.A. **2010**. Analysis of *Drosophila* TRPA1 reveals an ancient origin for human chemical nociception. *Nature*. 464:597–600.

Keller, T.A., Powell, I., and Weissburg, M.J. **2003**. Role of olfactory appendages in chemically mediated orientation of blue crabs. *Marine Ecology Progress Series*. 261:217–231.

Kelley, D.S., Karson, J.A., Früh-Green, G.L., Yoerger, D.R., Shank, T.M., Butterfield, D.A., Hayes, J.M., Schrenk, M.O., Olson, E.J., and Proskurowski, G. **2005**. A serpentinite-hosted ecosystem: the Lost City hydrothermal field. *Science*. 307:1428–1434.

Kenning, M., Müller, C., Wirkner, C.S., and Harzsch, S. **2013**. The Malacostraca (Crustacea) from a neurophylogenetic perspective: New insights from brain architecture in *Nebalia herbstii* Leach,

1814 (Leptostraca, Phyllocarida). *Zoologischer Anzeiger - A Journal of Comparative Zoology*. 252:319–336.

Kenning, M., Lehmann, P., Lindström, M., and Harzsch, S. **2015**. Heading which way? Y-maze chemical assays: not all crustaceans are alike. *Helgoland Marine Research*. 69:305.

Kim, S.L., Mullineaux, L.S., and Helfrich, K.R. **1994**. Larval dispersal via entrainment into hydrothermal vent plumes. *Journal of Geophysical Research: Oceans*. 99:12655–12665.

Klagges, B.R., Heimbeck, G., Godenschwege, T.A., Hofbauer, A., Pflugfelder, G.O., Reifegerste, R., Reisch, D., Schaupp, M., Buchner, S., and Buchner, E. **1996**. Invertebrate synapsins: a single gene codes for several isoforms in Drosophila. *Journal of Neuroscience*. 16:3154–3165.

Klevenz, V., Bach, W., Schmidt, K., Hentscher, M., Koschinsky, A., and Petersen, S. **2011**. Geochemistry of vent fluid particles formed during initial hydrothermal fluid–seawater mixing along the Mid-Atlantic Ridge. *Geochemistry, Geophysics, Geosystems*. 12.

Knecht, Z.A., Silbering, A.F., Ni, L., Klein, M., Budelli, G., Bell, R., Abuin, L., Ferrer, A.J., Samuel, A.D., Benton, R., and Garrity, P.A. **2016**. Distinct combinations of variant ionotropic glutamate receptors mediate thermosensation and hygrosensation in Drosophila. *ELife*. 5.

Koehl, M. **2011**. Hydrodynamics of sniffing by crustaceans. In: Breithaupt, T., Thiel, M. (Eds.), *Chemical Communication in Crustaceans*. Springer, New York. pp. 85–102.

Koh, T.-W., He, Z., Gorur-Shandilya, S., Menuz, K., Larter, N.K., Stewart, S., and Carlson, J.R. **2014**. The Drosophila IR20a clade of ionotropic receptors are candidate taste and pheromone receptors. *Neuron*. 83:850–865.

Komai, T., and Segonzac, M. **2003**. Review of the hydrothermal vent shrimp genus *Mirocaris*, redescription of *M-fortunata* and reassessment of the taxonomic status of the family Alvinocarididae (Crustacea : Decapoda : Caridea). *Cahiers de Biologie Marine*. 44:199–215.

Kreissl, S., Strasser, C., and Galizia, C.G. **2010**. Allatostatin immunoreactivity in the honeybee brain. *Journal of Comparative Neurology*. 518:1391–1417.

Krieger, J., Sombke, A., Seefluth, F., Kenning, M., Hansson, B.S., and Harzsch, S. **2012**. Comparative brain architecture of the European shore crab *Carcinus maenas* (Brachyura) and the common hermit crab *Pagurus bernhardus* (Anomura) with notes on other marine hermit crabs. *Cell and Tissue Research*. 348:47–69.

Krieger, J., Braun, P., Rivera, N.T., Schubart, C.D., Müller, C.H.G., and Harzsch, S. **2015**. Comparative analyses of olfactory systems in terrestrial crabs (Brachyura): evidence for aerial olfaction? *PeerJ*. 3:e1433.

Kwon, J.Y., Dahanukar, A., Weiss, L.A., and Carlson, J.R. **2007**. The molecular basis of CO_2 reception in Drosophila. *Proceedings of the National Academy of Sciences*. 104:3574–3578.

L

Lagerspetz, K.Y., and Vainio, L.A. **2006**. Thermal behaviour of crustaceans. *Biological Reviews*. 81:237–258.

Lakin, R.C., Jinks, R.N., Battelle, B.-A., Herzog, E.D., Kass, L., Renninger, G.H., and Chamberlain, S.C. **1997**. Retinal anatomy of *Chorocaris chacei*, a deep-sea hydrothermal vent shrimp from the mid-Atlantic ridge. *Journal of Comparative Neurology*. 385:503–514.

Lallier, F.H., and Truchot, J.-P. **1997**. Hemocyanin oxygen-binding properties of a deep-sea hydrothermal vent shrimp: Evidence for a novel cofactor. *Journal of Experimental Zoology*. 277:357–364.

Lalou, C., Reyss, J.-L., Brichet, E., Rona, P.A., and Thompson, G. **1995**. Hydrothermal activity on a 105-year scale at a slow-spreading ridge, TAG hydrothermal field, Mid-Atlantic Ridge 26° N. *Journal of Geophysical Research: Solid Earth*. 100:17855–17862.

Laverack, M.S. **1964**. The antennular sense organs of *Panulirus argus*. *Comparative Biochemistry and Physiology*. 13:301–321.

Le Bris, N., Sarradin, P.-M., and Caprais, J.-C. **2003**. Contrasted sulphide chemistries in the environment of 13°N EPR vent fauna. *Deep Sea Research Part I: Oceanographic Research Papers*. 50:737–747.

Le Bris, N., Zbinden, M., and Gaill, F. **2005**. Processes controlling the physico-chemical micro-environments associated with Pompeii worms. *Deep Sea Research Part I: Oceanographic Research Papers*. 52:1071–1083.

Le Bris, N., and Gaill, F. **2007**. How does the annelid *Alvinella pompejana* deal with an extreme hydrothermal environment? *Reviews in Environmental Science and Bio/Technology*. 6:197.

Le Bris, N., and Duperron, S. **2010**. Chemosynthetic communities and biogeochemical energy pathways along the Mid-Atlantic Ridge: The case of *Bathymodiolus Azoricus*. *Diversity of Hydrothermal Systems on Slow Spreading Ocean Ridges*. 409–429.

Lee, R.W. **2003**. Thermal tolerances of deep-sea hydrothermal vent animals from the northeast Pacific. *The Biological Bulletin*. 205:98–101.

Lee, Y., Lee, Y., Lee, J., Bang, S., Hyun, S., Kang, J., Hong, S.-T., Bae, E., Kaang, B.-K., and Kim, J. **2005**. Pyrexia is a new thermal transient receptor potential channel endowing tolerance to high temperatures in *Drosophila melanogaster*. *Nature Genetics*. 37:305–310.

Levin, L.A., and Michener, R.H. **2002**. Isotopic evidence for chemosynthesis-based nutrition of macrobenthos: The lightness of being at Pacific methane seeps. *Limnology and Oceanography*. 47:1336–1345.

Li, C.P., De Grave, S., Chan, T.-Y., Lei, H.C., and Chu, K.H. **2011**. Molecular systematics of caridean shrimps based on five nuclear genes: Implications for superfamily classification. *Zoologischer Anzeiger - A Journal of Comparative Zoology*. 250:270–279.

Limbaugh, C., Pederson, H., and Chace, F.A. **1961**. Shrimps that clean fishes. *Bulletin of Marine Science*. 11:237–257.

Ling, F., Dahanukar, A., Weiss, L.A., Kwon, J.Y., and Carlson, J.R. **2014**. The molecular and cellular basis of taste coding in the legs of Drosophila. *Journal of Neuroscience*. 34:7148–7164.

Little, S.A. **1988**. Fluid Flow and Sound Generation at Hydrothermal Vent Fields. PhD Thesis. Woods Hole Oceanographic Institution, Massachusetts.

Loesel, R., Wolf, H., Kenning, M., Harzsch, S., and Sombke, A. **2013**. Architectural principles and evolution of the Arthropod central nervous system. In: Minelli, A., Boxshall, G., Fusco, G. (Eds.), *Arthropod Biology and Evolution*. Springer, Berlin, Heidelberg. pp. 299–342.

Lonsdale, P. **1977**. Clustering of suspension-feeding macrobenthos near abyssal hydrothermal vents at oceanic spreading centers. *Deep Sea Research*. 24:857–863.

Lovell, J.M., Findlay, M.M., Moate, R.M., and Yan, H.Y. **2005**. The hearing abilities of the prawn *Palaemon serratus*. *Comparative Biochemistry and Physiology Part A: Molecular & Integrative Physiology*. 140:89–100.

M

Machon, J., Ravaux, J., Zbinden, M., and Lucas, P. **2016**. New electroantennography method on a marine shrimp in water. *Journal of Experimental Biology*. 219:3696–3700.

Machon, J., Lucas, P., Ravaux, J., and Zbinden, M. **2018**. Comparison of chemoreceptive abilities of the hydrothermal shrimp *Mirocaris fortunata* and the coastal shrimp *Palaemon elegans*. *Chemical Senses*. bjy041, https://doi.org/10.1093/chemse/bjy041

Martin, J.W., and Christiansen, J.C. **1995**. A new species of the shrimp genus *Chorocaris* Martin & Hessler, 1990 (Crustacea: Decapoda: Bresiliidae) from hydrothermal vent fields along the Mid-Atlantic Ridge. *Proceedings Biological Society of Washington*. 108:220–220.

Martin, J.W., and Hessler, R.R. **1990**. *Chorocaris vandoverae*, a new genus and species of hydrothermal vent shrimp (Crustaceae, Decapoda, Bresiliidae) from the western Pacific. *Contributions in Science, Natural History Museum of Los Angeles County*. 417:1–11.

Martinez, A.-S., Toullec, J.-Y., Shillito, B., Charmantier-Daures, M., and Charmantier, G. **2001**. Hydromineral regulation in the hydrothermal vent crab *Bythograea thermydron*. *The Biological Bulletin*. 201:167–174.

Matabos, M., Cuvelier, D., Brouard, J., Shillito, B., Ravaux, J., Zbinden, M., Barthelemy, D., Sarradin, P.M., and Sarrazin, J. **2015**. Behavioural study of two hydrothermal crustacean decapods: *Mirocaris fortunata* and *Segonzacia mesatlantica*, from the Lucky Strike vent field (Mid-Atlantic Ridge). *Deep Sea Research Part II: Topical Studies in Oceanography*. 121:146–158.

Matsuura, H., Sokabe, T., Kohno, K., Tominaga, M., and Kadowaki, T. **2009**. Evolutionary conservation and changes in insect TRP channels. *BMC Evolutionary Biology*. 9:228.

Maza, F.J., Sztarker, J., Shkedy, A., Peszano, V.N., Locatelli, F.F., and Delorenzi, A. **2016**. Context-dependent memory traces in the crab's mushroom bodies: Functional support for a common origin of high-order memory centers. *Proceedings of the National Academy of Sciences*. 113:E7957–E7965.

Mccall, J.R., and Mead, K.S. **2008**. Structural and functional changes in regenerating antennules in the crayfish *Orconectes sanborni*. *The Biological Bulletin*. 214:99–110.

McClintock, T.S., Ache, B.W., and Derby, C.D. **2006**. Lobster olfactory genomics. *Integrative and Comparative Biology*. 46:940–947.

McGrath, L.L., Vollmer, S.V., Kaluziak, S.T., and Ayers, J. **2016**. De novo transcriptome assembly for the lobster *Homarus americanus* and characterization of differential gene expression across nervous system tissues. *BMC Genomics*. 17:63.

Mead, K.S. **1998**. The biomechanics of odorant access to aesthetascs in the grass shrimp, *Palaemonetes vulgaris*. *The Biological Bulletin*. 195:184–185.

Mead, K.S. **2002**. From odor molecules to plume tracking: An interdisciplinary, multilevel approach to olfaction in stomatopods. *Integrative and Comparative Biology*. 42:258–264.

Mellon, D.F., Alones, V., and Lawrence, M.D. **1992**. Anatomy and fine structure of neurons in the deutocerebral projection pathway of the crayfish olfactory system. *Journal of Comparative Neurology*. 321:93–111.

Mellon, D. **2007**. Combining dissimilar senses: Central processing of hydrodynamic and chemosensory inputs in aquatic crustaceans. *The Biological Bulletin*. 213:1–11.

Mellon, D. **2012**. Smelling, feeling, tasting and touching: behavioral and neural integration of antennular chemosensory and mechanosensory inputs in the crayfish. *Journal of Experimental Biology*. 215:2163–2172.

Mellon, D., and Reidenbach, M.A. **2012**. Fluid mechanical problems in crustacean active chemoreception. In: Barth, F.G., Humphrey, J.A.C., Srinivasan, M.V. (Eds.), *Frontiers in Sensing*. Springer, Vienna. pp. 159–170.

Mellon, D. **2014**. Sensory systems of crustaceans. In: Derby, C., Thiel, M. (Eds.) *Crustacean Nervous System and their Control of Behavior*. Oxford University Press, New York. pp. 49–84.

Mestre, N.C., Thatje, S., and Tyler, P.A. **2009**. The ocean is not deep enough: pressure tolerances during early ontogeny of the blue mussel *Mytilus edulis*. *Proceedings of the Royal Society of London B: Biological Sciences*. 276:717–726.

Meth, R., Wittfoth, C., and Harzsch, S. **2017**. Brain architecture of the Pacific White Shrimp *Penaeus vannamei* Boone, 1931 (Malacostraca, Dendrobranchiata): correspondence of brain structure and sensory input? *Cell and Tissue Research*. 369:255–271.

Mickel, T.J., and Childress, J.J. **1982**. Effects of temperature, pressure, and oxygen concentration on the oxygen consumption rate of the hydrothermal vent crab *Bythograea thermydron* (Brachyura). *Physiological Zoology*. 55:199–207.

Miyake, H., Kitada, M., Tsuchida, S., Okuyama, Y., and Nakamura, K. **2007**. Ecological aspects of hydrothermal vent animals in captivity at atmospheric pressure. *Marine Ecology*. 28:86–92.

Mottl, M.J., and McConachy, T.F. **1990**. Chemical processes in buoyant hydrothermal plumes on the East Pacific Rise near 21°N. *Geochimica y Cosmochimica Acta*. 54:1911–1927.

N

Nagai, T. **1983**. On the relationship between the electroantennogram and simultaneously recorded single sensillum response of the European corn borer, *Ostrinia nubilalis*. *Archives of Insect Biochemistry and Physiology*. 1:85–91.

Nagai, T. **1985**. Summation and gradient characteristics of local electroantennogram response of the European corn borer, *Ostrinia nubilalis*. *Pesticide Biochemistry and Physiology*. 24:32–39.

Neal, K. **2008**. *Palaemon elegans,* a prawn. In: Tyler-Walters, H., Hiscock, K. (Eds.), *Marine Life Information Netword: Biology and Sensitivity Key Information Reviews*. Marine Biological Association of the United Kingdom. Available from: https://www.marlin.ac.uk/species/detail/2035

Neely, G.G., Keene, A.C., Duchek, P., Chang, E.C., Wang, Q.-P., Aksoy, Y.A., Rosenzweig, M., Costigan, M., Woolf, C.J., Garrity, P.A., and Penninger, J.M. **2011**. TrpA1 regulates thermal nociception in Drosophila. *PloS One*. 6:e24343.

Nelson, J.M., Mellon, D., and Reidenbach, M.A. **2013**. Effects of antennule morphology and flicking kinematics on flow and odor sampling by the freshwater crayfish, *Procambarus clarkii*. *Chemical Senses*. 38:729–741.

Ni, L., Bronk, P., Chang, E.C., Lowell, A.M., Flam, J.O., Panzano, V.C., Theobald, D.L., Griffith, L.C., and Garrity, P.A. **2013a**. A gustatory receptor paralogue controls rapid warmth avoidance in *Drosophila*. *Nature*. 500:580–584.

Ni, L., Klein, M., Svec, K.V., Budelli, G., Chang, E.C., Ferrer, A.J., Benton, R., Samuel, A.D., and Garrity, P.A. **2013b**. The ionotropic receptors IR21a and IR25a mediate cool sensing in Drosophila. *ELife*. 5.

Niven, J.E., and Laughlin, S.B. **2008**. Energy limitation as a selective pressure on the evolution of sensory systems. *Journal of Experimental Biology*. 211:1792–1804.

Nuckley, D.J., Jinks, R.N., Battelle, B.A., Herzog, E.D., Kass, L., Renninger, G.H., and Chamberlain, S.C. **1996**. Retinal anatomy of a new species of bresiliid shrimp from a hydrothermal vent field on the Mid-Atlantic Ridge. *The Biological Bulletin*. 190:98–110.

O

Obermeier, M., and Schmitz, B. **2004**. The modality of the dominance signal in snapping shrimp (*Alpheus heterochaelis*) and the corresponding setal types on the antennules. *Marine and Freshwater Behaviour and Physiology*. 37:109–126.

Oliphant, A., Thatje, S., Brown, A., Morini, M., Ravaux, J., and Shillito, B. **2011**. Pressure tolerance of the shallow-water caridean shrimp *Palaemonetes varians* across its thermal tolerance window. *Journal of Experimental Biology*. 214:1109–1117.

O'Neill, P.J., Jinks, R.N., Herzog, E.D., Battelle, B.-A., Kass, L., Renninger, G.H., and Chamberlain, S.C. **1995**. The morphology of the dorsal eye of the hydrothermal vent shrimp, *Rimicaris exoculata*. *Visual Neuroscience*. 12:861–875.

P

Pelli, D.G., and Chamberlain, S.C. **1989**. The visibility of 350 °C black-body radiation by the shrimp *Rimicaris exoculata* and man. *Nature*. 337:460–461.

Pelosi, P., Iovinella, I., Felicioli, A., and Dani, F.R. **2014**. Soluble proteins of chemical communication: an overview across arthropods. *Frontiers in Physiology*. 5.

Peñalva-Arana, D.C., Lynch, M., and Robertson, H.M. **2009**. The chemoreceptor genes of the waterflea *Daphnia pulex*: many Grs but no Ors. *BMC Evolutionary Biology*. 9:79.

Petersen, J.M., Ramette, A., Lott, C., Cambon-Bonavita, M.-A., Zbinden, M., and Dubilier, N. **2010**. Dual symbiosis of the vent shrimp *Rimicaris exoculata* with filamentous gamma- and epsilonproteobacteria at four Mid-Atlantic Ridge hydrothermal vent fields. *Environmental Microbiology*. 12:2204–2218.

Phillips, B.T., Gruber, D.F., Vasan, G., Pieribone, V.A., Sparks, J.S., and Roman, C.N. **2016**. First evidence of bioluminescenceon "black smoker" hydrothermal chimney. *Oceanography*. 29:10.

Polanska, M.A., Tuchina, O., Agricola, H., Hansson, B.S., and Harzsch, S. **2012**. Neuropeptide complexity in the crustacean central olfactory pathway: immunolocalization of A-type allatostatins and RFamide-like peptides in the brain of a terrestrial hermit crab. *Molecular Brain*. 5:29.

Polz, M.F., Robinson, J.J., Cavanaugh, C.M., and Dover, C.L.V. **1998**. Trophic ecology of massive shrimp aggregations at a Mid-Atlantic Ridge hydrothermal vent site. *Limnology and Oceanography*. 43:1631–1638.

Pomerol, C., Renard, M., and Lagabrielle, Y. **2005**. Eléments de géologie. Paris.

Pond, D.W., Segonzac, M., Bell, M.V., Dixon, D.R., Fallick, A.E., and Sargent, J.R. **1997**. Lipid and lipid carbon stable isotope composition of the hydrothermal vent shrimp *Mirocaris fortunata*: evidence for nutritional dependence on photosynthetically fixed carbon. *Marine Ecology Progress Series*. 157:221–231.

Pond, D.W., Gebruk, A., Southward, E.C., Southward, A.J., Fallick, A.E., Bell, M.V., and Sargent, J.R. **2000**. Unusual fatty acid composition of storage lipids in the bresilioid shrimp *Rimicaris exoculata* couples the photic zone with MAR hydrothermal vent sites. *Marine Ecology Progress Series*. 198:171–179.

Portail, M., Brandily, C., Cathalot, C., Colaço, A., Gélinas, Y., Husson, B., Sarradin, P.-M., and Sarrazin, J. **2018**. Food-web complexity across hydrothermal vents on the Azores triple junction. *Deep Sea Research Part I: Oceanographic Research Papers*. 131:101–120.

Powell, M.A., and Somero, G.N. **1986**. Adaptations to sulfide by hydrothermal vent animals: sites and mechanisms of detoxification and metabolism. *The Biological Bulletin*. 171:274–290.

Pradillon, F. **2012**. High hydrostatic pressure environments. In: Bell, E.M. (Ed.), *Life at Extremes: Environments, Organisms and Strategies for Survival*. CABI, Wallingford. pp. 271–295.

Pradillon, F., Shillito, B., Young, C.M., and Gaill, F. **2001**. Deep-sea ecology: Developmental arrest in vent worm embryos. *Nature*. 413:698–699.

Pradillon, F., Shillito, B., Chervin, J.-C., Hamel, G., and Gaill, F. **2004**. Pressure vessels for in vivo studies of deep-sea fauna. *High Pressure Research*. 24:237–246.

Pradillon, F., Bris, N.L., Shillito, B., Young, C.M., and Gaill, F. **2005**. Influence of environmental conditions on early development of the hydrothermal vent polychaete *Alvinella pompejana*. *Journal of Experimental Biology*. 208:1551–1561.

Pradillon, F., and Gaill, F. **2007**. Pressure and life: Some biological strategies. *Reviews in Environmental Science and Bio/Technology*. 6:181–195.

Puri, S., and Faulkes, Z. **2010**. Do decapod crustaceans have nociceptors for extreme pH? *PLoS One*. 5:e10244.

Puri, S., and Faulkes, Z. **2015**. Can crayfish take the heat? Procambarus clarkii show nociceptive behaviour to high temperature stimuli, but not low temperature or chemical stimuli. *Biology Open*. 4:441–448.

R

Ramirez-Llodra, E., Shank, T.M., and German, C.R. **2007**. Biodiversity and biogeography of hydrothermal vent species: thirty years of discovery and investigations. *Oceanography*. 20:30–41.

Ramm, T., and Scholtz, G. **2017**. No sight, no smell? – Brain anatomy of two amphipod crustaceans with different lifestyles. *Arthropod Structure & Development*. 46:537–551.

Rathke, M.H. **1837**. Bertrag zur fauna der krym. *Mémoires de l'Académie Impériale Des Sciences de St Petersbourg*. 3:371–380.

Ravaux, J., Gaill, F., Bris, N.L., Sarradin, P.-M., Jollivet, D., and Shillito, B. **2003**. Heat-shock response and temperature resistance in the deep-sea vent shrimp *Rimicaris exoculata*. *Journal of Experimental Biology*. 206:2345–2354.

Ravaux, J., Cottin, D., Chertemps, T., Hamel, G., and Shillito, B. **2009**. Hydrothermal vent shrimps display low expression of the heat-inducible hsp70 gene in nature. *Marine Ecology Progress Series*. 396:153–156.

Ravaux, J., Léger, N., Rabet, N., Morini, M., Zbinden, M., Thatje, S., and Shillito, B. **2012**. Adaptation to thermally variable environments: capacity for acclimation of thermal limit and heat shock response in the shrimp *Palaemonetes varians*. *Journal of Comparative Physiology B*. 182:899–907.

Ravaux, J., Léger, N., Rabet, N., Fourgous, C., Voland, G., Zbinden, M., and Shillito, B. **2016**. Plasticity and acquisition of the thermal tolerance (upper thermal limit and heat shock response) in the intertidal species *Palaemon elegans*. *Journal of Experimental Marine Biology and Ecology*. 484:39–45.

Regier, J.C., Shultz, J.W., Zwick, A., Hussey, A., Ball, B., Wetzer, R., Martin, J.W., and Cunningham, C.W. **2010**. Arthropod relationships revealed by phylogenomic analysis of nuclear protein-coding sequences. *Nature*. 463:1079–1083.

Renninger, G.H., Kass, L., Gleeson, R.A., Van Dover, C.L., Battelle, B.-A., Jinks, R.N., Herzog, E.D., and Chamberlain, S.C. **1995**. Sulfide as a chemical stimulus for deep-sea hydrothermal vent shrimp. *The Biological Bulletin*. 189:69–76.

Rittschof, D., Jr, R.B.F., Cannon, G., Welch, J.M., Jr, M.M., Holm, E.R., Clare, A.S., Conova, S., McKelvey, L.M., Bryan, P., and Van Dover, C.L. **1998**. Cues and context: Larval responses to physical and chemical cues. *Biofouling*. 12:31–44.

Robertson, H.M. **2015**. The insect chemoreceptor superfamily is ancient in animals. *Chemical Senses*. 40:609–614.

Rona, P.A., Hannington, M.D., Raman, C.V., Thompson, G., Tivey, M.K., Humphris, S.E., Lalou, C., and Petersen, S. **1993**. Active and relict sea-floor hydrothermal mineralization at the TAG hydrothermal field, Mid-Atlantic Ridge. *Economic Geology*. 88:8.

Rotjan, R.D., Chabot, J.R., and Lewis, S.M. **2010**. Social context of shell acquisition in *Coenobita clypeatus* hermit crabs. *Behavioral Ecology*. 21:639–646.

Rytz, R., Croset, V., and Benton, R. **2013**. Ionotropic Receptors (IRs): Chemosensory ionotropic glutamate receptors in Drosophila and beyond. *Insect Biochemistry and Molecular Biology*. 43:888–897.

S

Sandeman, D.C., and Luff, S.E. **1973**. The structural organization of glomerular neuropil in the olfactory and accessory lobes of an Australian freshwater crayfish, *Cherax destructor*. *Zitschrift für Zellforschung und Mikroskopische Anatomie*. 142:37–61.

Sandeman, D.C., and Denburg, J.L. **1976**. The central projections of chemoreceptor axons in the crayfish revealed by axoplasmic transport. *Brain Research*. 115:492–496.

Sandeman, D., Sandeman, R., Derby, C., and Schmidt, M. **1992**. Morphology of the brain of crayfish, crabs, and spiny lobsters: A common nomenclature for homologous structures. *The Biological Bulletin*. 183:304–326.

Sandeman, D.C., Scholtz, G., and Sandeman, R.E. **1993**. Brain evolution in decapod crustacea. *Journal of Experimental Zoology*. 265:112–133.

Sandeman, D., Kenning, M., and Harzsch, S. **2014**. Adaptive trends in malacostracan brain form and function related to behavior. In: Derby, C., Thiel, M. (Eds.), *Crustacean Nervous System and their Control of Behavior*. Oxford University Press, New York. pp. 11-48.

Sanders, N.K., Arp, A.J., and Childress, J.J. **1988**. Oxygen binding characteristics of the hemocyanins of two deep-sea hydrothermal vent crustaceans. *Respiration Physiology*. 71:57–67.

Sarradin, P.-M., Caprais, J.-C., Briand, P., Gaill, F., Shillito, B., and Desbruyères, D. **1998**. Chemical and thermal description of the environment of the Genesis hydrothermal vent community (13 degree N, EPR). *Cahiers de Biologie Marine*. 39:159-167.

Sarrazin, J., Robigou, V., Juniper, S.K., and Delaney, J.R. **1997**. Biological and geological dynamics over four years on a high-temperature sulfide structure at the Juan de Fuca Ridge hydrothermal observatory. *Marine Ecology Progress Series*. 153:5–24.

Sarrazin, J., and Juniper, S.K. **1999**. Biological characteristics of a hydrothermal edifice mosaic community. *Marine Ecology Progress Series*. 185:1–19.

Sarrazin, J., Juniper, S.K., Massoth, G., and Legendre, P. **1999**. Physical and chemical factors influencing species distributions on hydrothermal sulfide edifices of the Juan de Fuca Ridge, northeast Pacific. *Marine Ecology Progress Series*. 190:89–112.

Sarrazin, J., Levesque, C., Juniper, S., and Tivey, M. **2002**. Mosaic community dynamics on Juan de Fuca Ridge sulphide edifices: substratum, temperature and implications for trophic structure. *Cahiers de Biologie Marine*. 43:275–279.

Sarrazin, J., Blandin, J., Delauney, L., Dentrecolas, S., Dorval, P., Dupont, J., Legrand, J., Leroux, D., Leon, P., and Lévèque, J.P. **2007**. TEMPO: a new ecological module for studying deep-sea community dynamics at hydrothermal vents. In: *Oceans 2007-Europe*. pp. 1–4.

Sarrazin, J., Legendre, P., Busserolles, F. de, Fabri, M.-C., Guilini, K., Ivanenko, V.N., Morineaux, M., Vanreusel, A., and Sarradin, P.-M. **2015**. Biodiversity patterns, environmental drivers and indicator species on a high-temperature hydrothermal edifice, Mid-Atlantic Ridge. *Deep Sea Research Part II: Topical Studies in Oceanography*. 121:177–192.

Sato, K., Tanaka, K., and Touhara, K. **2011**. Sugar-regulated cation channel formed by an insect gustatory receptor. *Proceedings of the National Academy of Sciences*. 108:11680–11685.

Santonja, M., Greff, S., Le Croller, M., Thomas, O., and Perez, T. **2018**. Distance interaction between marine cave-dwelling sponges and crustaceans. *Marine Biology*. 165:121.

Schachtner, J., Schmidt, M., and Homberg, U. **2005**. Organization and evolutionary trends of primary olfactory brain centers in Tetraconata (Crustacea+Hexapoda). *Arthropod Structure & Development.* 34:257–299.

Schmidt, M., and Gnatzy, W. **1984**. Are the funnel-canal organs the 'campaniform sensilla' of the shore crab, *Carcinus maenas* (Decapoda, Crustacea)? *Cell and Tissue Research*. 237:81–93.

Schmidt, M., and Ache, B.W. **1996**. Processing of antennular input in the brain of the spiny lobster, *Panulirus argus*. *Journal of Comparative Physiology A*. 178:605–628.

Schmidt, M., and Ache, B.W. **1997**. Immunocytochemical analysis of glomerular regionalization and neuronal diversity in the olfactory deutocerebrum of the spiny lobster. *Cell and Tissue Research*. 287:541–563.

Schmidt, M., and Derby, C.D. **2005**. Non-olfactory chemoreceptors in asymmetric setae activate antennular grooming behavior in the Caribbean spiny lobster *Panulirus argus*. *Journal of Experimental Biology*. 208:233–248.

Schmidt, K., Koschinsky, A., Garbe-Schönberg, D., Carvalho, L.M. de, and Seifert, R. **2007**. Geochemistry of hydrothermal fluids from the ultramafic-hosted Logatchev hydrothermal field, 15°N on the Mid-Atlantic Ridge: Temporal and spatial investigation. *Chemical Geology*. 242:1–21.

Schmidt, C., Vuillemin, R., Le Gall, C., Gaill, F., and Le Bris, N. **2008**. Geochemical energy sources for microbial primary production in the environment of hydrothermal vent shrimps. *Marine Chemistry*. 108:18–31.

Schmidt, M., and Mellon, D. **2010**. Neuronal processing of chemical information in crustaceans. In: Breithaupt, T., Thiel, M. (Eds.), *Chemical Communication in Crustaceans*. Springer, New York. pp. 123–147.

Scott, K., Brady, R., Cravchik, A., Morozov, P., Rzhetsky, A., Zuker, C., and Axel, R. **2001**. A chemosensory gene family encoding candidate gustatory and olfactory receptors in Drosophila. *Cell*. 104:661–673.

Semm, P., and Beason, R.C. **1990**. Responses to small magnetic variations by the trigeminal system of the bobolink. *Brain Research Bulletin*. 25:735–740.

Shillito, B., Bris, N.L., Gaill, F., Rees, J.-F., and Zal, F. **2004**. First access to live alvinellas. *High Pressure Research*. 24:169–172.

Shillito, B., Le Bris, N., Hourdez, S., Ravaux, J., Cottin, D., Caprais, J.-C., Jollivet, D., and Gaill, F. **2006**. Temperature resistance studies on the deep-sea vent shrimp *Mirocaris fortunata*. *Journal of Experimental Biology*. 209:945–955.

Shillito, B., Hamel, G., Duchi, C., Cottin, D., Sarrazin, J., Sarradin, P.-M., Ravaux, J., and Gaill, F. **2008**. Live capture of megafauna from 2300m depth, using a newly designed Pressurized Recovery Device. *Deep Sea Research Part I: Oceanographic Research Papers*. 55:881–889.

Shillito, B., Ravaux, J., Sarrazin, J., Zbinden, M., Sarradin, P.-M., and Barthelemy, D. **2015**. Long-term maintenance and public exhibition of deep-sea hydrothermal fauna: The AbyssBox project. *Deep Sea Research Part II: Topical Studies in Oceanography*. 121:137–145.

Smith, R.P., and Gosselin, R.E. **1979**. Hydrogen sulfide poisoning. *Journal of Occupational Medicine: Official Publication of the Industrial Medical Association*. 21:93–97.

Smith, F., Brown, A., Mestre, N.C., Reed, A.J., and Thatje, S. **2013**. Thermal adaptations in deep-sea hydrothermal vent and shallow-water shrimp. *Deep Sea Research Part II: Topical Studies in Oceanography*. 92:234–239.

Sokabe, T., and Tominaga, M. **2009**. A temperature-sensitive TRP ion channel, Painless, functions as a noxious heat sensor in fruit flies. *Communicative & Integrative Biology*. 2:170–173.

Solari, P., Sollai, G., Masala, C., Loy, F., Palmas, F., Sabatini, A., and Crnjar, R. **2017**. Antennular morphology and contribution of aesthetascs in the detection of food-related compounds in the shrimp *Palaemon adspersus* Rathke, 1837 (Decapoda: Palaemonidae). *The Biological Bulletin*. 232:110–122.

Somero, G.N. **1992**. Adaptations to high hydrostatic pressure. *Annual Review of Physiology*. 54:557–577.

Stegner, M.E., Stemme, T., Iliffe, T.M., Richter, S., and Wirkner, C.S. **2015**. The brain in three crustaceans from cavernous darkness. *BMC Neuroscience*. 16:19.

Stemme, T., and Harzsch, S. **2016**. Remipedia. *Structure and Evolution of Invertebrate Nervous Systems*. 522–528.

Stensmyr, M.C., Erland, S., Hallberg, E., Wallén, R., Greenaway, P., and Hansson, B.S. **2005**. Insect-like olfactory adaptations in the terrestrial giant robber crab. *Current Biology*. 15:116–121.

Stepanyan, R., Hollins, B., Brock, S.E., and McClintock, T.S. **2004**. Primary culture of lobster (*Homarus americanus*) olfactory sensory neurons. *Chemical Senses*. 29:179–187.

Steullet, P., Cate, H.S., Michel, W.C., and Derby, C.D. **2000**. Functional units of a compound nose: Aesthetasc sensilla house similar populations of olfactory receptor neurons on the crustacean antennule. *Journal of Comparative Neurology*. 418:270–280.

Steullet, P., Dudar, O., Flavus, T., Zhou, M., and Derby, C.D. **2001**. Selective ablation of antennular sensilla on the Caribbean spiny lobster *Panulirus argus* suggests that dual antennular chemosensory pathways mediate odorant activation of searching and localization of food. *Journal of Experimental Biology*. 204:4259–4269.

Steullet, P., Krützfeldt, D.R., Hamidani, G., Flavus, T., Ngo, V., and Derby, C.D. **2002**. Dual antennular chemosensory pathways mediate odor-associative learning and odor discrimination in the Caribbean spiny lobster *Panulirus argus*. *Journal of Experimental Biology*. 205:851–867.

Strausfeld, N.J. **1998**. Crustacean – Insect relationships: The use of brain characters to derive phylogeny amongst segmented invertebrates. *Brain, Behavior and Evolution*. 52:186–206.

Strausfeld, N.J., and Andrew, D.R. **2011**. A new view of insect–crustacean relationships I. Inferences from neural cladistics and comparative neuroanatomy. *Arthropod Structure & Development*. 40:276–288.

Sullivan, J.M., and Beltz, B.S. **2001**. Neural pathways connecting the deutocerebrum and lateral protocerebrum in the brains of decapod crustaceans. *Journal of Comparative Neurology*. 441:9–22.

Sullivan, J.M., and Beltz, B.S. **2005**. Integration and segregation of inputs to higher-order neuropils of the crayfish brain. *Journal of Comparative Neurology*. 481:118–126.

Sun, S., Hui, M., Wang, M., and Sha, Z. **2018**. The complete mitochondrial genome of the alvinocaridid shrimp *Shinkaicaris leurokolos* (Decapoda, Caridea): Insight into the mitochondrial genetic basis of deep-sea hydrothermal vent adaptation in the shrimp. *Comparative Biochemistry and Physiology Part D: Genomics and Proteomics*. 25:42–52.

T

Tao, C., Chen, S., Baker, E.T., Li, H., Liang, J., Liao, S., Chen, Y.J., Deng, X., Zhang, G., Gu, C., and Wu, J. **2017**. Hydrothermal plume mapping as a prospecting tool for seafloor sulfide deposits: a case study at the Zouyu-1 and Zouyu-2 hydrothermal fields in the southern Mid-Atlantic Ridge. *Marine Geophysical Research*. 38:3–16.

Teague, J., Allen, M.J., and Scott, T.B. **2018**. The potential of low-cost ROV for use in deep-sea mineral, ore prospecting and monitoring. *Ocean Engineering*. 147:333–339.

Teixeira, S., Serrão, E.A., and Arnaud-Haond, S. **2012**. Panmixia in a fragmented and unstable environment: The hydrothermal shrimp *Rimicaris exoculata* disperses extensively along the Mid-Atlantic Ridge. *PloS One*. 7:e38521.

Teixeira, S., Olu, K., Decker, C., Cunha, R.L., Fuchs, S., Hourdez, S., Serrão, E.A., and Arnaud-Haond, S. **2013**. High connectivity across the fragmented chemosynthetic ecosystems of the deep Atlantic Equatorial Belt: efficient dispersal mechanisms or questionable endemism? *Molecular Ecology*. 22:4663–4680.

Thatje, S., Casburn, L., and Calcagno, J.A. **2010**. Behavioural and respiratory response of the shallow-water hermit crab *Pagurus cuanensis* to hydrostatic pressure and temperature. *Journal of Experimental Marine Biology and Ecology*. 390:22–30.

Tidau, S., and Briffa, M. **2016**. Review on behavioral impacts of aquatic noise on crustaceans. *Proceedings of Meetings on Acoustics*. 27:010028.

Tierney, A.J., Thompson, C.S., and Dunham, D.W. **1986**. Fine structure of aesthetasc chemoreceptors in the crayfish *Orconectes propinquus*. *Canadian Journal of Zoology*. 64:392–399.

Tokuda, G., Yamada, A., Nakano, K., Arita, N., and Yamasaki, H. **2006**. Occurrence and recent long-distance dispersal of deep-sea hydrothermal vent shrimps. *Biology Letters*. 2:257–260.

Tuchina, O., Koczan, S., Harzsch, S., Rybak, J., Wolff, G., Strausfeld, N.J., and Hansson, B.S. **2015**. Central projections of antennular chemosensory and mechanosensory afferents in the brain of the terrestrial hermit crab (*Coenobita clypeatus*; Coenobitidae, Anomura). *Frontiers in Neuroanatomy*. 9:94.

Tunnicliffe, V. **1991**. The biology of hydrothermal vents: Ecology and evolution. *Oceanographic Marine Biology Annual Reunions*. 29:319–407.

Tunnicliffe, V., McArthur, A.G., and McHugh, D. **1998**. A biogeographical perspective of the deep-sea hydrothermal vent fauna. In: Blaxter, J.H.S., Southward, A.J., Tyler, P.A. (Eds.), *Advances in Marine Biology*. Academic Press. pp. 353–442.

Tyler, P.A., and Young, C.M. **1999**. Reproduction and dispersal at vents and cold seeps. *Journal of the Marine Biological Association of the United Kingdom*. 79:193–208.

Tyler, P.A., and Young, C.M. **2003**. Dispersal at hydrothermal vents: a summary of recent progress. *Hydrobiologia*. 503:9–19.

U

Ukhanov, K., Bobkov, Y., and Ache, B.W. **2011**. Imaging ensemble activity in arthropod olfactory receptor neurons *in situ*. *Cell Calcium*. 49:100–107.

V

Van Dover, C.L., Fry, B., Grassle, J.F., Humphris, S., and Rona, P.A. **1988**. Feeding biology of the shrimp *Rimicaris exoculata* at hydrothermal vents on the Mid-Atlantic Ridge. *Marine Biology*. 98:209–216.

Van Dover, C.L. **2000**. The ecology of deep-sea hydrothermal vents. Princeton University Press.

Van Dover, C.L. **2011**. Tighten regulations on deep-sea mining. *Nature*. 470:31.

Van Dover, C.L., Arnaud-Haond, S., Gianni, M., Helmreich, S., Huber, J.A., Jaeckel, A.L., Metaxas, A., Pendleton, L.H., Petersen, S., Ramirez-Llodra, E., Steinberg, P.E., Tunnicliffe, V., and Yamamoto, H. **2018**. Scientific rationale and international obligations for protection of active hydrothermal vent ecosystems from deep-sea mining. *Marine Policy*. 90:20–28.

Van Dover, C.L., Szuts, E.Z., Chamberlain, S.C., and Cann, J.R. **1989**. A novel eye in "eyeless" shrimp from hydrothermal vents of the Mid-Atlantic Ridge. *Nature*. 337:458–460.

Van Drongelen, W., Holley, A., and Døving, K.B. **1978**. Convergence in the olfactory system: quantitative aspects of odour sensitivity. *Journal of Theoretical Biology*. 71:39–48.

Vereshchaka, A.L. **1996**. Comparative analysis of taxonomic composition of shrimps as edificators of hydrothermal communities in the Mid-Atlantic Ridge. *Biological Sciences*. 35:576-578.

Vereshchaka, A.L. **1997**. Comparative morphological studies on four populations of the shrimp *Rimicaris exoculata* from the Mid-Atlantic Ridge. *Deep Sea Research Part I: Oceanographic Research Papers*. 44:1905–1921.

Vereshchaka, A.L., Kulagin, D.N., and Lunina, A.A. **2015.** Phylogeny and new classification of hydrothermal vent and seep shrimps of the family Alvinocarididae (Decapoda). *PloS One*. 10:e0129975.

Vinogradov, M.E., and Vereshchaka, A.L. **1995**. The micro-scale distribution of the hydrothermal near-bottom shrimp fauna. *Deep-Sea Newsletter*. 23:18–21.

Vismann, B. **1996**. Sulfide species and total sulfide toxicity in the shrimp *Crangon crangon*. *Journal of Experimental Marine Biology and Ecology*. 204:141–154.

Vitzthum, H., Homberg, U., and Agricola, H. **1996**. Distribution of Dip-allatostatin I-like immunoreactivity in the brain of the locust *Schistocerca gregaria* with detailed analysis of immunostaining in the central complex. *Journal of Comparative Neurology*. 369:419–437.

Voigt, R., and Atema, J. **1992**. Tuning of chemoreceptor cells of the second antenna of the American lobster (*Homarus americanus*) with a comparison of four of its other chemoreceptor organs. *Journal of Comparative Physiology A*. 171:673–683.

W

Wachowiak, M., Diebel, C., and Ache, B. **1997**. Local interneurons define functionally distinct regions within lobster olfactory glomeruli. *Journal of Experimental Biology*. 200:989–1001.

Waeles, M., Cotte, L., Pernet-Coudrier, B., Chavagnac, V., Cathalot, C., Leleu, T., Laës-Huon, A., Perhirin, A., Riso, R.D., and Sarradin, P.-M. **2017**. On the early fate of hydrothermal iron at deep-sea vents: A reassessment after in situ filtration. *Geophysical Research Letters*. 44:4233–4240.

Williams, A.B., and Rona, P.A. **1986**. Two new caridean shrimps (Bresiliidae) from a hydrothermal field on the Mid-Atlantic Ridge. *Journal of Crustacean Biology*. 6:446–462.

Williams, A.B. **1988**. New marine decapod crustaceans from waters influenced by hydrothermal discharge, brine and hydrocarbon seepage. *Fishery Bulletin*. 86.

Wolff, T. **2005**. Composition and endemism of the deep-sea hydrothermal vent fauna. *Cahiers de Biologie Marine*. 46:97–104.

Wolff, G., Harzsch, S., Hansson, B.S., Brown, S., and Strausfeld, N. **2012**. Neuronal organization of the hemiellipsoid body of the land hermit crab, *Coenobita clypeatus*: Correspondence with the mushroom body ground pattern. *Journal of Comparative Neurology*. 520:2824–2846.

Wolff, G.H., and Strausfeld, N.J. **2015**. Genealogical correspondence of mushroom bodies across invertebrate phyla. *Current Biology*. 25:38–44.

Wolff, G.H., Thoen, H.H., Marshall, J., Sayre, M.E., and Strausfeld, N.J. **2017**. An insect-like mushroom body in a crustacean brain. *ELife*. 6.

Wyatt, T.D. **2014**. Pheromones and animal behavior: chemical signals and signatures. *Cambridge University Press*.

Y

Yoshino, M., Kondoh, Y., and Hisada, M. **1983**. Projection of statocyst sensory neurons associated with crescent hairs in the crayfish *Procambarus clarkii*. *Cell and Tissue Research*. 230:37–48.

Z

Zbinden, M., Le Bris, N., Gaill, F., and Compère, P. **2004**. Distribution of bacteria and associated minerals in the gill chamber of the vent shrimp *Rimicaris exoculata* and related biogeochemical processes. *Marine Ecology Progress Series*. 284:237–251.

Zbinden, M., Shillito, B., Le Bris, N., Villardi de Montlaur, C. de, Roussel, E., Guyot, F., Gaill, F., and Cambon-Bonavita, M.-A. **2008**. New insigths on the metabolic diversity among the epibiotic microbial communitiy of the hydrothermal shrimp *Rimicaris exoculata*. *Journal of Experimental Marine Biology and Ecology*. 359:131–140.

Zbinden, M., Berthod, C., Montagné, N., Machon, J., Léger, N., Chertemps, T., Rabet, N., Shillito, B., and Ravaux, J. **2017**. Comparative study of chemosensory organs of shrimp from hydrothermal vent and coastal environments. *Chemical Senses*. 42:319–331.

Zhang, J.-Z., and Millero, F.J. **1993**. The products from the oxidation of H_2S in seawater. *Geochimica y Cosmochimica Acta*. 57:1705–1718.

Zhang, D., Cai, S., Liu, H., and Lin, J. **2008**. Antennal sensilla in the genus *Lysmata* (Caridea). *Journal of Crustacean Biology*. 28:433–438.

Zhang, Y.-N., Jin, J.-Y., Jin, R., Xia, Y.-H., Zhou, J.-J., Deng, J.-Y., and Dong, S.-L. **2013.** Differential expression patterns in chemosensory and non-chemosensory tissues of putative chemosensory genes identified by transcriptome analysis of insect pest the purple stem borer *Sesamia inferens* (Walker). *PloS One*. 8:e69715.

Zhong, L., Bellemer, A., Yan, H., Honjo, K., Robertson, J., Hwang, R.Y., Pitt, G.S., and Tracey, W.D. **2012**. Thermosensory and nonthermosensory isoforms of *Drosophila melanogaster* TRPA1 reveal heat-sensor domains of a thermoTRP channel. *Cell Reports*. 1:43–55.

Zhu, J., Zhang, D., and Lin, J. **2011**. Morphology and distribution of antennal and antennular setae in *Lysmata* shrimp. *Journal of Shellfish Research*. 30:381–388.

Thesis publications

Machon Julia, Ravaux Juliette, Zbinden Magali, Lucas Philippe (2016). New electroantennography method on a marine shrimp in water. *Journal of Experimental Biology*, 219(23), 3696-3700.

Pages 186-190

Zbinden Magali, Berthod Camille, Montagné Nicolas, **Machon Julia**, Léger Nelly, Chertemps Thomas, Rabet Nicolas, Shillito Bruce, Ravaux Juliette (2017). Comparative study of chemosensory organs of shrimp from hydrothermal vent and coastal environments. *Chemical Senses*, 42(4), 319-331.

Pages 191-203

Machon Julia, Lucas Philippe, Ravaux Juliette, Zbinden Magali (2018). Comparison of chemoreceptive abilities of the hydrothermal shrimp *Mirocaris fortunata* and the coastal shrimp *Palaemon elegans*. *Chemical Senses*, bjy041, https://doi.org/10.1093/chemse/bjy041.

Pages 204-215

Submitted:

Zbinden Magali, Gallet Alison, Szafranski Kamil, **Machon Julia**, Ravaux Juliette, Léger Nelly, Duperron Sebastien. Blow your nose, shrimp! Unexpectedly dense bacterial communities occur on the antennae of hydrothermal vent shrimp. *Frontiers in Microbiology*.

In preparation:

Machon Julia, Krieger Jakob, Zbinden Magali, Ravaux Juliette, Chertemps Thomas, Montagné Nicolas, Meth Rebecca, Harzsch Steffen. Brain architecture of the deep-hydrothermal vent shrimp *Rimicaris exoculata* (Decapoda, Caridea, Alvinocarididae). *Proceedings of the Royal Society B*.

© 2016. Published by The Company of Biologists Ltd | Journal of Experimental Biology (2016) 219, 3696-3700 doi:10.1242/jeb.140947

New electroantennography method on a marine shrimp in water

Julia Machon[1,2], Juliette Ravaux[1], Magali Zbinden[1] and Philippe Lucas[2,*]

ABSTRACT

Antennular chemoreception in aquatic decapods is well studied via the recording of single chemoreceptor neuron activity in the antennule, but global responses of the antennule (or antennae in insects) by electroantennography (EAG) has so far been mainly restricted to aerial conditions. We present here a well-established underwater EAG method to record the global antennule activity in the marine shrimp *Palaemon elegans* in natural (aqueous) conditions. EAG responses to food extracts, recorded as net positive deviations of the baseline, are reproducible, dose-dependent and exhibit sensory adaptation. This new EAG method opens a large field of possibilities for studying *in vivo* antennular chemoreception in aquatic decapods, in a global approach to supplement current, more specific techniques.

KEY WORDS: Electroantennography, Shrimp, Olfaction, Antennule

INTRODUCTION

Crustaceans, in particular lobsters and crayfishes, have emerged as excellent models for research in chemoreception (Ache, 2002). They rely on antennular chemoreception for diverse behaviors such as food detection and social interactions (Derby and Sorensen, 2008). Their main olfactory organ is the antennule (Derby and Weissburg, 2014), the lateral flagellum of which bears presumably unimodal sensilla specialized in olfaction, the aesthetascs, innervated only by olfactory receptor neurons (ORNs) (Ghiradella et al., 1968). Antennular flagella also bear bimodal sensilla, innervated by mechanoreceptor and chemoreceptor neurons (Schmidt and Derby, 2005). Responses of crustacean chemoreceptor neurons to odor stimuli were classically recorded either extracellularly from their axons (Derby, 1989; Kamio et al., 2005) or intracellularly after the introduction of the patch-clamp method (Ache, 2002; Anderson and Ache, 1985; Bobkov et al., 2012).

Study of antennular chemoreception is essential for understanding the biology of our model species, the blind Alvinocarididae deep-sea hydrothermal shrimp. Despite the fact that the antennal appendages may play a major role in the detection of their environment (Chamberlain, 2000; Jinks et al., 1998; Renninger et al., 1995), there is still little information about their chemosensory sensitivity. Specimens of these species are extremely difficult to collect and maintain alive, and therefore are available in low numbers for experiments. The objective of this work was to develop a method with a high rate of success, allowing the recording of global responses of the antennule, in marine decapods. In insects, such a technique called electroantennography (EAG) (Schneider, 1957) is commonly used to measure the global response profile of antennal ORNs to odor stimuli. This technique is widely used in screening moth pheromones (Roelofs, 1984). In crustaceans, EAG measurements were performed in aerial conditions on two terrestrial crabs, the giant robber crab *Birgus latro* (Stensmyr et al., 2005) and the hermit crab *Coenobita clypeatus* (Krång et al., 2012), and in the marine hermit crab *Pagurus berhnardus* (Stensmyr et al., 2005). Two papers reported very briefly EAG recordings, with no technical demonstration, from freshwater crustaceans: the branchiopoda *Daphnia* spp. (Simbeya et al., 2012) and the crayfish *Procambarus clarkii* (Ameyaw-Akumfi and Hazlett, 1975).

We present here the first demonstration of an underwater EAG method established for shrimp. It was developed on the coastal marine species *Palaemon elegans* (Rathke, 1837) but it can easily be adapted to other marine or freshwater decapods.

MATERIALS AND METHODS

Animals

Caridean shrimp *Palaemon elegans* (Rathke, 1837) were collected from Saint-Malo Bay (France), housed communally in 100 liter aquaria with oxygenated artificial seawater (Red Sea Salt, Red Sea, Houston, TX, USA) at 15.5±0.5°C under a 12 h:12 h light:dark cycle, and fed twice a week with shrimp food pellets [Novo Prawn (NP), JBL, Neuhofen, Germany]. The specimens for experiments were transferred to a 25 liter aquarium maintained at room temperature (21±1°C) for at least 48 h of starvation to prevent any potential adaptation of their chemoreceptor neurons to food odors. The sex and age of animals were not determined.

Biological preparation

The animal was restrained in a 1 or 5 ml pipette tip cut according to the shrimp's size with the antennal appendages and the posterior part of the abdomen out at each extremity of the cone (Fig. 1). The shrimp was placed ventral side up. The preparation was attached to a UM-3C micromanipulator (Narishige, London, UK) and angled at approximately 45 deg so that the anterior part of the animal (i.e. antennal appendages) was submerged in a Petri dish filled with *Panulirus* saline (PS) and the posterior part (i.e. telson and abdomen) remained in air. The composition of PS was (in mmol l^{-1}): 486 NaCl, 5 KCl, 13.6 $CaCl_2$, 9.8 $MgCl_2$ and 10 Hepes, pH 7.8–7.9 (Hamilton and Ache, 1983). A gravity-fed PS perfusion was inserted in the pipette tip just over the cephalothorax, to irrigate the branchial cavity and keep the animal alive, and to renew the PS bath solution. The antennules were immobilized with U-shape tungsten hooks on a piece of Styrofoam stuck to the bottom of the Petri dish. The preparation was visualized under a dissecting microscope (M165C, Leica, Nanterre, France). Experiments were performed at room temperature (21±1°C).

[1]Sorbonne Universités, UPMC Univ Paris 06, MNHN, CNRS, IRD, UCBN, UAG, Unité de Biologie des organismes et écosystèmes aquatiques (BOREA, UMR 7208), Equipe Adaptations aux Milieux Extrêmes, 7 Quai Saint-Bernard, Bâtiment A, Paris 75005, France. [2]IEES-Paris, Department of Sensory Ecology, INRA, Route de Saint-Cyr, Versailles 78026, France.

*Author for correspondence (philippe.lucas@inra.fr)

P.L., 0000-0003-2166-8248

Received 31 March 2016; Accepted 13 September 2016

Journal of Experimental Biology (2016) 219, 3696-3700 doi:10.1242/jeb.140947

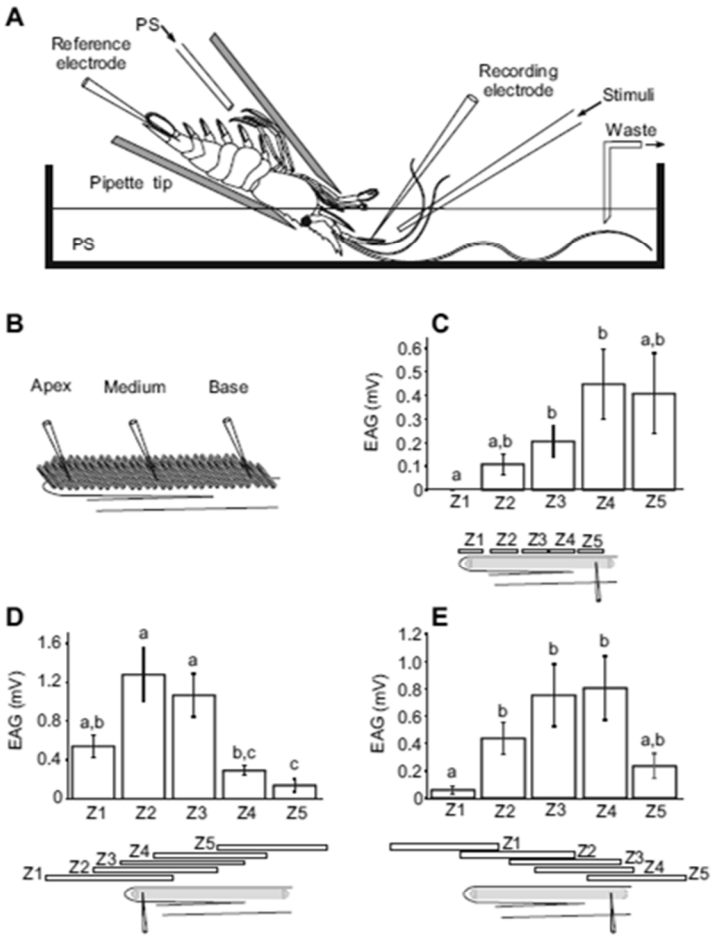

Fig. 1. Setup, electrode placements and electroantennography (EAG) responses from the marine shrimp *Palaemon elegans*. (A) Sketch of the setup used to record EAG responses. The shrimp, restrained in a cut pipette cone, is fixed head down in the bath solution, ventral side up, and is perfused with *Panulirus* saline (PS) solution near the branchial cavity. The recording electrode is inserted in the antennular lateral flagellum that bears the olfactory aesthetasc sensilla, and the reference electrode is inserted between the telson and the abdomen. The stimulus delivery system is placed approximately 1.5 mm from the lateral flagellum. Shrimp size (from telson tip to eyes) is 2.7±0.4 cm; antennae, antennules and materials are not to scale. (B) Sketch of *P. elegans* aesthetascs bearing antennular flagellum with the different electrode placements at the base, middle and apex regions. Not to scale. (C) EAG amplitudes recorded from the base region to narrow stimuli at different zones along the antennule (Z1, Z2, Z5, n=4; Z3, Z4, n=5). (D) EAG amplitudes recorded from the apex region to wide stimuli at different zones along the antennule (Z1, Z4, Z5, n=5; Z2, n=7; Z3, n=6). (E) EAG amplitudes recorded from the base region with wide stimuli at different zones along the antennule (Z1, Z2, Z3, n=7; Z4, n=6; Z5, n=4). In C–E, EAGs were recorded in response to Novo Prawn (NP) stimuli (0.2 g ml^{-1} of NP extract for 1 s in C, 0.5 s in D and E). Fast Green was used to visualize stimulated zones; it did not modify responses to NP stimuli. The gray zone on the antennule sketch represents the aesthetascs bearing area. Means±s.e.m. were compared with a one-way ANOVA with permutation test (C, P=0.04; D, P=0.002; E, P=0.01) and by multiple comparisons with two-sample permutation t-tests; Benjamini–Hochberg corrections were applied. Means with different letters are significantly different (P<0.05).

Electrophysiological recordings and data analysis

Electrodes were pulled from GB150F-8P glass capillaries (Science Products, Hofheim, Germany) using a P-97 puller (Sutter Instrument, Novato, CA, USA). They had a tip diameter of 1 to 2.5 µm and were filled with PS. The reference electrode was introduced through the soft articular membrane between the telson and the abdomen. The recording electrode was inserted with a NMM-25 micromanipulator (Narishige, London, UK) in the base, middle or apex region of the flagellum area bearing the aesthetascs, between two aesthetasc rows (Fig. 1B). Signals were amplified (×100) and filtered (0.1–1000 Hz) using an EX1 amplifier with a 4002 headstage (Dagan, Minneapolis, MN, USA), and digitized at 2 kHz by a 16-bit acquisition board (Digidata 1440A) under Clampex 10.3 (Molecular Devices, Sunnyvale, CA, USA). Data were analyzed using Clampfit (Molecular Devices). Signals were low-pass filtered offline at 20 Hz. Data are given as means±s.e.m.

Chemical stimuli preparation and delivery

An aqueous extract of shrimp food NP was used as odorant in most experiments. NP pellets were dissolved for 48 h at room temperature at 0.2 g ml^{-1} in PS. The extract was then centrifuged at 5900 ***g*** for 10, 15 and 20 min and the supernatant was collected after each centrifugation and filtered (0.45 µm), aliquoted and stored at −20°C until use. For dose–response experiments, NP extracts were diluted from 1:2 to 1:200 with PS. Aqueous extracts of green crab *Carcinus maenas*, blue mussel *Mytilus edulis* and dead *P. elegans* individuals were prepared from fresh material at approximately 0.1, 0.5 and 0.6 g ml^{-1} in PS, respectively, using the same protocol as for NP extract. Osmolarity (1050 mOsm l^{-1} with mannitol) and pH (7.85 with NaOH) were adjusted for all solutions.

To deliver chemical stimuli, we used a pressurized perfusion system with eight channels (AutoMate Scientific, Berkeley, CA, USA). Each reservoir was connected to one entry of an MPP-8 multi-barrel manifold (Harvard Apparatus, Les Ulis, France). A segment (60 mm) of deactivated gas chromatography (GC) column (0.25 mm internal diameter) was glued to the manifold exit. The manifold was mounted onto a UM-3C micromanipulator and the tip of the GC column was positioned approximately 1.5 mm from the recorded flagellum in its longitudinal axis. Stimuli were applied for 1 s at 5 psi (1.1 ml min^{-1}). Consecutive stimuli were delivered with

Journal of Experimental Biology (2016) 219, 3696-3700 doi:10.1242/jeb.140947

at least 2 min intervals to prevent chemosensory adaptation. To establish the dose–response relationship for NP extract, stimuli were applied in increasing concentrations. To analyze how global the responses are, glass capillaries with two diameters were used to stimulate wide and narrow portions of the antennule (0.86 mm and 100 µm internal diameter, respectively) perpendicular to the antennule axis. Responses to 0.1 or 0.2 g ml^{-1} of NP extract (positive control) were measured at the beginning and at the end of each experiment to ensure that the quality of recording remained constant throughout the experiment. PS was used as a negative control.

RESULTS AND DISCUSSION

We implemented a new EAG technique on a marine decapod while keeping both its antennule and the stimulus in their natural (marine) environment. This technique is derived from EAG on insects. Insect antennae have different shapes, which impacts the positioning of the recording electrode. In Lepidoptera, EAG is typically performed from whole insect preparations by cutting the tip of the antenna and inserting it in a glass electrode filled with electrolyte, with the reference electrode inserted in the insect body. Excised antenna can also be used but they have a shorter lifetime (Martinez et al., 2014). In Coleoptera, the recording electrode is inserted in the antenna (Roelofs, 1984). In aquatic species, having the two electrodes in water would result in a short circuit between them. We used the air–water interface to prevent this short circuit, putting the anterior part of the shrimp (i.e. antennular appendages, one lateral flagellum impaled by the recording electrode) in the bath solution and the posterior part (i.e. telson and abdomen, connected to the reference electrode) in the air. Because cutting the extremity of the antennule induced a prominent outflow of fluid, we inserted the recording electrode tip between aesthetascs.

Determination of recording parameters

To establish the best conditions to record EAG responses, NP extract stimuli were used. Responses to NP were positive deviations of the baseline, while control stimuli (PS) induced negative deviations of the baseline.

To estimate whether the recording electrode sampled the responses from a large or small portion of the antennule (i.e. global versus local response), different portions were stimulated with 0.2 g ml^{-1} of NP extract. When narrow stimuli were applied along the antennule while recording from the base region (Fig. 1C), the electrode recorded responses from zones stimulated far from the electrode location. Then, increasing lengths of the antennule were stimulated by moving a larger stimulation capillary along the antennule while recording from the apex (Fig. 1D) or the base (Fig. 1E) regions. For both electrode placements, the EAG amplitude increased with the size of the stimulated area. Thus, there is a good propagation of the chemosensory response within the antennule, so a large fraction of receptor neurons can be recorded. To maximize the amplitude of recorded responses (i.e. to record the largest number of receptor neurons), subsequent experiments were performed by placing the recording electrode in the middle region of the antennule (Fig. 1B).

In decapods, the antennule is not only equipped with unimodal (chemosensory) aesthetascs housing ORNs. It also carries bimodal (chemo- and mechanosensory) non-aesthetasc sensilla; however, in much lower density than aesthetascs (Cate and Derby, 2001; Hallberg et al., 1997; Obermeier and Schmitz, 2004; Steullet et al., 2002). Hence, both neurons innervating the aesthetascs and the non-aesthetasc sensilla can contribute to recorded chemical responses; selective ablation experiments could clarify this point. To verify whether control responses were mechanical, PS flows were applied at increasing pressures (2 to 10 psi). PS responses were pressure-dependent, with no significant response for the lowest pressure (2 psi) and significant response for pressure values of 4 psi and more (Fig. 2A,B), indicating that PS responses were likely mechanical. The response increase from 4 (−0.17±0.04 mV, n=24) to 10 psi (−0.32±0.09 mV, n=25) was not significant (one-way ANOVA with permutation test, P=0.8) because of a high variability of the amplitude of PS responses across recordings. We thus decided to adjust the pressure of all stimuli to 5 psi to facilitate stimulus access to aesthetascs through their dense packing and to distributed chemosensilla without eliciting strong mechanical responses that would have impeded the correct measurement of chemical responses.

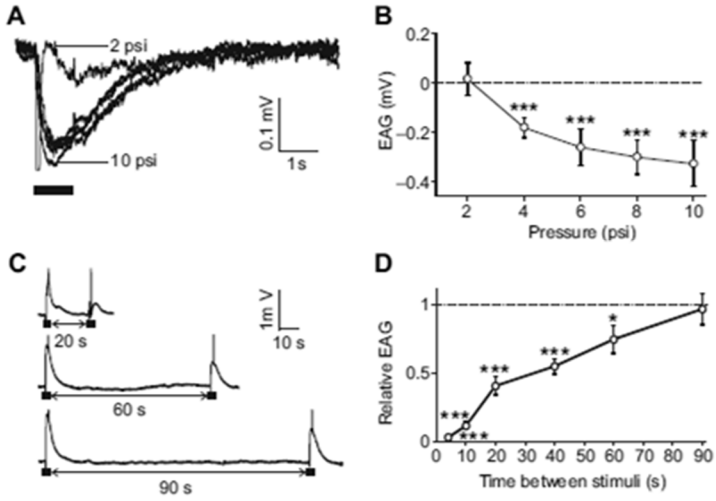

Fig. 2. EAG responses to mechanical and consecutive chemical stimuli. (A) Superimposed traces of EAG responses to *Panulirus* saline with increasing pressure, the upper trace corresponding to 2 psi, and the others to 4, 6, 8 and 10 psi. (B) EAG pressure–response curve to *Panulirus* saline (n=21 for 2 psi; n=24 for 4 psi; n=25 for 6, 8 and 10 psi). (C) Examples of EAG responses to two consecutive NP stimuli (0.1 g ml^{-1} of NP extract for 1 s at 5 psi) separated by 20, 60 and 90 s. (D) Amplitude of EAG responses to NP stimuli (same as in C) relative to the amplitude of EAG response to a previous identical stimulation, as a function of the time between the two stimuli (n=7 for 10, 60 and 90 s, n=9 for 4 and 40 s; n=11 for 20 s). In A and C, bars indicate the stimulus delivery. Transient peaks are valve opening artefacts. Means±s.e.m. were compared with a one-way ANOVA with permutation test (B, P=0.004; D, P<10^{-15}), and with a one-sample permutation t-test to reference values (0 in B, 1 in D). *P<0.05; ***P<0.001.

Journal of Experimental Biology (2016) 219, 3696-3700 doi:10.1242/jeb.140947

Responses of chemoreceptor neurons depend not only on the stimulus characteristics (quality, quantity), but also on previous chemosensory experience via the process of adaptation (Kaissling et al., 1987). When chemoreceptor neurons are adapted by a stimulus, responses to subsequent stimuli are reduced. The recovery from adaptation is time-dependent. To define a time interval between consecutive stimuli that could prevent measuring responses from adapted sensory neurons, we measured EAG responses to pairs of identical stimuli (0.1 g ml^{-1} of NP extract) with increasing inter-stimulus intervals (4 to 90 s) (Fig. 2C,D). As the inter-stimulus interval was increased, the average amplitude of the response to the second stimulus increased and eventually did not differ significantly from the amplitude of the first response when the interval was at least 90 s. For safety, in the following we kept an interval of at least 2 min between consecutive stimuli.

EAG responses according to defined recording parameters

All the responses to NP extracts were positive deviations of the baseline (Fig. 3A). Increasing concentrations of NP extract (0.001 to 0.2 g ml^{-1}) elicited dose-dependent responses with a threshold between 0.001 and 0.003 g ml^{-1} (Fig. 3B) and amplitudes reaching 2.6 mV for the highest concentration (0.2 g ml^{-1}). The delay between the electrovalve opening command and the beginning of the EAG response to 0.1 or 0.2 g ml^{-1} is 62±3 ms (n=20). Antennules were also stimulated with other food extracts made from green crabs, blue mussels and dead *P. elegans* individuals, and responses had the same polarity as those for NP extracts (Fig. 3C). A similar response profile to dead shrimp extract was obtained for the deep hydrothermal shrimp *Mirocaris fortunata* (Fig. 3D).

EAG responses to food-related odor in *P. elegans* are reproducible, dose-dependent and exhibit sensory adaptation, confirming we indeed recorded chemosensory responses. We could not reach the saturation level in the dose–response curve because we reached the saturating concentration of the NP extract. All stimuli we tested (extracts of NP, crab, mussel and dead shrimp) elicited positive EAGs in *P. elegans* whereas insect EAGs are usually negative (Roelofs, 1984), with some exceptions related to the chemical structure of single odorants (e.g. Pavis and Renou, 1990). The EAG response is assumed to represent the summation of receptor potentials of many synchronously activated chemoreceptor neurons (Schneider, 1957, 1999; Nagai, 1983; Mayer et al., 1984). As slow electrical events (e.g. receptor potentials) travel better than action potentials because of low-pass filtering of the extracellular space (Bedard et al., 2004), the fact that odor-evoked signals travelled far within the antennule suggests that EAGs in shrimp are also summed receptor potentials. In the terrestrial hermit crab *Coenobita clypeatus*, compounds with different chemical properties elicited EAG responses of opposite polarity (Krång et al., 2012), which has been proposed to result from activation of different signal transduction pathways. In lobsters, odors may depolarize or hyperpolarize ORNs, and different pathways are directly linked to opposing outputs: excitatory and inhibitory receptor potentials coexist in the same ORN and the response type (excitation or inhibition) is not a property of the stimulant but it depends on the ORN (Doolin et al., 2001; McClintock and Ache, 1989; Michel et al., 1991). Positive EAG responses were obtained in robber crab, hermit crab and daphnia (Krång et al., 2012; Simbeya et al., 2012; Stensmyr et al., 2005). In the marine hermit crab *P. bernhardus*, EAG responses to amines were positive, and responses to acids were negative (Krång et al., 2012). Here we worked with complex mixtures. Comparison of EAG responses to single odorants will allow determining whether different chemical groups also elicit different response polarities in *P. elegans*. Mechanical stimuli elicited negative EAGs. Recordings from single chemoreceptor neurons and single mechanoreceptor neurons could help clarify why chemical and mechanical responses have opposite polarities.

The development of the EAG method in shrimp opens a large field of possibilities for studying antennular chemoreception in decapods and maybe other crustaceans. This method is relatively easy to use on species larger than 1 cm, and it enables work on intact animals. EAG is complementary to other existing electrophysiological methods. It gives a more general idea of the animal sensitivity than single chemoreceptor neuron recordings, and is thus relevant in an ecological approach. EAG allows the screening of compounds eliciting electrophysiological response, before testing potential odor-gated behavioral responses.

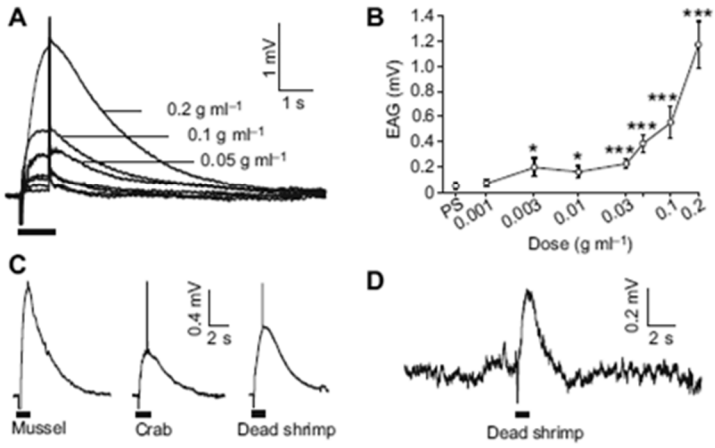

Fig. 3. EAG responses to odorant extracts in the marine shrimp *Palaemon elegans*.
(A) Superimposed traces of EAG responses to dilutions of NP extract (0.001, 0.003, 0.01, 0.03, 0.05, 0.1 and 0.2 g ml^{-1}). (B) EAG dose–response curve to dilutions of NP extract (n=10 for 0.05 g ml^{-1}; n=11 for 0.001 and 0.003 g ml^{-1}; n=12 for control; n=14 for 0.2 g ml^{-1}; n=16 for 0.01, 0.03 and 0.1 g ml^{-1}). Means±s.e.m. were compared with a one-way ANOVA with permutation test (P<10^{-15}), and with a two-sample permutation t-test to control stimuli (PS). *P<0.05; ***P<0.001. (C) EAG responses to fresh mussel extract, fresh green crab extract and extract of dead *P. elegans* individuals. The order of stimuli (mussel, crab, dead shrimp) was randomized. (D) EAG response to dead shrimp extract from the deep hydrothermal shrimp *Mirocaris fortunata*. In A, C and D, bold horizontal bars indicate the stimulus delivery. Transient peaks are valve opening artefacts.

Acknowledgements
The authors thank N. Rabet for collecting the shrimp used in this study, M. Dacher for his help with the statistical analysis and B. Shillito for managing the European MIDAS project, which funded this study.

Competing interests
The authors declare no competing or financial interests.

Author contributions
P.L., J.R. and M.Z. conceived the study and J.M. drafted the paper. J.M. performed all the experiments, with the help of P.L. All authors participated in data analysis and in writing the manuscript.

Funding
This research was funded by the European Union Seventh Framework Programme (FP7/2007-2013) under the MIDAS project (grant agreement no. 603418).

References

Ache, B. W. (2002). Crustaceans as animal models for olfactory research. In *Crustacean Experimental Systems in Neurobiology* (ed. K. Wiese), pp. 189-199. New York: Springer-Verlag.
Ameyaw-Akumfi, C. and Hazlett, B. A. (1975). Sex recognition in the crayfish *Procambarus clarkii*. *Science* **190**, 1225-1226.
Anderson, P. A. V. and Ache, B. W. (1985). Voltage- and current-clamp recordings of the receptor potential in olfactory receptor cells in situ. *Brain Res.* **338**, 273-280.
Bedard, C., Kroger, H. and Destexhe, A. (2004). Modeling extracellular field potentials and the frequency-filtering properties of extracellular space. *Biophys. J.* **86**, 1829-1842.
Bobkov, Y., Park, I., Ukhanov, K., Principe, J. and Ache, B. (2012). Cellular basis for response diversity in the olfactory periphery. *PLoS ONE* **7**, e34843.
Cate, H. S. and Derby, C. D. (2001). Morphology and distribution of setae on the antennules of the Caribbean spiny lobster *Panulirus argus* reveal new types of bimodal chemo-mechanosensilla. *Cell Tissue Res.* **304**, 439-454.
Chamberlain, S. C. (2000). Vision in hydrothermal vent shrimp. *Philos. Trans. R. Soc. B Biol. Sci.* **355**, 1151-1154.
Derby, C. D. (1989). Physiology of sensory neurons in morphologically identified cuticular sensilla of crustaceans. In *Functional Morphology of Feeding and Grooming in Crustacea* (ed. B. E. Felgenhauer, L. Watling and A. B. Thistle), pp. 27-48. Rotterdam: Balkema.
Derby, C. D. and Sorensen, P. W. (2008). Neural processing, perception, and behavioral responses to natural chemical stimuli by fish and crustaceans. *J. Chem. Ecol.* **34**, 898-914.
Derby, C. D. and Weissburg, M. J. (2014). The chemical senses and chemosensory ecology of crustaceans. In *Nervous Systems and Control of Behavior* (ed. C. D. Derby and M. Thiel), pp. 263-292. Oxford: Oxford University Press.
Doolin, R. E., Zhainazarov, A. B. and Ache, B. W. (2001). An odorant-suppressed Cl^- conductance in lobster olfactory receptor cells. *J. Comp. Physiol. A Neuroethol. Sens. Neural Behav. Physiol.* **187**, 477-487.
Ghiradella, H. T., Case, J. F. and Cronshaw, J. (1968). Structure of aesthetascs in selected marine and terrestrial decapods: chemoreceptor morphology and environment. *Am. Zool.* **8**, 603-621.
Hallberg, E., Johansson, K. U. I. and Wallén, R. (1997). Olfactory sensilla in crustaceans: morphology, sexual dimorphism, and distribution patterns. *Int. J. Insect Morphol. Embryol.* **26**, 173-180.
Hamilton, K. A. and Ache, B. W. (1983). Olfactory excitation of interneurons in the brain of the spiny lobster. *J. Comp. Physiol. A Neuroethol. Sens. Neural Behav. Physiol.* **150**, 129-140.
Jinks, R. N., Battelle, B. A., Herzog, E. D., Kass, L., Renninger, G. H. and Chamberlain, S. C. (1998). Sensory adaptations in hydrothermal vent shrimps from the Mid-Atlantic Ridge. *Cah. Biol. Mar.* **39**, 309-312.
Kaissling, K.-E., Zack Strausfeld, C. and Rumbo, E. R. (1987). Adaptation processes in insect olfactory receptors. Mechanisms and behavioral significance. *Ann. N. Y. Acad. Sci.* **510**, 104-112.
Kamio, M., Araki, M., Nagayama, T., Matsunaga, S. and Fusetani, N. (2005). Behavioral and electrophysiological experiments suggest that the antennular outer flagellum is the site of pheromone reception in the male helmet crab *Telmessus cheiragonus*. *Biol. Bull.* **208**, 12-19.
Krång, A.-S., Knaden, M., Steck, K. and Hansson, B. S. (2012). Transition from sea to land: olfactory function and constraints in the terrestrial hermit crab *Coenobita clypeatus*. *Proc. R. Soc. B Biol. Sci.* **279**, 3510-3519.
Martinez, D., Arhidi, L., Demondion, E., Masson, J.-B. and Lucas, P. (2014). Using insect electroantennogram sensors on autonomous robots for olfactory searches. *J. Vis. Exp.* **90**, e51704.
Mayer, M. S., Mankin, R. W. and Lemire, G. F. (1984). Quantitation of the insect electroantennogram: measurement of sensillar contributions, elimination of background potentials, and relationship to olfactory sensation. *J. Insect. Physiol.* **30**, 757-763.
McClintock, T. S. and Ache, B. W. (1989). Hyperpolarizing receptor potentials in lobster olfactory receptor cells: implications for transduction and mixture suppression. *Chem. Sens.* **14**, 637-647.
Michel, W. C., McClintock, T. S. and Ache, B. W. (1991). Inhibition of lobster olfactory receptor cells by and odor-activated potassium conductance. *J. Neurophysiol.* **65**, 446-453.
Nagai, T. (1983). On the relationship between the electroantennogram and simultaneously recorded single sensillum response of the european corn borer, *Ostrinia nubilalis*. *Arch. Insect Biochem. Physiol.* **1**, 85-91.
Obermeier, M. and Schmitz, B. (2004). The modality of the dominance signal in snapping shrimp (*Alpheus heterochaelis*) and the corresponding setal types on the antennules. *Mar. Fresh. Behav. Physiol.* **37**, 109-126.
Pavis, C. and Renou, M. (1990). Study of the shape of the electroantennogram responses in *Nezara viridula* (L.) (Heteroptera, Pentatomidae). *C. R. Acad. Sci. Paris.* **310**, 521-526.
Rathke, H. (1837). Zur fauna der krym. *Mém. Acad. Imp. Sci. St. Pétersbourg* **3**, 291-454.
Renninger, G. H., Kass, L., Gleeson, R. A., Van Dover, C. L., Battelle, B.-A., Jinks, R. N., Herzog, E. D. and Chamberlain, S. C. (1995). Sulfide as a chemical stimulus for deep-sea hydrothermal vent shrimp. *Biol. Bull.* **189**, 69-76.
Roelofs, W. L. (1984). Electroantennogram assays: rapid and convenient screening procedures for pheromones. In *Techniques in Pheromone Research* (ed. H. E. Hummel and T. A. Miller), pp. 131-159. New York: Springer Series in Experimental Entomology.
Schmidt, M. and Derby, C. D. (2005). Non-olfactory chemoreceptors in asymmetric setae activate antennular grooming behavior in the Caribbean spiny lobster *Panulirus argus*. *J. Exp. Biol.* **208**, 233-248.
Schneider, D. (1957). Electrophysiological investigation on the antennal receptors of the silk moth during chemical and mechanical stimulation. *Experientia* **13**, 89-91.
Schneider, D. (1999). Insect pheromone research: some history and 45 years of personal recollections. *IOBC-WPRS Bull* **22**. Available at http://www.phero.net/iobc/dachau/bulletin99/schneider.pdf.
Simbeya, C. K., Csuzdi, C. E., Dew, W. A. and Pyle, G. G. (2012). Electroantennogram measurement of the olfactory response of *Daphnia* spp. and its impairment by waterborne copper. *Ecotoxicol. Environ. Saf.* **82**, 80-84.
Stensmyr, M. C., Erland, S., Hallberg, E., Wallén, R., Greenaway, P. and Hansson, B. S. (2005). Insect-like olfactory adaptations in the terrestrial giant robber crab. *Curr. Biol.* **15**, 116-121.
Steullet, P., Krützfeldt, D. R., Hamidani, G., Flavus, T., Ngo, V. and Derby, C. D. (2002). Dual antennular chemosensory pathways mediate odor-associative learning and odor discrimination in the Caribbean spiny lobster *Panulirus argus*. *J. Exp. Biol.* **205**, 851-867.

Chemical Senses, 2017, Vol 00, 1–13
doi:10.1093/chemse/bjx007
Original Article

OXFORD

Original Article

Comparative Study of Chemosensory Organs of Shrimp From Hydrothermal Vent and Coastal Environments

Magali Zbinden[1], Camille Berthod[1], Nicolas Montagné[2], Julia Machon[1], Nelly Léger[1], Thomas Chertemps[2], Nicolas Rabet[3], Bruce Shillito[1] and Juliette Ravaux[1]

[1]Sorbonne Universités, Univ Paris 06, UMR CNRS MNHN 7208 Biologie des Organismes Aquatiques et Ecosystèmes (BOREA), Equipe Adaptation aux Milieux Extrêmes, Bât. A, 4e étage, 7 Quai St Bernard, 75005 Paris, France, [2]Sorbonne Universités, Univ Paris 06, Institut d'Ecologie et des Sciences de l'Environnement (iEES-Paris), 4 place Jussieu, 75005 Paris, France and [3]Sorbonne Universités, Univ Paris 06, UMR CNRS MNHN 7208 Biologie des Organismes Aquatiques et Ecosystèmes (BOREA), Département des milieux et peuplements aquatiques, CP26, 43 rue Cuvier, 75005 Paris, France

Correspondence to be sent to: Magali Zbinden, Université Pierre et Marie Curie, UMR 7208 BOREA, 7 quai St Bernard - Bat A, 4ème étage, pièce 417 (Boite 5), 75252 Paris Cedex 05, France. e-mail: magali.zbinden@upmc.fr

Editorial Decision 24 January 2017.

Abstract

The detection of chemical signals is involved in a variety of crustacean behaviors, such as social interactions, search and evaluation of food and navigation in the environment. At hydrothermal vents, endemic shrimp may use the chemical signature of vent fluids to locate active edifices, however little is known on their sensory perception in these remote deep-sea habitats. Here, we present the first comparative description of the sensilla on the antennules and antennae of 4 hydrothermal vent shrimp (*Rimicaris exoculata*, *Mirocaris fortunata*, *Chorocaris chacei*, and *Alvinocaris markensis*) and of a closely related coastal shrimp (*Palaemon elegans*). These observations revealed no specific adaptation regarding the size or number of aesthetascs (specialized unimodal olfactory sensilla) between hydrothermal and coastal species. We also identified partial sequences of the ionotropic receptor IR25a, a co-receptor putatively involved in olfaction, in 3 coastal and 4 hydrothermal shrimp species, and showed that it is mainly expressed in the lateral flagella of the antennules that bear the unimodal chemosensilla aesthetascs.

Key words: aesthetascs, decapod, hydrothermal shrimp, IR25a, olfaction

Introduction

Chemical senses are crucial in mediating important behavioral patterns for most animals. In crustaceans, chemical senses have been shown to play a role in various social interactions, search and evaluation of food, as well as in evaluation and navigation in the habitat (Steullet et al. 2001; Derby and Weissburg 2014). Chemoreception in decapod crustaceans is mediated by chemosensory sensilla that are mainly localized on the first antennae (antennules), pereiopod dactyls and mouthparts (Ache 1982; Derby et al. 2016). Chemoreception has been proposed to be differentiated into 2 different modes (Schmidt and Mellon 2011; Mellon 2014; Derby et al. 2016): 1) "olfaction" mediated by olfactory receptor neurons (ORNs) housed in specialized unimodal olfactory sensilla (the aesthetascs), restricted to the lateral flagella of the antennules (Laverack 1964; Grünert and Ache 1988;

Cate and Derby 2001) and projecting to the olfactory lobe of the brain (Schmidt and Ache 1996b) and 2) "distributed chemoreception" mediated by numerous bimodal sensilla (containing mecano- and chemo-receptor neurons) occurring on all appendages, projecting to the second antenna and lateral antennular neuropils and the leg neuromeres (Schmidt and Ache 1996a). Although the molecular mechanisms of olfaction have been well studied in insects, they remain largely unknown in crustaceans, and the existing knowledge is restricted to a few number of model organisms (lobsters, crayfish, and the water flea *Daphnia pulex*; review in Derby et al. 2016). In particular, the nature of crustacean odorant receptors has remained elusive until recently, since searches for the traditional insect olfactory receptors have been unsuccessful. A new family of receptors involved in odorant detection, named the Ionotropic Receptors (IRs), was recently described in *Drosophila melanogaster*, and was subsequently shown to be conserved in Protostomia, including the crustacean *D. pulex* (Benton et al. 2009; review in Croset et al. 2010). Lately, several IRs were identified in other crustaceans, the spiny lobster *Panulirus argus* (Corey et al. 2013), the American lobster *Homarus americanus* (Hollins et al. 2003), the hermit crabs *Pagurus bernhardus* (Groh et al. 2014) and *Coenobita clypeatus* (Groh-Lunow et al. 2015), and were proposed to mediate the odorant detection in the antennules. In the lobster, the authors propose that IRs function as heteromeric receptors, with IR25a and IR93a being common subunits that associate with other IR subunits to determine the odor sensitivity of ORNs.

Chemoreception in crustaceans has been largely studied in large decapods like lobsters (Devine and Atema 1982; Cowan 1991; Moore et al. 1991; Derby et al. 2001; Shabani et al. 2008; and see review in Derby et al. 2016). However, this research theme remains poorly investigated in shrimp, especially in deep-sea species. Deep-sea hydrothermal vent shrimp inhabit patchy and ephemeral environments along the mid-oceanic ridges. Inhabiting such sparsely distributed habitats presents challenges for the detection of active emissions by endemic fauna, especially in the absence of light. In the early developmental stages, after release and dispersal in the water column, sometimes tens or hundreds of kilometers from their starting point, larvae need to locate a vent site to settle and begin their adult life (Pond et al. 1997; Herring and Dixon 1998). Later as adults, mobile vent fauna may need to evaluate their environment, to find hydrothermal fluid either to feed their symbiotic bacteria or just to be able to detect the appropriate habitat, in an environment characterized by steep physicochemical gradients (Sarradin et al. 1999; Sarrazin et al. 1999; Le Bris et al. 2006). Chemical compounds like sulfide, temperature and dim light emitted by vents have been proposed to be potential attractants for detection of hydrothermal emissions (Van Dover et al. 1989; Renninger et al. 1995; Gaten et al. 1998).

Only a few studies on olfaction in the hydrothermal shrimp *Rimicaris exoculata* have been published (Renninger et al. 1995; Chamberlain et al. 1996; Jinks et al. 1998), providing the first, brief, description of the sensilla on the antennules and antennae of this species. These authors also reported preliminary behavioral observations, suggesting an attraction to sulfide, and registered electrophysiological responses to sulfide in antennal filaments (but surprisingly not in the antennular lateral ones bearing aesthetascs).

Here, we present a comparative morphological description of antennae and antennules of 4 hydrothermal vent shrimp (*R. exoculata*, *Mirocaris fortunata*, *Chorocaris chacei*, and *Alvinocaris markensis*). We also identified partial sequences of the candidate co-receptor IR25a and studied its expression pattern in the different species. All the approaches were conducted in parallel on a closely related coastal shrimp (*Palaemon elegans*), to give insights in the potential adaptations of sensory organs in deep-sea species. Comparisons within hydrothermal species were also conducted to examine possible specific adaptations related to their different environments and lifestyles, as previous studies showed that chemical senses of crustaceans rapidly evolve and present specialized adaptations according to phylogeny, lifestyle and habitat, as well as to trophic levels (Beltz et al. 2003; Derby and Weissburg 2014). Knowledge of the sensory capabilities of hydrothermal species is especially relevant with the growing interest of mining companies for extraction of seafloor massive sulfides hydrothermal deposits (Hoagland et al. 2010). Possible impacts of sulfide exploitation on vent species encompass habitat destruction, increase of suspended particles and the presence of higher levels of toxic elements, leading to physiological disturbances and to potential alteration of their ability to perceive their environment (Lahman and Moore 2015) and detect hydrothermal emissions.

Materials and methods

Choice of models

Shrimp are one of the dominant macrofaunal taxa of hydrothermal sites in the Mid-Atlantic Ridge (Desbruyères et al. 2000, 2001). They are highly motile, and according to species, occupy different habitats, exhibit different food diets, and show various degrees of association with bacteria. Therefore they provide good models for studying olfactory capabilities since individuals belonging to different species are potentially not sensitive to the same attractants. *Rimicaris exoculata* lives in dense swarms (up to 2500 ind/m^2, Desbruyères et al. 2001) on the chimney walls, at around 20–30 °C, near the fluid emissions in order to feed their dense symbiotic chemoautotrophic bacterial community (Van Dover et al. 1988; Zbinden et al. 2004, 2008). *Chorocaris chacei* is much less abundant (locally 2–3 ind/dm^2) than *R. exoculata*, but may live close to it. It is also found as on sulfide blocks, in areas of weak fluid emissions (Desbruyères et al. 2006; Husson et al. 2016). *Chorocaris* also harbors a bacterial symbiotic community, though less developed than in *Rimicaris* (Segonzac 1992). *Mirocaris fortunata* lives at lower temperature (4.8–6.1 °C, Husson et al. 2016), in diffuse flow habitats and among *Bathymodiolus* mussel assemblages (Sarrazin et al. 2015). *Mirocaris* is opportunistic and feeds on mussel tissue, shrimp and other invertebrates, being reported as predators and/or scavengers (Gebruk et al. 2000; De Busserolles et al. 2009). *Alvinocaris markensis* occurs as solitary individuals, at the base of and on the walls of active edifices, close to *R. exoculata* aggregates, and also on mussel assemblages. It has been reported as necrophagous (Desbruyères et al. 2006), but also as a predator (Segonzac 1992).

In order to identify potential adaptations of hydrothermal shrimp sensory faculties, comparisons were made with the related shallow-water palaemonid species *P. elegans*. The description of palaemonid antennal structures is also interesting per se since olfaction is poorly analyzed in shrimp in general. Two additional palaemonid species, *Palaemon serratus* and *Palaemonetes varians*, were used for identifying the IR25a sequence.

Animal collection, conditioning, and maintenance

Specimens of Alvinocarididae *M. fortunata*, *R. exoculata*, *C. chacei*, and *A. markensis* were collected during the Momarsat 2011 and 2012, Biobaz 2013, and Bicose 2014 cruises, on the Mid-Atlantic Ridge (see Table 1 for cruises and sites). Shrimp were collected with the suction sampler of the ROV "Victor 6000" operating from the

RV "Pourquoi Pas?". Immediately after retrieval, living specimens were dissected and tissues of interest (see below) were fixed in a 2.5% glutaraldehyde/seawater solution for morphological observations or frozen in liquid nitrogen for molecular biology experiments.

Specimens of Palaemonidae *P. elegans*, *P. serratus*, and *P. varians* were collected from Saint-Malo region (France; 48°64′N, –2°00′W), between October 2011 and January 2015, using a shrimp hand net. They were transported to the laboratory and transferred to aerated aquaria with a 12 h:12 h light:dark cycle, a salinity of 35 g/L, and a water temperature of 18 °C. The shrimp were regularly fed with granules (JBL Novo Prawn). Tissues of interest were also fixed in a 2.5% glutaraldehyde/seawater solution for morphological observations or frozen in liquid nitrogen for molecular biology experiments.

Tissue collection

For morphological observations, antennae and antennules (both medial and lateral flagella) were used. For molecular biology experiments, the following organs were dissected for *P. elegans*: the antennular medial and lateral flagella (internal and external ramus separated), the antennae, the mouthparts (mandibles and 2 pairs of maxillae), the first and second walking legs and the eyestalks. For the hydrothermal shrimp, the dissection included the following organs: the antennular medial and lateral flagella, the antennae, and abdominal muscles.

Scanning electron microscopy

Samples were post-fixed in osmium tetroxide 1% once in the lab and dehydrated through an ethanol series. They were then critical-point-dried (CPD7501, Quorum Technologies) and platinum-coated in a Scancoat six Edwards sputter-unit prior to observation in a scanning electron microscope (Cambridge Stereoscan 260), operating at 20 kV.

RNA extraction and reverse transcription

Frozen shrimp tissues were ground in TRIzol Reagent (Thermo Fisher Scientific) with a Minilys homogenizer (Bertin Corp). Total RNA was isolated according to the manufacturer's protocol, and quantified by spectrophotometry and electrophoresis in a 1.2% agarose gel under denaturing conditions. RNA (500 ng) was DNAse treated to remove contamination using the TURBO DNAse kit (Thermo Fisher Scientific) and then reverse transcribed to cDNA with the Superscript II reverse transcriptase kit (Thermo Fisher Scientific) using a oligo$(dT)_{18}$ primer according to the manufacturer's instructions.

IR25a sequencing and mRNA expression (reverse transcription polymerase chain reaction)

The cDNA fragments encoding IR25a were amplified by 2 rounds of polymerase chain reaction (PCR). Oligonucleotide primers were designed from a multiple-sequence alignment of IR25a sequences of crustaceans (*D. pulex*, Croset et al. 2010; *H. americanus* AY098942, Hollins et al. 2003, *Lepeophtheirus salmonis* PRJNA280127 genome sequencing project), insects (*Acyrthosiphon pisum, Aedes aegypti, Anopheles gambiae, Apis mellifera, Bombyx mori, Culex quinquefasciatus, D. melanogaster, Nasonia vitripennis, Pediculus humanus, Tribolium castaneum*, Croset et al. 2010), gastropod molluscs (*Aplysia californica*, *Lottia gigantea*, Croset et al. 2010), nematods (*Caenorhabditis briggsae* XM_002643827, Stein et al. 2003, *Caenorhabditis elegans* NM_076040, The *C. elegans* Sequencing Consortium) and an annelid (*Capitella capitata*, Croset et al. 2010) (primer sequences are listed in Supplementary Table S1). PCR amplification reactions were performed in a 20 µL volume containing 1 µL of cDNA template, 2 µL of each primer [10 µM], 11.7 µL of H_2O, 2 µL of PCR buffer [10×], 0.8 µL of MgCl2 [50 mM], 0.4 µL of dNTP [10 mM] and 0.1 µL of BIOTAQ polymerase [5 U/µL] (Eurobio AbCys). The thermal profile consisted of an initial denaturation (94 °C, 3 min), followed by 35 cycles of denaturation (94 °C, 30 s), annealing (45 to 55 °C, 45 s) and extension (72 °C, 2 min), and a final extension (72 °C, 10 min) step. The PCR products were separated on a 1.5% agarose gel, purified with the GeneClean kit (MP Biomedicals), and cloned into a pBluescript KS plasmid vector using the T4 DNA ligase (Thermo Fisher Scientific). The ligation product was introduced in competent *Escherichia coli* cells (DH5alpha) that were cultured at 37 °C overnight. The clone screening was performed through PstI/HindIII (Thermo Fisher Scientific) digestion of plasmid DNA after plasmid extraction. Positive clones were sequenced on both strands (GATC Biotech). The resulting nucleotide sequences were deposited in the GenBank database under the accession numbers KU726988 (*M. fortunata* IR25a; consensus sequence from 6 clones), KU726987 (*R. exoculata* IR25a; consensus sequence from 3 clones), KU726989 (*C. chacei* IR25a; consensus sequence from 4 clones), KU726990 (*A. markensis* IR25a; consensus sequence from 4 clones), KU726984 (*P. elegans* IR25a; consensus sequence from 11 clones), KU726985 (*P. varians* IR25a; consensus sequence from 12 clones), and KU726986 (*P. serratus* IR25a; consensus sequence from 3 clones). Specific primers were further designed to amplify IR25a sequences in diverse tissues of the 4 alvinocaridid species and the palaemonid *P. elegans* (Supplementary Table S1). PCR amplifications were performed using BIOTAQ polymerase (Eurobio, AbCys) in a thermocycler (Eppendorf, Hamburg, Germany) with the following program: 94 °C for 3 min, 35 cycles of (94 °C for 30 s, 55 °C for 45 s, 72 °C for 2 min), and 72 °C for 10 min, with minor modifications of annealing temperature for different primer pairs.

Sequence analyses

A dataset of IR amino acid sequences was created, including the IR25a sequences identified in shrimp (present study), in other decapods (*P. argus*, Corey et al. 2013; *C. clypeatus*, Groh-Lunow et al. 2015; *H. americanus* AY098942, Hollins et al. 2003) and

Table 1. Cruises, locations and depths of the different sampling sites of the samples used in this study

Sites	Lat.	Long.	Depth (m)	Cruise, year	Ship/ submersible	Chief scientist
Menez Gwen	37°51′N	31°31′W	840	Biobaz, 2013	Pourquoi Pas? / ROV Victor	F. Lallier
Lucky Strike	37°17′N	32°16′W	1700	Biobaz, 2013	Pourquoi Pas? / ROV Victor	F. Lallier
				Momarsat, 2011	Pourquoi Pas? / ROV Victor	M. Cannat
				Momarsat, 2012	Thalassa / ROV Victor	M. Cannat and P. M. Sarradin
Rainbow	36°13′N	33°54′W	2260	Biobaz, 2013	Pourquoi Pas? / ROV Victor	F. Lallier
TAG	26°08′N	44°49′W	3600	Bicose, 2014	Pourquoi Pas? / ROV Victor	M. A. Cambon-Bonavita
Snake Pit	23°23′N	44°58′W	3480	Bicose, 2014	Pourquoi Pas? / ROV Victor	M. A. Cambon-Bonavita

in other crustaceans (*D. pulex*, Croset et al. 2010; *L. salmonis* PRJNA280127) together with IR sequences from the insects *B. mori*, *D. melanogaster*, *A. mellifera*, and *T. castaneum* (Croset et al. 2010). *Drosophila melanogaster* ionotropic glutamate receptor sequences were also included to serve as an out-group, and the final data set contained 173 sequences. These amino acid sequences were aligned with MAFFT v.6 (Katoh and Toh 2010) using the FFT-NS-2 algorithm and default parameters. The alignment was then manually curated to remove highly divergent regions (500 amino acid positions conserved in the final dataset). The phylogenetic reconstruction was carried out using maximum-likelihood. The LG+I+G+F substitution model (Le and Gascuel 2008) was determined as the best-fit model of protein evolution by ProtTest 1.3 (Abascal et al. 2005) following Akaike information criterion. Rate heterogeneity was set at 4 categories, and the gamma distribution parameter was estimated from the data set. Tree reconstruction was performed using PhyML 3.0 (Guindon et al. 2010), with both Subtree Pruning and Regrafting (SPR) and Nearest Neighbour Interchange (NNI) methods for tree topology improvement. Branch support was estimated by approximate likelihood-ratio test (aLRT) (Anisimova et al. 2006). Images were created using the iTOL web server (Letunic and Bork 2011).

Results

Morphology of the chemosensory organs: description and distribution of setal types on the antennae and antennules

In the 5 shrimp species studied for morphology (*P. elegans*, *M. fortunata*, *R. exoculata*, *C. chacei*, and *A. markensis*), antennae and antennules both consist of a peduncle and segmented flagella (one for the antennae and 2 for the antennules: an outer or lateral, and an inner or medial). In the 3 flagella, the diameter and length of the annuli vary, being large and short at the base and becoming thinner and longer towards the apex. The aesthetasc dimensions vary also along the flagella, being thinner and shorter at the base and growing toward the apex. The set of values (maximum, minimum, mean and standard deviation of diameter and length) for aesthetasc, as well as for non-aesthetasc sensilla, are given in Supplementary Table S2.

Palaemon elegans

The antennules are made of 3 basal annuli and 2 distal flagella. The lateral flagella are divided in 2 rami after a short fused basal part: a long external one and a shorter internal one (1/3 of the long one, n = 12, SD = 0.61) (Figure 1A). The aesthetascs are localized

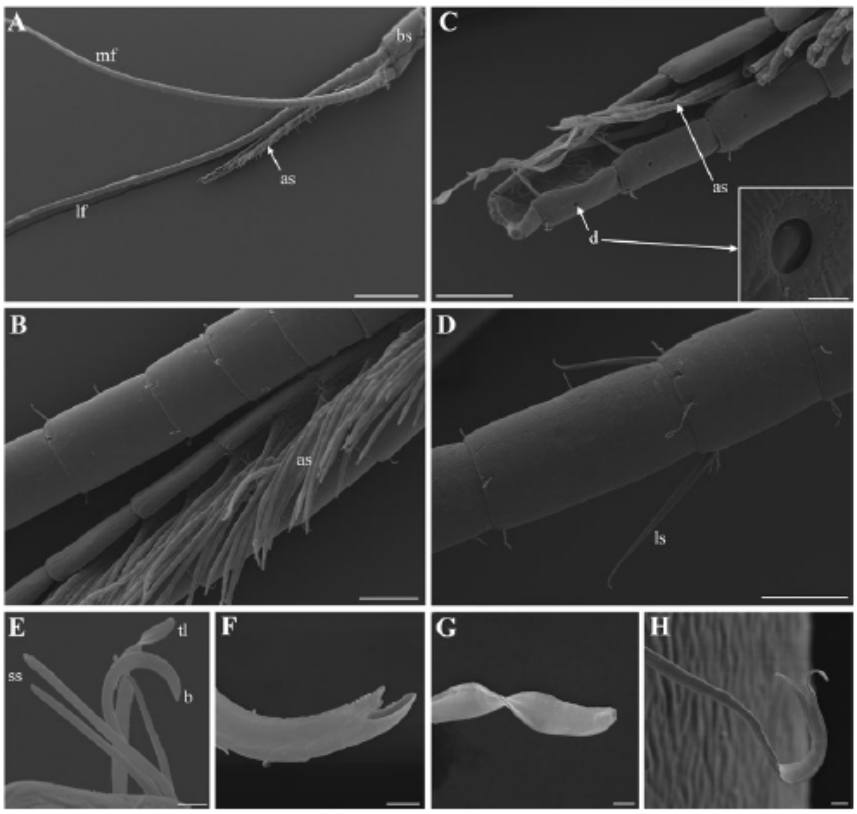

Figure 1. Morphology of antennules and setal types of *Palaemon elegans*. (A) Antennules are made of 3 basal annuli (bs) and 2 flagella: a medial (mf) and a lateral one (lf), which is divided in 2 rami: a long (outer) and a short (inner), bearing the aesthetascs (as). (B) Close-up on the ventral side of the furrow on the shorter ramus of the lateral flagellum bearing the aesthetascs. (C) Apex of the shorter ramus, showing the absence of aesthetascs on the last 2 annuli and the occurrence of small cuticular depressions (d), enlarged in insert. (D) Medial antennular flagellum showing the long simple seta (ls). (E) Tuft of 3 simple short (ss), one twisted flat (tf) and one beaked scaly (b) setae. (F) Beaked scaly seta. (G) Twisted flat seta. (H) Bifid seta. Scale bars: A = 1 mm; B, C, D = 100 μm; E = 10 μm; F, G, H = 2 μm. Scale bar in insert in C = 5 μm.

ventrally, in a furrow on the shorter ramus (Figure 1B). They are present from the basal fused part of the antennules to the apex of the short ramus (except from the last 2 annuli, Figure 1C). Two rows of 5 to 6 aesthetascs occur on each annulus (one row at the distal part of the annulus and the other at the middle part) (Figure 1B). The 2 or 3 basal and apical annuli have a smaller number of aesthetascs, giving a total number of approximately 140 aesthetascs per ramus (Table 2). Aesthetascs are up to 20.3 µm in diameter (n = 14) and 393 µm in length (n = 10) (Supplementary Table S2). They bear annulation throughout their length (short at the base and longer towards the apex), and lack a terminal pore.

Non-aesthetasc setae are also present on all the annuli of the 3 flagella (antennae and antennules), where they are distributed (up to 8) around the distal part of each annulus (Figure 1D). Five setal types are observed on the flagella, named after their morphology (dimensions are given in Table 2): 1) short simple seta (Figure 1E), 2) long simple seta (Figure 1D), 3) beaked scaly seta (Figure 1F), 4) twisted flat seta (Figure 1G), and 5) bifid seta (Figure 1H). All these 5 types appear to have a terminal pore. Short simple, beaked scaly and twisted flat setae are present on the antennae, the medial flagella of the antennules and the long ramus of the lateral flagella of the antennules. They occur as tufts of 5 setae, containing 3 simple short, one twisted flat and one beaked scaly seta (Figure 1E). These tufts are present on each annulus near the base but are spaced further apart towards the apex. The bifid setae are found only on the 2 flagella of the antennules, whereas the long simple are only found on medial flagella of the antennules (2 every 5 annuli, on each side of the flagellum). Small round cuticular depressions (5,5 to 6,7 µm in diameter) are observed on the medial side of the short ramus of the lateral flagella of the antennules, as well as on the antennae (insert in Figure 1C).

Mirocaris fortunata

In *M. fortunata*, as well as in the 3 other hydrothermal species, the antennules are also made of 3 basal annuli and 2 distal flagella (lateral and medial) (Figure 2A). In *M. fortunata*, the aesthetascs are localized latero-ventrally on the inner side of the lateral flagella, from the base to 2/3 of the flagella. One row of 3 to 4 aesthetascs occurs on the distal part of each annulus (Figure 2B), leading to a total number of approximately 60 aesthetascs per ramus (Table 2). Aesthetascs are up to 18.3 µm in diameter (n = 21) and 290.3 µm in length (n = 46) (Supplementary Table S2). They bear annulation on the apical half, and lack a terminal pore.

The rows of aesthetascs are flanked on the inner side by non-aesthetasc setae, organized as follows: one intermediate seta (thinner and shorter than the aesthetascs) and 2 or 3 short thin setae (thinner and shorter than the former) (Figure 2B). The intermediate setae have a peculiar apex shape with no obviously visible pore (Figure 2D), whereas the short setae are simple with a clearly visible pore at the apex (Figure 2E).

Intermediate and short simple setae also occur along with a sparse third type of non-aesthetasc setae (Figure 2F) on the 2 other flagella (medial flagella of the antennules and the antennae), distributed around the distal part of each annulus (about 10 over the entire circumference by extrapolation of what is seen on one face). Small round cuticular depressions (7 to 10 µm in diameter) are observed on the lateral flagella of the antennules, on the medial side of the aesthetascs (Figure 2B). Flagella are often densely covered by a thick bacterial layer of filamentous and rod-shaped bacteria (Figure 2C), which was never observed on *P. elegans*. Rod-shaped bacteria also sometimes covered the entire aesthetasc surface (not shown).

Rimicaris exoculata

The aesthetascs are localized laterally on the medial side of the lateral flagella, from the base (except the 2 or 3 first annuli) up to the apex (except for the 4 last annuli). One row of 3 to 4 aesthetascs occurs on the distal part of each annulus (Figure 3A), leading to a total number of approximately 108 aesthetascs per ramus. Aesthetascs are up to 22 µm in diameter (n = 22) and 191 µm in length (n = 26) (Supplementary Table S2). They bear annulation on the apical half, and lack a terminal pore.

Table 2. Comparative table of aesthetascs setae characteristics in different species of decapods

Species	Total number	Number per row	Dimensions (diameter × length in µm)	Reference
Lobster				
Panulirus argus (20–60 cm)	2000 to 4000	9–10	40 × 1000	Gleeson et al. 1993 Laverack 1964
Homarus americanus (20–60 cm)	2000	10–12	20 × 600	Guenther and Atema 1998
Crayfish				
Orconectes propinquus (4–10 cm)	160	3–6	12 × 150	Tierney et al. 1986
Cherax destructor (10–20 cm)	260[a]	2–5	18 × 100	Sandeman and Sandeman 1996 Beltz et al. 2003
Crab				
Callinectes sapidus (23 cm)	1400	~20	12 × 795	Gleeson et al. 1996
Carcinus maenas (9 cm)	100–300	8–10	13 × 750	Fontaine et al. 1982
Shrimp				
Lysmata[b] (5–7 cm)	210–460	3–5	20 × 800	Zhang et al. 2008
Palaemon elegans (7 cm)	280	5–6	14 × 230	This study
Mirocaris fortunata (3 cm)	120[a]	3–4	16 × 234	This study
Rimicaris exoculata (5.5 cm)	206[a]	3–4	20 × 170	This study
Chorocaris chacei (5.5 cm)	226[a]	2–4	19 × 251	This study
Alvinocaris markensis (8.2 cm)	220[a]	3–4	21 × 531	This study

Rough animal lengths are given for comparison. Total length is given for lobster, crayfish and shrimp, carapace width for crabs.

[a]Species with only one row of aesthetascs per annuli.

[b]Study realized on *Lysmata boggessi*, *L. wurdemanni*, *L. amboinensis*, and *L. debelius*.

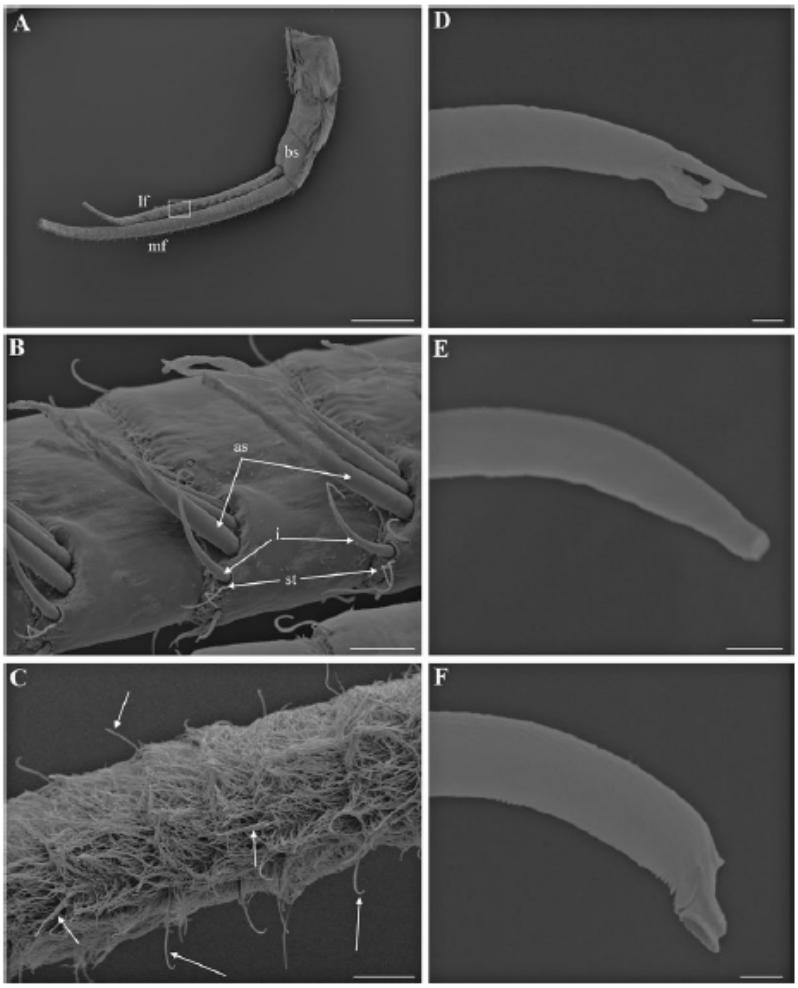

Figure 2. Morphology of antennule and setal types of *Mirocaris fortunata*. (A) Antennules are made of 3 basal annuli (bs) and 2 flagella: a medial (mf) and a lateral one (lf), bearing the aesthetascs (as). Box: area enlarged in B. (B) Close-up on the lateral flagellum bearing the aesthetascs, and intermediate (i) and short thin setae (st). (C) Lateral flagellum covered by dense filamentous and rod-shaped bacteria. Some setae are visible, protruding from the layer of bacteria (arrows). (D) Apex of the intermediate simple setae. (E) Short setae are simple with a clear pore at the apex. (F) Third setal type. Scale bars: A = 1 mm; B = 50 μm; C = 100 μm; D, E, F = 1 μm

The arrangement pattern of the non-aesthetasc setae around the aesthetascs is quite similar to that observed in *M. fortunata*, but with different setal types: 1 long thick beaked seta, 1 intermediate beaked seta and 6 or 7 short thin beaked setae (Figure 3B). All these setae have a pore at the apex (Figure 3C), but they are devoid of scales unlike the beaked setae observed in *P. elegans*.

Long thick, intermediate and short thin beaked setae also occur on the outer side of the lateral flagella, on the medial flagella of the antennules, and on the antennae, distributed over the circumference (20–25 over the entire circumference by extrapolation of setae seen on one face, or counted on the periphery of the apex), with a tight tuft of 6–8 setae on the inner side.

Small round cuticular depressions were (rarely) observed (6 to 8 μm in diameter) in *R. exoculata*, but they are barely observable due to a dense rod-shaped bacterial coverage. Indeed, for this species too, we have observed that the flagella (even the aesthetascs) can be covered by layer of filamentous and rod-shaped bacteria (not shown).

Chorocaris chacei

The aesthetascs are localized laterally on the medial side of the lateral flagella, from the base (except the 4 or 5 first annuli) to 2/3 of the flagella. One row of 2 to 4 aesthetascs occurs on the distal part of each annulus (Figure 3D), leading to a total number of approximately 113 aesthetascs per ramus. Aesthetascs are up to 23.2 μm in diameter (n = 50) and 339.5 μm in length (n = 58) (Supplementary Table S2). They bear annulation on the apical half, and lack a terminal pore.

The arrangement pattern of the non-aesthetasc setae around the aesthetascs is also quite similar to that observed in *M. fortunata* with one intermediate beaked seta, and 1 to 3 short simple or beaked thin setae on both the medial and lateral sides (Figures 3E and F).

Intermediate beaked and short setae (either simple or beaked shaped) also occur on the medial flagella of the antennules, and on the antennae, distributed over the circumference, roughly equidistant (around 15 over the entire circumference by extrapolation of

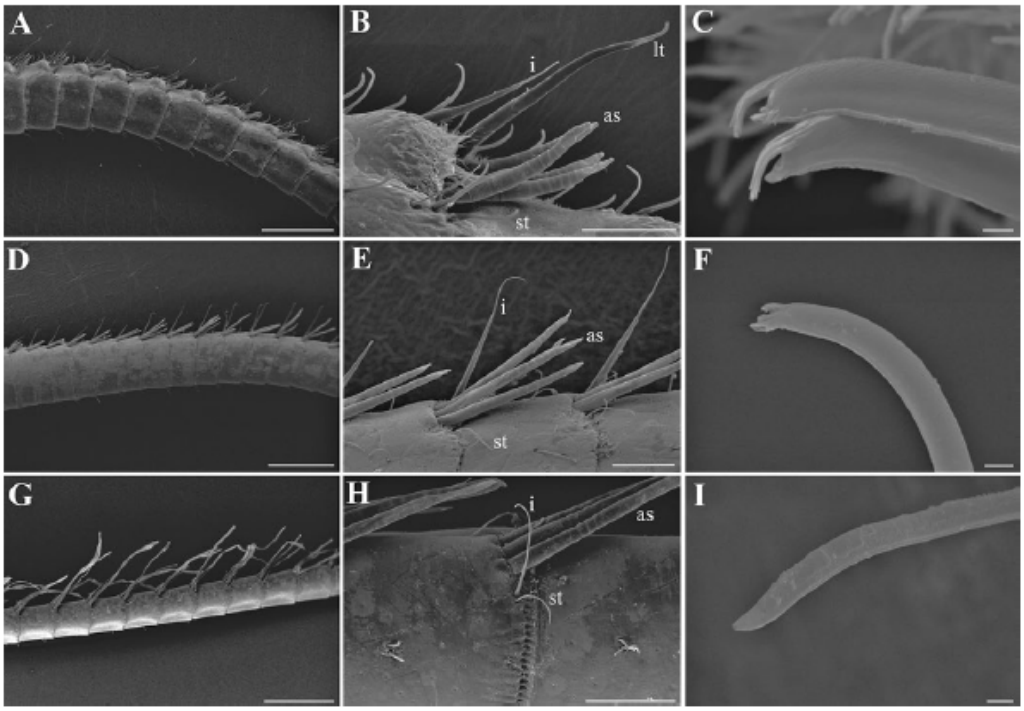

Figure 3. Morphology of lateral flagella and setal types of *Rimicaris exoculata* (A, B, C), *Chorocaris chacei* (D, E, F) and *Alvinocaris markensis* (G, H, I). as: aesthetascs, lt: long thick seta, i: intermediate seta, st: short thin seta, Scale bars: A, D, G = 500 µm; B, E, H = 100 µm; C, F, I = 2 µm.

setae seen on one face, or counted on the periphery of the apex), with a tight tuft of 8 to 10 setae on the inner side.

Small cuticular depressions (5 to 5.5 µm in diameter) are observed on the lateral flagella of the antennules, on the medial side of the aesthetascs but are difficult to observe as they are covered by rod-shaped bacteria. For this species again, the flagella (and even the aesthetascs) can be covered by filamentous and rod-shaped bacteria (not shown).

Alvinocaris markensis

The aesthetascs are localized laterally on the medial side of the lateral flagella, from the base (except the 3 or 4 first annuli) up to half of the flagella. One row of 3 to 4 aesthetascs (rarely 5) occurs on the distal part of each annulus (Figure 3G), leading to a total number of approximately 110 aesthetascs per ramus. Aesthetascs are up to 25.2 µm in diameter (n = 39) and 879.1 µm in length (n = 49) (Supplementary Table S2). They bear annulation almost throughout their length (short at the base and longer towards the apex), and lack a terminal pore.

The arrangement pattern of the non-aesthetasc setae around the aesthetascs is quite similar to that observed in *M. fortunata* with 1 intermediate seta and 1 short thin seta (Figure 3H). Two (sometimes 3 or 4) short setae occur at mid-length of each annulus. Intermediate and short thin setae all seem to all be simple, with a pore (Figure 3I). They also occur on the medial flagella of the antennules and on the antennae, in fewer numbers than observed in the other species (4–6 over the entire circumference, mostly on the medial side). Long simple setae also occur on few basal annuli on the medial flagella of the antennules and of the antennae.

Small cuticular depressions (4.5 to 7.5 µm diameter) were also observed in *A. markensis*, on the lateral flagella of the antennules, on the distal part of the annuli, occurring by one, 2 or sometimes 3, which had not been observed in other species (not shown). They are also observed on the antennae. Only a few rod-shaped bacteria occurred on the 2 specimens observed.

Identification and expression of the putative olfactory co-receptor IR25a in hydrothermal vent and coastal shrimp

In order to identify the regions of antennules and antennae putatively involved in olfaction, we studied the expression pattern of the IR IR25a, which belongs to a conserved family of olfactory receptors amongst Protostomia (review in Croset et al. 2010), involved in olfaction, taste, thermosensation, and hygrosensation. Recently the homologue of IR25a was identified in the lobster, and had been associated with olfactory sensilla (Corey et al. 2013). Using homology-based PCR with primers designed from the alignment of IR25a sequences from diverse organisms, we obtained partial sequences for 7 species of shrimp: 903 bp for *R. exoculata*, *P. elegans*, and *P. varians*, 763 bp for *M. fortunata*, *C. chacei*, and *A. markensis*, and 881 bp for *P. serratus* (Figures 4A and B). A phylogenetic analysis confirmed that these sequences are IR25a orthologs (Figure 5). All shrimp sequences grouped with IR25a sequences from other arthropods, and were closely related to IR25a sequences from the decapod crustaceans *P. argus* (Corey et al. 2013), *H. americanus* (Hollins et al. 2003) and *C. chypeatus* (Groh-Lunow et al. 2015). The Palaemonidae and Alvinocarididae sequences formed distinct clusters within the shrimp sequences, therefore being congruent with the phylogeny of these groups (Figure 6). The IR25a partial amino acid sequences obtained in this study are about 250 to 300 amino acids in length, which represents 25 to 30% of the total length expected for such sequences (Figure 4). They include the ligand-gated ion channel

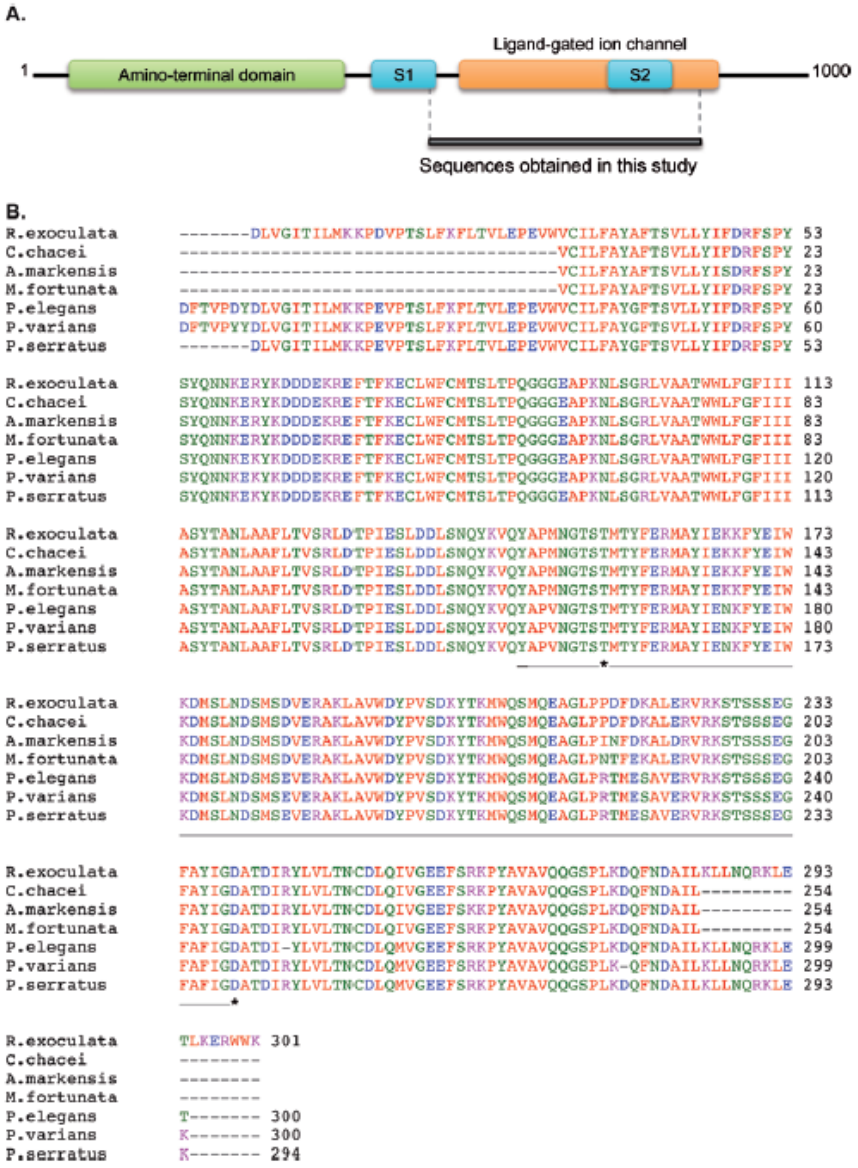

Figure 4. IR25a partial sequences obtained for hydrothermal and coastal shrimp. (A) IR25a protein domain organization (modified from Croset et al. 2010) showing the position of the shrimp partial sequences obtained in the present study. The ligand-binding domains are named S1 and S2. (B) Alignement of shrimp IR25a sequences. The ligand-binding S2 domain is underlined, and putative ligand-binding residues are indicated by an asterisk.

and the ligand-binding S2 domain, localized in the C-terminal part of the protein. When considering the ligand-binding S2 domain, the threonine and aspartate, which are characteristic glutamate binding residues, are conserved among shrimp sequences.

Then, we studied the expression pattern of IR25a in antennules, antennae, mouthparts and walking legs, as well as in non-chemosensory tissues (abdominal muscles, eye), from the 4 hydrothermal vent shrimp and the coastal shrimp *P. elegans* (Figure 7). IR25a was predominantly expressed in the lateral antennular flagella (A1 lateral) for all shrimp. In *P. elegans*, a weaker expression was observed in the external ramus (A1 lateral R2) than in the internal ramus of the lateral antennular flagella (A1 lateral R1), which bear the aesthetascs. A weak expression was also detected in the medial antennular flagella of *R. exoculata* and *C. chacei* (A1 medial), and in the antennae (A2) of *R. exoculata*. IR25a transcripts were undetectable in other tissues.

Discussion

Comparative morphology of sensilla of antennae and antennules among decapods, and in coastal palaemonid versus hydrothermal alvinocarid shrimp

Setae are outgrowths of the arthropod integument presenting a multitude of sizes and shapes. These ubiquitous features of crustacean

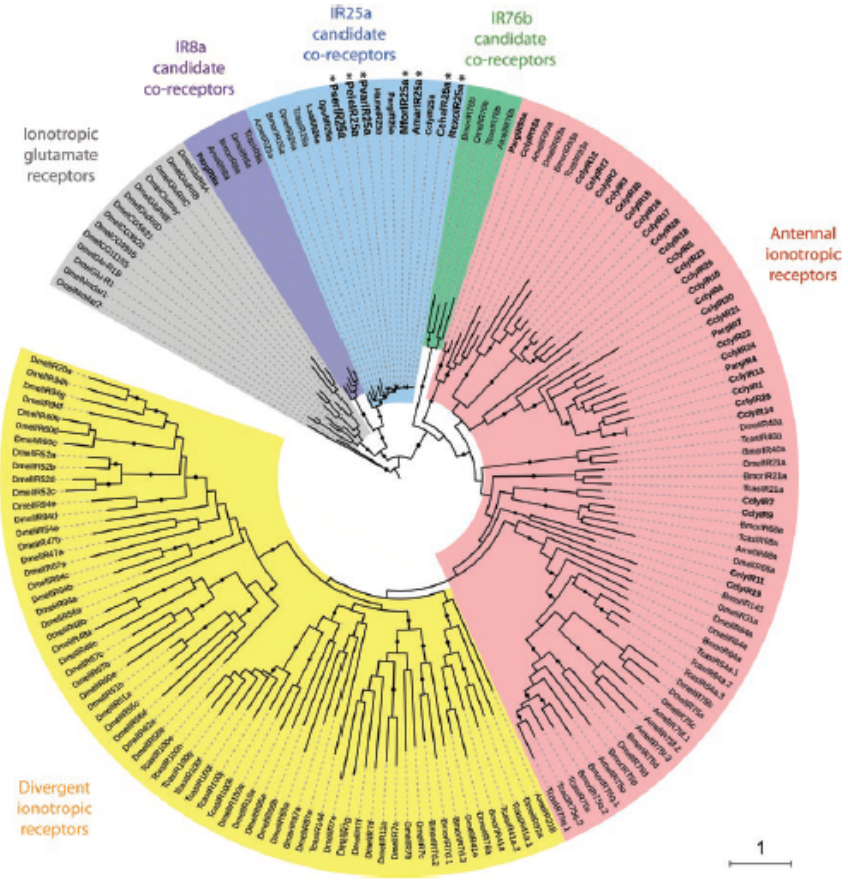

Figure 5. Phylogeny of insect and crustacean ionotropic receptors (IRs). This tree is based on a maximum-likelihood analysis of an amino acid dataset. *Drosophila melanogaster* ionotropic glutamate receptor sequences were used as an out-group. Branch support was estimated by approximate likelihood-ratio test (aLRT) (circles: >0.9). The scale bar corresponds to the expected number of amino acid substitutions per site. Crustacean IRs are in bold and the new IRs identified in this study are in larger font size, and highlighted with an asterisk. Amar, *Alvinocaris markensis*; Amel, *Apis mellifera*; Bmor, *Bombyx mori*; Ccha, *Chorocaris chacei*; Ccly, *Coenobitus clypeatus*; Dmel, *Drosophila melanogaster*; Dpul, *Daphnia pulex*; Hame, *Homarus americanus*; Lsal, *Lepeophtheirus salmonis*; Mfor, *Mirocaris fortunata*; Parg, *Panulirus argus*; Pele, *Palaemon elegans*; Pser, *Palaemon serratus*; Pvari, *Palaemon varians*; Rexo, *Rimicaris exoculata*; Tcas, *Tribolium castaneum*.

integuments are involved in a variety of vital functions including locomotion, feeding, sensory perception and grooming (Felgenhauer 1992). Sensilla (setae innervated by sensory cells) were shown to present a great inter- and intra-specific diversity in crustaceans (see references in the paragraphs below).

In the most studied large decapods like lobsters and crayfish, the aesthetascs are localized in tufts on the distal half or two-thirds of the ventral side of each lateral antennular flagellum (*P. argus*, Cate and Derby 2001; *H. americanus*, Guenther and Atema 1998; *Orconectes sanborni*, McCall and Mead 2008; *O. propinquus*, Tierney et al. 1986; *Procambarus clarkii*, Mellon 2012). The localization at the tip of the antennules may increase the spatial resolution of the chemical environment, but could also increase their chance of damage during encounters with the environment or other animals. On the contrary, in shrimp (the 4 alvinocaridid species and *P. elegans* [this study], as well as other palaemonid species like *P. serratus* and *Macrobrachium rosenbergii* [Hallberg et al. 1992]), the aesthetascs are localized on the basal half or two-thirds of the lateral flagella (for the alvinocarididae) or on the basal part of the short ramus of the lateral flagella (for the palaemonidae). The aesthetascs are thus less likely to be lost or damaged, but this arrangement may decrease spatial resolution.

The aesthetascs are usually organized in 2 successive rows (in the different lobsters and crayfishes cited above and also in *Lysmata* shrimp, Zhang et al. 2008) or in 2 juxtaposed rows in the short antennules of the crab *Carcinus maenas* (Fontaine et al. 1982). Surprisingly, there is only one row of aethetascs on each annulus in the 4 hydrothermal species (an exception also occurs in the crayfish *Cherax destructor*, see Table 2). Nevertheless, comparisons of the total number of aesthetascs in diverse decapod species (Table 2) revealed that this number is relatively similar among shrimp group and other decapods of comparable size (the crayfish *Orconectes propinquus* or the crab *C. maenas*) (Table 2 and see Beltz et al. 2003 for more comprehensive data). Hydrothermal shrimp do not seem to present any specific adaptation regarding this character. The total number, as well as the size of aesthetascs seems related to the size of the animal rather than to its environment. Indeed, based on a study of 17 Reptentia decapods, Beltz et al. (2003) found a strong linear relationship between the number of aesthetascs and carapace

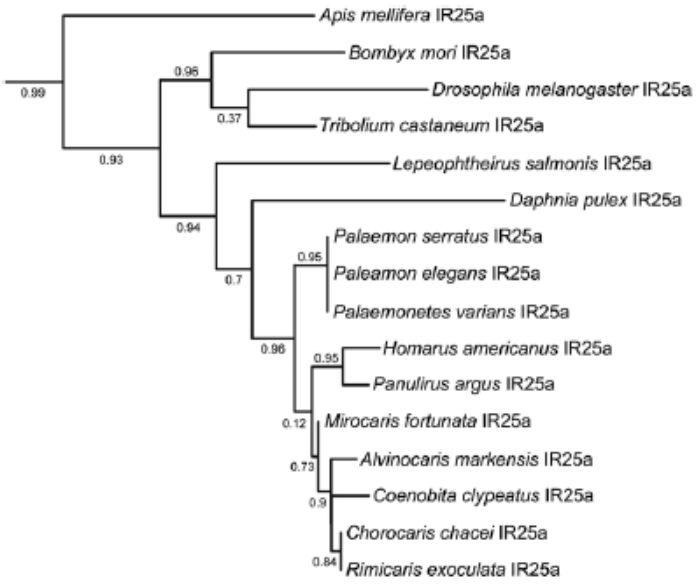

Figure 6. Detail of the IR25a clade of the IR phylogeny. This sub-tree is a zoom of the IR25a clade from the tree depicted in Figure 5.

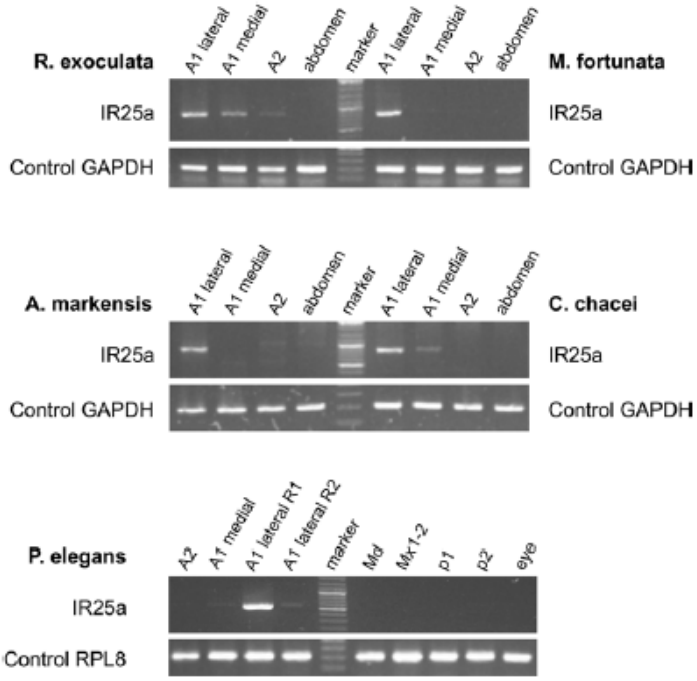

Figure 7. IR25a gene expression in hydrothermal vent shrimp Rimicaris exoculata, Mirocaris fortunata, Alvinocaris markensis, Chorocaris chacei, and in the coastal shrimp *P. elegans*. Control RT-PCR products for comparative analysis of gene expression correspond to the glycolysis enzyme GAPDH for hydrothermal vent shrimp, and to the ribosomal protein gene RPL8 for *P. elegans*. No amplification was detected in the absence of template (data not shown). A1, antennules; R1, internal ramus of the lateral antennular flagella; R2, external ramus of the lateral antennular flagella; A2, second antennae; Md, mandibles; Mx1-2, maxillae; p1 and p2, first and second walking legs.

length, which was also reported earlier for the crayfish *C. destructor* by Sandeman and Sandeman (1996). Among hydrothermal species, it can however be noted that the aesthetascs of *A. markensis* are longer than those of the 3 other species, with the maximum length being 2 to 4 times higher than for the 3 other species (see Supplementary Table S2). The adult hydrothermal shrimp lack the usual externally differentiated eye (eye-stalked), having instead a pair of large, highly reflective, dorsal organs (Van Dover et al. 1989). These modifications

have been reported to be an adaptation for the detection of extremely faint sources of light emitted by the vents (Pelli and Chamberlain 1989). These eyes are unusual in having no image-forming optics, but a solid wall of light-sensitive rhabdom containing rhodopsin, with the exception of *A. markensis*, which also lacks this photoreceptor and is completely blind (Wharton et al. 1997; Gaten et al. 1998). The longer olfactory sensilla observed in this species may possibly be interpreted as a development of the olfactory capacity to compensate for the lack of vision. Zhang et al. (2008) showed for *Lysmata* species that shrimp living in aggregations (*L. boggessi* and *L. wurdemanni*, 460 aesthetascs) possess a significantly higher number of aethetascs than pair-living species (*L. amboinensis* and *L. debelius*, 210 aesthetascs), suggesting a possible correlation between the number of aesthetascs and the social behavior. Our results do not support this hypothesis, since no significant differences were observed between vent species living in dense swarms (*R. exoculata*) and the others.

Most studies on olfaction in crustaceans have focused on aesthetascs. Several lines of evidence however suggest that non-aesthetasc bimodal chemosensilla (innervated by mecano- and chemo-receptive cells, also called distributed chemosensilla [Schmidt and Mellon 2011]) or non-olfactory sensilla (Derby and Weissburg 2014), distributed over both flagella of the antennules, as well as on the antennae, also play a role in the detection of water-borne chemicals (Guenther and Atema 1998; Cate and Derby 2001). Non-aesthetasc setae exhibit a wide variety of sizes and morphologies. These setae are named in the literature according to their morphology, size or location on the flagellum. For example, there are 9 setal types in *P. argus* (hooded, plumose, short setuled, long simple, medium simple, short simple, guard, companion, and asymmetric: Cate and Derby 2001), but only 1 type in the shrimp *Thor manningi* (curved simple: Bauer and Caskey 2006). The role of these setae is still poorly known and whether their diversity corresponds to a multiplicity of perceived stimuli remains an open question (Cate and Derby 2001; Derby and Steullet 2001). Among the shrimp studied here, the coastal shrimp *P. elegans* showed the highest diversity in non-aesthetasc setal types (5 setal types: short simple, long simple, beaked scaly, twisted flat, bifid) when compared with the 4 hydrothermal species (2 or 3 types). Among hydrothermal species, the setal types vary essentially by their size (long, intermediate or short) and less by their morphology (all simple in *Alvinocaris*, all beaked in *Rimicaris*, a mix of the 2 in *Chorocaris*, whereas *Mirocaris* exhibit more original morphologies [see Figures 2D and 2F]). At this point of our knowledge, it is difficult to explain the observed differences and even more to speculate on the functions of these different setae.

Surprisingly, dense bacterial populations were often observed on the antennae and antennules of the 4 hydrothermal shrimp (see e.g., *Mirocaris*, Figure 2C), sometimes even covering the whole surface of aesthetacs (not shown), whereas no bacterial coverage was ever observed in the coastal *P. elegans* specimens. The type of bacteria present on the antennae of hydrothermal shrimp, as well as their potential impact on olfaction or other role for the shrimp should be investigated in future studies.

Comparative expression of the putative olfactory co-receptor IR25a in hydrothermal vent and coastal shrimp

We identified, in the 4 alvinocaridid hydrothermal shrimp and in 3 palaemonid species (*P. elegans*, *P. varians*, and *P. serratus*), a member of the IR family, which was recently proposed to be involved in the odorant detection in crustaceans: the common IR25a subunit (Corey et al. 2013). In the 5 shrimp species tested, IR25a was predominantly expressed in the lateral antennular flagella that bear the aesthetascs olfactory sensilla (Figure 7), consistent with the expression pattern of this IR subunit in *H. americanus* (iGluR1, Stepanyan et al. 2004), *P. argus* (Corey et al. 2013), and *C. clypeatus* (Groh-Lunow et al. 2015). IR25a expression in other chemosensory tissues than the lateral antennular flagella varies amongst decapod crustacean species, with either no detection (for *M. fortunata*, *A. markensis*, *P. elegans*: this study; for *H. americanus*: Stepanyan et al. 2004), or detection in different organs (medial antennular flagella in *R. exoculata* and *C. chacei*: this study; mouth and 2 first walking legs in *P. argus*: Corey et al. 2013). Taken together, these results raise the question of whether IR25a may play a more general role in decapod crustacean chemosensation beyond just mediating odor detection (Corey et al. 2013), or if organs other than the aesthetascs bearing flagella can also have an olfactory role, as Keller et al. (2003) suggested for the antennae and walking legs of the blue crab *Callinectes sapidus*. According to several recent studies and reviews (Schmidt and Mellon 2011, Mellon 2014; Derby and Weissburg 2014; Derby et al. 2016), only the aesthetascs are considered as olfactory sensilla, which rather plead for the first hypothesis.

Among hydrothermal species, the different patterns of IR25a expression obtained for *R. exoculata* and *C. chacei* on one hand and for *M. fortunata* and *A. markensis* on the other hand, would suggest different chemosensory mechanisms in these 2 shrimp groups. This may be related to their diet and thus to their direct dependence to the hydrothermal fluid. Indeed, *Rimicaris* and *Chorocaris* to a lesser extent live in symbiosis with chemoautotrophic bacteria from which they derive all or part of their food (Segonzac et al. 1993; Ponsard et al. 2013), forcing them to stay permanently close to hydrothermal emissions to supply their bacteria in reduced compounds necessary for chemosynthesis. These 2 species are also phylogenetically closely related, which recently led Vereshchaka et al. (2015) to propose to synonymize all the genus *Chorocaris* with *Rimicaris*. On the other hand, *Mirocaris* and *Alvinocaris* are secondary consumers, scavenging on local organic matter and living at greater distances from the vent emissions. Regarding the IR25a expression pattern, the coastal shrimp *P. elegans* has a profile similar to hydrothermal secondary consumers *Mirocaris* and *Alvinocaris*, itself having an opportunistic omnivorous diet of invertebrate tissues.

In future studies, we will attempt to identify, and subsequently localize, other receptors of the IR family that could be involved in olfaction, and in particular the members generally found associated with IR25a (like IR93a and IR8a). We recently developed an electrophysiological method that allows the recording of shrimp ORNs activity (Machon et al. 2016). This method will be used to conduct a comparative study of the global antennule activity upon exposure to environmental stimuli, in the hydrothermal species *M. fortunata* and the coastal species *P. elegans*. An ultrastructural approach could help to refine the morphological comparison between hydrothermal and coastal species, by analyzing other characteristics like the number of ORNs per aesthetascs, the number of outer dendritic segments per ORNs or the aesthetasc cuticle thickness. This combined morphological and functional approach will provide insights into deep-sea vent shrimp olfaction, and ultimately in the potential adaptations of the sensory organs to their peculiar environment.

Supplementary Material

Supplementary data are available at *Chemical Senses* online.

Funding

This work was supported by the European Union Seventh Framework Programme (FP7/2007–2013) under the MIDAS project [grant agreement n° 603418].

Acknowledgments

The authors thank the electronic microscopy platform of the Institute of Biology Paris-Seine (IBPS), and especially V. Bazin and M. Trichet. We also thank the 2 chief scientist of the Momarsat 2011 and 2012 cruise M. Cannat and P. M. Sarradin, the chief scientist of the Biobaz 2013 (F. Lallier) and the Bicose 2014 (MA Cambon-Bonavita) cruises, as well as Jozée Sarrazin for hydrothermal shrimp sampling.

References

Abascal F, Zardoya R, Posada D. 2005. ProtTest: selection of best-fit models of protein evolution. *Bioinformatics*. 21(9):2104–2105.

Ache B. 1982. Chemoreception and thermoreception. In: Bliss D, editor, *The Biology of Crustacea*. Vol 3. New York: Academic Press. p. 369–398.

Anisimova M, Gascuel O. 2006. Approximate likelihood-ratio test for branches: a fast, accurate, and powerful alternative. *Syst Biol*. 55(4):539–552.

Bauer R, Caskey J. 2006. Flagellar setae of the second antennae in decapod shrimps: sexual dimorphism and possible role in detection of contact sex pheromones. *Invertebr Reprod Dev*. 49(1–2):51–60.

Beltz BS, Kordas K, Lee MM, Long JB, Benton JL, Sandeman DC. 2003. Ecological, evolutionary, and functional correlates of sensilla number and glomerular density in the olfactory system of decapod crustaceans. *J Comp Neurol*. 455(2):260–269.

Benton R, Vannice KS, Gomez-Diaz C, Vosshall LB. 2009. Variant ionotropic glutamate receptors as chemosensory receptors in *Drosophila*. *Cell*. 136(1):149–162.

Cate HS, Derby CD. 2001. Morphology and distribution of setae on the antennules of the Caribbean spiny lobster *Panulirus argus* reveal new types of bimodal chemo-mechanosensilla. *Cell Tissue Res*. 304(3):439–454.

Chamberlain S, Battelle B, Herzog E, Jinks R, Kass L, Renninger G. 1996. *Sensory neurobiology of hydrothermal vent shrimp from the Mid-Atlantic Ridge. Abstract*. FARA-IR Mid-Atlantic Ridge Symposium. Reykjavik, Iceland.

Corey EA, Bobkov Y, Ukhanov K, Ache BW. 2013. Ionotropic crustacean olfactory receptors. *PLoS One*. 8(4):e60551.

Cowan D. 1991. The role of olfaction in courtship behavior of the American lobster *Homarus americanus*. *Bio Bull*. 181:402–407.

Croset V, Rytz R, Cummins SF, Budd A, Brawand D, Kaessmann H, Gibson TJ, Benton R. 2010. Ancient protostome origin of chemosensory ionotropic glutamate receptors and the evolution of insect taste and olfaction. *PLoS Genet*. 6(8):e1001064.

De Busserolles F, Sarrazin J, Gauthier O, Gelinas Y, Fabri MC, Sarradin PM, Desbruyeres D. 2009. Are spatial variations in the diets of hydrothermal fauna linked to local environmental conditions? *Deep-Sea Res II*. 56:1649–1664.

Derby CD, Steullet P. 2001. Why do animals have so many receptors? The role of multiple chemosensors in animal perception. *Biol Bull*. 200(2):211–215.

Derby C, Steullet P, Horner A, Cate H. 2001. The sensory basis of feeding behavior in the Caribbean spiny lobster, *Panulirus argus*. *Mar Freshwater Res*. 52:1339–1350.

Derby C, Weissburg M. 2014. The chemical senses and chemosensory ecology of Crustaceans. In: Derby C, Thiel M, editors, *The Natural History of the Crustacea.- Vol. 3: Nervous Systems and Control Behavior*. New York: Oxford Univ. Press. p. 263–292.

Derby CD, Kozma MT, Senatore A, Schmidt M. 2016. Molecular mechanisms of reception and perireception in crustacean chemoreception: a comparative review. *Chem Senses*. 41(5):381–398.

Desbruyères D, Almeida A, Biscoito M, Comtet T, Khripounoff A, Le Bris N, Sarradin PM, Segonzac M. 2000. A review of the distribution of hydrothermal vent communities along the northern Mid-Atlantic Ridge: dispersal vs. environmental controls. *Hydrobiologia*. 440:201–216.

Desbruyères D, Biscoito M, Caprais JC, Colaço A, Comtet T, Crassous P, Fouquet Y, Khripounoff A, Le Bris N, Olu K, *et al*. 2001. Variations in deep-sea hydrothermal vent communities on the Mid-Atlantic Ridge near the Azores plateau. *Deep-Sea Res I*. 48:1325–1346.

Desbruyères D, Segonzac M, Bright M. 2006. Handbook of deep-sea hydrothermal vent fauna. Second completely revised edition. Linz (Austria): Denisia.

Devine D, Atema J. 1982. Function of chemoreceptor organs in spatial orientation of the lobster, *Homarus americanus*: differences and overlap. *Bio Bull*. 163:144–153.

Felgenhauer B. 1992. External anatomy and integumentary structures of the Decapoda. In: Harrison F, Humes A, editors, *Microscopic Anatomy of Invertebrates*. New York: Wiley-Liss. p. 7–43.

Fontaine M, Passelecq-Gerin E, Bauchau A. 1982. Structures chemoreceptrices des antennules du crabe *Carcinus maenas* (L.) (Decapoda Brachyura). *Crustaceana*. 43(3):271–283.

Gaten E, Herring P, Shelton P, Johnson M. 1998. The development and evolution of the eyes of vent shrimps (Decapoda: Bresiliidae). *Cah Biol Mar*. 39:287–290.

Gebruk A, Southward E, Kennedy H, Southward A. 2000. Food sources, behaviour, and distribution of hydrothermal vent shrimp at the Mid-Atlantic Ridge. *J Mar Biol Ass UK*. 80:485–499.

Gleeson R, Carr W, Trapido-Rosenthal H. 1993. Morphological characteristics facilitating stimulus access and removal in the olfactory organ of the spiny lobster, *Panulirus argus*: insight from the design. *Chem Senses*. 18(1):67–75.

Gleeson R, McDowell L, Aldrich H. 1996. Structure of the aesthetasc (olfactory) sensilla of the blue crab, *Callinectes sapidus*: transformations as a function of salinity. *Cell Tissue Res*. 284:279–288.

Groh K, Vogel H, Stensmyr M, Grosse-Wilde E, Hansson B. 2014. The hermit crab's nose—antennal transcriptomics. *Front Neurosci*. 7:Article 266. doi:210.3389/fnins.2013.00266.

Groh-Lunow K, Getahun M, Grosse-Wilde E, Hansson B. 2015. Expression of ionotropic receptors in terrestrial hermit crab's olfactory sensory neurons. *Front. Cell Neurosci*. 8:Article 448. doi:410.3389/fncel.2014.00448.

Grünert U, Ache B. 1988. Ultrastructure of the aesthetasc (olfactory) sensilla of the spiny lobster, *Panulirus argus*. *Cell Tissue Res*. 251:95–103.

Guenther C, Atema J. 1998. Distribution of setae on the *Homarus americanus* lateral antennular flagella. *Biol Bull*. 195:182–183.

Guindon S, Dufayard JF, Lefort V, Anisimova M, Hordijk W, Gascuel O. 2010. New algorithms and methods to estimate maximum-likelihood phylogenies: assessing the performance of PhyML 3.0. *Syst Biol*. 59(3):307–321.

Hallberg E, Johansson KU, Elofsson R. 1992. The aesthetasc concept: structural variations of putative olfactory receptor cell complexes in Crustacea. *Microsc Res Tech*. 22(4):325–335.

Hallberg E, Skog M. 2011. Chemosensory sensilla in Crustaceans. In: Breithaupt T, Thiel M, editors, *Chemical communication in Cristaceans*. New York: Springer Science+ Business Media. p. 103–121.

Herring P, Dixon DR. 1998. Extensive deep-sea dispersal of postlarval shrimp from a hydrothermal vent. *Deep-Sea Res I*. 45:2105–2118.

Hoagland P, Beaulieu S, Tivey M, Eggert R, German C, Glowka L, Lin J. 2010. Deep-sea mining of seafloor massive sulfides. *Marine Policy*. 34(3):728–732.

Hollins B, Hardin D, Gimelbrant AA, McClintock TS. 2003. Olfactory-enriched transcripts are cell-specific markers in the lobster olfactory organ. *J Comp Neurol*. 455(1):125–138.

Husson B, Sarradin P, Zeppilli D, Sarrazin J. 2016. Picturing thermal niches and biomass of hydrothermal vent species. *Deep-sea Res. II*. In press. doi:http://doi.org/10.1016/j.dsr2.2016.05.028

Jinks R, Battelle B, Herzog E, Kass L, Renninger G, Chamberlain S. 1998. Sensory adaptations in hydrothermal vent shrimps from the Mid-Atlantic Ridge. *Cah Biol Mar*. 39:309–312.

Katoh K, Toh H. 2010. Parallelization of the MAFFT multiple sequence alignment program. *Bioinformatics*. 26(15):1899–1900.

Keller T, Powell I, Weissburg M. 2003. Role of olfactory appendages in chemicammy mediated orientation of blue crabs. *Mar Ecol Prog Ser*. 261:217–231.

Lahman SE, Moore PA. 2015. Olfactory sampling recovery following sublethal copper exposure in the rusty crayfish, *Orconectes rusticus*. *Bull Environ Contam Toxicol*. 95(4):441–446.

Laverack MS. 1964. The antennular sense organs of *Panulirus argus*. *Comp Biochem Physiol*. 13:301–321.

Le SQ, Gascuel O. 2008. An improved general amino acid replacement matrix. *Mol Biol Evol*. 25(7):1307–1320.

Le Bris N, Govenar B, Le Gall C, Fisher C. 2006. Variability of physico-chemical conditions in 9 degrees 50' NEPR diffuse flow vent habitats. *Mar Chem*. 98(2–4):167–182.

Letunic I, Bork P. 2011. Interactive Tree Of Life v2: online annotation and display of phylogenetic trees made easy. *Nucleic Acids Res*. 39:W475–W478.

Machon J, Ravaux J, Zbinden M, Lucas P. 2016. New electroantennography method on a marine shrimp in water. *J Exp Biol*. 219(Pt 23):3696–3700.

McCall JR, Mead KS. 2008. Structural and functional changes in regenerating antennules in the crayfish *Orconectes sanborni*. *Biol Bull*. 214(2):99–110.

Mellon D Jr. 2012. Smelling, feeling, tasting and touching: behavioral and neural integration of antennular chemosensory and mechanosensory inputs in the crayfish. *J Exp Biol*. 215(Pt 13):2163–2172.

Mellon D. 2014. Sensory Systems of Crustaceans. In: Derby C, Thiel M, editors, *The Natural History of the Crustacea. Vol. 3: Nervous Systems and Control Behavior*. New York: Oxford Univ. Press.

Moore PA, Scholz N, Atema J. 1991. Chemical orientation of lobsters, *Homarus americanus*, in turbulent odor plumes. *J Chem Ecol*. 17(7):1293–1307.

Pelli DG, Chamberlain SC. 1989. The visibility of 350 degrees C blackbody radiation by the shrimp *Rimicaris exoculata* and man. *Nature*. 337(6206):460–461.

Pond DW, Segonzac M, Bell MV, Dixon DR, Fallick AE, Sargent JR. 1997. Lipid and lipid carbon stable isotope composition of the hydrothermal vent shrimp *Mirocaris fortunata*: evidence for nutritional dependance on photosynthetically fixed carbon. *Mar Ecol Prog Ser*. 157:221–231.

Ponsard J, Cambon-Bonavita MA, Zbinden M, Lepoint G, Joassin A, Corbari L, Shillito B, Durand L, Cueff-Gauchard V, Compère P. 2013. Inorganic carbon fixation by chemosynthetic ectosymbionts and nutritional transfers to the hydrothermal vent host-shrimp *Rimicaris exoculata*. *ISME J*. 7(1):96–109.

Renninger GH, Kass L, Gleeson RA, Van Dover CL, Battelle BA, Jinks RN, Herzog ED, Chamberlain SC. 1995. Sulfide as a chemical stimulus for deep-sea hydrothermal vent shrimp. *Biol Bull*. 189(2):69–76.

Sandeman R, Sandeman D. 1996. Pre- and postembryonic development, growth and turnover of olfactory receptor neurones in crayfish antennules. *J Exp Biol*. 199(Pt 11):2409–2418.

Sarradin P, Caprais J, Riso R, Kerouel R. 1999. Chemical environment of the hydrothermal mussel communities in the LuckyStrike and Menez Gwen vent fields, Mid Atlantic ridge. *Cah Biol Mar*. 40(1):93–104.

Sarrazin J, Juniper K, Massoth G, Lehgendre P. 1999. Physical and chemical factors influencing species distributions on hydrothermal sulfide edifices of the Juan de Fuca Ridge, northeast Pacific. *Mar Ecol Prog Ser*. 190:89–112.

Sarrazin J, Legendre P, De Brusserolles F, Fabri M, Guilini K, Ivanenko V, Morineaux M, Vanreusel A, Sarradin P. 2015. Biodiversity patterns, environmental drivers and indicator species on a High-temperature Hydrothermal edifice, mid-Atlantic ridge. *Deep-sea Res II*. 121:177–192.

Schmidt M, Ache B. 1996a. Processing of antennular input in the brain of the spiny lobster, *Panulirus argus*. I. Non-olfactory chemosensory and mechanosensory pathway of the lateral and median antennular neuropils. *J Comp Physiol A*. 178:579–604.

Schmidt M, Ache B. 1996b. Processing of antennular input in the brain of the spiny lobster, *Panulirus argus*. II. The olfactory pathway. *J Comp Physiol A*. 178:605–628.

Schmidt M, Mellon D. 2011. Neuronal processing of chemical information in crustaceans. In: Breithaupt T, Thiel M, editors, *Chemical communication in Cristaceans*. New York: Springer Science+ Business Media. p. 123–147.

Segonzac M. 1992. Les peuplements associés à l'hydrothermalisme océanique du Snake Pit (dorsale médio-Atlantique, 23°N, 3480m): composition et microdistribution de la mégafaune. *CR Acad Sci*. 314, série III:593–600.

Segonzac M, de Saint-Laurent M, Casanova B. 1993. L'énigme du comportement trophique des crevettes Alvinocaridídae des sites hydrothermaux de la dorsale médio-atlantique. *Cah Biol Mar*. 34:535–571.

Shabani S, Kamio M, Derby CD. 2008. Spiny lobsters detect conspecific blood-borne alarm cues exclusively through olfactory sensilla. *J Exp Biol*. 211(Pt 16):2600–2608.

Shillito B, Ravaux J, Sarrazin J, Zbinden M, Barthélémy D, Sarradin P. 2015. Long-term maintenance and public exhibition of deep-sea fauna: the AbyssBox Project. *Deep-Sea Res I*. 121:137–145.

Stein L, Bao Z, Blasiar D, Blumenthal T, Brent M, Chen N, Chinwalla A, Clarke L, Clee C, Coghlan A, *et al*. 2003. The genome sequence of *Caenorhabditis briggsae*: a platform for comparative genomics. *PLoS Biol*. 1(2):e45. doi:10.1371/journal.pbio.0000045.

Stepanyan R, Hollins B, Brock SE, McClintock TS. 2004. Primary culture of lobster (*Homarus americanus*) olfactory sensory neurons. *Chem Senses*. 29(3):179–187.

Steullet P, Dudar O, Flavus T, Zhou M, Derby CD. 2001. Selective ablation of antennular sensilla on the Caribbean spiny lobster Panulirus argus suggests that dual antennular chemosensory pathways mediate odorant activation of searching and localization of food. *J Exp Biol*. 204(Pt 24):4259–4269.

Tierney A, Thompson C, Dunham D. 1986. Fine structure of aethetasc chemoreceptors in the crayfish Oronectes propinquus. *Can J Zool*. 64:392–399.

The C. *elegans* Sequencing Consortium. 1998. Genome sequence of the nematode C. *elegans*: a platform for investigating biology. *Science*. 282(5396):2012–2018.

Van Dover C, Fry B, Grassle J, Humphris S, Rona P. 1988. Feeding biology of the shrimp *Rimicaris exoculata* at hydrothermal vents on the Mid-Atlantic Ridge. *Mar Biol*. 98:209–216.

Van Dover CL, Szuts EZ, Chamberlain SC, Cann JR. 1989. A novel eye in 'eyeless' shrimp from hydrothermal vents of the Mid-Atlantic Ridge. *Nature*. 337(6206):458–460.

Vereshchaka AL, Kulagin DN, Lunina AA. 2015. Phylogeny and new classification of hydrothermal vent and seep shrimps of the family alvinocarididae (decapoda). *PLoS One*. 10(7):e0129975.

Wharton D, Jinks R, Herzog E, Battelle B, Kass L, Renninger G, Chamberlain S. 1997. Morphology of the eye of the hydrothermal vent shrimp *Alvinocaris markensis*. *J Mar Biol Ass UK*. 77:1097–1108.

Zbinden M, Le Bris N, Gaill F, Compère P. 2004. Distribution of bacteria and associated minerals in the gill chamber of the vent shrimp *Rimicaris exoculata* and related biogeochemical processes. *Mar Ecol Prog Ser*. 284:237–251.

Zbinden M, Shillito B, Le Bris N, De Vilardi de Montlaur C, Roussel E, Guyot F, Gaill F, Cambon-Bonavita M-A. 2008. New insights on the metabolic diversity among the epibiotic microbial community of the hydrothermal shrimp *Rimicaris exoculata*. *J Exp Mar Biol Ecol*. 159(2):131–140.

Zhang D, Cai S, Liu H, Lin J. 2008. Antennal sensilla in the genus *Lysmata* (Caridea). *J Crust Biol*. 28(3):433–438.

Chemical Senses, 2018, Vol XX, 1–13
doi:10.1093/chemse/bjy041
Original Article
Advance Access publication 20 June 2018

OXFORD

Original Article

Comparison of Chemoreceptive Abilities of the Hydrothermal Shrimp *Mirocaris fortunata* and the Coastal Shrimp *Palaemon elegans*

Julia Machon[1], Philippe Lucas[2], Juliette Ravaux[1] and Magali Zbinden[1]

[1]Sorbonne Université, UPMC Univ Paris 06, MNHN, CNRS, IRD, UCBN, UAG, Unité de Biologie des organismes et écosystèmes aquatiques (BOREA, UMR 7208), Equipe Adaptations aux Milieux Extrêmes, 7 Quai Saint-Bernard, Bâtiment A, 75005 Paris, France and [2]Department of Sensory Ecology, INRA, iEES-Paris, Route de Saint-Cyr, 78026 Versailles, France

Correspondence to be sent to: Magali Zbinden, BOREA UMR7208, Sorbonne Université, Paris, France. e-mail: magali.zbinden@upmc.fr

Editorial Decision 12 June 2018.

Abstract

Chemoreception might play an important role for endemic shrimp that inhabit deep and dark hydrothermal vents to find food sources and to locate active edifices that release specific chemicals. We compared the chemosensory abilities of the hydrothermal shrimp *Mirocaris fortunata* and the coastal related species, *Palaemon elegans*. The detection of diverse ecologically relevant chemical stimuli by the antennal appendages was measured with electroantennography. The 2 species can detect food-related odor and sulfide, a short-distance stimulus, via both their antennae and antennules. Neither iron nor manganese, considered as long-distance stimuli, was detected by the antennal appendages. Investigation of the ultrastructure of aesthetasc sensilla revealed no specific features of the hydrothermal species regarding innervation by olfactory sensory neurons. Pore-like structures occurring in the aesthetasc cuticle and dense bacterial covering seem to be unique to hydrothermal species, but their potential link to chemoreception remains elusive.

Key words: aesthetasc, chemoreception, electroantennography, hydrothermal vent, sulfide

Introduction

Alvinocaridid shrimp are emblematic of deep hydrothermal vents in the Mid-Atlantic Ridge (MAR, Desbruyères et al. 2000, 2001). They inhabit patchy, ephemeral, and dark environments, depending on hot and potentially toxic fluid emissions. Several studies show that these shrimp possess a range of morphological, anatomical, and physiological adaptations to the hydrothermal environment, related to ectosymbiosis with bacteria (Casanova et al. 1993; Ponsard et al. 2013), respiration in sometimes hypoxic conditions (Lallier and Truchot 1997; Hourdez and Lallier 2007), or thermal stress (Cottin et al. 2010) for instance. However, adaptations of sensory systems have been only partially investigated (Jinks et al. 1998). Vent fauna communities are always spread around active chimneys, suggesting that they must detect attractants to choose their microhabitat, such as food sources or fluid emissions (Sarradin et al. 1999; Sarrazin et al. 1999; Le Bris et al. 2006). Among the sensory modalities that can be involved in the detection of the habitat, chemoreception might be relevant since active vents are characterized by an extensive release of various chemicals (Charlou et al. 2000). However, chemical attractants and vent shrimp chemosensory specificities are largely unknown, despite their importance for understanding how the shrimp detect their local dim environment, or new venting sites to settle in.

Considering food sources, invertebrate tissues or bacterial mats might be major attractants for scavenger species such as the hydrothermal shrimp *Mirocaris fortunata* (Gebruk et al. 2000). For the detection of hydrothermal fluid emissions, the chemicals released might be used as orientation cues. The chemical composition of fluids varies

were filled with *Panulirus* saline (PS, composition in chemical stimuli). The reference electrode was introduced through the soft articular membrane between the telson and the abdomen. The recording electrode was inserted with a NMN-25 micromanipulator (Narishige, London, United Kingdom) in the middle region of the flagellum area bearing the aesthetascs, between 2 aesthetasc rows, for the lateral flagellum of the antennule (referred as "antennule" further in the text), and between 2 annuli of the proximal region (first quarter) for the antenna. Signals were amplified (×100) and filtered (0.1–1000 Hz) using an EX1 amplifier with a 4002 headstage (Dagan, Minneapolis, MN), and digitized at 2 kHz by a 16-bit acquisition board (Digidata 1440A) under Clampex 10.3 (Molecular Devices, Sunnyvale, CA). Data were analyzed using Clampfit (Molecular Devices). Signals were low-pass filtered offline at 20 Hz.

A gravity-fed PS perfusion was positioned over the branchial cavity to maintain the shrimp alive. For *M. fortunata*, the PS perfusion was maintained at 9 ± 1 °C using ice packs. Chemical stimuli were delivered by a pressurized perfusion system with 8 channels (AutoMate scientific, Berkeley, CA). To prevent oxidation of the iron, manganese, and sulfide solutions within reservoirs, the system was pressurized under nitrogen gas. Reservoirs were connected to a segment (70 mm) of deactivated gas chromatography (GC) column (0.25 mm internal diameter). The tip of the GC column was positioned with a UM-3C micromanipulator at ~1 mm from the recorded flagellum, and ~45° from its longitudinal axis.

Stimuli were applied for 1 s at 5 psi (1.1 mL.min^{-1}). Consecutive stimuli were delivered with at least 90 s intervals to prevent chemosensory adaptation (Machon et al. 2016). In addition to continuous renewing of the PS bath solution with a gravity-fed perfusion, half of the medium was replaced after applying each stimulus with new PS using a 10 mL syringe. Between stimuli, the dead volume of the stimulus device (GC column) was rinsed outside of the Petri dish, first with PS and then with the solution of the next stimulus. To establish the dose–response relationship for each stimulus, stimuli were applied in increasing concentrations, always starting with the negative control (PS). Responses to the positive control (aqueous extract of shrimp food, see below) were applied at the end of the experiment to ensure the recording quality. Recordings of low quality were excluded from the analysis by discarding experiments for which the amplitudes of responses to the positive control were smaller than 0.3 and 0.08 mV for the antennule and the antenna, respectively. When responses to the negative control had different amplitudes at the beginning and at the end of an experiment, the average of the 2 values was used.

Chemical stimuli

PS was used to prepare all stimuli and as a negative control. The composition of PS was (in mmol.L^{-1}) 486 NaCl, 5 KCl, 13.6 $CaCl_2$, 9.8 $MgCl_2$, and 10 HEPES, pH: 7.8–7.9 (Hamilton and Ache 1983), with osmolarity adjusted to 1050 mOsm/L with mannitol.

An aqueous extract of shrimp Novo Prawn food pellets (NP) was used as positive control in all experiments. Food pellets were dissolved for 48 h at room temperature at 0.2 g.mL^{-1} in PS. The extract was then centrifuged at 5900 g for 10, 15, and 20 min and the supernatant was collected after each centrifugation and filtered (0.45 µm), aliquoted and stored at −20 °C until use.

Aqueous extracts of dead *M. fortunata* and dead *P. elegans* individuals were prepared in PS from material kept for 48 h at room temperature at approximately 75 mg.mL^{-1}. Extracts were then centrifuged at 2000 g with a Galaxy MiniStar microcentrifuge and the supernatant was filtered (0.45 µm), aliquoted and stored at −20 °C. Before use, pH was adjusted to 7.8–7.9 and solutions were diluted 10 and 100 times.

For stimuli characteristic of hydrothermal fluids (sulfide, iron, and manganese), dose–response relationships were established with concentrations in the range of those that *M. fortunata* is likely to encounter its environment (sulfide, 2–20 µmol.L^{-1}; iron, 0.2–2.5 µmol.L^{-1} [Sarrazin et al. 2015]; manganese, 0.004–4.8 µmol.L^{-1} [Aumond 2013]) to concentrations in the range of those of the hydrothermal fluid at the Lucky Strike vent site (sulfide, 2–15 mmol.L^{-1} [Renninger et al. 1995]; iron, 30–863 µmol.L^{-1}; manganese, 50–450 µmol.L^{-1} [Charlou et al. 2000]). To minimize oxidation, all solutions were prepared under a funnel connected to a nitrogen gas bottle, with PS previously deoxygenated by bubbling nitrogen for 5–10 min. All dilutions were made the day of use. Stimuli, concentrations, and controls used for EAG are given in Table 1.

In order to simulate the concentrations that *M. fortunata* encounters in its environment, stock solutions were prepared at 2 mmol.L^{-1} in deoxygenated PS, with pH adjusted to 2 for $FeCl_2$ (reference 372870, Sigma-Aldrich) and $MnCl_2$ (reference M8054, Sigma-Aldrich) solutions, and to 9 for Na_2S (reference 208043, Sigma-Aldrich) solution. Stock solutions were diluted with deoxygenated PS. The concentrations 40 µmol.L^{-1} for Na_2S and 5 µmol.L^{-1} for $FeCl_2$ and $MnCl_2$ correspond to the estimated concentrations in the environment of *M. fortunata* (Sarrazin et al. 2015 for iron and sulfide, Aumond 2013 for manganese). For higher concentrations, 4 concentrations were chosen on a logarithmic scale, the lowest corresponding to the estimated concentration in the environment of *M. fortunata*, and the second highest corresponding to the concentration measured in the pure fluid at the Lucky Strike vent site (Charlou et al. 2000). Solutions were prepared in deoxygenated PS with serial dilutions from the highest concentration. For $FeCl_2$ solutions, pH was adjusted to 6 to avoid iron precipitation. PS adjusted to pH 6 was used as a pH control for $FeCl_2$ stimulation series, and PS adjusted to pH 11 was used as a pH control for Na_2S stimulation series, to match the pH of the highest concentrated Na_2S solution (14 mmol.L^{-1}).

Statistical analysis

For EAG data, 1-way ANOVA with permutation test was used to test differences among amplitudes of EAG responses to concentrations of each stimulus. For significant results, 2-sided 2-sample permutation test using Welsh's t test was performed to investigate the difference with the negative control for each concentration. Data are given as means (standard deviation [SD]).

Data analyses were carried out using RStudio v.1.0.136 software.

Transmission electron microscopy

For anatomical observations, lateral flagella of the antennules were used. Tissues were postfixed in osmium tetroxide 1%, dehydrated in ethanol and propylene oxide series, and further embedded in epoxy resin (Agar Scientific). Ultrathin sections were made from the middle region of lateral flagella on a Leica Ultramicrotome (Ultracut R) using a diamond knife, and were laid on 150 or 200-mesh copper grids and stained with saturated solution of uranyl acetate at 60 °C. Observations were carried out on a Hitachi H7100 transmission electron microscope operating at 75 kV.

Ultrastructural analysis

Anatomical traits of the aesthetascs, the cuticle thickness and the number of inner and outer dendritic segments (respectively IDSs and ODSs; Figure 1), were estimated from TEM observations, using ImageJ software. Measurements of cuticle thickness were made on sections at various levels of 20 and 30 aesthetascs for *M. fortunata* (5 individuals)

Table 1. Solutions and number (*n*) of antennules and antennae tested for each condition in EAG

Stimulus	Concentrations, dilutions, controls	*N*			
		Antennules		Antennae	
		Mirocaris fortunata	*Palaemon elegans*	*Mirocaris fortunata*	*Palaemon elegans*
Figure 2					
Shrimp food extract	0.2 g.mL^{-1}	44	58	13	27
PS	—				
Dead shrimp extract	Non-diluted; 1:10; 1:100	7	8	—	—
Figure 3					
Na_2S	PS (negative control)	9	12	4	8
	PS pH 11 (pH control)	4	7	4	8
	0.04, 0.1, 0.4, 1, 4 µmol.L^{-1}	5	5	—	—
	40 µmol.L^{-1}	8	12	4	8
	300, 2000, 14 000 µmol.L^{-1}	4	7	4	8
$FeCl_2$	PS (negative control)	11	15	5	9
	PS pH 6 (pH control)	6	10	5	9
	0.05, 0.1, 0.5, 1 µmol.L^{-1}	5	5	—	—
	5 µmol.L^{-1}	10	15	5	9
	60, 900, 10 000 µmol.L^{-1}	6	10	5	9
$MnCl_2$	PS (negative control)	10	17	4	10
	0.05, 0.1, 0.5, 1 µmol.L^{-1}	5	6	—	—
	5 µmol.L^{-1}	9	17	4	10
	50, 500, 3500 µmol.L^{-1}	5	11	4	10

and *P. elegans* (4 individuals), respectively. Data for cuticle thickness are given as minimum and maximum values. The number of IDSs per aesthetasc was estimated from counts in several 25 to 150 µm^2 portions of sections from the base of the sensilla, on 11 and 13 aesthetascs for *M. fortunata* (3 individuals) and *P. elegans* (2 individuals), respectively. The number of ODSs per aesthetasc was estimated from counts in several 4 to 30 µm^2 portions of the sensilla judged to contain the highest number of ODSs containing single microtubules, on 7 and 28 aesthetascs for *M. fortunata* (4 individuals) and *P. elegans* (4 individuals), respectively. Data for IDS and ODS are given as range.

Results

EAG responses to chemicals

Stimulations of the antennal appendages with a shrimp food extract (NP, positive control) always triggered positive deviations of the baseline (Figure 2A). Antennular responses to NP extract had a significantly higher amplitude in *P. elegans* than in *M. fortunata*. By contrast, the amplitude of antennal responses to the NP extract were significantly higher in *M. fortunata* than in *P. elegans*. Responses to the negative control (PS) were always negative deviations of the baseline for the antennule, but were either positive or negative for the antenna (Figure 2B). Responses to PS from the antenna were much lower than responses from the antennule for both species.

Responses of the antennule to dead shrimp extracts were dose-dependent (Figure 2C), with a threshold dilutions between 1:100 and 1:10 for *P. elegans*, and between 1:10 and non-diluted for *M. fortunata*, and amplitudes reaching 250 and 70 µV for the non-diluted extract for *P. elegans* and *M. fortunata*, respectively.

At concentrations of *M. fortunata* environment, for the stimuli tested (Na_2S: 0.04–40 µmol.L^{-1}; $FeCl_2$ and $MnCl_2$: 0.05–5 µmol.L^{-1}) responses from the antennule of *M. fortunata* and *P. elegans* did not depend on stimulus concentrations (Figure 3A,C,E, white bars).

At higher concentrations, Na_2S elicited dose-dependent responses from both the antennules and antennae of *M. fortunata* and *P. elegans* (Figures 3A,B and 4). Thresholds were between 0.3 and 2 mmol.L^{-1} for the antennules of both species and for the antennae of *M. fortunata*, and between 2 and 14 mmol.L^{-1} for the antennae of *P. elegans*. For *M. fortunata*, amplitudes for the highest concentration (14 mmol.L^{-1}) reached 120 µV for the antennule and 50 µV for the antenna. For *P. elegans*, they reached 20 µV for the antennule and 110 µV for the antenna. Increasing concentration of $FeCl_2$ (0.005–10 mmol.L^{-1}) and $MnCl_2$ (0.005–3.5 mmol.L^{-1}) solutions did not trigger dose-dependent responses from the antennules and the antennae (Figure 3C,D,E,F) for both species.

pH control solutions were used to distinguish responses triggered by the chemicals or by the pH of the solutions (pH 11 for Na_2S 14 mmol.L^{-1}, and pH 6 for all high concentration $FeCl_2$ solutions). Mean response of *P. elegans* antennae to pH control solution (pH: 11) significantly differed from the negative control (PS) and from the response to the highest Na_2S concentration (14 mmol.L^{-1}) (Figure 3B). This pH control solution did not trigger response different from the negative control (PS) for the antenna of *M. fortunata*, and for the antennules of the 2 species (Figure 3A,B). The pH control solution for high concentration $FeCl_2$ series (pH 6) did not elicit any significant response for both antennae and antennules for the 2 species (Figure 3C,D).

Aesthetascs cuticle and innervation

The thickness and ultrastructure of the cuticle of aesthetascs vary over the length of the sensilla (Table 2). From the base to the transitional zone (see Figure 1), the aesthetasc cuticle is thick for the 2 species, from 0.8 to 1.8 µm (minimum and maximum values) in *M. fortunata* and from 0.6 to 1.3 µm in *P. elegans*. Just distal to the transitional zone, in *P. elegans* the cuticle becomes thin (0.6–0.3 µm) on almost all the distal part of the sensilla (80% of the length), with the cuticle at the tip of the aesthetasc thinning to 0.15 µm. In

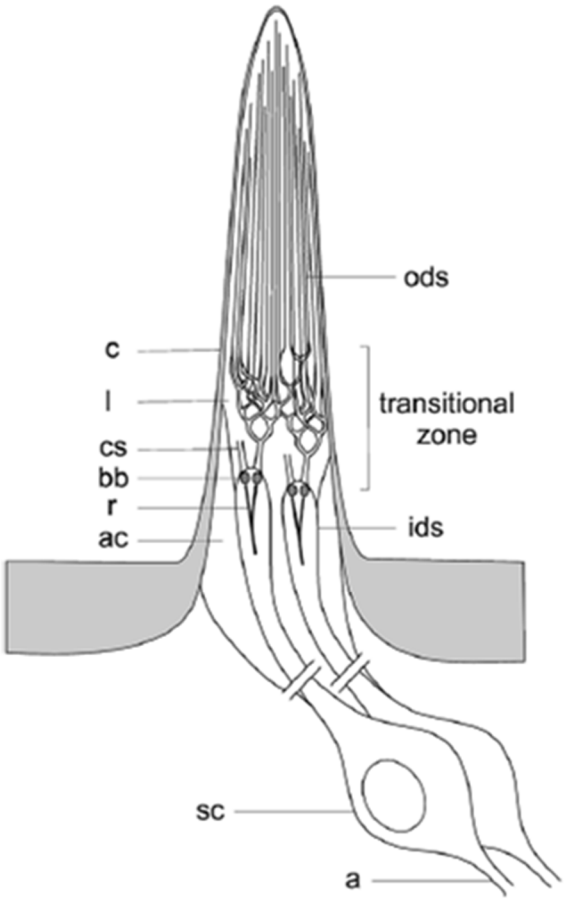

Figure 1. Schematic representation of an aesthetasc from a marine crustacean decapod. Only 2 of approximately 100–400 bipolar olfactory sensory neurons that innervate each aesthetasc are shown, and for each neuron only 1 cilium branching is shown. The transitional zone refers to the zone where the inner dendritic segments give rise to 2 ciliary segments, each starting to divide dichotomously in outer dendritic segments. Axon (a); accessory cell (ac); basal bodies (bb); cuticle (c); ciliary segment (cs); inner dendritic segment (ids); outer dendritic segment (ods); ciliary rootlet (r); lumen (l); sensory cell somata (sc). Not to scale.

M. fortunata the cuticle remains thick on the first half of the aesthetasc length, and becomes thin on the distal half of the sensilla, from 0.8 to 0.15 µm. For each species, the thick cuticle has a lamellar structure (Figure 5A,B), which gradually becomes loose when thinning (Figure 5C,D). In *M. fortunata*, pore-like structures occur in the lamellar cuticle (Figures 5A,E and 6C). They can reach approximately 0.2 µm in diameter, open to the inner side of the aesthetasc and are separated from the outside by a cuticle layer that thins from 0.4 to 0.06 µm. They are present from the transitional zone to approximately 50 % of the aesthetasc length, when the cuticle starts to thin, and are no longer present in the loose part of the cuticle (Figure 5C). These pore-like structures were also observed in the same region of the aesthetascs in the hydrothermal shrimp *R. exoculata* (Figure 5F), with a diameter slightly larger (up to 0.4 µm). For these 2 hydrothermal species, the aesthetascs are often covered by bacteria (Figure 5C,E,F) over their entire length. Neither pore-like structures, nor bacteria have ever been observed in *P. elegans*.

A schematic view of the dendrites regionalization (with IDSs, ODSs, and transitional zone) within an aesthetasc is presented in Figure 1. IDSs are surrounded by auxiliary cells (Figure 6B) and extend into the lumen of the aesthetasc, where they terminate at various levels within the transitional zone. They contain mitochondria, microtubules, vesicles, and a ciliary rootlet (Figure 6A,B). Each aesthetasc contains approximately 90 to 223 IDSs for *M. fortunata* and 177 to 519 IDSs for *P. elegans*, meaning each aesthetasc is innervated by approximately 90 to 223 and 177 to 519 OSNs for *M. fortunata* and *P. elegans*, respectively (Table 2). ODSs are not surrounded by auxiliary cells, the remaining area is filled with lymph (Figure 6C,D). Swellings occur along the entire length of the outer dendritic segments (Figure 6C,D). There is approximately 2545 to 5383 and 1568 to 10637 ODSs per aesthetasc for *M. fortunata* and *P. elegans*, respectively (Table 2).

Discussion

Detection of food-related odor mixtures

M. fortunata exhibits an opportunistic feeding behavior, scavenging on tissues of mussel, shrimp, and other invertebrates when available, as well as grazing bacteria on sulfide surfaces (Gebruk et al. 2000; Colaço et al. 2002; Busserolles et al. 2009). We used an extract of dead *M. fortunata* as an environmental relevant food-odor stimulus to test whether the detection of food is mediated by the antennule for this species. This stimulus elicited dose-dependent responses from the antennule, confirming its presumed role in food detection. An extract of dead *P. elegans* also stimulated the antennule of *P. elegans*. These results are consistent since *P. elegans* and *M. fortunata* have a similar food profile, being secondary consumers. EAG responses to positive control (NP), from both the antennule and the antenna, suggest that the antenna is also involved in the chemodetection of food sources in both species. The detection of food sources by the antennal appendages of *M. fortunata* indicates that this hydrothermal species may rely on food-related odors to detect its habitat as can do coastal species, but the influence of food stimuli in maintaining shrimp around vent chimneys need to be further investigated with behavioral experiments.

Detection of hydrothermal fluid stimuli

Chemicals and their concentrations were chosen regarding the chemical composition of the hydrothermal fluids (Radford-Knoery et al. 1998; Charlou et al. 2000) and in the shrimp vicinity (Aumond 2013; Sarrazin et al. 2015) at the Lucky Strike hydrothermal vent site, where *M. fortunata* specimens were sampled. Each chemical presents different removal rates, associated to reaction with seawater, other hydrothermal fluid constituents, dissolved organic matter, and to consumption by chemoautotrophic bacteria. Sulfide removal rate is high and sulfide is thus considered as a short-distance stimulus, detectable near hydrothermal fluid emission points, whereas manganese and iron are more stable, detectable far from the source, thus are considered as long-distance stimuli (Radford-Knoery et al. 1998; Aumond 2013; Waeles et al. 2017). To investigate if vent shrimp use such hydrothermal fluid compounds as orientation cues for both near-field and distant perception of the habitat, we tested the detection of selected chemicals by the antennular and antennal appendages of *M. fortunata*, as well as those of the coastal shrimp *P. elegans*, to check for potential hydrothermal shrimp specificity. Each chemical was first tested on the antennules at concentrations that *M. fortunata* is likely to encounter in its environment, but none elicited responses distinct from responses to the negative control.

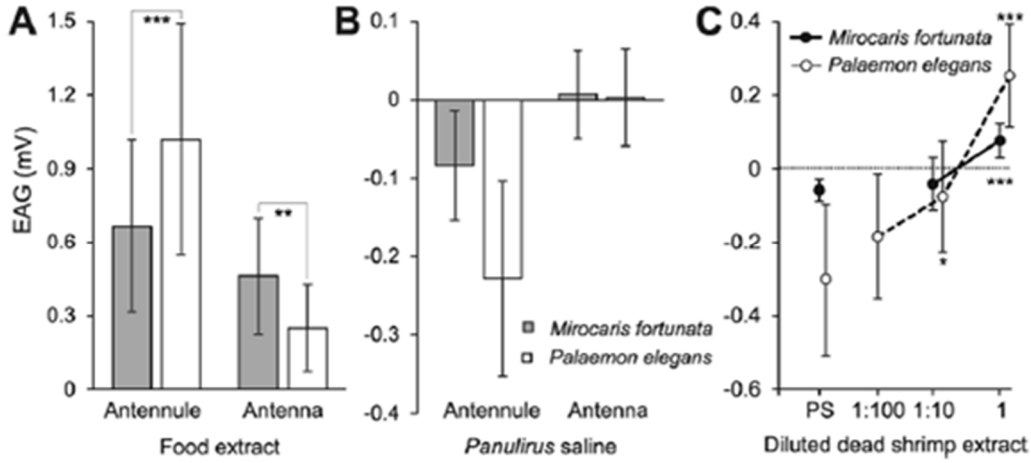

Figure 2. EAG responses to food extract stimulus, to negative control, and to dead shrimp extracts. Responses to (A) a shrimp food extract 0.2 g.mL^{-1} and to (B) PS (negative control) recorded from the antennules and antennae (gray, *Mirocaris fortunata*; white, *Palaemon elegans*), and to (C) dead shrimp extracts recorded from the antennules. For (A) and (B), means (SD) were compared between 2 species for each organ and stimulus with a 2-sample permutation *t*-test. For (C), means (SD) were compared with a 1-way ANOVA with permutation test ($P < 10^{-15}$) and with a 2-sample permutation *t*-test to control stimuli (PS). $^{**}P < 0.01$, $^{***}P < 0.005$. The *n* numbers of antennules and antennae tested for each species and for each condition are presented in Table 1.

We then used high concentrations, up and beyond to the concentrations measured in the pure fluid of the Lucky Strike vent site, on the antennule and antenna of both species. Sulfide elicited responses in a concentration-dependent manner for both the antennules and the antennae in *M. fortunata*. Thus sulfide is detected by bimodal sensilla from the antennae, but for the antennules we cannot distinguish the role played by aesthetascs and bimodal sensilla in sulfide detection. Renninger et al. (1995) recorded trains of action potentials from nerve fibers of the 3 antennal appendages of the hydrothermal shrimp *R. exoculata*, and found that only the antennae respond in a graded way to sulfide. This absence of concentration-dependent responses for the antennule in *R. exoculata* might be due to technical limitations rather than no detection. Recording from nerve fibers implies that only a fraction of axons are connected to the electrode opening, and thus action potentials are recorded from only a minority of neurons. The EAG method overcomes this problem since the electrode records neuron activation from almost the whole length of the flagellum (Machon et al. 2016). Hence at least 2 hydrothermal shrimp species are physiologically able to detect sulfide via their antennal appendages, supporting the hypothesis that sulfide could serve as an effective orientation cue at short distance of the hydrothermal vent. Yet because the sulfide concentrations that triggered significant EAG responses were equivalent to those encountered in the pure fluid, there is some doubt about the ecological relevance of the responses obtained since *M. fortunata* inhabits diffuse vents with low chemical concentrations (Cuvelier et al. 2011), and *R. exoculata* lives closer to vent chimneys but still in fluid-diluted areas. However, convergence of sensory inputs onto higher-level neurons occurs in the chemosensory pathway of crustaceans (Mellon 2000), as in vertebrates and insects (Van Drongelen et al. 1978). This convergence makes second-order neurons in the central nervous system more sensitive than peripheral chemosensory neurons (Rospars et al. 2014). Hence, behavioral responses to chemical stimuli can potentially be observed at concentrations that do no trigger EAG responses, and questions regarding the relevance of the sulfide concentrations tested could be addressed with behavior experiments. Antennules and antennae of the coastal shrimp *P. elegans* were also responsive to sulfide in this study, meaning that sulfide detection is not specific to vent species and is likely not an adaptation to the hydrothermal environment. Again, behavior experiments are needed to investigate if hydrothermal species present specific responses to sulfide, such as attraction behavior, compared to coastal species.

P. elegans antenna was also significantly responsive to a control pH 11 stimulus, as observed by Renninger et al. (1995) for the coastal shrimp *Palaemonetes aztecus* antenna exposed to a pH 13 stimulus. But the response to pH 13 in *P. aztecus* was not significantly different from the response to a pH 13 sulfide solution (1300 mmol.L^{-1}). In this study, response of the antenna in *P. elegans* to pH 11 significantly differs in amplitude from the response to pH 11 sulfide solution (Na_2S 14 mmol.L^{-1}), meaning there is detection of both sulfide and high pH by the antenna of *P. elegans*. The confounded responses to sulfide and pH 13 stimulus in *P. aztecus* (Renninger et al. 1995) might be due to the low number of specimens tested ($1 < n < 4$), insufficient to bring out a significant difference between these 2 stimuli. Responses to high pH stimuli could be specific to coastal species, because neither *M. fortunata* antenna (this study) nor *R. exoculata* antenna (Renninger et al. 1995) were significantly responsive to basic pH solutions. However, in shallow habitats extreme pH are rarely encountered and may appear as ecologically irrelevant stimuli that should not evoke any behavioral response (Puri and Faulkes 2010). Note that pH 11 stimulus was used in this study as a control for the highest concentrated sulfide solution, not as a pH stimulus. To investigate the detection of pH variations as an orientation cue for hydrothermal shrimp, acid pH solutions should be tested because in Lucky Strike hydrothermal fluid pH ranges from 3.84 to 6.45 (Charlou et al. 2000), and from 6.1 to 7.3 in the shrimp habitat (Desbruyères et al. 2001).

Detection of manganese and iron by a vent shrimp was tested here for the first time, and the 2 stimuli did not trigger responses at any concentration tested. This suggests but does not definitely proves that shrimp cannot detect these compounds since the sensitivity of the EAG method is limited. EAG represents the summation of receptor potentials generated by many sensory neurons responding simultaneously (Nagai 1985). Thus, if iron and manganese stimulate only a low number of chemosensory neurons, the sensitivity of the EAG

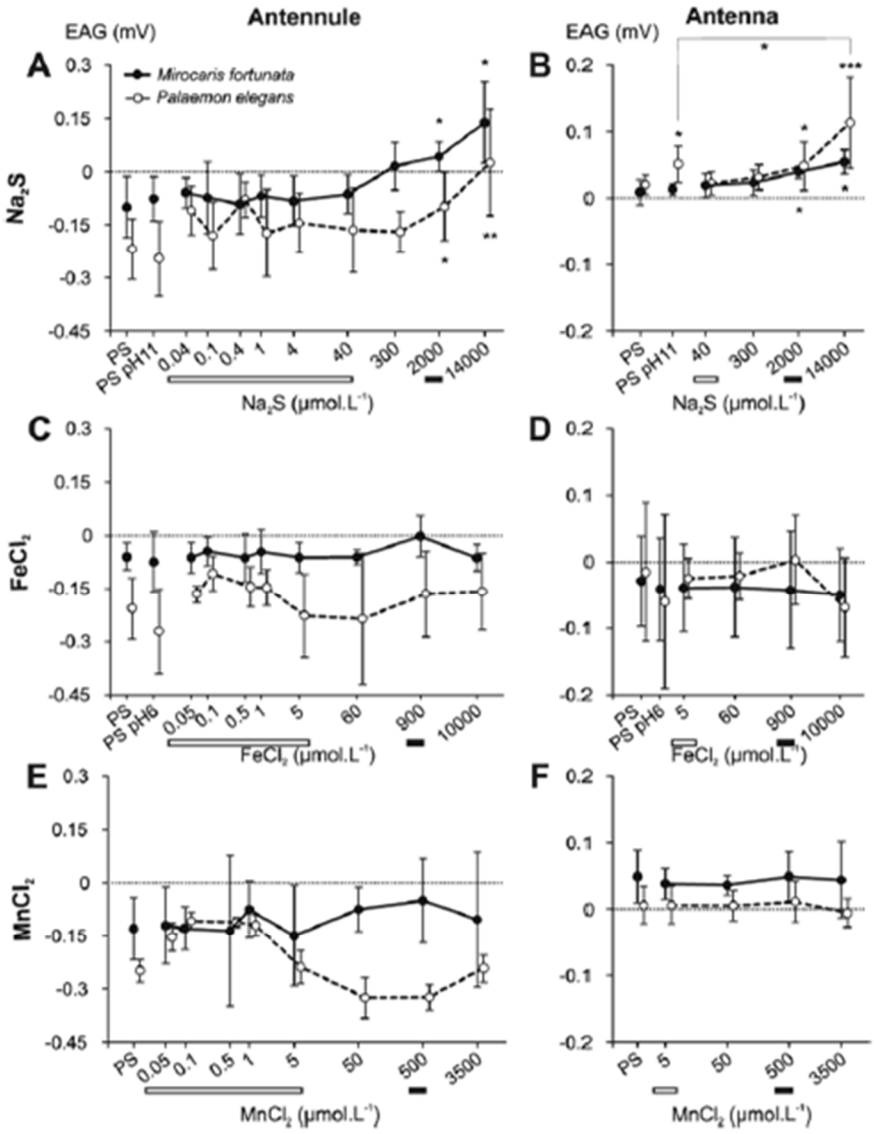

Figure 3. EAG responses from the antennules and the antennae to hydrothermal fluid compounds. EAG responses to increasing concentrations for Na_2S, $FeCl_2$, and $MnCl_2$ in *Mirocaris fortunata* (black dots) and *Palaemon elegans* (white dots). (A) Responses to Na_2S recorded from the antennules. (B) Responses to Na_2S recorded from the antennae. For (A) and (B), pH control is set to 11 and corresponds to the pH of the 14 000 µmol.L^{-1} Na_2S solution. (C) Responses to $FeCl_2$ recorded from the antennules. (D) Responses to $FeCl_2$ recorded from the antennae. For (C) and (D) pH control is set to 6 and corresponds to the pH of the 5–10000 µmol.L^{-1} $FeCl_2$ solutions. (E) Responses to $MnCl_2$ recorded from the antennules. (F) Responses to $MnCl_2$ recorded from the antennae. Under the *x* axis, white bars indicate concentrations that *M. fortunata* is likely to encounter in its environment, and black bars indicate concentrations measured in the pure fluid at the Lucky Strike vent field. Means (SD) were compared with a 1-way ANOVA with permutation test ($P < 10^{-15}$ for sodium sulfide dose-responses) and with a 2-sample permutation *t*-test to control stimuli (PS). *$P < 0.05$, **$P < 0.01$, ***$P < 0.001$. The *n* numbers of antennules and antennae tested for each species and for each condition are presented in Table 1.

method is most likely not sufficient to detect a response. However, the alternative that manganese and iron are actually not detectable by vent shrimp raises questioning about the relative importance of chemoreception for these animals. Manganese and iron are relevant stimuli for long-distance detection of hydrothermal fluids, which is a fundamental issue regarding vent shrimp lifestyle. Because hydrothermal vents are dynamic and ephemeral ecosystems, vent animals need to detect new venting sites to settle in, and the extremely high abundances of shrimp on MAR sites (Polz et al. 2003; Martin and Haney 2005) suggest that they are successful colonizers. Which fluid attractants are used for the long-distance detection of active sites, in addition to which stage of life are involved (Herring and Dixon 1998; Tyler and Young 2003), is still uncertain. Since sulfide, although emblematic of vent chemicals, is not a relevant stimulus in this context, the prospective that vent shrimp cannot detect manganese and iron makes the distant chemodetection of hydrothermal

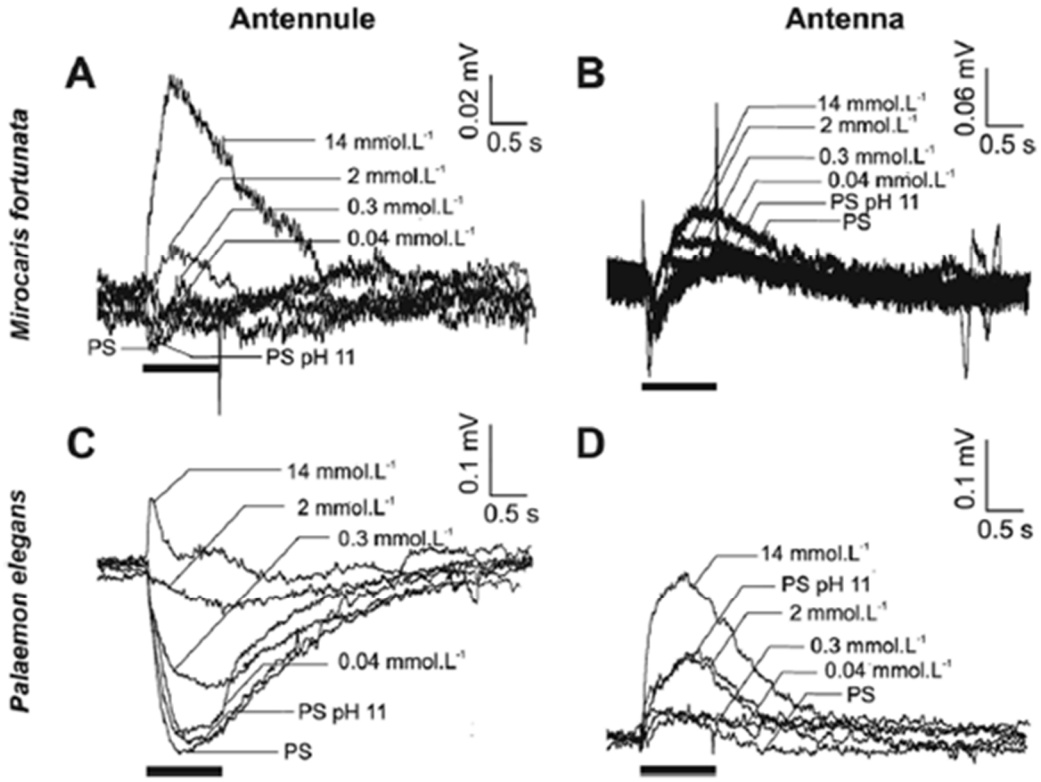

Figure 4. Dose-dependent EAG responses to Na_2S solution from the antennule and the antenna of the 2 shrimps. Superimposed traces of EAG responses to PS, to increasing concentrations of Na_2S (0.04, 0.3, 2, 14 mmol.L^{-1}) and to pH control solution (PS at pH 11) from the antennule (A, C) and the antenna (B, D) in *Mirocaris fortunata* (A, B) and *Palaemon elegans* (C, D). Horizontal bars indicate stimulus delivery. Transient peaks in A, B, and D are valve opening artifacts.

Table 2. Comparison of cuticle thickness and number of IDSs and ODSs in aesthetascs of marine crustacean decapod species

Species	Thickness of "thick" cuticle (µm)	Thickness of "thin" cuticle (µm)	Number of IDSs per aesthetasc[a]	Number of ODSs per aesthetasc[a]	References
Marine crab					
Cancer productus	2.1	1.1	100	—	Ghiradella et al. 1968
Callinectes sapidus	—	—	105	1420	Gleeson et al. 1996
Marine hermit crab					
Pagurus hirsutiusculus	1.3	0.4	400	6000–8000	Ghiradella et al. 1968
Spiny lobster					
Panulirus interruptus	4	1	300	—	Spencer and Linberg 1986
Panulirus argus	3	0.8	300–350	8000–10 000	Grünert and Ache 1988
Caridean shrimp					
Palaemon adspersus	1	0.4	—	—	Solari et al. 2017
Palaemon elegans	1.3	0.14	177–519	1568–10 637	This study
Mirocaris fortunata	1.5	0.15	90–223	2545–5383	This study

[a]Estimations presented as range.

plume doubtful. Detection of other long-distance relevant chemicals such as methane (de Angelis et al. 1993) should be tested, as well as other possible long-distance attractants such as noise (Crone et al. 2006) or temperature (Baker et al. 2016). Chemoreception abilities of other life stages should also be investigated, although larval dispersal is thought to play a role in colonization processes (Lutz et al. 1984) and aesthetasc sensilla are present in Alvinocaridid first zoeal stages (Hernandez-Avila et al. 2015).

Comparison of aesthetasc cuticle and innervation

Differences in chemosensitivity between 2 species, as specific adaptations to a particular environment, may be reflected by anatomical dissimilarities (Beltz et al. 2003). Although the general organization of aesthetascs and OSNs is analogous between decapod species (Ghiradella et al. 1968), the aesthetasc cuticle thickness and the numbers of IDSs and ODSs can vary. The cuticle thickness relates to the permeability of the aesthetasc, thus the ability to detect

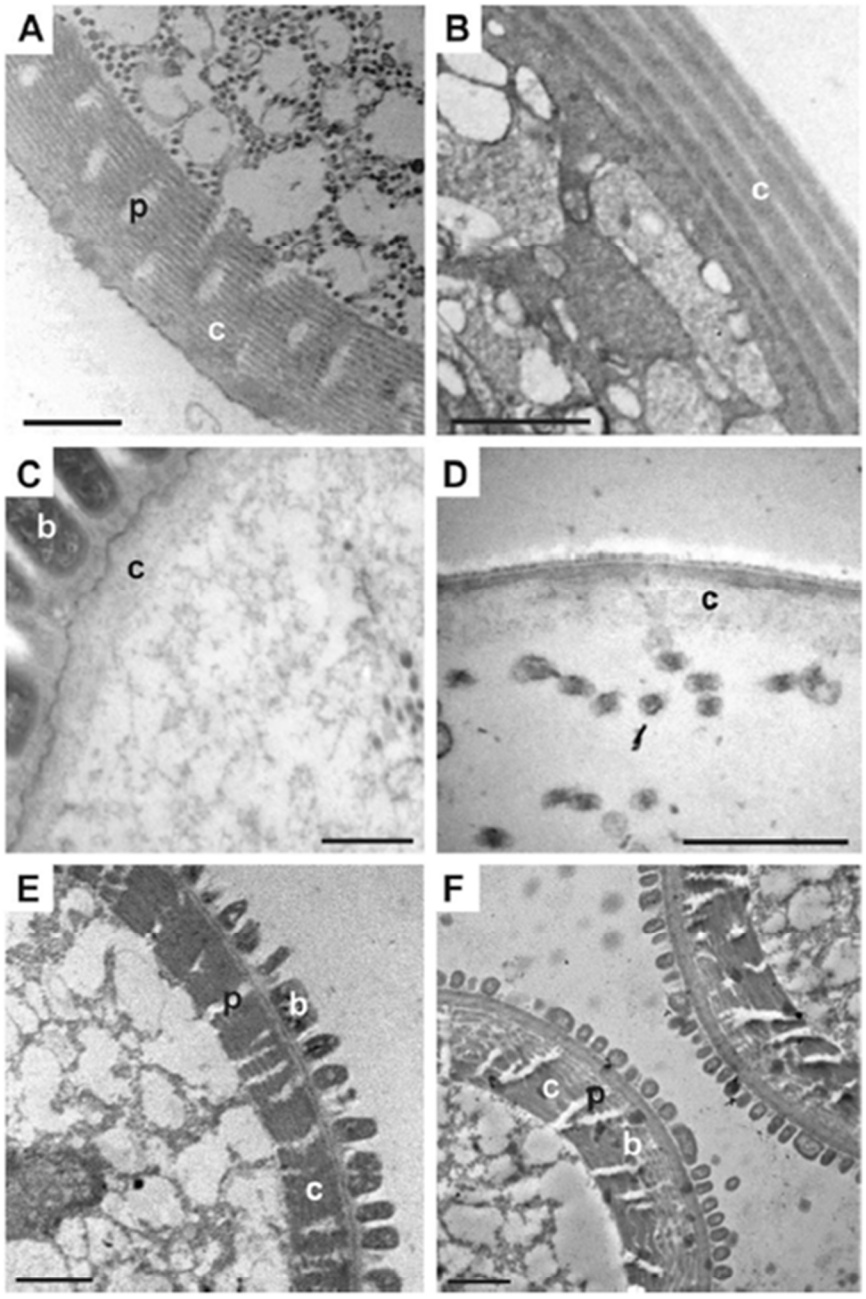

Figure 5. Cuticle of aesthetasc sensilla of *Mirocaris fortunata* (A, C, E), *Palaemon elegans* (B, D), and *Rimicaris exoculata* (F). Cross sections through the base (B), the middle (A, E, F), and the apex region (C, D) of the aesthetascs. Bacterium (b); cuticle (c); pore-like structure (p). Scale bar = 1 μm.

soluble odorants. IDSs and ODSs refer respectively to the number of OSNs and dendrites innervating the aesthetasc, and could be linked to odorant discrimination ability (Derby and Weissburg 2014). Aesthetasc ultrastructure has been well described for several decapod models (Table 2; Laverack and Ardill 1965; Ghiradella et al. 1968; Snow 1973; Hallberg and Chaigneau 2004), but for caridean shrimp species only the aesthetasc external morphology is described (Table 2; Bauer 1977; Hallberg et al. 1992; Mead 1998; Obermeier and Schmitz 2004; Zhang et al. 2008; Zhu et al. 2011; Solari et al. 2017; Zbinden et al. 2017) and no information is available on the ultrastructure. Aims of the present approach were to investigate potential specificities of the hydrothermal shrimp chemosensory system regarding the aesthetasc cuticle structure and innervation, as well as to provide observations on shrimp aesthetasc ultrastructure to enhance the general knowledge on decapods olfactory systems diversity.

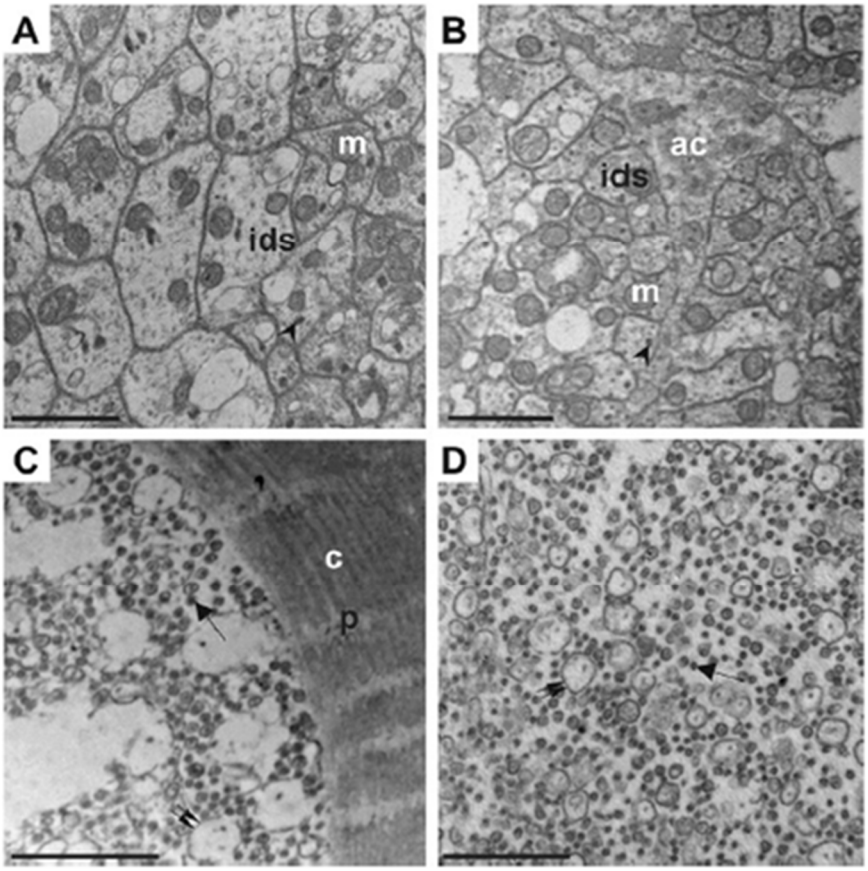

Figure 6. Inner and outer dendritic segments of aesthetasc sensilla of *Mirocaris fortunata* (A, C) and *Palaemon elegans* (B, D). Cross sections through the base (A, B) and the middle (C, D) region of the aesthetasc, showing the inner and outer dendritic segments, respectively. Cuticle (c); auxiliary cell (ac); inner dendritic segment (ids); mitochondrion (m); outer dendritic segment (arrow); pore-like structure (p); ciliary rootlet (arrow head); swelling of dendritic membrane (double arrows). Scale bar = 1 μm.

Aesthetascs of marine decapods are characterized by a thin (0.4–2.1 μm thick, Table 2), poreless cuticle, unlike bimodal sensilla that have a pore at their tip (Garm et al. 2003) and a thick cuticle (e.g., from 2 to 7 μm thick for the distal part of an antennular bimodal sensilla in *R. exoculata*; Machon, personal communication). The aesthetasc cuticle looks spongy, especially in the distal part, possibly functioning as a molecular sieve through which appropriate odorants move quickly to activate OSNs, as reported in spiny lobster (Derby et al. 1997) and crayfish (Tierney et al. 1986). Therefore, the cuticle thickness and structure along the aesthetasc may define the portion of sensilla permeable to soluble odorants. Comparison of aesthetascs from *M. fortunata* and *P. elegans*, and other marine decapod species, reveals similarities in cuticle thickness in the basal region of aesthetascs among the caridean shrimp group, marine crabs and the hermit crab (Table 2), and also in structure, being lamellar (Ghiradella et al. 1968; Grünert and Ache 1988; Gleeson et al. 1996). In our study, the distal region of aesthetascs has a thinner cuticle than described for other decapod species (Table 2), but similar to the thickness of *Daphnia* aesthetasc cuticle (Hallberg et al. 1992), and identical between *M. fortunata* and *P. elegans*. Regarding the cuticle, the spongy nonlamellar cuticle most likely corresponds to the odorant-permeable region. A portion of 50 and 80% of the aesthetasc length has a thin and spongy cuticle in *M. fortunata* and *P. elegans*, respectively. Although the 2 species have a similar aesthetasc length (Zbinden et al. 2017), *P. elegans* aesthetascs appear to have a larger surface area permeable to odorants than *M. fortunata*, which could lead to better sampling of the environment and spatial resolution.

Pore-like structures occur in the aesthetasc cuticle of *M. fortunata* from and beyond the transitional zone, but are absent in the thin cuticle of the distal part of the aesthetasc. These structures and pattern were also found in the hydrothermal shrimp *R. exoculata*, but not in the coastal shrimp *P. elegans*. Other types of pore-like structures have been described in the basal region of the aesthetasc for some marine decapods. Pore canals perforate the lamellar cuticle of the basal tenth of the aesthetascs in the hermit crab *Pagurus hirsutiusculus* (Ghiradella et al. 1968), proximal to the ciliary segments of the transitional zone, and pore-like structures occur from the base to the transitional zone in the lobster *Panulirus argus*, and contain extensions of the auxiliary cells (Grünert and Ache 1988). However, in *M. fortunata* these pore-like structures appear only from and beyond the transitional zone, where the auxiliary cells end. In addition these pore-like structures are much more abundant than those described in *P. hirsutiusculus* and *P. argus*, and are longer, crossing almost the entire thickness of the

cuticle, making them likely a feature specific to hydrothermal shrimp. The function of these pore-like structures is unknown. Although the cuticle layer separating the inner side of the pore-like structures with the outside is extremely thin, they could facilitate the passage of odorant molecules through the thick lamellar cuticle and thus enhance the sampling of the environment by compensating the small surface permeable to odorants in *M. fortunata* aesthetascs.

The presence of a thick layer of bacteria covering the aesthetascs is also likely a feature specific to hydrothermal shrimp. Indeed, dense bacterial populations have been observed on the antennae and antennules of 4 hydrothermal shrimp species (Zbinden et al. 2017; Figure 6C,E,F), sometimes covering the major surface of the aesthetascs, whereas no bacterial coverage was ever observed with the coastal shrimp *P. elegans*. Identification of the different bacteria types present on each species is needed to discuss on their potential role or impact on shrimp sensory perception.

Increased IDSs and ODSs numbers could be associated to a better discrimination of the chemical environment (Derby and Weissburg 2014) because the OSNs (whose number is reflected by the number of IDSs) express different olfactory receptors, beared by the ODSs. The number of IDSs per aesthetasc for *M. fortunata* and *P. elegans* fits within the range of about 100–400 displayed by several Malacostracan taxons (Table 2; Harzsch and Krieger 2018). Compared to *P. elegans*, aesthetascs of *M. fortunata* house fewer OSNs and contain fewer ODSs, suggesting the hydrothermal species is not likely to have an enhanced chemosensitivity regarding this character. However, these data need to be completed by identifying and quantifying the receptor proteins expressed by OSNs for each species, to investigate potential adaptations of the hydrothermal species at the molecular level.

Conclusions and perspectives

This study presents the first insights into the detection of various organic and chemical compounds by hydrothermal shrimp using an EAG approach. Sulfide was detected by both the antennule and the antenna, suggesting that hydrothermal shrimp may be able to sense sulfide concentrations occurring naturally in the near field of the vents. However, this detection is not specific to hydrothermal species. Neurons responding to sulfide are presumably present at least in Palaemonidae and Alvinocarididae shrimp groups, but the behavioral responses triggered by this detection remains unknown. Sulfide is a good candidate as a short-distance orientation cue in hydrothermal environments, as well as food-related odors, and behavioral designs are being experimented to see whether *M. fortunata* use these chemical sources for orientation around vent chimneys. In contrast, manganese and iron did not trigger significant EAG responses, which puts in doubt the significance of chemoreception for long-distance detection of active vents. Chemoreception abilities of other life stages should also be investigated, because dispersal and colonization processes occur at the larval stage (Lutz et al. 1984), which may be more sensitive to long-distance stimuli than adults. Furthermore, behavioral responses to both short- and long-distance stimuli must be investigated for *M. fortunata* and other hydrothermal species using pressurized aquaria (Shillito et al. 2014). Shrimp species occupy distinct microhabitats around vent chimneys, thus may not be sensitive to the same attractants and could exhibit different chemosensory abilities.

Comparative description of the aesthetasc ultrastructure gave insights into features of the hydrothermal shrimp, including cuticular pore-like structures and large bacteria covering. Bacterial functional types are being identified by sequencing approaches to ultimately discuss their potential influence on vent shrimp chemosensory abilities. Examination of the aesthetasc cuticle thickness and the numbers of IDSs and ODSs innervating aesthetascs did not reveal noticeable specializations of the hydrothermal species. Molecular studies are being conducted to further investigate adaptations of hydrothermal species by identifying, quantifying and localizing the chemoreceptors expressed by OSNs.

Funding

This work was supported in part by Sorbonne Université, UPMC and by the European Union Seventh Framework Programme (FP7/2007-2013) under the MIDAS project [grant agreement n°603418].

Acknowledgements

We thank the chief scientists of the Momarsat 2011, 2012, and 2016 cruises (Mathilde Cannat and Pierre-Marie Sarradin), and the chief scientist of the Biobaz 2013 cruise (François Lallier). We also thank Jozée Sarrazin and Nicolas Rabet for hydrothermal and coastal shrimp sampling, respectively, and Cécile Konn for her help with the preparation of chemical stimuli. TEM was performed at the "Plateforme de Microscopie Electronique" (MNHN) with the help of Chakib Djediat.

Conflict of interest

We have no conflict of interest to declare.

References

Ache BW. 1982. Chemoreception and thermoreception. In: Bliss D, editor. *The biology of Crustacea*, Vol. 3. New York: Academic Press. p. 369–398.

Ache BW, Derby CD. 1985. Functional organization of olfaction in crustaceans. *Trends Neurosci.* 8:356–360.

Altner H, Prillinger L. 1980. Ultrastructure of invertebrate chemo-, thermo-, and hygroreceptors and its functional significance. *Int Rev Cytol.* 67:69–139.

Aumond V. 2013. *Spéciation du cuivre en milieu hydrothermal profond et dans les zones de suintements froids* [dissertation]. Université de Bretagne occidentale-Brest.

Baker ET, Resing JA, Haymon RM, Tunnicliffe V, Lavelle JW, Martinez F, Ferrini V, Walker SL, Nakamura K. 2016. How many vent fields? New estimates of vent field populations on ocean ridges from precise mapping of hydrothermal discharge locations. *Earth Planet Sci Lett.* 449:186–196.

Bargmann CI. 2006. Comparative chemosensation from receptors to ecology. *Nature*. 444:295–301.

Bauer RT. 1977. Antifouling adaptations of marine shrimp (Crustacea: Decapoda: Caridea): functional morphology and adaptive significance of antennular preening by the third maxillipeds. *Mar Biol.* 40:261–276.

Beltz BS, Kordas K, Lee MM, Long JB, Benton JL, Sandeman DC. 2003. Ecological, evolutionary, and functional correlates of sensilla number and glomerular density in the olfactory system of decapod crustaceans. *J Comp Neurol.* 455:260–269.

Blaustein DN, Simmons RB, Burgess MF, Derby CD, Nishikawa M, Olson KS. 1993. Ultrastructural localization of 5'AMP odorant receptor sites on the dendrites of olfactory receptor neurons of the spiny lobster. *J Neurosci.* 13:2821–2828.

Carr WE, Ache BW, Gleeson RA. 1987. Chemoreceptors of crustaceans: similarities to receptors for neuroactive substances in internal tissues. *Environ Health Perspect.* 71:31–46.

Casanova B, Brunet M, Segonzac M. 1993. L'impact d'une épibiose bactérienne sur la morphologie fonctionnelle de crevettes associées à l'hydrothermalisme médio-Atlantique. *Cah Biol Mar.* 34:573–588.

Cate HS, Derby CD. 2001. Morphology and distribution of setae on the antennules of the Caribbean spiny lobster *Panulirus argus* reveal new types of bimodal chemo-mechanosensilla. *Cell Tissue Res.* 304:439–454.

Chamberlain SC. 2000. Vision in hydrothermal vent shrimp. *Philos Trans R Soc Lond B Biol Sci*. 355:1151–1154.

Charlou JL, Donval JP, Douville E, Jean-Baptiste P, Radford-Knoery J, Fouquet Y, Dapoigny A, Stievenard M. 2000. Compared geochemical signatures and the evolution of Menez Gwen (37°50′ N) and Lucky Strike (37°17′ N) hydrothermal fluids, south of the Azores Triple Junction on the Mid-Atlantic Ridge. *Chem Geol*. 171:49–75.

Colaço A, Dehairs F, Desbruyères D. 2002. Nutritional relations of deep-sea hydrothermal fields at the Mid-Atlantic Ridge: a stable isotope approach. *Deep Sea Res I*. 49:395–412.

Cottin D, Shillito B, Chertemps T, Thatje S, Léger N, Ravaux J. 2010. Comparison of heat-shock responses between the hydrothermal vent shrimp *Rimicaris exoculata* and the related coastal shrimp *Palaemonetes varians*. *J Exp Marine Biol Ecol*. 393:9–16.

Cowen JP, Massoth GJ, Feely RA. 1990. Scavenging rates of dissolved manganese in a hydrothermal vent plume. *Deep Sea Res I*. 37:1619–1637.

Crone TJ, Wilcock WS, Barclay AH, Parsons JD. 2006. The sound generated by mid-ocean ridge black smoker hydrothermal vents. *PLoS One*. 1:e133.

Cuvelier D, Sarradin PM, Sarrazin J, Colaço A, Copley TJ, Desbruyères D, Glover AG, Santos RS, Tyler PA. 2011. Hydrothermal faunal assemblages and habitat characterization at the Eiffel Tower edifice (Lucky Strike, Mid-Atlantic Ridge). *Mar Ecol*. 32:243–255.

De Angelis MA, Lilley MD, Baross JA. 1993. Methane oxidation in deep-sea hydrothermal plumes of the endeavour segment of the Juan de Fuca Ridge. *Deep Sea Res I*. 40:1169–1186.

Derby CD. 1982. Structure and function of cuticular sensilla of the lobster *Homarus americanus*. *J Crustac Biol*. 2:1–21.

Derby CD. 1995. Single unit electrophysiological recordings from crustacean chemoreceptor neurons. In: Spielman AI, Brand JG, editors. *Experimental cell biology of taste and olfaction: current techniques and protocols*. Boca Raton (FL): CRC Press. p. 241–250.

Derby CD, Cate HS, Gentilcore LR. 1997. Perireception in olfaction: molecular mass sieving by aesthetasc sensillar cuticle determines odorant access to receptor sites in the Caribbean spiny lobster *Panulirus argus*. *J Exp Biol*. 200:2073–2081.

Derby CD, Kozma MT, Senatore A, Schmidt M. 2016. Molecular mechanisms of reception and perireception in crustacean chemoreception: a comparative review. *Chem Senses*. 41:381–398.

Derby CD, Weissburg MJ. 2014. The chemical senses and chemosensory ecology of crustaceans. In: Derby CD, Thiel M, editors. *Crustacean nervous systems and their control of behavior*. New York: Springer. p. 263–293.

Desbruyères D, Almeida A, Biscoito M, Comtet T, Khripounoff A, Le Bris N, Sarradin PM, Segonzac M. 2000. A review of the distribution of hydrothermal vent communities along the northern Mid-Atlantic Ridge: dispersal vs. environmental controls. *Hydrobiologia*. 440:201–216.

Desbruyères D, Biscoito M, Caprais JC, Colaço A, Comtet T, Crassous P, Fouquet Y, Khripounoff A, Le Bris N, Olu K, *et al*. 2001. Variations in deep-sea hydrothermal vent communities on the Mid-Atlantic Ridge near the Azores plateau. *Deep Sea Res II*. 48:1325–1346.

Doolin RE, Zhainazarov AB, Ache BW. 2001. An odorant-suppressed Cl- conductance in lobster olfactory receptor cells. *J Comp Physiol A*. 187:477–487.

Fuzessery ZM, Childress JJ. 1975. Comparative chemosensitivity to amino acids and their role in the feeding activity of bathypelagic and littoral crustaceans. *Biol Bull*. 149:522–538.

Garm A, Hallberg E, Høeg JT. 2003. Role of maxilla 2 and its setae during feeding in the shrimp *Palaemon adspersus* (Crustacea: Decapoda). *Biol Bull*. 204:126–137.

Garm A, Walting K. 2013. The crustacean integument: setae, setules, and other ornamentation. *Funct Morphol Divers*. 1:167–198.

Gaten E, Herring PJ, Shelton PMJ, Johnson ML. 1998. Comparative morphology of the eyes of postlarval bresiliid shrimps from the region of hydrothermal vents. *Biol Bull*. 194:267–280.

Gebruk AV, Southward EC, Kennedy H, Southward AJ. 2000. Food sources, behaviour, and distribution of hydrothermal vent shrimps at the Mid-Atlantic Ridge. *J Mar Biol Assoc UK*. 80:485–499.

Ghiradella HT, Case JF, Cronshaw J. 1968. Structure of aesthetases in selected marine and terrestrial decapods: chemoreceptor morphology and environment. *Am Zool*. 8:603–621.

Gleeson RA, McDowell LM, Aldrich HC. 1996. Structure of the aesthetasc (olfactory) sensilla of the blue crab, *Callinectes sapidus*: transformations as a function of salinity. *Cell Tissue Res*. 284:279–288.

Grünert U, Ache BW. 1988. Ultrastructure of the aesthetasc (olfactory) sensilla of the spiny lobster, *Panulirus argus*. *Cell Tissue Res*. 251:95–103.

Hallberg E, Chaigneau J. 2004. Non-visual sense organs. In: Forest J, von Vaupel Klein JC, editors. *Treatise on zoology, Crustacea*, Vol. 1. Leiden (NL): Brill Academic Publishers. p. 301–380.

Hallberg E, Johansson KU, Elofsson R. 1992. The aesthetasc concept: structural variations of putative olfactory receptor cell complexes in Crustacea. *Microsc Res Tech*. 22:325–335.

Hallberg E, Skog M. 2010. Chemosensory sensilla in crustaceans. In: Breithaupt T, Thiel M, editors. *Chemical communication in crustaceans*. New York: Springer. p. 103–121.

Hamilton KA, Ache BW. 1983. Olfactory excitation of interneurons in the brain of the spiny lobster. *J Comp Physiol*. 150:129–140.

Harzsch S, Krieger J. 2018. Crustacean olfactory systems: a comparative review and a crustacean perspective on insect olfactory systems. *Prog Neurobiol*. 161:23–60.

Hernández-Ávila I, Cambon-Bonavita MA, Pradillon F. 2015. Morphology of first zoeal stage of four genera of alvinocaridid shrimps from hydrothermal vents and cold seeps: implications for ecology, larval biology and phylogeny. *PLoS One*. 10:e0144657.

Herring PJ, Dixon DR. 1998. Extensive deep-sea dispersal of postlarval shrimp from a hydrothermal vent. *Deep Sea Res I*. 45:2105–2118.

Hourdez S, Lallier FH. 2007. Adaptations to hypoxia in hydrothermal-vent and cold-seep invertebrates. *Rev Environ Sci Biotechnol*. 6:143–159.

Jinks RN, Battelle BA, Herzog ED, Kass L, Renninger GH, Chamberlain SC. 1998. Sensory adaptations in hydrothermal vent shrimps from the Mid-Atlantic Ridge. *Cab Biol Mar*. 39: 309–312.

Klevenz V, Bach W, Schmidt K, Hentscher M, Koschinsky A, Petersen S. 2011. Geochemistry of vent fluid particles formed during initial hydrothermal fluid-seawater mixing along the Mid-Atlantic Ridge. *Geochem Geophys Geosyst*. 12:Q0AE05. doi:10.1029/2011GC003704.

Lagerspetz KY, Vainio LA. 2006. Thermal behaviour of crustaceans. *Biol Rev Camb Philos Soc*. 81:237–258.

Lallier FH, Truchot JP. 1997. Hemocyanin oxygen-binding properties of a deep-sea hydrothermal vent shrimp: evidence for a novel cofactor. *J Exp Zool*. 277:357–364.

Laverack MS. 1964. The antennular sense organs of *Panulirus argus*. *Comp Biochem Physiol*. 13:301–321.

Laverack MS. 1988. The diversity of chemoreceptors. In: Atema J, Fay RR, Tavolga WN, editors. *Sensory biology of aquatic animals*, Vol. 3. New York: Springer-Verlag. p. 287–312.

Laverack MS, Ardill DJ. 1965. The innervation of the aesthetasc hairs of *Panulirus argus*. *J Cell Sci*. 3:45–60.

Le Bris N, Govenar B, Le Gall C, Fisher CR. 2006. Variability of physico-chemical conditions in 9°50′ N EPR diffuse flow vent habitats. *Mar Chem*. 98:167–182.

Lutz RA, Jablonski D, Turner RD. 1984. Larval development and dispersal at deep-sea hydrothermal vents. *Science*. 226:1451–1454.

Machon J, Ravaux J, Zbinden M, Lucas P. 2016. New electroantennography method on a marine shrimp in water. *J Exp Biol*. 219:3696–3700.

Martin JW, Christiansen JC. 1995. A new species of the shrimp genus *Chorocaris* Martin & Hessler, 1990 (Crustacea: Decapoda: Bresiliidae) from hydrothermal vent fields along Mid-Atlantic Ridge. *Proc Biol Soc Wash*. 108:220–227.

Martin JW, Haney TA. 2005. Decapod crustaceans from hydrothermal vents and cold seeps: a review through 2005. *Zool J Linn Soc*. 145:445–522.

Matabos M, Cuvelier D, Brouard J, Shillito B, Ravaux J, Zbinden M, Barthelemy D, Sarradin PM, Sarrazin J. 2015. Behavioural study of two hydrothermal crustacean decapods: *Mirocaris fortunata* and *Segonzacia mesatlantica*, from the Lucky Strike vent field (Mid-Atlantic Ridge). *Deep Sea Res II*. 121:146–158.

Mead KS. 1998. The biomechanics of odorant access to aesthetascs in the grass shrimp, *Palaemonetes vulgaris*. *Biol Bull*. 195:184–185.

Mellon D Jr. 2000. Convergence of multimodal sensory input onto higher-level neurons of the crayfish olfactory pathway. *J Neurophysiol*. 84:3043–3055.

Monteclaro HM, Anraku K, Matsuoka T. 2010. Response properties of crayfish antennules to hydrodynamic stimuli: functional differences in the lateral and medial flagella. *J Exp Biol*. 213:3683–3691.

Mottl MJ, McConachy TF. 1990. Chemical processes in buoyant hydrothermal plumes on the East Pacific Rise near 21°N. *Geochim Cosmochim Acta*. 54:1911–1927.

Nagai T. 1985. Summation and gradient characteristics of local electroantennogram response of the European corn borer, *Ostrinia nubilalis*. *Pestic Biochem Physiol*. 24:32–39.

Obermeier M, Schmitz B. 2004. The modality of the dominance signal in snapping shrimp (*Alpheus heterochaelis*) and the corresponding setal types on the antennules. *Mar Freshwater Behav Physiol*. 37:109–126.

Pelli DG, Chamberlin SC. 1989. The visibility of 350 degrees C black-body radiation by the shrimp *Rimicaris exoculata* and man. *Nature*. 337:460–461.

Polz MF, Robinson JJ, Cavanaugh CM, Van Dover CL. 2003. Trophic ecology of massive shrimp aggregations at a Mid-Atlantic Ridge hydrothermal vent site. *Limnol Oceanogr*. 43:1631–1638.

Ponsard J, Cambon-Bonavita MA, Zbinden M, Lepoint G, Joassin A, Corbari L, Shillito B, Durand L, Cueff-Gauchard V, Compère P. 2013. Inorganic carbon fixation by chemosynthetic ectosymbionts and nutritional transfers to the hydrothermal vent host-shrimp *Rimicaris exoculata*. *ISME J*. 7:96–109.

Puri S, Faulkes Z. 2010. Do decapod crustaceans have nociceptors for extreme pH? *PLoS One*. 5:e10244.

Radford-Knoery J, Charlou JL, Donval JP, Aballea M, Fouquet Y, Ondreas H. 1998. Distribution of dissolved sulfide, methane, and manganese near the seafloor at the Lucky Strike (37°17′N) and Menez Gwen (37°50′N) hydrothermal vent sites on the mid-Atlantic Ridge. *Deep Sea Res I*. 45:367–386.

Rathke H. 1837. Zur Fauna der Krym. *Mémoires de l'Académie Impériale des Sciences de St. Pétersbourg*. 3:291–454.

Ravaux J, Cottin D, Chertemps T, Hamel G, Shillito B. 2009. Hydrothermal vent shrimps display low expression of the heat-inducible hsp70 gene in nature. *Mar Ecol Prog Ser*. 396:153–156.

Renninger GH, Kass L, Gleeson RA, Van Dover CL, Battelle BA, Jinks RN, Herzog ED, Chamberlain SC. 1995. Sulfide as a chemical stimulus for deep-sea hydrothermal vent shrimp. *Biol Bull*. 189:69–76.

Rospars JP, Grémiaux A, Jarriault D, Chaffiol A, Monsempes C, Deisig N, Anton S, Lucas P, Martinez D. 2014. Heterogeneity and convergence of olfactory first-order neurons account for the high speed and sensitivity of second-order neurons. *PLoS Comput Biol*. 10:e1003975.

Sarradin PM, Caprais JC, Riso R, Kerouel R, Aminot A. 1999. Chemical environment of the hydrothermal mussel communities in the lucky strike and Menez Gwen vent fields, Mid Atlantic Ridge. *Cah Biol Mar*. 40:93–104.

Sarrazin J, Juniper SK, Massoth G, Legendre P. 1999. Physical and chemical factors influencing species distributions on hydrothermal sulfide edifices of the Juan de Fuca Ridge, northeast Pacific. *Mar Ecol Prog Ser*. 190:89–112.

Sarrazin J, Legendre P, De Busserolles F, Fabri MC, Guilini K, Ivanenko VN, Morineaux M, Vanreusel A, Sarradin PM. 2015. Biodiversity patterns, environmental drivers and indicator species on a high-temperature hydrothermal edifice, Mid-Atlantic Ridge. *Deep Sea Res II*. 121:177–192.

Sarrazin J, Sarradin PM, Allais AG. 2006. MoMARETO: a cruise dedicated to the spatio-temporal dynamics and the adaptations of hydrothermal vent fauna on the Mid-Atlantic Ridge. *InterRidge News*. 15:24–33.

Schmidt M, Ache BW. 1996. Processing of antennular input in the brain of the spiny lobster, *Panulirus argus*. *J Comp Phys A*. 178:605–628.

Schmidt M, Mellon F. 2010. Neuronal processing of chemical information in crustaceans. In: Breithaupt T, Thiel M, editors. *Chemical communication in crustaceans*. New York: Springer. p. 123–147.

Shillito B, Gaill F, Ravaux J. 2014. The IPOCAMP pressure incubator for deep-sea fauna. *J Mar Sci Tech*. 22:97–102.

Shillito B, Hamel G, Duchi C, Cottin D, Sarrazin J, Sarradin PM, Ravaux J, Gaill F. 2008. Live capture of megafauna from 2300 m depth, using a newly designed pressurized recovery device. *Deep Sea Res I*. 55:881–889.

Shillito B, Ravaux J, Sarrazin J, Zbinden M, Sarradin PM, Barthelemy D. 2015. Long-term maintenance and public exhibition of deep-sea hydrothermal fauna: the AbyssBox project. *Deep Sea Res II*. 121:137–145.

Snow PJ. 1973. Ultrastructure of the aesthetase hairs of the littoral decapod, *Paragrapsus gaimardii*. *Z Zellforsch Mikrosk Anat*. 138:489–502.

Solari P, Sollai G, Masala C, Loy F, Palmas F, Sabatini A, Crnjar R. 2017. Antennular morphology and contribution of aesthetascs in the detection of food-related compounds in the shrimp *Palaemon adspersus* Rathke, 1837 (Decapoda: Palaemonidae). *Biol Bull*. 232:110–122.

Spencer M, Linberg KA. 1986. Ultrastructure of aesthetasc innervation and external morphology of the lateral antennule setae of the spiny lobster *Panulirus interruptus* (Randall). *Cell Tissue Res*. 245:69–80.

Tierney AJ, Thompson CS, Dunham DW. 1986. Fine structure of aesthetasc chemoreceptors in the crayfish *Orconectes propinquus*. *Can J Zool*. 64:392–399.

Toner BM, Santelli CM, Marcus MA, Wirth R, Chan CS, McCollom T, Bach W, Edwards KJ. 2009. Biogenic iron oxyhydroxide formation at mid-ocean ridge hydrothermal vents: Juan de Fuca Ridge. *Geochim Cosmochim Acta*. 73:388–403.

Tyler PA, Young CM. 2003. Dispersal at hydrothermal vents: a summary of recent progress. *Hydrobiologia*. 503:9–19.

Ukhanov K, Bobkov Y, Ache BW. 2011. Imaging ensemble activity in arthropod olfactory receptor neurons *in situ*. *Cell Calcium*. 49:100–107.

Van Dover CL, Szuts EZ, Chamberlain SC, Cann JR. 1989. A novel eye in 'eyeless' shrimp from hydrothermal vents of the Mid-Atlantic Ridge. *Nature*. 337:458–460.

van Drongelen W, Holley A, Døving KB. 1978. Convergence in the olfactory system: quantitative aspects of odour sensitivity. *J Theor Biol*. 71:39–48.

Waeles M, Cotte L, PErnet-Coudrier B, Chavagnac V, Cathalot C, Leleu T, Laës-Huon A, Perhirin A, Riso RD, Sarradin PM. 2017. On the early fate on hydrothermal iron at deep-sea vents: a reassessment after in situ filtration. *Geophys Res Let*. 44:4233–4240.

Zbinden M, Berthod C, Montagné N, Machon J, Léger N, Chertemps T, Rabet N, Shillito B, Ravaux J. 2017. Comparative study of chemosensory organs of shrimp from hydrothermal vent and coastal environments. *Chem Senses*. 42:319–331.

Zbinden M, Shillito B, Le Bris N, de Montlaur CDV, Roussel E, Guyot F, Gaill F, Cambon-Bonavita MA. 2008. New insights on the metabolic diversity among the epibiotic microbial community of the hydrothermal shrimp *Rimicaris exoculata*. *J Exp Mar Biol Ecol*. 359:131–140.

Zhang D, Cai S, Liu H, Lin J. 2008. Antennal sensilla in the genus *Lysmata* (Caridea). *J Crustac Biol*. 28:433–438.

Zhang JZ, Millero FJ. 1993. The products from the oxidation of H_2S in seawater. *Geochim Cosmochim Acta*. 57:1705–1718.

Zhu J, Zhang D, Lin J. 2011. Morphology and distribution of antennal and antennular setae in *Lysmata* shrimp. *J Shellfish Res*. 30:381–388.

Communications

- 19th annual meeting of the French Club for Invertebrate Neurobiology (CNI)

May 24-25, 2018, INRA, Campus de Versailles

Machon Julia, Ravaux Juliette, Zbinden Magali, Lucas Philippe, Chertemps Thomas, Montagné Nicolas, Harzsch Steffen, Krieger Jakob, Meth Rebecca, Shillito Bruce

Talk: « Insights into the chemosensory system of the deep hydrothermal vent shrimp *Mirocaris fortunata* »

- French-American Doctoral Exchange Program on Ocean (FadexO)

October 20, 2017, MNHN, Paris

Machon Julia, Lucas Philippe, Zbinden Magali, Ravaux Juliette

Talk: « Comparative study of sensory abilities in deep hydrothermal shrimp *Mirocaris fortunata* and coastal shrimp *Palaemon elegans* »

- Teaching to master students, course unit: "Biologie et Adaptations en Milieux Extrêmes »

September 12,. 2017, Sorbonne Université, Paris

Machon Julia

Lesson title: « Adaptations sensorielles (photo-et chimio-réception) chez les crevettes hydrothermales profondes »

- 6th International symposium on chemosynthesis-based ecosystems (CBE6)

August 27 – September 1, 2017, Woods Hole Oceanographic Institution (USA)

Machon Julia, Zbinden Magali, Ravaux Juliette, Barthelemy Dominique, Lucas Philippe, Sarrazin Jose, Sarradin Pierre-Marie, Shillito Bruce

Poster: « AbyssBox: Public exhibition of deep-sea hydrothermal fauna and associated research projects »

Page 228

- Journées scientifiques de l'UMR BOREA

July 6-8, 2016

July 5-7, 2017, Caen

Machon Julia, Ravaux Juliette, Zbinden Magali

Talks: « Adaptations sensorielles chez les crevettes hydrothermales profondes »

- MIDAS 2nd and final meeting (Managing impacts of deep-sea ressources exploitation)

November 16-19, 2015, Sintra (Portugal)

October 3-7, 2016, Gent (Belgium)

Machon Julia, Zbinden Magali, Lucas Philippe, Shillito Bruce, Léger Nelly, Montagné Nicolas, Chertemps Thomas, Ravaux Juliette

Talks: « Comparative study of chemo- and thermosensory abilities in hydrothermal Alvinocaridid and coastal Palaemonid shrimp »

- Colloque national sur la biologie et l'écologie des ecosystèmes à base de chimiosynthèse (CONNECT2)

May 11-13, 2016, Ifremer, Brest

Machon Julia, Zbinden Magali, Lucas Philippe, Shillito Bruce, Léger Nelly, Montagné Nicolas, Chertemps Thomas, Ravaux Juliette

Talk: « Comparaison des facultés chimio- et thermo-sensorielles chez les crevettes hydrothermales Alvinocarididés et cotières Palaemonides »

- 3rd Young Natural History Scientists Meeting (YNHM3)

February 2-6, 2016, MNHN, Paris

Machon Julia, Zbinden Magali, Lucas Philippe, Léger Nelly, Montagné Nicolas, Chertemps Thomas, Ravaux Juliette

Poster: « Sensorial adaptations in deep hydrothermal shrimp »

Page 229

AbyssBox :

Public exhibition of deep-sea hydrothermal fauna and associated research projects

Machon J.[1], Zbinden M.[1], Ravaux J.[1], Barthélémy D.[2], Lucas P.[3], Sarrazin J.[4], Sarradin P-M.[4], Shillito B.[1].

[1] Sorbonne Universités, UPMC Univ Paris 06, UMR CNRS 7208 BOREA, Adaptations aux Milieux Extrêmes, 75005 Paris, France
[2] Océanopolis, Port de Plaisance du Moulin Blanc, 29210 Brest Cedex 1, France
[3] iEES, Institut of Ecological and Environmental Sciences – UPMC, UMR 7618, Dpt Sensorial Ecology, Paris-Versailles, France
[4] Ifremer, Centre de Bretagne, REM/EEP, Laboratoire Environnement Profond, Institut Carnot EDROME, 29280 Plouzané, France

The AbyssBox pressurized aquarium : long-term maintenance of deep-sea invertebrates

A valuable approach to better understand ecosystem functioning is the **experimentation on live animals**, but deep-sea organisms usually have low tolerance to sampling and prolonged exposure at atmospheric pressure.

The AbyssBox project, at the Oceanopolis aquarium (Brest, France) aims to provide the **first permanent public exhibition of live hydrothermal invertebrates maintained at *in situ* pressure** : the vent shrimp *Mirocaris fortunata* and crab *Segonzacia mesatlantica*, sampled at 1700 m depth in the Lucky Strike vent field on Mid-Atlantic Ridge.

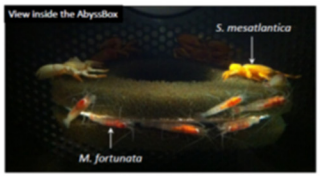


Dr. Bruce Shillito presenting the two Abyssboxes exhibited at the Océanopolis public aquarium

Volume 16.5L – pressure up to 20MPa – temperature 2-40°C – flow rates up to 10L/h

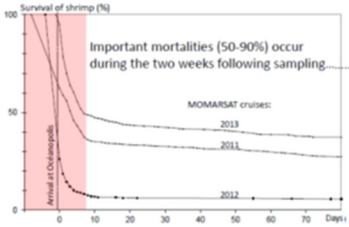

but then survivors stay alive for years :

	M. fortunata	*S. mesatlantica*
In situ pressure (AbyssBox)	1097 days	731 days
Atmospheric pressure	> 2 years	few days

Maximum lifespan observed in captivity

Designed to function permanently, AbyssBox is also available to the scientific community for long-term rearing of deep-sea fauna, at the **scale of years**, giving informations on lifespan, reproduction cycles and species interactions, which are often poorly characterized.

➔ **The AbyssBox is one of the most useful tools for long-term (over years) maintenance and observation of hydrothermal fauna at *in situ* pressure**

Comparative study of chemo-reception in deep hydrothermal shrimp *Mirocaris fortunata* and coastal shrimp *Palaemon elegans*

Does *M. fortunata* present specific adaptations of its chemo-sensory system to detect the environment, using hydrothermal fluid emissions ?

Which organs are involved in chemo-reception ?

The **antenna** and **antennules** are associated to various sensory modalities

Localisation of the chemo-receptor IR25a in the lateral antennule

The lateral antennule bears **aesthetasc sensilla** specialized in chemo-reception

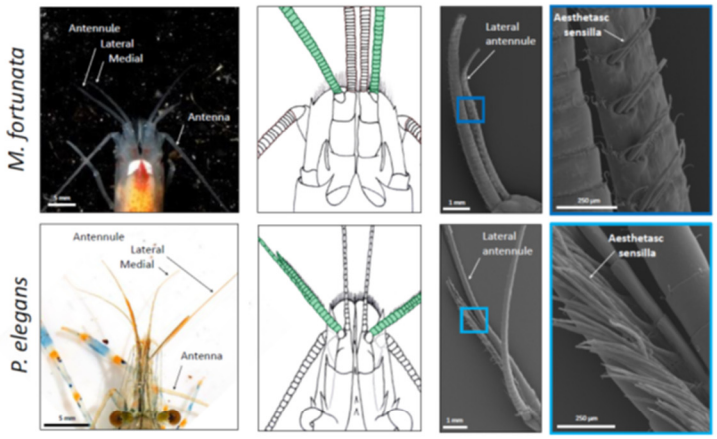

Which chemical stimuli are detected ?

We developped the first underwater electroantennography (EAG) method on **live** shrimp, to record the **electrical responses of the chemo-receptor neurons innervating the aesthetasc sensilla.**

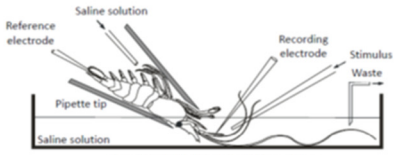

Experimental design of the EAG on shrimp

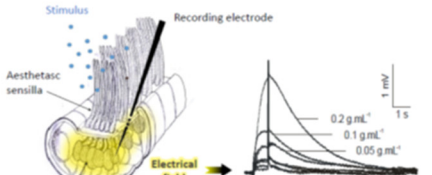

EAG responses of *P. elegans* antennule to increasing concentrations of food extract

Current projects

We are estimating the **number of dendrites per aesthetascs**, since an enhanced dendritic number may be correlated to life style and/or chemo-reception efficiency.

We are lauching a **transcriptomic study on 4 hydrothermal shrimps** (*M. fortunata, R. exoculata, Chorocaris chacei* and *Alvinocaris markensis*) that live at different distances from vent chimneys, in order **to identify chemo-receptors** expressed in their antennules, antenna and mouth parts.

Detection of hydrothermal stimuli (**sulfide, iron and manganese**) is being tested with the EAG method. The compounds eliciting positive responses will be used for **behavior experiments (e.g. attraction or repulsion)**, to determine if *M. fortunata* uses the chemical signature of the hydrothermal fluid for orientation in its environment.

Temperature variations around vent chimneys are also a potential attractant for hydrothermal shrimp. We are testing the **attraction to warm temperature** and searching for **thermo-receptors** expressed in the antennal appendages.

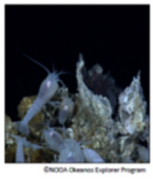
©NOAA Okeanos Explorer Program

Selected publications :

- Shillito, B., Ravaux, J., Sarrazin, J., Zbinden, M., Sarradin, P.M., & Barthelemy, D. (2015). Long-term maintenance and public exhibition of deep-sea Hydrothermal fauna: the AbyssBox project. *Deep Sea Research Part I: Topical Studies in Oceanography*, *121*, 137-143.
- Zbinden, M., Berthet, C., Montagné, N., Machon, J., Léger, N., Chertemps, T., Rabet N., Shillito B. & Ravaux, J. (2017). Comparative Study of Chemosensory Organs of Shrimp From Hydrothermal Vent and Coastal Environments. *Chemical Senses*, *42*(4), 319-331.
- Matabos, M., Cuvelier, D., Breusot, J., Shillito, B., Ravaux, J., Zbinden, M., Barthelemy D., Sarradin PM. & Sarrazin J. (2015). Behavioural study of two hydrothermal crustacean decapods: Mirocaris fortunata and Segonzacia mesatlantica, from the Lucky Strike vent field (Mid-Atlantic Ridge). *Deep Sea Research Part I: Topical Studies in Oceanography*, *121*, 148-158.
- Machon, J., Ravaux, J., Zbinden, M., & Lucas, P. (2018). New electroantennography method on a marine shrimp in water. *Journal of Experimental Biology*, *221*(23), 1666-5700.

Fundings :

The AbyssBox project is funded by the Oceanopolis public aquarium
The work is funded by the FP7 european project MIDAS (n° 603418)

MIDAS MANAGING IMPACTS OF DEEP SEA RESOURCE EXPLOITATION

Acknowledgements :

Aquariology team, Océanopolis public aquarium
NBO team, ECOSENS department, iEES, IRAs Versailles
Service de microscopie électronique à Balayage, UPMC – V. Bazin & M. Yéchat

Julie.Machon@LIVE.FR

YNHM YOUNG NATURAL HISTORY SCIENTISTS MEETING

Sensorial adaptations in deep hydrothermal shrimp :

Comparison of sensory abilities of hydrothermal shrimp *Mirocaris fortunata* and coastal species *Palaemon elegans*

Machon J.[1], Zbinden M.[1], Lucas P.[2], Léger N.[1], Montagné N.[2], Chertemps T.[2], Ravaux J.[1]

[1] Université Pierre et Marie Curie – Paris VI (UPMC), UMR 7208 BOREA, équipe Adaptations aux Milieux Extrêmes, 75005 Paris, France
[2] iEES, Institut of Ecological and Environmental Sciences – UPMC, UMR 7618, Dpt Ecologie sensorielle, Paris-Versailles, France

Hydrothermal vent ecosystems are scarce and ephemere environments along the mid-oceanic ridges. **Detection of hydrothermal emissions** is crucial for endemic fauna, either to find fluid to feed their symbiotic bacteria, to remain in an appropriate range of physiochemical conditions, or to detect new venting sites during dispersion. Hydrothermal activity has specific **chemical signatures**, as well as **thermal gradients**, which may be used to locate hydrothermal vent emissions.

To date, only a few studies are available on **chemoreception** in hydrothermal shrimp (Renninger et al. 1995; Chamberlain et al. 1996; Jinks et al. 1998), whereas it is primordial for the understanding of their life cycle, maintening and long-term evolution. For **thermoreception**, no study has been performed in hydrothermal species.

In the present study we foccus on chemoreception, more precisely on **olfaction** (i.e. « distant » chemoreception) : sensilla respond to highly soluble compounds, detected in very low concentrations at distance from the source (Bauer & Caskey 2006). In decapods, chemoreceptors are located mainly on the antennule (or first antenna; for olfaction) and pereiopods dactyls and mouthparts (for gustation, Ache 1982).

The shrimp *Mirocaris fortunara* are among the dominant species of hydrothermal sites in Mid-Atlantic Ridge and are good models for studying olfactory capacities. The closely related coastal shrimp *Palaemon elegans* has been chosen for comparison to discuss **potential adaptations of deep-sea shrimp related to their environment.**


Mirocaris fortunata


Palaemon elegans

MORPHOLOGY OF ANTENNULAR SENSILLA

In Crustacea, the main olfactory organ is the **antennule**, the lateral flagellum of which bears specialized sensilla called **aesthetascs**. Their cuticule is permeable to chemicals and they are innervated only by chemoreceptor neurons.

Non-aesthetasc sensilla are present on both antenna and antennules, and are innervated by chemo- and mecano-receptor neurons.

Hydrothermal shrimp *Mirocaris fortunata*

The antennule is divided in lateral and medial flagella

Aesthetascs are located on the ventral face of the lateral flagellum, with one row of 3 to 4 aesthetascs per segment
→ ~ 60 aesthetascs per lateral flagellum

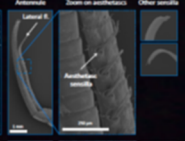

Coastal shrimp *Palaemon elegans*

The antennule is divided in lateral and medial flagella, and the lateral one is bipartite, with an extern filament similar to the medial flagellum, and a shorter intern filament

Aesthetascs are located on the ventral face of the intern filament of the lateral flagellum, with 2 rows of 5 to 6 aesthetasc per segment.

→ ~ 150 aesthetascs per lateral flagellum

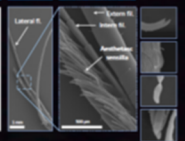

Legend : R. flagellum ; RL. filament

→ Relative to the antennule size, total number of aesthetascs is quite similar, showing no particularities in hydrothermal specie

RESEARCH OF IONOTROPIC RECEPTORS

We sequenced a receptor involved in olfaction, called **IR25a**, in 4 hydrothermal shrimp and 3 coastal Palaemonids.

The receptor IR25a was discovered in 2008 and is part of the ionotropic receptor (IR) family. Irs are involved in the detection of odors, and are located in the membrane of the Olfactory Receptor Neurons (ORNs).

Because these receptors are well conserved among Arthropods, we managed to sequence about 1/3 of the sequence.

Phylogenetic relationship in arthroped IR25a olfactory receptor

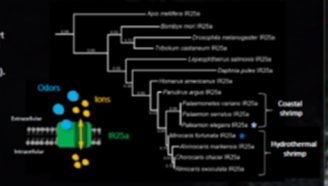

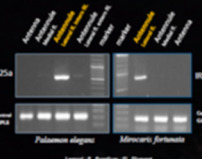

IR25a gene products were next located in the antennular appendages in P. elegans and M. fortunata, by RT-PCR.

In both species, IR25a is expressed only in the flagellum that bears aesthetasc sensilla.

→ The high expression of the olfactory receptor IR25a in the lateral antennule confirms the major role of this organ in shrimp olfaction

BEHAVIOURAL EXPERIMENTS

The shrimp were placed in a tank for 5 min with no odor source. Food and lure bags were than immersed and shrimp were observed for 5 min.

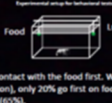

3 batches of shrimp (n=3x20) were tested :
* Intact antennules (intact A1)
* Lateral antennules ablated (Lat. A1 ablated)
* Whole antennules ablated (A1 ablated)

In *P. elegans*, majority (45%) of intact shrimp make a contact with the food first. With the ablation of the lateral antennule (i.e. aesthetasc ablation), only 20% go first on food. Whole antennule ablated shrmp were mostly inactive (65%).
For *M. fortunata*, the bioassat was not conclusive since the majority of intact shrimp was attracted to the lure.

→ The ablation of the lateral antennule impaired the food source detection in *P. elegans*, which confirms its involvement in olfaction

In vivo studies were conducted on hydrothermal shrimp *M. fortunata* and *Rimicaris exoculata*, with the pressurized aquarium IPOCAMP.

The setup allow the delivery of chemical stimuli as well as warm temperature, and shrimp behavior is video-recorded.

→ The hydrothermal species showed attraction for high temperature, but no for sulfides in opposition to previous experiments on *R. exoculata* (Renninger *et al.* 1995)

Results need to be reproduced on the coastal specie *P. elegans*

IPOCAMP aquarium
Shillito et al. 2015

ELECTROPHYSIOLOGY STUDY

When odor molecules bind to olfactory receptors on the dendrite membrane of Olfactory Receptor Neurons (ORNs), it triggers a **receptor potential** around the cell bodies of ORNs activated simultaneously.

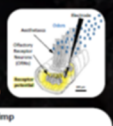

We developped a method to record this receptor potential with electrodes, to test if shrimp are able to detect hydrothermal stimuli via olfaction.

This setup is derived from **electroantennography** (EAG) on insects. The animal is fixed with the aesthetascs up, antennules being immersed in saline solution, also perfused on the gills. The recording electrode in inserted between the aesthetascs, the reference electrode at the base of telson. Stimulus delivery via a capillary is controled with Clampex software.

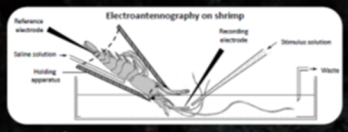

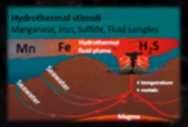

Stimulus	Attraction	Repulsion
Food	+	-
Saline	-	-
Vent fluid	+	-
Fe	+	-
Mn	+	-
H_2S	+	-
Acid saline	+	-

The results confirm the reproductibility, the concentration dependence and adaptation of the response to a stimulus
→ We record a chemosensory response

→ *P. elegans* and *M. fortunata* detected the same stimuli
More data will be produce to consider the amplitude of the responses and make quantitative comparison

We present here the **first detailed morphological description of the olfactory aesthetasc sensilla**, as well as the **first ionotropic receptor identification and localisation in hydrothermal shrimp**. Ablation experiments confirmed that the lateral antennule play a major role in olfaction. We also developed the **first extracellular recording technique of the global activity of the antennule in aquatic crustacean**.

The validation of the EAG on shrimp opens a wide field of possibilities to refine the results obtained, both in detection of chemicals (to test other concentrations, or other potential attractants, and potential behaviors associated) and in shrimp olfactory capacity (spectrum of response, interaction between compounds...).

The **detection of temperature** could also be a promising line of work, as suggested by preliminary data on *R. exoculata* and *M. fortunata* in IPOCAMP experiments.

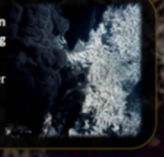

References

Ache 1982, Chemoreception and thermoreception. Atlas D (ed) The Biology of Crustacea, Academic Press, New York, 3 369-398
Bauer B, Caskey 2006, Flagellar setae of the second antennae in Artemia sp. shrimp: sexual dimorphism and possible role in detection of contact sex pheromones. Invertebr Reprod. Dev. 49(1-2):53-63
Chamberlain, Battelle, Herzog, Jinks, Kass and Renninger 1996, Sensory neurobiology of hydrothermal vent shrimp from the Mid-Atlantic Ridge. Abstract. TAMU-IR-MAR Symposium,Reykjavik, Iceland
Jinks, Battelle, Herzog, Kass, Renninger and Chamberlain 1998, Sensory adaptations in hydrothermal vent shrimps from the MAR-Atlantic Ridge. Cahiers de Biologie Marine 39 309-312
Renninger, Kass, Gleeson, Van Dover, Battelle, Jinks, Herzog and Chamberlain 1995, Sulfide as chemical stimulus for deep-sea hydrothermal vent shrimps. Biological Bulletin 189 69-76
Shillito, Ravaux, Sarrazin, Zbinden, Barthélémy and Sarradin 2015, Long-term maintenance and public exhibition of deep-sea fauna : the Abyssbox project. Deep-sea Research II.

Acknowledgements

- The work is funded by the FP7 european project MIDAS (n° 603418)
- iFRED Service de Microscopie Electronique à Balayage, UPMC – V.Kientz & M. Vrchet
- Oceanopolis, Brest, France – D. Barthélémy & the aquariology team

MIDAS MANAGING IMPACTS OF DEEP SEA RESOURCE EXPLOITATION

Glossary

Aesthetasc: tubular, thin-walled sensilla found on the antennules of crustaceans (the lateral antennules in decapods), innervated by olfactory sensory neurons that project to the olfactory lobes in the brain.

Allatostatins: neuropeptide hormones that inhibit the generation of the juvenile hormone, which regulates many aspects of insect and crustacean physiology.

Antennal neuropil: first-order neuropil that receives afferent fibers from the sensory neurons innervating the sensilla on the antennae (second antennae).

Basaltic (rock): volcanic mafic (rich in silica) rock formed from the rapid cooling of lava.

Bimodal sensilla: sensilla with a terminal pore found on the antennal appendages, mouthparts, walking appendages and the body surface of crustaceans, innervated by chemo- and mechanosensory neurons that project to the lateral and medial antennular neuropils.

Calcium imaging: technique used to investigate neuronal activity, by visualizing changes in intracellular calcium concentration, with fluorescent molecules that respond to the binding of Ca^{2+} ions by changing their fluorescence properties.

Distributed chemodetection: one chemosensory pathway in crustaceans (in parallel to Olfaction), mediated by bimodal sensilla, and comprising contact chemodetection ("taste") and "chemical senses" with specialized function, such the control of antennular grooming, coordination of mating…

Flicking: movement of the antennules (the lateral flagellum is quickly depressed from its normal posture and then returned at slower speed) that enhances odorant capture by exposing the aesthetasc sensilla to new water samples ("sniffing").

Grooming: crustacean behavior to keep the body free of microbial and particulate fouling, for exemple by preening the antennules with setal brushes on the third maxillipeds.

Hemiellipsoid bodies: second-order neuropils that process information from various sensory modalities, likely with the medulla terminalis.

Homeoviscous adaptation: adaptation of the cell membrane lipid composition to keep the adequate membrane fluidity.

Lateral antennular neuropil: first-order neuropil that receives afferent fibers from the sensory neurons innervating the sensilla on the antennules (first antennae), except from the olfactory sensory neurons innervating the aesthetascs.

Lecithotrophy: form of development in which the larva receives nutritional supply only from its stock of lipids.

Manifold: stimulator device that has several openings to allow the passing of liquids or gases.

Medulla terminalis: second-order neuropils that might be involved in multi-sensory integration, together with the hemiellipsoid bodies.

Neuropil: synaptically dense region in the central nervous system, composed of glial cells, axons and dendrites, but not the somata, of sensory, inter- and projection neurons.

Olfaction: one chemosensory pathway in crustaceans (in parallel to Distributed chemodetection), mediated by aesthetascs, and comprising to the distant detection of odorant molecules.

Olfactory lobe: first-order neuropil that receives afferent fibers from the olfactory sensory neurons innervated the aesthetascs on the lateral antennules.

Olfactory sensory neuron: chemosensory neuron innervating the aesthetascs and projecting to the olfactory lobes in the brain.

Patch-clamp: recording technique of ionic currents in isolated individual cells, tissues sections or patches of cell membrane, especially in neurons to record action potentials and nerve activity.

Peripheral nervous system: neurons, nerves and ganglia outside the brain and the ventral nerve cord.

Plume: column of one fluid moving through another (e.g. hydrothermal fluid or mining wastes mixing with the ambient seawater).

Receptor potential: generally a depolarization consecutive to the activation of a sensory receptor, which can eventually trigger the corresponding sensory neuron to emit action potentials.

Sensillum (Sensilla): cuticular expansion innervated by sensory neurons.

Seta (Setae): cuticular expansion with no sensory function (or for which innervation by sensory neurons has not been demonstrated).

Single sensillum recording: electrophysiology technique to perform extracellular recording of action potentials from single sensory neurons innervating a sensilla.

Statocyst: balance sensory receptor in some aquatic invertebrates, consisting of a sac-like structure containing a mineralized mass and numerous sensory hairs.

Synapsins: family of proteins implicated in the regulation of neurotransmitter release at synapses.

Ultramafic (rock): dominant rock type of the Earth's upper mantle (also known as peridotite), which undergoes near the seafloor hydration and metamorphic transformation into serpentinite minerals, which produces hydrogen gas.

Abbreviations

AnN: Antennal Neuropil (see Glossary)

BALIST: Biology of Alvinella Isobaric Sampling and Transfer

EAG: ElectroAntennoGraphy

GR: Gustatory Receptor

HB: Hemiellipsoid Bodies

IPOCAMP: Incubateur Pressurisé pour l'Observation et la Culture d'Animaux Marins Profonds

IR: Ionotropic Receptor

LAN: Lateral Antennular Neuropil (see Glossary)

MAR: Mid-Atlantic Ridge

MT: Medulla Terminalis

NP: Novo Prawn

OL: Olfactory Lobe (see Glossary)

OSN: Olfactory Sensory Neuron (see Glossary)

PBS: Phosphate Buffered Saline

PERISCOP: Projet d'Enceinte et de Récupération Isobare Servant à la Collecte d'Organismes Profonds

PS: *Panulirus* Saline

TRP: Transient Receptor Potential channel

Ifremer: Institut FRançais pour l'Exploitation de la MER

WHOI: Woods Hole Oceanographic Institution